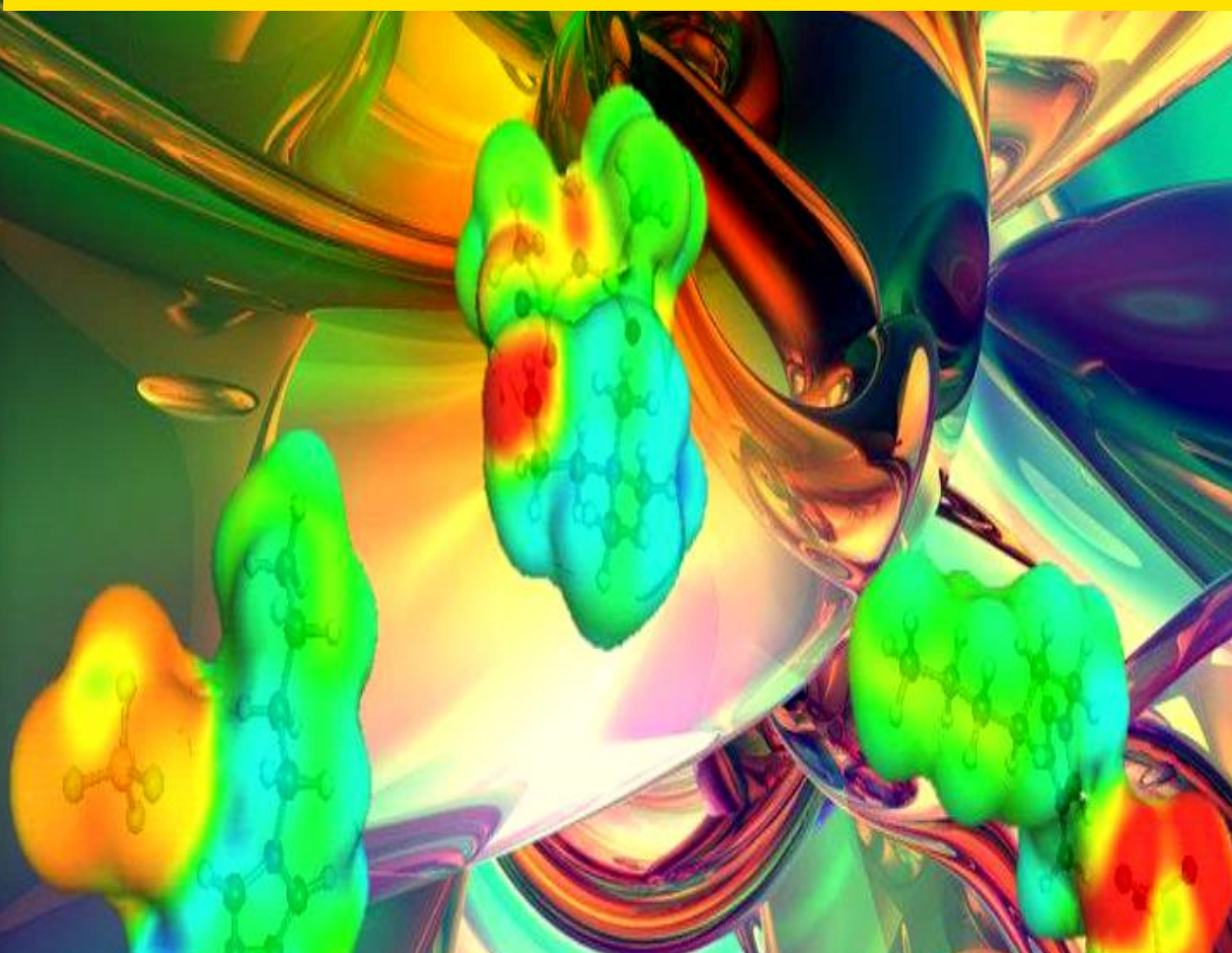


Multiscale Approach for the Conceptual Development of Industrial Processes Based on Ionic Liquids



PhD Thesis
Elia Ruiz Pachón





UNIVERSIDAD AUTÓNOMA DE MADRID

Facultad de Ciencias

Multiscale approach for the conceptual development of industrial processes based on ionic liquids

Elia Ruiz Pachón

Dirigido por:

Dr. Víctor Ferro Fernández

Dr. José Palomar Herrero

Tesis Doctoral presentada para optar al grado de Doctor con mención de “Doctorado Internacional” por la Universidad Autónoma de Madrid

Madrid, 2013

Los profesores de la Sección Departamental de Ingeniería Química (Departamento de Química Física Aplicada) de la Universidad Autónoma de Madrid: **Prof. Dr. Víctor Roberto Ferro Fernández** y **Prof. Dr. José Francisco Palomar Herrero**,

CERTIFICAN:

Que la presente memoria '*Multiscale approach for the conceptual development of industrial processes based on ionic liquids*' ha sido realizada bajo nuestra dirección en la Sección Departamental de Ingeniería Química (Departamento de Química Física Aplicada) de la Facultad de Ciencias de la Universidad Autónoma de Madrid por **Dña. Elia Ruiz Pachón** y que constituye su tesis para optar al grado de **Doctor con Mención Internacional**.

Y para que conste, firmamos la presente certificación en Madrid, a 15 de octubre de 2013.

Fdo: Víctor R. Ferro Fernández

Fdo: José F. Palomar Herrero

Agradecimientos

Los méritos y aciertos se deben a mis directores de tesis y los errores son sólo imputables a mi persona. Llegados a este punto, procedo a exponer los resultados de mi trabajo de los últimos años, y como se diría en las universidades medievales... Hora est!

A mis padres

‘La humanidad también necesita soñadores, para quienes el desarrollo desinteresado de una pasión sea tan cautivador que les resulte imposible dedicar su atención a su propio beneficio material. Sin duda, estos soñadores no merecen la riqueza, porque no la desean. Aun así, una sociedad bien organizada debe garantizar a tales trabajadores los medios para llevar a cabo su labor con eficacia, en una vida libre de cuidados materiales y libremente consagrada a la investigación.’

Marie Curie

Resumen

Esta tesis doctoral se orienta al desarrollo de una estrategia de investigación multi-escala que emplea la simulación molecular, la simulación de procesos y la experimentación a escala de laboratorio para el diseño conceptual de aplicaciones industriales basadas en líquidos iónicos. Este procedimiento permite principalmente seleccionar y/o diseñar líquidos iónicos con propiedades optimizadas para una tarea de interés, así como establecer las óptimas condiciones de operación de aquellos procesos en los que encuentran aplicación.

El desarrollo y aplicación de esta metodología se realiza a través de un conjunto de tareas, sistemas y procesos escogidos de forma intencionada para poner de manifiesto sus principales desafíos y ventajas. Para ello, (i) mediante simulación molecular se analizan las propiedades termodinámicas de mezclas acetona - líquido iónico y de mezclas multi-componentes parafinas/olefinas - líquido iónico, (ii) se simula la regeneración del líquido iónico de sus mezclas con otros disolventes, así como un ciclo de refrigeración por absorción empleando amoníaco - líquido iónico utilizando un simulador de procesos comercial y, (iii) por último, se aplica la estrategia multiescala en la selección del líquido iónico óptimo para el proceso de absorción de tolueno.

Este trabajo se ha realizado en la Sección de Ingeniería Química (Departamento de Química-Física Aplicada) de la Universidad Autónoma de Madrid (España). Se ha desarrollado en el marco del proyecto S2009/PPQ-1545(LIQUORGPAS) financiado por la Comunidad de Madrid, y con la tutela de los directores de tesis Prof. Dr. Víctor Ferro Fernández y Prof. Dr. José Palomar Herrero. La formación de la candidata a doctora ha sido completada mediante una estancia de una semana en la empresa COSMOlogic (Leverkusen, Alemania) bajo la supervisión del Dr. Andreas Klamt, un curso de simulación dinámica de procesos con HYSYS y un curso sobre Visual Basic en la Facultad de Químicas (Ciudad Real, España) de la Universidad de Castilla-La Mancha bajo la supervisión del Prof. Dr. José Luis Valverde Palomino, dos cursos de entrenamiento en Aspen Tech sobre el manejo de la herramienta Aspen Simulation Workbook celebrados en Madrid bajo la dirección de Roly Pemberton, y una estancia de cuatro meses en el

departamento de Chemical and Biomolecular Engineering de la University of California, Berkeley (USA) bajo la supervisión del Prof. Dr. John M. Prausnitz.

El proyecto de investigación en el que se incluye esta tesis tiene como objetivo el empleo de líquidos iónicos como alternativa a los disolventes orgánicos en procesos avanzados de separación. La necesidad de implementar tecnologías más limpias en la industria es un hecho destacado en la actualidad. Muchas líneas de investigación surgen con la idea de ofrecer a la industria nuevos procesos o modificaciones de los ya existentes, planteando otras opciones más atractivas por ser menos contaminantes. El uso de los líquidos iónicos constituye una de las posibles alternativas a los compuestos orgánicos convencionales más contaminantes. Los líquidos iónicos poseen propiedades excepcionales, tales como su baja volatilidad, su gran capacidad disolvente y su elevada estabilidad química y térmica. Además, una gran ventaja es que según la combinación catión-anión se pueden lograr numerosos líquidos iónicos con diferentes propiedades. Esto permite diseñar líquidos iónicos con propiedades adecuadas para una tarea específica. Sin embargo, muchos de ellos poseen alguna propiedad poco deseable como su elevada viscosidad (que otorga dificultades en los fenómenos de transporte) y, además, suelen ser caros. Esto dificulta su investigación y, por tanto, retrasa su implementación a escala industrial. Para conseguir un mayor rendimiento en la investigación con líquidos iónicos, se podría limitar la experimentación sólo a los candidatos más apropiados para un proceso de interés. Esto implica tanto conocer las propiedades termodinámicas de los líquidos iónicos y sus mezclas con todos los componentes del proceso, como evaluar a priori propiedades y comportamientos en procesos que aún no se han llevado a la práctica. Debido al elevado número de líquidos iónicos posibles, los estudios de simulación proporcionan información para elegir buenos candidatos según criterios relacionados con los datos de equilibrio entre fases, la entalpía de exceso de una mezcla, la volatilidad relativa, el estudio cinético y termodinámico de un determinado proceso, las condiciones de operación o el rendimiento energético de un proceso, incluyendo la estimación de costes tanto operacionales como de inmovilizado. La aplicación de una estrategia multiescala que implica simulación molecular - experimentación - simulación de procesos, permite analizar con detalle el comportamiento de los líquidos iónicos en un determinado proceso para diseñar/seleccionar los que ofrezcan propiedades optimizadas para su uso en una aplicación industrial de interés.

Esta tesis se desarrolla a través de un conjunto independiente de casos que pretenden ejemplificar la metodología multiescala propuesta. Cada tema individual se explica en un

capítulo por separado y se clasifican en tres bloques, de acuerdo con el carácter multidisciplinar propio de la técnica empleada.

El capítulo I contiene una introducción sobre los líquidos iónicos y las herramientas utilizadas en la elaboración de esta tesis, como son la simulación molecular y la de procesos. También presenta las ventajas de los simuladores de procesos de Aspen Tech para la creación de componentes (los líquidos iónicos no se encuentran en las bases de datos de los simuladores de procesos comerciales) y para la integración de la herramienta de modelización molecular utilizada. Al final del capítulo introductorio, se enumeran los objetivos generales de esta tesis.

El capítulo II explica detalladamente el fundamento de las herramientas de simulación molecular y de procesos. Se explica cómo a través del programa COSMOthermX se pueden calcular propiedades termodinámicas tanto de líquidos iónicos como de su mezclas con otros compuestos orgánicos. También se presentan las ventajas que ofrece la etapa de simulación molecular en la herramienta multiescala. La principal es que permite seleccionar un conjunto de líquidos iónicos con propiedades termodinámicas adecuadas para una tarea de interés. Después se explica la etapa de simulación de procesos, describiéndose la implementación de los líquidos iónicos en el simulador Aspen Plus. Para ello, es necesario aportar información acerca de cada uno de ellos y especificar el modelo termodinámico adecuado para llevar a cabo la simulación del proceso. Finalmente se presentan las ventajas que ofrece esta etapa, siendo la principal la de establecer criterios económicos y operacionales en la selección del líquido iónico óptimo para un proceso de interés.

El primer bloque integra los capítulos III y IV centrados en la aplicación de la herramienta de simulación molecular (COSMO-RS). Al principio de ambos capítulos, se presenta una evaluación de la capacidad predictiva del método. En el Capítulo III se lleva a cabo un análisis de interacciones moleculares. Se utiliza el programa COSMOthermX para calcular las entalpías de exceso de diversas mezclas acetona - líquido iónico. Este estudio permite evaluar la fortaleza y el carácter predominante de las interacciones entre los componentes de dichas mezclas. En el Capítulo IV, se presenta un trabajo de selección de los mejores líquidos iónicos para llevar a cabo la separación de olefinas de parafinas utilizando el método COSMO-RS. En este caso, el criterio de selección se basa en la volatilidad relativa y la selectividad de mezclas parafina/olefina con un líquido iónico, de tal forma que se optimice la separación deseada.

Los capítulos V y VI se incluyen dentro del bloque en el que se utiliza la herramienta

de simulación de procesos. Al principio de ambos capítulos, se presenta una evaluación de la capacidad predictiva del método de integración simulación molecular el simulador de procesos. En el capítulo V se estudia la separación de mezclas líquido iónico - componente orgánico por destilación como vía para recuperar el disolvente (líquido iónico). Para seleccionar el líquido iónico óptimo en este proceso se establecen criterios basados en la estimación de costes. En el capítulo VI se lleva a cabo la simulación de ciclos de refrigeración por absorción, utilizando el amoníaco como refrigerante y líquidos iónicos como absorbentes. Mediante la simulación del proceso, se realiza una evaluación termodinámica del ciclo y se establecen criterios de selección de líquido iónico basados en el rendimiento.

El tercer bloque comprende el Capítulo VII, donde se presenta la herramienta multi-escala completamente desarrollada para resolver un problema específico. Primero se utiliza la simulación molecular para elegir un conjunto de líquidos iónicos comerciales adecuados para absorber un compuesto orgánico volátil contaminante, como es el tolueno. En este caso, el criterio de selección se basa en la constante de Henry y la entalpía de exceso de una mezcla tolueno - líquido iónico. En segundo lugar, se evalúa experimentalmente la termodinámica y la cinética del proceso de absorción de tolueno con los líquidos iónicos seleccionados. Estos ensayos se realizaron en los laboratorios de la Sección de Ingeniería Química de la Universidad Autónoma de Madrid. Por último, se utiliza el simulador de procesos para evaluar la eficacia de la separación utilizando líquidos iónicos como absorbentes en columnas de relleno y de platos, comparando los resultados con aquellos utilizando disolventes orgánicos convencionales.

Finalmente, en el Capítulo VIII se presentan las conclusiones globales de esta tesis doctoral y, además, se proponen perspectivas para continuar en esta línea de investigación en el futuro.

Abstract

This PhD thesis is focused on the development of a multiscale approach using molecular simulation, experimental measurements and process simulation for the conceptual design of industrial processes based on ionic liquids (ILs). This procedure allows selecting ionic liquids with optimized properties for a specific task, as well as establishing the operating conditions of the IL-based processes.

The development and application of this methodology is carried out through a set of particular tasks, systems and processes. To do that, (i) thermodynamic properties are analyzed using molecular simulation for the acetone-IL binary mixtures and for the paraffin/olefin multicomponent mixtures, (ii) the IL regeneration from their mixtures with organic solvents coming from a separation process, and the absorption refrigeration cycle using ammonia-IL as working pair are simulated using process simulation, finally (iii) the multiscale approach is applied in the selection of the optimal ionic liquid for toluene absorption.

This thesis has been carried out in Sección de Ingeniería Química (Departamento de Química-Física Aplicada) of Universidad Autónoma of Madrid (Spain). It has been developed in the framework of the project S2009/PPQ-1545(LIQUORGPA) funded by Comunidad de Madrid, and supervised by Prof. Dr. Víctor Ferro Fernández and Prof. Dr. José Palomar Herrero. The formation of the PhD candidate has been completed through several visits and courses. Elia stayed one week in the COSMOlogic Company (Leverkusen, Germany) under supervision of Prof. Dr. Andreas Klamt. She took lessons of dynamic process simulation using HYSYS in Facultad de Químicas (Ciudad Real, Spain) of Universidad de Castilla-La Mancha under supervision of Prof. Dr. José Luis Valverde Palomino, two training courses of Aspen Tech on the handling of Aspen Simulation Workbook held in Madrid taught by Roly Pemberton. The PhD candidate was visiting researcher for four months in the Chemical and Biomolecular Engineering department of University of California, Berkeley (USA) supervised by Prof. Dr. John M. Prausnitz.

The aim of the research project including this PhD thesis is the use of ionic liquids as an alternative to the organic solvents in advanced separation processes. The need to implement cleaner technologies in the industry is a striking fact today. Many research lines arise with the idea of providing the industry with new processes or changes to the existing ones, proposing more attractive and less polluting alternatives. The use of ILs represents one of the possible alternatives to the most polluting conventional organic compounds. Ionic liquids possess exceptional properties such as their low volatility, potential solvent capacity and high thermal and chemical stability.

These features have led to the great attention that the ILs research is receiving in the last few years. However, a few ionic liquids have some undesirable property such as high viscosity (hindering transport phenomena) and they may also be expensive. These facts make the research with ILs difficult and, consequently, their implementation in industry is delayed. A way to optimize the ILs research is to experiment only with the most suitable ones for a process of interest. This implies both to know the thermodynamic properties of ILs and their mixtures, as well as to evaluate *a priori* the behavior in processes that have not yet been put into practice. Due to the large amount of possible ILs, simulation studies allow to choose good candidates according to established criteria related to phase equilibrium data, excess properties of mixture, relative volatility, kinetics and thermodynamics of a specific process, and economics or energy performance taking into account operating and fixed costs. This multiscale strategy involving molecular simulation - experiment - process simulation enables to analyze the ILs behavior in a specific process in order to design/select those providing optimized properties for their use in an industrial application of interest.

This PhD thesis is developed through a set of independent cases that exemplify the multiscale methodology proposed. Each individual topic is explained in a separate chapter. The chapters are classified into three parts, according to the multidisciplinary nature of the technique.

Chapter I introduces the ionic liquids and the tools used in the development of the PhD thesis, such as the molecular and process simulation. It also presents the advantages of using AspenTech process simulators for the creation of components (since the ionic liquids are not available in commercial process simulators databases) and for the integration of the molecular simulation results in process simulation. The scope of this PhD thesis is presented at the end of the chapter where the overall objectives are listed.

Chapter II details the fundamental of the molecular and process simulation tools. The

use of COSMOthermX for calculating thermodynamic properties of pure ILs and their mixtures with other components is explained. The advantages of using molecular simulation in the multiscale strategy are presented. The main advantage is that of selecting a set of promising ionic liquids for a task of interest. Then, process simulation stage is explained. The implementation of ILs in Aspen Plus process simulator is described. Some information is required to create the ILs in the simulator as well as to fully specify the thermodynamic property package. Finally, the process simulation advantages are presented. The goal of using process simulation is to establish economic and operating criteria for selecting an optimal IL for a process of interest.

Part I integrate chapters III and IV focused on the application of molecular simulation. Firstly, the predictive capacity of the COSMO-RS method is presented. In chapter III, an intermolecular interaction analysis is carried out. The COSMOthermX program is used to calculate the excess enthalpy of many acetone-IL binary mixtures. This study allows for the strength evaluation and characterization of the main interactions established in such mixtures. In Chapter IV, the selection of most promising ILs to separate different paraffin/olefin systems using COSMO-RS is displayed. Here, the selection criterion is based on the relative volatility and selectivity of paraffin/olefin-IL systems.

Part II includes the chapters V and VI where the process simulation tool is used. Firstly, the predictive capacity is evaluated for the integration of molecular simulation results in process simulation. In Chapter V, the IL-organic mixtures are separated using flash distillation in the simulator as a way to simulate the IL solvent regeneration. In order to select the optimal IL for this process, techno-economic criteria are established. In chapter VI the absorption refrigeration chiller using ammonia as refrigerant and IL as absorbent is simulated. IL selection criteria based on the cycle's performance are established using process simulation.

Part III comprises Chapter VII, where the multiscale approach is applied for a case study. In a first step, a set of suitable ionic liquid for toluene absorption is selected using molecular simulation. Here, the selection criterion is based on toluene Henry's constant and the excess enthalpy of IL-toluene mixtures. In a second step, thermodynamics and kinetics of the toluene absorption process is evaluated through experimental measurements. These assays were performed in the laboratories of Sección de Ingeniería Química of Universidad Autónoma of Madrid. Last, process simulation is used to evaluate the efficiency of the separation using ILs as toluene absorbents in tray and packed columns. The results are compared with those obtained conventional organic solvents.

Finally, the overall conclusions of this PhD thesis are set forth in Chapter VIII. In addition, general prospects for the future are announced in the last paragraphs.

Contents

1	Introduction	1
1.1	Ionic Liquids	2
1.1.1	Physical and chemical properties of ionic liquids	3
1.1.2	Applications of ionic liquids	4
1.2	Molecular and process simulations	6
1.2.1	Introduction	6
1.2.2	Molecular simulation involving ionic liquids	7
1.2.3	Process Simulation involving ionic liquids	8
1.3	Thesis scope and outline	10
2	Multiscale approach development	11
2.1	Molecular Simulation	13
2.1.1	Introduction to the “Conductor-like Screening Model for Real Solvents” COSMO-RS	13
2.1.1.1	Fundamentals	14
2.1.1.2	The COSMO view of molecular interactions	16
2.1.1.3	Calculation methodology	18
2.1.1.4	Further developments of the COSMO-RS method	20
2.1.2	Application of the COSMO-RS method to ionic liquids	21
2.1.2.1	Calcualtion methodology: molecular model, geometry optimization and computational level	22
2.1.2.2	Prediction of thermodynamic properties using COSMO-thermX	24

2.2	Process Simulation	28
2.2.1	The aspenONE Engineering	28
2.2.2	Strategies for integrating COSMO-based results in Aspen Tech process simulators	30
2.2.3	Integration of the COSMO-based results in Aspen Tech process simulators	32
2.2.4	Implementation of Ionic Liquids in the Aspen Plus property packages	33
2.3	Statistical procedure for the evaluation of the predictive tools	35
2.4	Evaluation of the transferability of COSMO-RS results to process simulation	36
2.5	Concluding remarks	43
I	MOLECULAR SIMULATION	45
3	Interactions of ionic liquids and acetone: thermodynamic properties, quantum-chemical calculations, and NMR analysis	47
3.1	Introduction	48
3.2	Computational details	51
3.2.1	COSMO-RS calculations	51
3.2.2	Quantum-chemical description of the acetone-IL interactions	51
3.3	NMR spectroscopic analysis procedure	51
3.4	Results	52
3.4.1	h^E calculation in (organic + IL) mixtures	52
3.4.1.1	Contributions to h^E	58
3.4.2	COSMO-RS description of acetone and ILs	59
3.4.3	Thermodynamic analysis of the Gas-Liquid and Vapor-Liquid equilibria in terms of the IL-acetone interactions	62
3.4.4	Molecular overview of the acetone-IL interactions	63
3.5	Concluding remarks	69
4	Separation of small paraffin-olefin mixtures with an ionic liquid. Thermodynamic study using COSMO-RS	71

4.1	Introduction	72
4.2	Thermodynamic analysis	72
4.3	Computational method	74
4.4	Results	76
4.4.1	Henry's law constants calculation	76
4.4.2	Differences between [CA] and [C+A] models in Henry's constants calculation	79
4.4.3	Data for the ethane/Ethylene-IL systems	79
4.4.4	Data for the propane/propylene-IL systems	82
4.4.5	Data for the systems: butane/butene, pentane/pentene or hexane/hexene with an ionic liquid	84
4.5	Concluding remarks	86

II PROCESS SIMULATION 87

5	Ionic liquids design/selection for separation processes based on opera- tional and economic criteria through the example of their regeneration	89
5.1	Introduction	90
5.2	Computational details	94
5.3	Results	95
5.3.1	Prediction of VLE in the (organic solvent-IL) mixtures using COSMO- RS	95
5.3.2	Prediction of VLE in the (organic solvent-IL) mixtures using Aspen HYSYS	98
5.3.3	Prediction of ILs heat capacities using Aspen HYSYS	98
5.3.4	Operating conditions and energy consumption of the IL recovery . .	100
5.3.4.1	Operating conditions for the VL separator	103
5.3.4.2	Energy consumptions of the IL recovery process	105
5.3.5	A case of study: the separation of aromatic/aliphatic hydrocarbons using ILs	107
5.4	Concluding remarks	110

6	Evaluation of ionic liquids as absorbents for ammonia absorption refrigeration cycles using COSMO-based process simulations	111
6.1	Introduction	112
6.2	Computational details	116
6.2.1	Quantum chemical calculations	116
6.2.2	Property package creation	116
6.2.3	Process simulations	117
6.2.4	Evaluation of the cycle's performances	119
6.3	Results	120
6.3.1	Prediction of pure component and (NH ₃ + IL) binary mixture properties	120
6.3.1.1	Prediction of ammonia properties	120
6.3.1.2	Prediction of IL properties	120
6.3.1.3	Density and viscosity of the (NH ₃ + IL) binary mixtures	122
6.3.1.4	Vapor-liquid behavior of (NH ₃ + IL) binary mixtures	124
6.3.2	Cycle performance	127
6.3.2.1	Overall cycle's results	127
6.3.2.2	Optimizing cycle's behavior	129
6.4	Concluding remarks	133
 III MULTISCALE APPROACH: A case study		 135
7	Optimized ionic liquids for toluene absorption	137
7.1	Introduction	138
7.2	Procedure	141
7.2.1	Molecular simulation: computational details of COSMO-RS calculations	141
7.2.2	Experimental section	141
7.2.2.1	Materials	141

CONTENTS

7.2.2.2	Absorption/desorption experiment	142
7.2.3	Process simulation details	143
7.3	Results	147
7.3.1	COSMO-RS screening to select ILs for toluene absorption	147
7.3.2	Toluene absorption experiments	152
7.3.3	Process simulation	160
7.4	Concluding remarks	164
8	Conclusions and prospects for the future	165
8	Conclusiones globales y perspectivas para el futuro	167
A	Acronyms for ionic liquids	171
	List of Figures	175
	List of Tables	183
	List of References	187
	CD-ROM: PhD Thesis and Publications	225

CONTENTS

Chapter 1

Introduction

The use of clean technologies has become a major concern throughout both industry and academia. The search for alternatives to the most pollutant solvents has become a high priority. Solvents are high on the list of damaging chemicals for two reasons: they are used in huge amounts and they are usually volatile liquids that are difficult to contain. Volatile organic solvents are useful because they can dissolve oils, fats, resins, rubber, and plastics, and they represent the normal media for the industrial synthesis of organic chemicals (petrochemical, chemical and pharmaceutical). However, the environmental impact of these solvents is significant. The Montreal Protocol ([Tripp, 1987](#)) has resulted in a compelling need to re-evaluate many chemical processes that have proved satisfactory for much of this century. There are four strategies to avoid using conventional organic solvents: the solvent-free synthesis, or the use of water, supercritical fluids, or ionic liquids as solvents.

The easiest way to avoid problems with solvents is not to use them, an approach that has been widely exploited in the paints and coatings industries. [Cave et al. \(2001\)](#) described organic reactions that can be carried out merely by grinding the reagents together with a catalyst, a process that is both cleaner and quicker than the conventional reactions. Most reactions do, however, require a solvent, and a green chemical process must necessarily involve an environmentally acceptable solvent ([DeSimone, 2002](#)). The use of water can be advantageous but many organic compounds are difficult to dissolve in water, and disposing of contaminated aqueous streams is expensive. Much current research

focuses on supercritical fluids and ionic liquids as alternative solvents. Supercritical fluids are gases that are nearly as dense as liquids ([Jessop and Leitner, 2008](#)). Because they have both gas- and liquid-like properties, they are highly versatile solvents for chemical synthesis ([Poliakoff et al., 2002](#)). Ionic liquids and supercritical fluids provide a range of options to industrialists looking to minimize the environmental impact of their processes. This thesis is focused in investigating the ionic liquids option.

1.1 Ionic Liquids

Ionic liquids are low-melting-point salts that are composed entirely of ions ([Seddon, 1995](#)). Most of the ionic liquids appearing in literature are liquid at room temperature. The liquid state is thermodynamically favorable in these electrolytes due to the large size and conformational flexibility of the ions which leads to small lattice enthalpies and large entropy changes that favor the liquid state ([Krossing et al., 2006](#)). They are typically formed by a large organic cation and an organic or inorganic anion. Because of the huge number of anions and cations, an extensive amount of different ionic liquids with potential properties for specific applications can be achieved.

The field of ionic liquids began in 1914 with an observation by Paul Walden. He reported the physical properties of ethylammonium nitrate (melting point of 12 °C), which was formed by neutralization of ethylamine with concentrated nitric acid ([Walden, 1914](#)). The first industrial process involving ionic liquids was the BASILTM (Biphasic Acid Scavenging utilizing Ionic Liquids) process ([Freemantle, 2003](#); [Seddon, 2003](#); [Rogers and Seddon, 2003](#); [Maase, 2005](#); [Maase and Massonne, 2005](#)). It was introduced to the BASF site in Ludwigshafen, Germany, in 2002. The BASILTM process is used for the production of the generic photoinitiator precursor alkoxyphenylphosphines. Although the BASILTM process was the first publicly announced room-temperature ionic liquid process, and was launched with a significant amount of publicity, Eastman Chemical Company had been running a process for the isomerization of 3,4-epoxybut-1-ene to 2,5-dihydrofuran since December 1996 ([Falling et al., 2005](#); [Holbrey et al., 2006](#)). This was operated by the Texas Eastman Division, in Longview until the end of 2004. Whereas Eastman Chemical Company and BASF commercialized the first ionic liquid process, IFP was the first to operate an ionic liquid pilot plant ([IFP, 2004](#)).

The reality is that ionic liquids have received much attention in the last few years. At present there is a high interest in investigation of new ionic liquids and their industrial

applications. One of the primary driving forces behind research into ionic liquids is the perceived benefit of substituting traditional industrial solvents. However, ionic liquids are not intrinsically “green” - some are extremely toxic - and they are quite expensive. Interestingly they can be designed to be environmentally benign, with large potential benefits for sustainable chemistry ([Freemantle, 1998](#)).

1.1.1 Physical and chemical properties of ionic liquids

Ionic liquids have remarkable properties that confer significant potential for industrial application ([Sheldon, 2001](#); [Gordon, 2001](#)). The main advantages of using a room-temperature ionic liquid (RTIL) in an industrially relevant process are:

- Relatively high thermal stability in a wide range of temperatures. The thermal decomposition of ionic liquids ranges between 300 and 400 °C, however a few of them begin to decompose at c.a. 200 °C ([MacFarlane et al., 2002](#); [Fredlake et al., 2004](#); [Crosthwaite et al., 2005a](#); [Meindersma and De Haan, 2012](#))
- High chemical stability. Most of RTILs are chemically inert and non-flammable.
- Negligible vapor pressure at near ambient conditions. Due to their ionic nature and the fact that their chemical and thermal stability can be designed to be high, ionic liquids possess negligibly small vapor pressures, even at high temperatures. Ionic liquids cannot evaporate from the reaction vessel. Thus they may be used in high-vacuum systems and eliminate many containment problems ([Welton, 1999](#); [Heintz, 2005](#); [Rebelo et al., 2005](#)). Nonetheless, [Earle et al. \(2006\)](#) reports that many ionic liquids which had been believed to be nonvolatile (such as $[C_n\text{mim}][\text{NTf}_2]$) can be distilled without decomposition at high temperatures and low pressures (eg, 300°C and 0.1 mbar). Moreover, many ionic liquids where the cation is protonated can be distilled via neutral intermediates ([Kreher et al., 2004](#); [Yoshizawa et al., 2003](#)). Thus, ionic liquids can be designed to be volatile, if that offers a processing advantage.
- Low melting point. Ionic liquids have melting points below the room temperature, being some of them fluid at temperatures as low as -100°C.
- Good electrochemical properties, such as high stability to oxidation/reductions resisting a broad range of potentials, and highly conducting.
- Ionic liquids can solvate a wide range of species, such as organic and inorganic compounds, or gases (CO_2 , SO_2 , NH_3 , etc.)

1.1. Ionic Liquids

- RTILs are colourless and easily handled. Their density is higher than that of water (ranging between 1.12 g/cm³ and 2.24 g/cm³).
- Ionic liquids are considered “design solvents” (Freemantle, 1998), i.e. depending on the application, the ionic liquid can be designed for performance. Seddon and co-workers (Abdul-Sada et al., 1995), and Wilkes and Zaworotko (1992) proved the concept that the systematic alteration of the cation and the anion, respectively, can be used to “fine-tune” the properties of an ionic liquid. The choice of the anion and cation not only influences the physical properties, but also, if used as solvent, the thermodynamics and the kinetics of a reaction. Thus, by optimizing the solvent, the reaction outcome can be improved and controlled. At a zeroth level approximation, the anion controls the chemistry, and the cation fine-tunes the physical properties such as solubility, density, viscosity, etc. As an example, the nature of the anion may determine if the ionic liquid will be hydrophilic (e.g., Cl⁻) or hydrophobic (e.g., [NTf₂]⁻). Thus tuning the properties of the solvent to suit a particular application is feasible (Holbrey and Seddon, 1999a). At least one million simple ionic liquids and one trillion ternary ILs are potentially possible (Seddon, 1999). The first choice is to control and define the chemistry. Then, a second ionic liquid may be added to fine tune the physical properties of the system (viscosity, density or thermal conductivity). Finally, a third cheaper (but inert) ionic liquid can be added to lower the cost of the system.

Therefore ionic liquids offer a freedom and flexibility for process design previously unknown (Seddon, 1995, 1997; Freemantle, 1998). However, some drawbacks limit the extensive and definitive application of ILs in industrial processes. Probably, their high viscosity (from 10 to more than 10⁵ cP) (Bonhote et al., 1996) is one of the most significant practical disadvantages. Their viscosity exceeds that of conventional solvents. Nonetheless, the viscosity of ILs strongly depends on the temperature, showing a typical exponential decay for temperatures frequently used in common industrial applications.

1.1.2 Applications of ionic liquids

The ionic liquids were first synthesized for electrochemical purposes as battery components (Wilkes, 2002). Because they were found to be useful as reaction media in both chemical and biochemical processes, the study and development of new ionic liquids were consolidated (Parshall, 1972b,a; Rogers et al., 2002). In recent years, ionic liquids have

1. Introduction

been used for a wide variety of applications (Rogers et al., 2002; Atkins et al., 2002), such as the recovery of biofuels (Fadeev and Meagher, 2001) and the deep desulfurization of diesel oil (Bösmann et al., 2001) by extraction of butanol or sulfur-containing compounds, respectively, into the ionic liquid. Ionic liquids also have potential as lubricants (Ye et al., 2001), in solar cells (Papageorgiou et al., 1996; Grätzel, 1995; Kubo et al., 2002), for heat storage (Blake et al., 2002), in nuclear fuel processing (Thied et al., 1999; Jeapes et al., 2000; Bradley et al., 2002), in membrane technology as a highly permeable and selective transport medium (Koch et al., 1996; Doyle et al., 2000; Fuller et al., 1997), as sol-gel templates (Rogers et al., 2002), and in the dissolution of cellulose (Swatloski et al., 2002). Ionic liquids have also shown promise in some startling applications, such as embalming and tissue preservation (Majewski et al., 2003). The [emim][NTf₂] ionic liquids was studied as a propellant for colloid thrusters. These may become important for the positioning of small satellites or space missions, where accurate location of the spacecraft is required (Gamero-Castaño and Hruby, 2001). Ionic liquids can form versatile biphasic systems for separations (Gutowski et al., 2003), be media for a wide range of organic and inorganic reactions (Zhang, 2006), or absorbents of refrigerants in absorption refrigeration cycles (Yokozeki and Shiflett, 2010). The use of ionic liquids as media for CO₂ gas separations appears especially promising, as CO₂ is more highly soluble than the rest of the gases (Anthony et al., 2002; Bates et al., 2002; Bara et al., 2009a). Process temperature and the chemical structures of the cation and the anion have significant impacts on gas solubility and gas pair selectivity (Anthony et al., 2005).

Processes involving ionic liquids have to be designed and evaluated before changing any other plant or implant a new one. Crucial to the implementation of ILs on a larger scale is the knowledge of their physical properties. There is a continuous progress in the experimental determination of thermophysical properties of ILs and their mixtures. This information is compiled in databases such as the IUPAC Ionic Liquid database (ILthermo, 2006; Dong et al., 2007) or the Dortmund Databank (Gmehling, 1985; (DDBSP GmbH, 1989). These databases provide up-to-date information on ILs publications with over 94600 and 112000 total data points at the moment, respectively. Because the experimental way to determine IL thermophysical properties is a large resource and time consuming task, and many ILs are not even synthesized yet, there is a persistent lack of information for tailoring task-specific ILs. The development of efficient predictive methods for thermophysical properties of ILs and their mixtures could be helpful to organize experimentation (Rogers and Voth, 2007). Several methods have been applied to predict IL thermophysical properties or the thermodynamic behavior of different compounds with ILs. They range

from molecular dynamics (MD) using atomistic force fields, over quantitative structure-property relationship (QSPR) models, to classical thermodynamic models, such as NRTL, UNIQUAC or UNIFAC (Kato and Gmehling, 2005b). However most of the parameters of these models must be determined from experimental data, and they are not available for the vast majority of ionic liquids. The quantum chemistry based on the “conductor-like screening model for real solvents” (COSMO-RS) method seems to be an attractive predictive way to the full range of ILs avoiding experimentation (Diedenhofen and Klamt, 2010). Supported by predictive methods, different computational approaches (Jork et al., 2005; Lei et al., 2006; Palomar et al., 2008, 2009b) have been developed to design new ILs with specific properties. It means that counterions (cation and anion) are combined in such a way the properties of the IL correspond the target.

Process simulation could also be helpful to avoid some experimental work for the development of new applications involving ionic liquids. The operating conditions, equipment sizing, operational and fixed costs, performance or even the feasibility of a process can be analyzed by process simulation. However, ionic liquids are not currently available in the database of commercial process simulators. Achieving an insertion of these components in a process simulator without needing experimental data would be a relevant step in the research with ionic liquids.

There is much work to be done to advance in the burgeoning ionic liquids field of great current importance. To convince the community that ionic liquids are powerful candidates for their use in industry we should prove what they might offer. The next decade should see ionic liquids being used in many applications where conventional organic solvents are used today. Furthermore, ionic liquids will enable new applications that are not possible with conventional solvents.

1.2 Molecular and process simulations

1.2.1 Introduction

Nowadays, molecular and process simulators play an important role in chemical engineering for the development of new processes. Molecular simulation encompasses all theoretical methods and computational techniques used to model or mimic the structure of molecules. On the other hand, process simulation describes processes in flow diagrams using different models and methods for the calculation of properties. The goal of both kind of model-

ing is to reproduce the real characteristics of a given pure component, multicomponent mixture or process. In correspondence, the simulation allows finding optimal conditions for a process of interest. The combined use of molecular and process simulation can be helpful to create and evaluate new processes, such as in this particular case, the industrial applications based on ionic liquids.

1.2.2 Molecular simulation involving ionic liquids

Ionic liquids are being investigated in a variety of fields involving chemistry, biochemistry, engineering, pharmacology and many other areas. Depending on the chemical nature of the IL and the other components in the fluid, different intermolecular interactions can be established. The efficiency of several potential IL applications such as absorption, distillation, liquid-liquid extraction and others, depends on these intermolecular interactions (Anthony et al., 2005; Zhao et al., 2005; Seiler et al., 2004). Because of the tunable properties of ILs (e.g. solvent capacity), the optimal anion-cation combination selected among a huge number of ions is determinant in the development of potential IL-based applications. However, the vast amount of possible ionic liquids hinders the availability of experimental thermodynamic data for systematic analysis. In this context, molecular simulation including computational predictive methods, such as the quantum-chemical statistical thermodynamic approach COSMO-RS developed by Klamt (1995), is of great utility.

COSMO-RS (Klamt and Schüürmann, 1993) is a novel and efficient method for the *a priori* prediction of thermophysical data of liquids. It is based on unimolecular quantum chemical calculations combined with a statistical thermodynamics. Besides organic components, the COSMO-RS method has been shown as a valuable method for predicting a variety of thermodynamic properties of mixtures containing ILs. (Diedenhofen and Klamt, 2010; Manan et al., 2009; Ferreira et al., 2011; Lei et al., 2007; Verma and Banerjee, 2010).

Great advance in the understanding of ionic liquids - and the relationship between their structure and their properties - has been achieved thanks to the molecular simulation works (Jork et al., 2005; Lei et al., 2006; Palomar et al., 2008, 2009b). COSMOthermX, the software implementing the COSMO-RS method, has greatly helped in understanding the local structure, the transport and thermodynamic properties of pure ionic liquids or their mixtures with other compounds (e.g. organic solvents, gases, etc.) (Palomar et al., 2007b, 2010, 2011b; Navas et al., 2009). In addition, this software enables the property screening of multiple mixtures at once. This makes molecular simulation a useful and

powerful computational tool to design ILs with specific properties (Palomar et al., 2008, 2009b).

Therefore the COSMO-RS method is considered in this thesis to study both the ionic liquids properties and their behavior in mixtures with other components. In this sense, the molecular simulation is used in the multiscale approach to design/select a set of suitable ionic liquids with optimized properties for a specific task.

1.2.3 Process Simulation involving ionic liquids

Process simulation is likewise a useful tool in the design, development, analysis, and optimization of technical processes. Programs such as Aspen Plus, Aspen HYSYS, ChemCad, Speedup, Promax, and UniSim are broadly used in the chemical engineering field. In process simulation, the knowledge of thermophysical properties (Rhodes, 1996) of pure components and mixtures is required. These inputs enable the calculation of a process in computers once the mathematical models of the process operations are implemented. The success of the process simulation relies heavily on the accessibility and accuracy of physical and kinetic information for the components involved (Black, 1986; Arlt et al., 2004; O’Connell et al., 2009; Hendriks et al., 2010).

Process simulation can be based on simple equations and correlations where parameters are fitted to experimental data or on predictive methods where properties are *a priori* estimated. The disadvantage of correlations comes from the need of getting a large amount of experimental data to obtain reliable parameters. Commercial simulators contain very large databases including this information for every databank component. Nonetheless processes involving non-databank components are being increasingly developed, especially in the fine chemical and pharmaceutical industries or in those opting for the incorporation of new solvents (such as ionic liquids).

Fulfilling the process simulator databases using experimental data is a largely resource and time-consuming task. This is a severe limitation and often hinders progress and the exploration of unconventional strategies using non-databank components (Franke, 2007). Theoretical methods seem to be suitable candidates to provide the information needed in the implementation of non-databank components (Arlt et al., 2004; O’Connell et al., 2009; Franke, 2007). It has been reported the ability of the COSMO-based methods such as COSMO-RS (Klamt, 1995) and COSMO-SAC Lin and Sandler (2002a) to predict thermophysical data for liquids without needing a extremely large number of experimental

data. The integration of COSMO-based methodologies into commercial process simulators for developing the conceptual design of new processes results a goal subject for many researchers and engineers (Aspen Technology, 2004b, 2011b; Eckert et al., 2006; Eckert, 2007; Cadoret et al., 2009; Tian et al., 2010). aspenONE (Aspen Plus, 2010) has enabled the incorporation of the COSMO-based methods to estimate activity coefficients through the so-called COSMOSAC property model (Aspen Technology, 2004a). At present, it is entirely possible to transit from molecular modeling to process simulation following the route:

Quantum chemical calculations \longrightarrow COSMO-based estimates for fluid properties \longrightarrow aspenONE process simulations. To our knowledge, only a few attempts have explored this strategy (Eckert et al., 2006; Eckert, 2007; Cadoret et al., 2009; Tian et al., 2010).

Process simulation studies could be oriented towards the selection of suitable components and conditions in IL-based applications. Since ionic liquids are not available in the databases of commercial process simulators, they have to be created as non-databank components providing some thermodynamic properties as input variables. However, the models and computational routes implemented as default in process simulators to estimate the properties of non-databank components have not been developed for ionic liquids. The COSMO-RS method has been previously presented as *a priori* predictive method for calculating ionic liquid properties. Because the equations of the COSMO-based methodologies are those including in the COSMOSAC property model, aspenONE seem to be a promising option for implementing the ionic liquids in process simulation.

In this thesis, a new multiscale approach is developed using molecular and process simulation tools in combination. Three stages comprise this strategy: molecular simulation, experimental work and process simulation. Every step is required for achieving an overall understanding of the examined process involving ionic liquids. However, a fine tuning process is essential before extending this new technique: assessment of the actual functionality of the tools, implementation of efficient processes and result validations comparing with experiment.

1.3 Thesis scope and outline

The multiscale approach presented in this doctoral thesis is based on the use of two commercial simulation tools: COSMOthermX and aspenONE, as well as on experimental work. However, this thesis is mainly focused on the conceptual development of the strategy, i.e. an interim step between basic and applied research.

This PhD thesis has the following specific targets:

1. Evaluating the capability of the COSMO-RS method for predicting properties of ionic liquids and their binary mixtures with organic compounds.
2. Using molecular simulation to analyze the intermolecular interactions of acetone - ionic liquid binary mixtures. Comparing molecular simulation results with NMR spectroscopic analysis.
3. Applying the COSMO-RS method in the selection of promising ionic liquids for paraffin/olefin separation by absorption.
4. Implementing ionic liquids in Aspen Plus by transferring the information provided by molecular simulation to the process simulator. Validating the transferability of the COSMO-RS results to the Aspen Plus/Aspen HYSYS process simulators.
5. Simulating the regeneration of the ionic liquid from its mixture with an organic solvent in Aspen Plus/Aspen HYSYS. Using process simulation results to select ionic liquids for separation processes taking into account operational and economic criteria related to their regeneration.
6. Simulating the absorption refrigeration cycle using ammonia - ionic liquid as working pair. Using process simulation to select suitable ionic liquids as ammonia absorbents in absorption chillers basing on cycle's performance.
7. Applying the multiscale approach here developed to select ionic liquids with optimized properties for toluene absorption.

Chapter 2

Multiscale approach development

THE multiscale tool proposed in this thesis is designed in order to select optimal ionic liquids (ILs) and operating conditions for a process of interest. It is structured in three stages: (1)- molecular simulation, (2)- experimental work and (3)- process simulation. Every stage allows to accomplish a particular study (Figure 2.1) and is essential to address any of the other two. The sequence can be modified but the stage 1 should remain always as first step. Once the methodology is evaluated and fine tuning, the steps 1 and 3 may be performed before experiment to evaluate the viability of a proposed IL-based process from the point of view of the conceptual design. Molecular simulation enables to analyze and interpret the intermolecular interactions in IL-based systems, as well as to predict their thermodynamic properties of mixture taking into account a wide range of ILs. Thus we can select those cations and anions providing *a priori* an optimal IL solvent for a specific task. The COSMOthermX commercial program is used in this stage to support the thermodynamic and transport properties calculations. Experimental work should be always performed to compare and validate the thermodynamic properties predicted by molecular simulation. In this thesis, thermal gravimetric analyses (TGA) with ionic liquids are performed to provide information about the physical phenomena of gas-liquid absorption. In addition, the presence or strength of interactions occurring between the components of a mixture is studied using NMR spectroscopy. All these studies are conducted only for some systems evaluated in this thesis. Finally, the third step implies the conceptual design of the process of interest involving ILs using a process simulator. This is one of the most significant contributions of this work since ionic liquids are not

available in the database of commercial process simulators. Molecular simulation supplies the required information at the Simulation Basis Environment. This stage allows us to take advantage of all the possibilities offered by a commercial process simulator for the case of a process involving ILs, such as cost evaluation, operational details, performance optimization, debottlenecking, etc. Thus technical and economic criteria can be established to select the optimal IL for the considered application.

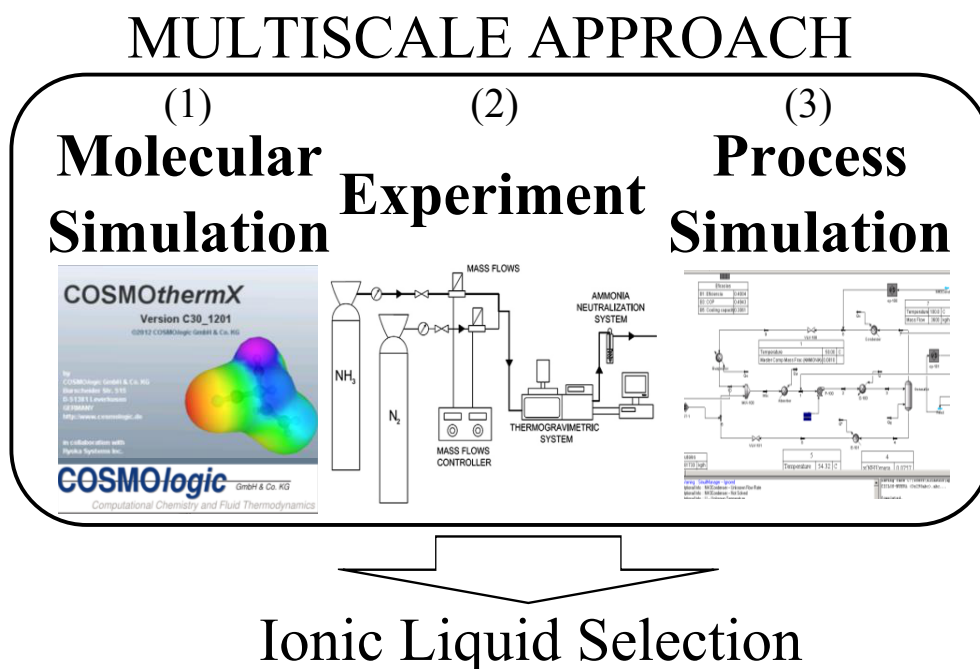


Figure 2.1: The three stages comprising the multiscale approach proposed.

A last step to complete the multiscale strategy should be to carry out experiments of the designed operations at pilot plant scale. We were not able to cover this stage so far, but this work is scheduled to be addressed in a short-term.

In this chapter, we provide a general view of the computational procedure used to carry out both molecular and process simulation stages that are part of the development of the presented multiscale approach.

2.1 Molecular Simulation

2.1.1 Introduction to the “Conductor-like Screening Model for Real Solvents” COSMO-RS

The “COnductor-like Screening MOdel for Real Solvents” COSMO-RS (Klamt, 1995) predicts thermophysical data of liquids without making an extensive use of experiments. COSMO-RS provides information about molecular interactions in solution from quantum chemical calculations on the chemical compounds. The condensed phase is characterized by molecules that are strongly interacting with each other. Intermolecular interactions are responsible of most of the properties (such as thermodynamic, thermophysical, transport, etc.) that determine the physicochemical (macroscopic) behavior of fluids. In the COSMO-RS approach the interaction energy between molecules in liquid phase is expressed by a generic functional of local surface descriptors. The descriptor used is the local polarization charge density σ (also called screening charge density), which would be induced on the molecular surface if the molecule is embedded in an ideal conductor. σ is calculated at reasonable costs by quantum chemical programs using the COnductor-like Screening Model (COSMO) (Klamt and Schüürmann, 1993). The COSMO method describes the screening charge density on the molecular surface through the so called σ -profile. Further, in the COSMO-RS method, the macroscopic properties of the fluid are estimated from COSMO calculations by a statistical thermodynamic procedure that uses the σ -profile of the compound as binding element. In a series of publications (Klamt and Eckert, 2000; Schäfer et al., 2000; Klamt et al., 1998), it was shown that COSMO-RS is a valuable tool for handling of chemical and engineering thermodynamics properties. COSMO-RS is capable of predicting partition coefficients (Mokrushina et al., 2007), vapor pressures (Eckert and Klamt, 2001), boiling points (Hervier and Klamt, 2006), solvation free energies of neutral compounds (Klamt et al., 2009), pKa constants of acids (Klamt et al., 2003). COSMO-RS is also capable to predict mixture thermodynamics (Klamt and Eckert, 2000; Eckert and Klamt, 2001). Infinite dilution activity coefficients (Putnam et al., 2003), vapor-liquid (Eckert and Klamt, 2001), liquid-liquid (Banerjee et al., 2007) and solid-liquid (Klamt et al., 2002) binary phase equilibrium diagrams, excess properties (COSMOlogic GmbH & Co. KG) and Henry’s constants (Schröder et al., 2010) can be predicted for binary systems using the COSMO-RS model. In all these cases the correspondence between experiment and the COSMO-RS predictions is qualitatively very accurate (Eckert and Klamt, 2001; Klamt and Eckert, 2000; Klamt et al., 2010a).

2.1.1.1 Fundamentals

COSMO (Klamt and Schüürmann, 1993) is a quantum chemical continuum solvation model (CSM) for describing liquid phases. This model considers the molecule (the solute) to be located within a molecular shaped “cavity” (Figure 2.2). Out of the cavity, the solvent is represented as a continuum ideal conductor media with an infinite dielectric constant $\epsilon \rightarrow \infty$ (boundary condition in CSMs) (Andzelm et al., 1995). In such an environment, the solute molecule induces a screening charge density σ on the interface between the molecule and the conductor, i.e. on the inner surface of the cavity. These charges act back on the solute and modify the charge distribution on the molecular surface with respect to vacuum (Figure 2.2). In COSMO calculations both molecular and cavity surfaces are discretized in segments to describe the local screening charge distribution. Each segment i of the surface is characterized by its area a_i and the screening charge density σ_i . Thus, each segment of the molecular surface with a specific charge corresponds to a segment in the solvent with opposite charge. The COSMO method calculates the proper charge distribution that minimizes the energy (Klamt and Schüürmann, 1993; Andzelm et al., 1995; Klamt and Eckert, 2000). The calculations end when the optimal energy state of the solute in the solvent is achieved. This is the ideal screening state, where the molecule is ideally screened and a screening charge distribution on the molecular surface is obtained. Then the COSMO-RS methodology develops a statistical-thermodynamic procedure to calculate the chemical potential of the molecule.

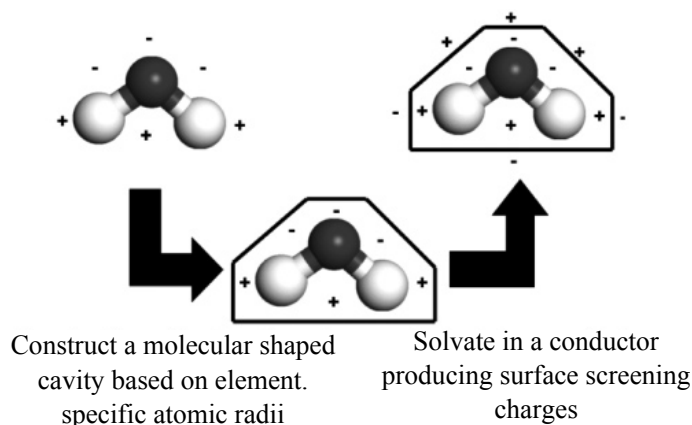


Figure 2.2: Representation in the COSMO method of the cavity embedding the molecule and the solute-solvent interactions in the COSMO method (Mullins et al., 2006).

The total intermolecular interaction energy $E(\sigma, \sigma')$ (see next paragraph) in the liquid

2. Multiscale approach development

system depends on the screening charge density (σ) and it is calculated by COSMO. Once this energy is calculated, a statistical thermodynamic method is used to evaluate the thermodynamics of the fluid. The equation used in this method, which is characteristic of COSMO-RS, is:

$$\mu_S(\sigma) = -R \cdot T \cdot \ln \left\{ \int p_S(\sigma') \cdot \exp \left(\frac{\mu_S(\sigma') - a_{\text{eff}} \cdot E(\sigma, \sigma')}{R \cdot T} \right) - d\sigma' \right\} \quad (2.1)$$

where $\mu_S(\sigma)$ is the chemical potential of the average molecular contact area (a_{eff}) and screening charge density σ in the system S at temperature T. In fact, $\mu_S(\sigma)$ is a measure for the affinity of the system S to a surface of polarity σ . It is a characteristic function of each system and is called “ σ -potential”. Thus the COSMO-RS representations of molecular interactions, the σ -profiles and σ -potentials of compounds and mixtures, contain valuable information qualitatively as well as quantitatively, respectively.

The chemical potential (the partial Gibbs free energy) of molecule X in system S is:

$$\mu_S^{X_i} = \mu_{C,S}^{X_i} + \mu_{R,S}^{X_i} \quad (2.2)$$

where $\mu_{C,S}^{X_i}$ and $\mu_{R,S}^{X_i}$ are the combinatorial and residual contributions to the chemical potential. The residual contribution is related to the energy and it is calculated by integration of $\mu_S(\sigma)$ over the entire surface of compound X_i . The combinatorial term is added to take into account size and shape differences of the molecules in the system. This term depends on the area and volume of all compounds in the mixture and three adjustable parameters.

Finally, once the chemical potential is calculated, a wide variety of thermodynamic properties can now be calculated, e.g. the activity coefficient:

$$\gamma_S^X = \exp \left(\frac{\mu_S^X - \mu_X^X}{R \cdot T} \right) \quad (2.3)$$

where μ_S^X is the chemical potential of compound X in the solvent S, and μ_X^X is the chemical potential of the pure compound X.

In summary, the stages carried out in the calculation of physical and chemical properties of compounds and their mixtures in liquid phase are two (Figure 2.3). First, the COSMO (quantum chemical) calculations are computed to describe the solute-solvent

2.1. Molecular Simulation

interactions. Finally, the σ -profile and the statistical thermodynamic procedure for the molecular interactions (σ -potential) are calculated to estimate fluid properties. This final step provides the COSMO-RS results.

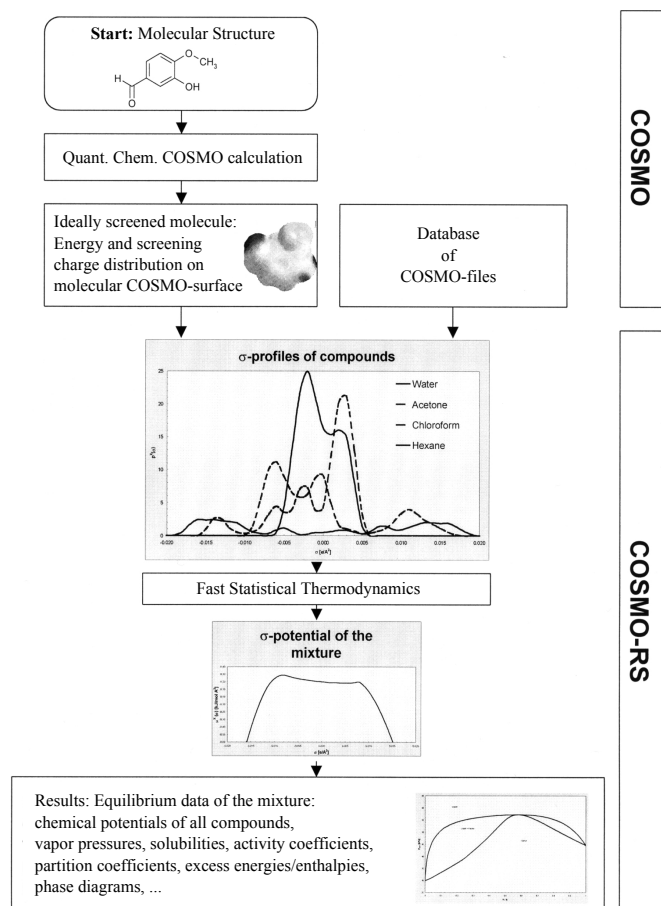


Figure 2.3: Flowchart of a property calculation using COSMO-RS (Eckert and Klamt, 2002).

2.1.1.2 The COSMO view of molecular interactions

The solute-solvent interaction energy is calculated by integrating over the total contact area the energy needed to separate the segments σ and σ' a distance where the electric potential is computationally null ($\sigma' = -\sigma$). The interactions between molecules considered in the COSMO method are (Klamt and Schüürmann, 1993; Klamt, 1995; Andzelm et al., 1995; Klamt et al., 1998; Klamt and Eckert, 2000):

2. Multiscale approach development

- **Dispersive or Van der Waals (vdW) interactions:** They are the most generally occurring class of intermolecular interactions in the condensed phase. Dispersive interactions are short-range forces of molecular surfaces. They are the sum of two parts: (1) an attractive part arising from the intermolecular correlation of the electrons in the vicinity of the adjacent molecular surfaces; (2) a repulsive term arising from the quantum chemical Pauli repulsion, which tends to restrict the interpenetration of the occupied molecular orbitals of different molecules. The vdW energy is dependent only on the element type of the atoms that are involved in surface contact. It is spatially non-specific.
- **Misfit interactions:** they are the electrostatic interactions between the charged particles of the system (nuclei and electrons), between groups with permanent polarity (dipole-dipole), and the induced electrostatic interactions (polarizability). The energy of this interaction is the energy needed to remove the residual screening charge density from the contact. Apparently, in the special situation of $\sigma = -\sigma'$, there is nothing to remove and hence, the interaction energy is zero. However, in the general case, there is some misfit of the partners, i.e. where $\sigma + \sigma'$ does not vanish, the energy of removal is given by E_{misfit} . The gain in electrostatic energy strongly depends on the choice of the right partner of opposite polarity. *Misfit* interaction energies are considered as long range and they are stronger than those of the vdW ones.
- **Hydrogen bonding (HB) interactions:** they are presented in systems containing strongly positively polar hydrogen atoms as donors and negatively polar heteroatomic lone pairs as acceptors. Donors and acceptors may form a very short-ranged and a directed pseudobond, the hydrogen bond. Hydrogen bonding strongly depends on the right choice of the nearest neighbor contact partner and even on its orientation. Thus, it is even more specific than the *Misfit* interaction. Hydrogen bonding comes into play if two sufficiently polar pieces of surface of opposite polarity are in contact. Because positive molecular regions get negative screening charge, the negative σ is now the donor part of the H-bond. The positive σ is the acceptor.

The interactions of molecular surfaces in COSMO-RS are given by the interaction energy functional:

$$E(\sigma, \sigma') = E_{Misfit}(\sigma, \sigma') + E_{HB}(\sigma, \sigma') \quad (2.4)$$

which does only depend on the screening charge densities of the interacting surfaces, plus a vdW contribution which is subsumed in the reference state energy. Thus, the generic interaction functional $E(\sigma, \sigma')$ has three adjustable parameters while the vdW term has two adjustable parameter, one per element in contact. The screening charge densities and parameterization depend on the element-specific radii used in the cavity construction. Thus, there are three general parameters plus two parameters per element. This is almost negligible compared to the several thousands of group interaction parameters needed for the groups in UNIFAC (Fredenslund et al., 1975). The greatest advantage of COSMO-RS is the fact that it is an a priori predictive method without needing an extensive amount of experimental data. It only requires 5 intrinsic parameters regardless of the type of compound, in fact, these parameters have been defined with database of more than 4000 compounds (Klamt et al., 1998). This causes a rather general applicability to almost the entire organic chemistry.

2.1.1.3 Calculation methodology

The COSMO-RS calculations required to address three successive stages:

1. **Optimization of the molecular structure used to describe the compounds.**

Once the molecular structure of a compound is defined, its molecular geometry must be optimized. The geometry of a molecule determines many of its physical and chemical properties. The objective of the geometry optimization is to find an atomic arrangement which makes the molecule most stable at the considered conditions (such as vacuum or solvent presence). The bond angles, bond distances, and dihedral angles are, as a rule, modified in order to get an optimized geometry. The molecular geometry optimization needs long time and hardware resource consumption.

In this thesis, the molecular geometry of compounds are optimized at the B3LYP/6-31++G** computational level in ideal gas phase using the quantum chemical Gaussian03 package (Frisch et al., 2003). In addition, the optimization of the molecular geometry can be subsequently performed to consider solvent effects. They are incorporated through the conductor-like polarizable continuum model (Klamt, 1995; Tomasi et al., 2005) taking a hypothetical solvent having dielectric constant $\epsilon \rightarrow \infty$ and using the Klamt atomic radii (Klamt et al., 1998) for all the atoms. This is the geometry optimization used in the creation of the COSMOlogic TZVP database. The type of geometry optimization directly influences in the accuracy of the prop-

2. Multiscale approach development

erty predictions.

Harmonic vibrational frequency calculations are performed on each optimized structure to establish the nature of the stationary points, i.e. to confirm the presence of an energy minimum state.

2. **The quantum-chemical COSMO calculations.** The ideal screening charge distribution on the surface of a molecule whose geometry has already been optimized is calculated by the COSMO calculations. The quantum-chemical calculations (including the geometry optimization and COSMO calculations) need hardware resource consumption. However, the software implementing COSMO allows recording the σ -profile output in .cosmo files. Thus quantum chemical calculations have to be performed only once for each molecule of interest. The COSMO model is available in several quantum chemistry program packages: Turbomole (Schäfer et al., 2000), DMOL3 (Andzelm et al., 1995; Delley, 2006), Gaussian (Frisch et al., 2003), GAMESS-US (Baldridge and Klamt, 1997), PQS (Pulay et al., 2003), Molpro (Amos et al., 2002), Columbus (Lischka et al., 2003) and ORCA (Neese, 2009).

In this thesis, Gaussian03 or Turbomole suit (v 3.1) quantum chemistry program packages are used to accomplish the quantum-chemical calculations. The ideal screening charges on the molecular surface for each species are calculated by the continuum solvation COSMO model using BVP86/TZVP/DGA1 level of theory. This means that the COSMO calculations are computed with the BVP86 density functional using the TZVP/DGA1 basis sets by the COSMO-RS self-consistent field method (Klamt and Eckert, 2000).

3. **Thermodynamic properties calculations using the COSMO-RS method.** COSMOtherm (Eckert and Klamt, 2010, 2008; Diedenhofen et al., 2012) is a command line program that uses the COSMO-RS method to compute some thermodynamic properties. It allows the calculation of any solvent or solvent mixture and solute or solute system at variable temperature and pressure. COSMOtherm also provides the smoothed σ -profile and σ -potential histograms of pure compounds. COSMOthermX is the graphical user interface to the COSMOtherm code, developed by the COSMO and COSMO-RS authors and commercially distributed by COSMOlogic GmbH & Co. KG. The required inputs in COSMOthermX to provide the COSMO-RS results are the .cosmo files. These files can be selected from the BP-TZVP-COSMO database developed by COSMOlogic, or they can be generated as explained before. There are some other optional input files that may improve the COSMO-RS predictions:

2.1. Molecular Simulation

- .energy files: contain the gas phase energy of the compounds. They are used to estimate the vapor pressures of pure compounds.
- .vap files: read the experimental vapor pressures of molecules using coefficients of empirical equations. They are not available for all compounds in the COSMOlogic database.

The versions C21_0111 and C30_1201 of COSMOthermX were used in this thesis to accomplish the thermodynamic properties calculations and to generate the σ -profile of the studied compounds. If several conformers are possible for a molecule, the conformer treatment implemented in COSMOtherm is used for estimating their thermophysical properties. Because the quality, accuracy, and systematic errors of the electrostatics resulting from the COSMO calculations depend on the quantum chemical method as well as on the basis set, COSMOtherm needs a particular parameterization for each method / basis set combination (COSMOthermX, 2011). According to our selected quantum chemical method, the functional and the basis set level, we use the corresponding parameterization (BP_TZVP_C21_0111 or BP_TZVP_C30_1201) (Klamt et al., 1998) containing intrinsic parameters of COSMOthermX as well as specific parameters.

2.1.1.4 Further developments of the COSMO-RS method

Some alternatives to the COSMO-RS method have been reported by other authors. The major changes published in literature include (i)- the COSMO-SAC method developed by Lin and Sandler (2002a) explained in next paragraphs; (ii)- the COSMO-RS (OI) method developed by Grensemann and Gmehling (2005) to better reproduce the hydrogen bonds interactions (Mu et al., 2007a,b); and (iii) the reparameterization developed by Banerjee et al. (2006) to improve the estimations of the liquid-liquid and vapor-liquid equilibriums. These contributions have been developed using computational codes developed by the authors, instead of using COSMOtherm (Eckert and Klamt, 2008).

The COSMO-SAC method is a modification of COSMO-RS (Lin and Sandler, 2002a; Klamt, 2002; Mullins et al., 2006; Wang et al., 2007c; Sandler et al., 2008; Klamt and Eckert, 2008). As in the COSMO-RS method, Lin and Sandler (2002a) consider the solute to be embedded in a continuum solvent. However, COSMO-SAC is based on the Group Contribution Solvation (GCS) model developed by Lin and Sandler (1999) It also defines the combinatorial term in a different way to COSMO-RS and uses other adjustable parameters (parameterization). In the COSMO-SAC method, the activity coefficient of a surface

2. Multiscale approach development

segment (Segment Activity Coefficient) is calculated for a solute molecule embedded in a continuum solvent. As in the COSMO-RS method, the thermodynamic description of the process only depends on the screening charge density distribution on the molecular surface, but the combinatorial term of the chemical potential in COSMO-SAC is calculated like in other classical activity models such as UNIQUAC or UNIFAC (Abrams and Prausnitz, 1975; Fredenslund et al., 1975). The COSMO-SAC method uses eight adjustable parameters: (i) five elements for the element specific radii, (ii) a threshold screening charge density to difference donor from acceptor groups in the hydrogen bond interactions, (iii) a parameter related to the effective surface of a standard segment; and (iv) a coefficient for segments capable of forming hydrogen bonds. The last two values were obtained in the primary formulation of COSMO-SAC (Lin and Sandler, 2002a). The remain parameters are those proposed by Klamt and Eckert (2000).

There is a controversial relationship between COSMO-SAC and COSMO-RS (Klamt, 2002; Klamt and Eckert, 2008) mainly based on three issues: (i)- the thermodynamic consistence of the chemical potential in a surface segment, (ii)- the distinguishability of the surface segment and, (iii)- the combinatorial term in the chemical potential. Nonetheless, the COSMO-SAC method has received a remarkable relevance: the implementation of the COSMO-based methodologies in the Aspen Technology as property package is generically called COSMOSAC (Aspen Technology, 2004a). Sandler et al. later developed a modification of COSMO-SAC to improve the vapor pressure and enthalpy of vaporization predictions in hydrogen-bonding systems (Lin et al., 2002). Since it modifies the hydrogen bond (HB) term of the original COSMO-SAC equation (Lin and Sandler, 2002a), the description of strongly non-ideal systems seems to be improved. COSMOSAC implemented in the Aspen Technology allows for the use of these three equations: COSMO-SAC (Lin and Sandler, 2002a), COSMO-RS (Klamt, 1995) and the modification of COSMO-SAC (Lin et al., 2002). There are some differences between these equations, but results are generally quite similar.

2.1.2 Application of the COSMO-RS method to ionic liquids

In the introduction of this thesis, COSMO-RS has been presented as a useful and powerful tool to *a priori* estimate the behavior of pure ionic liquids and their mixtures with other compounds (e.g. organic solvents or gases). In addition, COSMOthermX allows for the screening of thermodynamic properties of a big number of IL-based systems at once in a short time. This method can be used to analyze intermolecular interactions of

2.1. Molecular Simulation

mixtures containing ionic liquids and to screen predictions of their thermodynamic properties. Moreover, the need of some thermodynamic and transport properties of pure ILs in the process simulation step is complemented using the COSMOthermX software.

Molecular simulation is a determinant step in the designed multiscale approach. For this reason, we decided to boot this strategy with the full knowledge of the IL-based systems behavior to select suitable ILs for a specific application. A major highlight before using COSMOthermX is to decide the structure to model the IL. After that, the type of geometry optimization and computational level have to be chosen to prepare the COSMOthermX input files.

2.1.2.1 Calculation methodology: molecular model, geometry optimization and computational level

As explained before, we have to define the molecular structure and optimize the geometry of the compounds before performing the COSMO-RS calculations. In the case of ILs, the molecular structure is not trivial as they are composed of ions. Two possible molecular structures to simulate the IL solvents have been considered in our computational approaches:

- The [C+A] model, where the IL is regarded as independent counterions. ILs are treated as equimolar mixtures of cations and anions. The ions can be combined as in a matrix to screen multiple ILs properties calculated by COSMOtherm. The geometry optimization of an ion is faster and easier than that of the ionic liquid as a neutral molecule. Thus the [C+A] model is recommended for screening purposes.
- The [CA] model, where the IL is considered as an ion-paired structure. Here the cation-anion interactions are taken into account. Some studies reported that the [CA] model is slightly more accurate than [C+A] to predict Henry’s constants of solutes absorbed in ionic liquids (Fallanza et al., 2013; Palomar et al., 2011b). This is because in the [CA] structure the ion character of the molecule is reduced respecting to the [C+A] structure, where the ions are presented as charged species in an equimolar mixture. However, the geometry optimization of the [CA] IL structure can be complicated. In fact, sometimes, using the [CA] structural model, the calculation of the geometry optimization considering solvent effects does not even converge to the steady state. This may be due to the consideration of the cation-anion interactions providing multiple possible conformers.

2. Multiscale approach development

The two structural models reflect the main trends of the thermodynamic behavior of ILs and their mixtures. However, depending on the type of desired analysis, the considered system or the property to be calculated using COSMO-RS, one model may offer more advantages than the other.

According to the molecular model of the IL, as well as to the type of optimization selected for its geometry, the COSMO-RS calculations have been performed in this thesis using different IL databases. These IL databases are applied or developed by us, and they contain the ILs inputs simulated by:

1. The **[C+A] gas** model. The molecular structures of the ions are defined following the [C+A] model. The geometries of the ions have been optimized in ideal gas phase.
2. The **[CA] gas** model. The molecular structures of the ILs are defined following the [CA] model. The geometries of the ILs have been optimized in ideal gas phase.
3. The **[C+A] solvent effects** model. The molecular structures of the ions are defined following the [C+A] model. The geometries of the ions have been optimized in condensed phase considering the solvent effects. This is the TZVP-parameterized ILDB-C21-0110 database developed and commercially distributed by COSMOlogic.
4. The **[CA] solvent effects** model. The molecular structures of the ILs are defined following the [CA] model. The geometries of the ILs have been optimized in condensed phase considering the solvent effects.

In the version C30_1201 of COSMOthermX some quantitative structure-property relationships (QSPR) models has been implemented to predict thermo physical properties of ionic liquids. These QSPR models have been designed for the ILDB-C21-0110 database distributed by COSMOlogic, i.e. the [C+A] model solvent effects database. In summary, one of the main advantages of the COSMO-RS method for estimating IL properties is the multiple options offering to improve their predictions: the [CA] and [C+A] structural models to simulate the ILs, and the two ways to optimize their geometry: ideal gas phase and condensed phase considering solvent effects, all of them are valid to define the geometry of the molecules. After that, the standard procedure applied for the COSMO-RS calculations are in the same way that explained before.

2.1.2.2 Prediction of thermodynamic properties using COSMOthermX

Some of the thermodynamic properties calculated in this thesis using the COSMOthermX program are introduced as follows:

1. Pure compounds

(a) Vapor pressure

COSMO-RS allows for the estimation of pure compound vapor pressures at a given temperature. The energy of the gas phase is required for the calculation of vapor pressures. It can be taken from a gas phase quantum chemical calculation (recorded in the .energy file) or estimated by COSMOtherm. Vapor pressures of ILs can be calculated using both the [CA] and [C+A] models. It has been reported that COSMO-RS underestimates the vapor pressures of [c_nmim][NTf₂] ionic liquids by roughly 0.5-4 log units dependent on the IL and approach used ([Diedenhofen et al., 2007](#)).

(b) Boiling point

This option enables the iterative optimization of the temperature at a vapor pressure of 1 atm. The temperature of the system is varied and for each temperature the vapor pressure is calculated. This is repeated until difference between the COSMOtherm prediction of the total vapor pressure and 1 atm is below a certain accuracy threshold. Boiling points of ILs can be calculated using both the [CA] and [C+A] models. To our knowledge, no boiling points predictions for ILs using COSMO-RS have been reported. Nonetheless, [Diedenhofen et al. \(2007\)](#) showed that vapor pressures and enthalpies of vaporization predicted by COSMO-RS reasonably reproduce the experimental data. These considerations lead to the use of COSMO-RS in this thesis to estimate normal boiling points (NBPs) of ionic liquids.

(c) Density

The liquid density of a pure compound *i* (ρ_i) is computed as:

$$\rho_i = \frac{MW_i}{\tilde{V}_i \cdot N_A} \quad (2.5)$$

Where \tilde{V}_i is the corrected molar liquid volume of the compound, MW_i is the molecular weight of the compound and N_A is Avogadro's constant. The cor-

rected molar liquid volume \tilde{V}_i is computed from a QSPR model. The model contains 7 parameters which can be read from the COSMOtherm parameterization file (CTDATA-file). Because density equation does not include a temperature dependency term, these parameters are valid for room temperature data. Densities of ILs can be calculated using both the [CA] and [C+A] models. [Palomar et al. \(2007b\)](#) showed that, regardless of the molecular model, the COSMOtherm IL density predictions satisfactory agree the experiment.

(d) **Heat capacity**

The heat capacity, C_p , of the ionic liquids at a given temperature is computed using the QSPR model developed by [Preiss et al. \(2009\)](#) implemented in COSMOthermX. The model uses two parameters and the molecular volume of ions predicted with COSMO calculations. The parameters are obtained from empirical equations and they depend on the temperature selected for the C_p calculation. The parameters are valid for the ions available in the ILDB-C21-0110 databank ([C+A] solvent effects).

(e) **Viscosity**

The pure ionic liquid viscosity in dependence with a specified temperature is another property that can be calculated from the two QSPR models developed by [Eiden et al. \(2010\)](#) and implemented in COSMOthermX. One of the QSPR models allows for calculating the IL viscosity at 298 K and it contains 4 regression parameters from experimental data. The other QSPR method enables the calculation of the IL viscosity at a specified temperature containing 6 regression parameters. The parameters are valid for the ions available in the ILDB-C21-0110 databank ([C+A] solvent effects).

2. Mixtures

(a) Excess enthalpy

In COSMO-RS, the excess enthalpy of a binary mixture is calculated by the algebraic sum of contributions associated with the three types of interactions, thus

$$h^E = h^E(MF) + h^E(HB) + h^E(vdW) \quad (2.6)$$

where MF, HB and vdW are the *Misfit*, hydrogen bond and van der Waals interactions respectively. The summands of Eq.2.6 result from the contribution of each component of the mixture to the interaction, so that

$$h^E(Interaction) = x_1[h_1^E(Interaction)] + x_2[h_2^E(Interaction)] \quad (2.7)$$

The contributions of each summand in Eq.2.7 to the final values of h^E are obtained from the expression:

$$h_i^E(Interaction) = h_{i,Mixture}(Interaction) - h_{i,Pure}(Interaction) \quad (2.8)$$

where the enthalpy of the compound i at a given mixture composition, $h_{i,Mixture}$, is computed as the expectation value of the partition sum of the microscopic segment-segment interaction enthalpies (Klamt, 2005). The three contributions to the total h^E (h_{HB}^E , h_{MF}^E and h_{vdW}^E) are printed in the COSMOtherm table and output files.

(b) Henry's law constant

The Henry's law constant, H, for compound i is calculated from the activity coefficient and the vapor pressure of the compounds.

$$H_i = \gamma_i^\infty \cdot P_i^\circ \quad (2.9)$$

where P_i° is the vapor pressure for compound i and γ_i^∞ is the activity coefficient at infinite dilution of the compound i in the mixture as predicted by COSMOtherm. The γ_i^∞ is calculated from the chemical potential of compounds as shown in Eq.2.3.

There are several possibilities to calculate or approximate the vapor pressure of solutes. In order to increase the accuracy, one of these options can be selected:

2. Multiscale approach development

- The use of the COSMOtherm approximation for vapor pressure, using the approximated gas phase energy of the compound. This is the default and requires no additional input.
- The use of the COSMOtherm approximation for vapor pressure, using the exact gas phase energy of the compound, given via the .energy input file.
- The use of an empirical equation to compute the vapor pressure at the given temperature. The parameters of the equation are given in the .vap input file.
- Giving the exact value of the vapor pressure for this temperature via the compound property options.

(c) **Total pressure of mixture** The binary option of VLE/LLE panel allows for the automatic computation of phase diagrams of two component mixtures. The program automatically computes a list of concentrations covering the whole range of possible mole fractions of the binary mixture. For a given temperature, COSMOtherm automatically calculates partial pressures for each compound and the total pressure.

The total pressures used in the computation of a phase diagram are obtained from

$$P_{Total} = \sum_i P_i^o x_i \gamma_i^\infty = \sum_i P_i \quad (2.10)$$

P_i^o are the partial pressures of compounds. They are printed in the COSMOtherm table files.

2.2 Process Simulation

2.2.1 The aspenONE Engineering

AspenTech has gathered its efforts on the cross-discipline integration of modeling tools. The integration has caused a huge impact on the selection of the best design options, the overall quality of the designs, and the safe and profitable operation of process plants. AspenTech is a supplier of aspenONE software that optimizes process manufacturing for industries involving chemical processes by increasing capacity, improving margins, reducing costs, and becoming more energy efficient. It offers several products, among which aspenONE Engineering is found. aspenONE Engineering is a suite of products focused on process optimization and complements innovations in process engineering. It implements the integrated conceptual engineering workflow, which involves the conceptual design, basic engineering, detailed engineering and operations/maintenance stages (Figure 2.4).

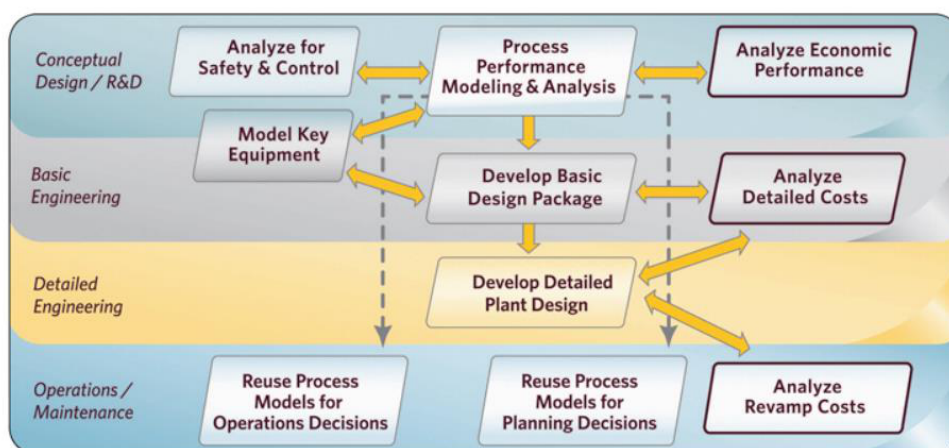


Figure 2.4: aspenONE Engineering enables an integrated engineering solution for process design and development ([Aspen Technology](#)).

The aspenONE Engineering suite of programs integrates (1)- **Aspen Plus** and (2)- **Aspen HYSYS** process simulators. The suit also includes other programs for (3)- equipment design (**Aspen Exchanger Design and Rating**), (4)- cost estimation (**Economic Evaluation**), (5)- process optimization (**Energy Optimization**), (6)- increasing productivity and agility (**Aspen Basic Engineering**), (7)- using Microsoft Excel to generate simulation results (**Aspen Simulation Workbook**), (8)- to continuously evaluate the

2. Multiscale approach development

process simulation by looking at energy economics and plant data (**Activation**), (9)- to learn more about the products (**Aspen Online Training**), (10)- to improve process safety (**Aspen Flare System Analyzer**) and (11)- to compare results to real-time data on the simulation flowsheet (**Enhanced Search**) (Figure 2.5).

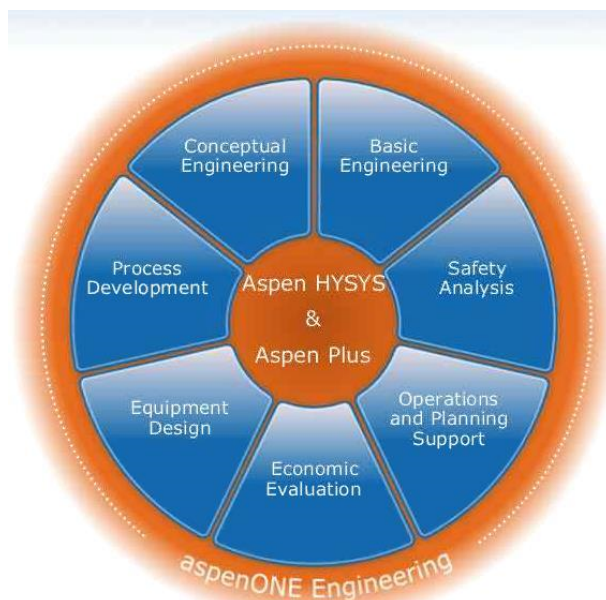


Figure 2.5: aspenONE Engineering ([Aspen Technology](#)).

The core of the integrated workflow is process modeling (Aspen Plus and Aspen HYSYS), which provides the capability to understand and predict process behavior and optimize asset performance. Aspen Plus serves the needs of the chemical industry and provides additional modules for polymer and custom modeling. Aspen HYSYS is aimed at the energy industry and provides value-added modules for Petroleum Refining and Upstream Oil and Gas. Aspen Plus and Aspen HYSYS both have capabilities to integrate economic analysis, equipment modeling, sizing, detailed heat exchanger analysis and economic analysis inside the simulation environment simultaneously. In addition, both simulation products provide direct access to energy analysis so that promising conceptual options for energy saving can be identified during process design. It is possible to screen multiple conceptual design alternatives quickly and reliably, resulting in capital and operating cost savings ([Kapavarapu and Kuwait Oil Company, 2011](#)).

A very useful innovation introduced by AspenTech is the Aspen Properties enterprise database which makes larger the set of thermo-physical properties accessible to modelers.

2.2. Process Simulation

This tool enables to read the experimental data inside the process modeling environment by using the National Institute of Standards and Technology (NIST) database. It also allows integrating a property database made by the user with the databases from Aspen-Tech and NIST. Thus, Aspen Properties, serving both Aspen Plus and Aspen HYSYS simulation software, has expanded its capabilities to cover over 4 million experimental data points, 30,000 binary pairs of compounds and 24,000 pure components. Expanded properties database reduces the time to develop physical properties from weeks to minutes.

Aspen HYSYS allows for importing property packages created in Aspen Plus. In this way, the conceptual design can be performed in either of the two environments. This is very important for the development of the simulations tackled in this thesis. Furthermore, the results from steady-state models can be used in the dynamic modeling environment for safety and controllability analysis.

Besides process simulators, some other products of the aspenONE Engineering suite of programs are finally commented. The Aspen Simulation Workbook (ASW) enables to work in Microsoft Excel to analyze what-if scenarios. ASW easily links process models with Excel to enable operational decision support for the manufacturing staff ([Gislason et al., 2008](#); [Schumann et al., 2009](#)). The introduced Microsoft Excel-based export/import facility in AspenTech creates fillable equipment and bulks lists that can be provided to the fabricator and supplier to fill in and return to the estimator team for automated loading into the estimating system. This tool allows saving time spent in re-typing and checking this information. Aspen Search is an application working as an integral part of Aspen Plus and Aspen HYSYS. It enables to quickly identify an appropriate model available within the organization. This eliminates the need to develop a new model for every project. Users can also link models to plant data and visualize the real-time data, side by side the flowsheet inside the simulation environment. Conceptual designs from Aspen Plus and Aspen HYSYS are brought into the basic engineering environment with Aspen Basic Engineering. The economic analysis developed during the conceptual design can be reused to develop detailed cost estimates during the basic engineering stage with Aspen Economic Evaluator.

2.2.2 Strategies for integrating COSMO-based results in Aspen Tech process simulators

Although COSMO-RS and COSMO-SAC are essentially similar in origin ([Lin and Sandler, 2002a](#); [Klamt, 2002](#); [Lin and Sandler, 2002b](#)) they have had theoretical and com-

2. Multiscale approach development

putational developing trajectories rather different. Therefore, at present there are two well-differentiated procedures to apply their results within process modeling and engineering simulations: using the CAPE-OPEN property package or the COSMOSAC property model.

- **CAPE-OPEN:** The COSMOlogic GmbH & Co. KG has developed the COSMOthermCO (Eckert, 2007), a CAPE-OPEN (Barrett and Yang, 2005; CO-LaN) interface between the COSMOthermX software and the CAPE-OPEN compliant process simulators. The aim is to apply thermodynamical data computed by COSMOthermX within process modeling and engineering simulations (Eckert et al., 2006; Eckert, 2007). Thus, activity coefficients calculated by COSMO-RS can be automatically exported through the COSMOthermCO interface (Eckert and A.) to the property packages created in a CAPE-OPEN compliant process simulator. This property package can be finally imported from Aspen Plus using its Import/Export CAPE-OPEN property package capabilities (Aspen Technology, 2010). In the bridging role described before has been explored (Eckert et al., 2006; Eckert, 2007), the free-on-charge CAPE-OPEN compliant steady-state simulation environment COCO (CAPE-OPEN to CAPE-OPEN). This procedure works well (Eckert et al., 2006; Eckert, 2007) if the considered components in the simulation are included in the COCO database; however, it exhibits some limitations when non-databank components, such as ionic liquids, have to be created.
- **COSMOSAC:** The COSMOSAC property model have been implemented in Aspen Plus since its version 12.0 (Aspen Technology, 2004b). COSMOSAC includes the primary version of the COSMO-SAC method developed by Lin and Sandler (2002a). Nevertheless two other equations are available in COSMOSAC: the COSMO-RS method (Klamt, 1995) or the later modification of COSMO-SAC (Lin et al., 2002). Using an option code the desired equation can be selected. In aspenONE v7.0 and further versions, the VT Sigma Profile Database created by the COSMO-SAC formalism (Mullins et al., 2006, 2008; Virginia Tech, 2006) has been incorporated to the Aspen Plus database of pure compounds (Aspen Technology, 2011b). However, the COSMOSAC property model can be specified by the user giving both the molecular volume and the σ -profile of individual compounds. The COSMO-SAC σ -profile of compounds not included in the VT Sigma Profile Database can be generated by the open Fortran program “Sigma-average.exe” available at the homepage (Virginia Tech, 2006). The computational support of the COSMOSAC method available

for users in the web site ([Virginia Tech, 2006](#)) also includes the “COSMOSAC-VT-2005.exe” code. This program uses the σ -profiles of two components to calculate the liquid-phase activity coefficients in solution. Hence, supplementary computational codes are needed to calculate thermophysical properties of individual compounds or equilibrium data, such as VLE, for mixtures. This is an instrumental limitation when trying to integrate the COSMO-SAC results to process simulators for extensive uses in process engineering, particularly when a set of properties should be collected for creating non-databank compounds.

COSMOthermX has already been presented as a commercial program that calculates, based on the COSMO-RS model, the σ -profiles and the σ -potentials of individual compounds. This program can provide a set of thermophysical, equilibrium, and transport properties of pure compounds and mixtures. Taking into account both circumstances discussed above, a hybrid approach is applied in this thesis: the results of COSMO-RS calculations are used to create non-databank components and to specify the COSMOSAC property package in Aspen Plus.

2.2.3 Integration of the COSMO-based results in Aspen Tech process simulators

The integration of COSMO-RS methodology into the Aspen Technology’s commercial process simulators for designing a new process is organized in this work as follows:

1. First, the properties of the compound such as normal boiling point, molecular weight, mass density, molecular volume and σ -profile, are computed in COSMOthermX.
2. The calculated properties are required both to create non-databank pseudocomponents in Aspen Plus (normal boiling point, molecular weight and mass density) and to specify COSMOSAC as property model (molecular volume and σ -profile).
3. Then, the COSMO-based property predictions in Aspen Plus/Aspen HYSYS are compared with experiment whenever possible, or with other prediction models based on experimental data (such as activity models or group contribution methods). Unfortunately, experimental data on the thermophysical and equilibrium properties of ionic liquids are not always available.

4. Finally, the aspenONE Engineering suite of programs vs.7.3 is used to simulate a specific process.

The use of COSMO-based outputs directly into process simulations was proved for mixtures of organic compounds and water (Ferro et al., 2012) where non-databank components were created in Aspen Plus. However, it should be demonstrated for systems containing ILs. In this thesis, we focus on the integration of the COSMO-RS results into the Aspen Technology’s commercial process simulators for designing new processes involving ILs.

2.2.4 Implementation of Ionic Liquids in the Aspen Plus property packages

The procedure developed in this thesis to implement the ionic liquids in process simulation using the aspenONE suit of packages, involves the following stages:

1. The non-databank ionic liquids are defined in Aspen Plus as pseudocomponents. As explained above, this type of components are specified with the normal boiling point, molecular weight and mass density calculated in COSMOthermX.
2. The COSMOSAC model is selected as property method. The parameters required for the fully specification of COSMOSAC are the molecular volume and the σ -profile of the pure compounds.
3. The components available in the Aspen Plus database are selected as conventional components. There are some components available in the Aspen Plus database but not available in the VT Sigma Profile Database (such as nitrogen). These components are selected as conventional components from the Aspen Plus database adding their σ -profiles and molecular volumes calculated by COSMO-RS. The COSMOSAC property model is simultaneously used in process simulations to calculate the activity coefficients in the liquid phase and to model the vapor phase.
4. Additionally, the coefficients of the Andrade equation for the viscosity-to-temperature dependency are usually specified depending of the simulation proposed. The Andrade equation for liquid viscosity is:

$$\ln \eta_i^{*,l} = A_i + \frac{B_i}{T} + C_i \ln T \quad \text{for } T_l \leq T \leq T_h \quad (2.11)$$

2.2. Process Simulation

The temperature limits (T_l , T_h) are always interpreted in user input units (0, 500 by default). The Andrade coefficients can be regressed from experimental data or from those calculated by the QSPR model implemented in COSMOthermX.

5. For improving the VLE description, we have found that the solute should be specified as Henry component. For this purpose, the coefficients A, B and C are specified in Aspen Plus following the equation:

$$H = \exp \left(A + \frac{B}{T} + C \cdot \ln T \right) \quad (2.12)$$

where H is the Henry's constant and T is the absolute temperature. These coefficients are regressed from experimental VLE (or H vs. T) data.

Once the basic specifications are fulfilled the remainder properties of pseudocomponents are predicted by the corresponding methods, models, and calculation routes implemented as default in Aspen Plus (v7.3).

2.3 Statistical procedure for the evaluation of the predictive tools

The thermodynamic properties calculated in this thesis are compared with experimental data to evaluate the predictive capacity of the used method. The Absolute Average Deviation (AAD), the Relative Absolute Average Deviation (RAAD), the Root Mean Square Deviation (RMSD), or the Mean Relative Deviation (MRD) are employed for quantifying the goodness of the predictions with respect to the experimental values. They are computed as:

$$AAD = \frac{1}{n} \cdot \sum_{i=1}^n |x_i^{Calc.} - x_i^{Exp.}| \quad (2.13)$$

$$RAAD(\%) = \frac{100}{n} \cdot \sum_{i=1}^n \frac{|x_i^{Calc.} - x_i^{Exp.}|}{x_i^{Exp.}} \quad (2.14)$$

$$RMSD = \sqrt{\frac{\sum_{i=1}^n (x_i^{Calc.} - x_i^{Exp.})^2}{n - 1}} \quad (2.15)$$

$$MRD(\%) = 100 \cdot \sqrt{\frac{\sum_{i=1}^n \frac{(x_i^{Calc.} - x_i^{Exp.})^2}{x_i^{Exp.}}}{n - 1}} \quad (2.16)$$

where n is the total number of data used, $x_i^{Calc.}$ is the considered variable calculated by the predictive method and $x_i^{Exp.}$ is the corresponding experimental value. In addition, calculated and experimental data are fitted by linear regressions. The square correlation coefficient R^2 and the standard deviation SD are presented to express the goodness of fit.

2.4 Evaluation of the transferability of COSMO-RS results to process simulation

The predictive capacity of the COSMO-RS method has to be evaluated for estimating the ILs properties required as inputs in process simulation. Because of this, the estimates of boiling point, density and viscosity are firstly validated in COSMO-RS. As a rule, the models and methods used by Aspen Plus to calculate the properties of pure compounds and mixtures in the Simulation Environment are different to those used in the Basis Environment. Because of this, the properties of ionic liquids such as density or viscosity are evaluated in Aspen Plus/Aspen HYSYS despite being inputs in the pseudocomponent generation.

1. Boiling point

Normal boiling points of ionic systems are high because strong, long-range Coulomb interactions prevent the particle's separation into the gas phase. However, this is a theoretical assumption because ILs decompose before achieving their boiling point which hinders their study. Due to the thermal decomposition of ILs, their boiling points cannot be directly determined by experiment but several methods have been developed to estimate them. There are methods based on experimental properties physically related to the boiling temperature. [Rebelo et al. \(2005\)](#) use densities and surface tensions through the Eötvös and Guggenheim empirical equations. However, these predictions provide relatively lower boiling points with respect to other methods (see Table 2.1). [Zaitsau et al. \(2006\)](#) uses experimental vapor pressures and the Antoine equation to estimate the equilibrium temperature. The problem is that they calculate boiling points at extremely low pressures, so then they have to extrapolate at 101.3 kPa to get NBPs. This extrapolation between such different values of pressures may lead to important errors. [Jones et al. \(2007\)](#) apply Trouton's rule ([Trouton, 1883, 1884](#)) to calculate NBPs after estimating $\Delta H_{\text{vap}}^{298}$. They use the experimental enthalpies of vaporization ($\Delta H_{\text{vap}}(T,P)$) obtained under ultrahigh vacuum ([Armstrong et al., 2007](#)) to predict $\Delta H_{\text{vap}}^{298}$. Trouton's rule may be a promising option due to the accuracy and quantity of ΔH_{vap} experimental data for ILs ([Armstrong et al., 2007](#); [Deyko et al., 2009](#)). In addition, enthalpy of vaporization can also be estimated by theoretical methods based on molecular dynamic ([Kelkar and Maginn, 2007](#); [Raabe and Köhler, 2008](#); [Deyko et al., 2009](#)) or quantum chemical and statistical thermodynamics ([Ludwig, 2008](#)). However, the Trouton's rule is met in many fluids, but not in many others. Therefore this as-

2. Multiscale approach development

Table 2.1: Boiling point estimates of some ILs using the COSMO-RS calculations and those reported by other authors in literature. The optimization and structural models for the ILs COSMO-RS calculations are [CA] gas and solvent phases.

Ionic Liquid	I	II	III	IV	V	COSMO-RS [CA]gas	COSMO-RS [CA]solvent
[emim][NTf ₂]	725	660	806	907	910	998	859
[bmim][NTf ₂]	646	607	852	933	910	1035	1086
[hxmmim][NTf ₂]	580	559	898	885	930	1070	1289
[omim][NTf ₂]	-	-	954	857	990	1108	1485
[emim][C ₂ H ₅ SO ₄]	-	-	713	-	1070	908	-
[emim][BF ₄]	-	-	439	-	-	914	2032
[bmim][BF ₄]	744	695	495	-	-	938	561
[hxmmim][BF ₄]	-	-	541	-	-	970	688
[omim][BF ₄]	616	594	576	-	1060	1016	-
[emim][PF ₆]	-	-	509	-	-	957	-
[bmim][PF ₆]	712	661	555	-	-	997	637
[hxmmim][PF ₆]	665	630	600	-	-	1025	-
[omim][CF ₃ SO ₃]	-	-	799	-	1000	1080	-
[omim][Cl]	559	581	650	-	-	933	-
[omim][Br]	514	478	-	-	-	945	-

^I [Rebello et al. \(2005\)](#)(Eötvös Eq.)

^{II} [Rebello et al. \(2005\)](#)(Guggenheim Eq.)

^{III} [Valderrama and Robles \(2007a\)](#)

^{IV} [Zaitsau et al. \(2006\)](#)

^V [Jones et al. \(2007\)](#)

sumption cannot be applied for all ionic liquids without further analysis ([Valderrama and Robles, 2007b](#)). Group contribution methods (GCMs) have also been used to estimate boiling points of ionic liquids ([Valderrama and Robles, 2007a](#)). The use of GCMs to calculate IL boiling points has been criticized by [Jones et al. \(2007\)](#). However these methods allow fast and direct predictive calculations being accurate enough for engineering calculations. [Ludwig \(2008\)](#) combined ab initio quantum and thermodynamics-statistics methods to determine thermodynamic properties of ILs using clusters of cations and anions. Nonetheless, these methods are demanding of large computational resources. [Diedenhofen et al. \(2007\)](#) showed that vapor pressures and enthalpies of vaporization predicted by COSMO-RS reproduce the experiment. All these considerations lead to the use of COSMO-RS in this thesis to estimate NBP of ionic liquids.

2.4. Evaluation of the transferability of COSMO-RS results to process simulation

The first question to be solved is related to the structural model to be used for representing the IL in the NBP calculations. The NBP of $[\text{emim}][\text{C}_2\text{H}_5\text{SO}_4]$ was calculated using different molecular structure models where C^+ and A^- were established at different distances (Figure 2.6). Thus, intermediate states for the IL dissociation $[\text{C} \dots \text{A}]$ are considered between the $[\text{CA}]$ and $[\text{C+A}]$ molecular models. The boiling points predicted for $[\text{emim}][\text{C}_2\text{H}_5\text{SO}_4]$ were 916 K using the $[\text{CA}]$ model, 1066 K when $d[\text{C} \dots \text{A}] = 4.5 \text{ \AA}$, and 2267 K using the $[\text{C+A}]$ model.

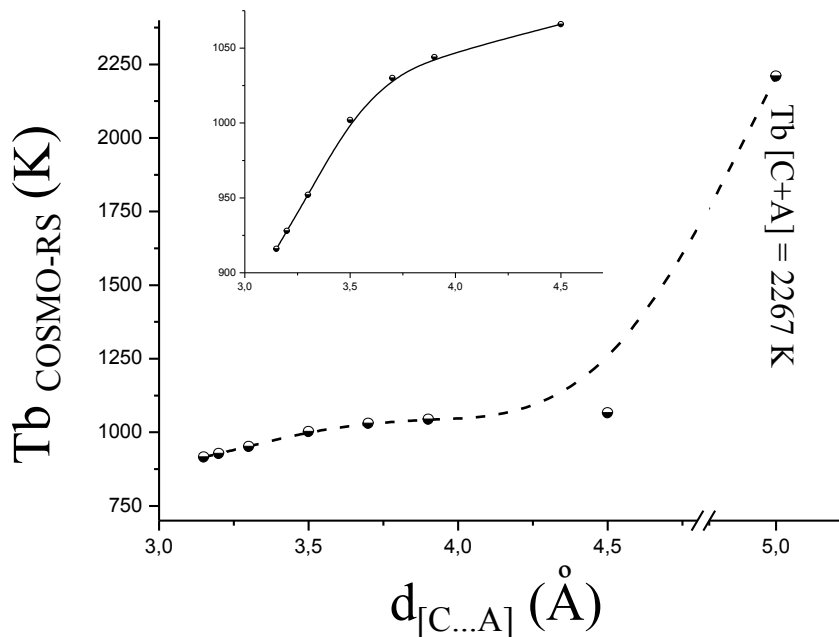


Figure 2.6: Normal boiling points calculated by COSMO-RS for different aggregates $[\text{C} \dots \text{A}]$ in $[\text{emim}][\text{C}_2\text{H}_5\text{SO}_4]$.

The normal boiling points of 52 ILs have been calculated by COSMO-RS in this work. When the $[\text{CA}]$ structural model and their geometries optimized in gas or solvent phases are used to estimate NBPs, our predictions are higher than those obtained by the methods based on Eötvös and Guggenheim empirical equations, about 200 K higher than using GCMs, and similar to those obtained using the Trouton’s rule. The predicted NBPs for this set of ILs are in the range of c.a. 800-1000 K using the $[\text{CA}]$ model. On the other hand, predictions using the $[\text{C+A}]$ COSMO model are always c.a. 2000 K, too far to the boiling temperatures predicted by other authors or the $[\text{CA}]$ model. Due to the large deviation obtained with the $[\text{C+A}]$ model, we use the $[\text{CA}]$ structural model to calculate boiling points of ILs by COSMO-RS. Table 2.1 shows differences between NBP estimates for some ILs using different methods.

2. Multiscale approach development

It can be seen that estimates obtained by GCM and those based on the Trouton’s rule are similar to the COSMO-RS predictions. These three methods show higher NBPs if the alkyl chain of the cation increases. On the other hand, [Rebello et al. \(2005\)](#) and [Zaitsau et al. \(2006\)](#) report lower boiling points of ILs as increasing the alkyl chain of cation. Since GCMs and Trouton’s rule seem to be consistent, the COSMO-RS method can be validated for estimating NBTs. Other important validation (not available on Table 2.1) is the one calculated for the [mmim][SCN] ionic liquid by [Ludwig \(2008\)](#). He obtained that $T_{\text{boil}} = 940$ K, relatively near to the 979 K obtained in this work using the [CA] structural model and considering gas phase optimization. However, it should be pointed out that COSMO-RS calculations are faster and they consume less computational resource than *ab initio* quantum-chemical and thermodynamics-statistics methods. The boiling point predictions obtained in COSMOthermX were compared with those calculated in Aspen HYSYS. Relative differences between the boiling points calculated by both methods were lower than 1% for all the studied ionic liquids.

2. Density

Density is probably the most measured property of ILs. One reason is that its determination is straightforward and can be very accurate if the appropriate equipment, usually a pycnometer or densimeter, is used ([Lazzús, 2010](#); [Wasserscheid and Welton, 2008](#)). Different theoretical methods for IL density predictions have also been successfully applied. [Lazzús \(2009\)](#) developed a model based on a QSPR that involved 11 molecular descriptors for estimating IL densities. The obtained R^2 and RAAD values are 0.93 and 2.0%, respectively. [Valderrama and Zarricueta \(2009\)](#) used a simple and accurate model to predict the density of ionic liquids. They proposed a model based on a generalized correlations to predict ionic liquid densities where RAAD lies in the range (4-9)%. [Ye and Shreeve \(2007\)](#) proposed a method to estimate volumetric properties of ILs based on group contribution methods. They estimated the density of a small range of ILs with accuracy ($\text{AAD}=0.007$ g/cm³), but its application is restricted to 298.15 K and atmospheric pressure. [Gardas and Coutinho \(2008\)](#) proposed an extension of the Ye and Shreeve GCM for the estimates of ILs densities. The presented new version allows not only the estimation of densities over wide ranges of temperature and pressure, but also for a small range of ILs. For the limited set of ILs they obtained RAAD of 1.5%. [Valderrama et al. \(2009\)](#) used a hybrid procedure including GCMs and neuronal networks to predict IL densities. RAAD found between predicted and experimental densities was 0.26%.

2.4. Evaluation of the transferability of COSMO-RS results to process simulation

Raabe and Köhler (2008) obtained very accurate density predictions using methods based on molecular dynamic simulations. Palomar et al. (2007b) estimated density of ionic liquids using COSMO-RS. They obtained $R^2 > 0.99$ for the linear regression between calculated and experiment and a standard deviation lower than 20 kg/m^3 for 40 ILs using the [CA] COSMO model. In this thesis, the set of ILs is extended.

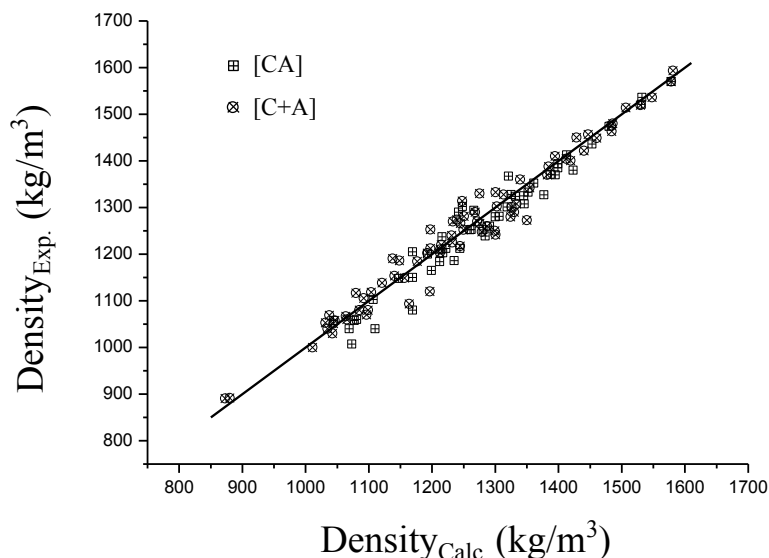


Figure 2.7: Comparison between experiment and Aspen HYSYS predictions for the density of ionic liquids at 298K. Solid line represents perfect agreement. The [CA] and [C+A] models are used to simulate the ILs structures.

We calculate IL densities using the [CA] and [C+A] COSMO models (optimization in solvent phase) for 50 and 75 ILs respectively (Figure 2.7). The calculations are performed in the Aspen HYSYS process simulator. The RAAD are 2.1% using the [CA] COSMO model and 2.5% using [C+A] to simulate the IL. Basing on these results, the viability of using COSMO-RS to predict densities of ILs is remarkable. Moreover, the relative differences between density calculated by COSMOtherm and Aspen HYSYS are lower than 1%, so the transferability of the information generated in the molecular simulation step is well-founded. These calculations validate the integration of the COSMO-RS results in the Aspen Plus/Aspen HYSYS process simulators, i.e. the computational procedure as a whole.

3. Viscosity

The viscosity of ionic liquids is very sensitive to impurities as well as to the kind of measurement. In addition, most of ILs show a great change in their viscosity at

2. Multiscale approach development

room temperature because this temperature is close to their melting point (Eiden et al., 2010). Thus, great care has to be ensured when tempering the sample during the measurement. Eiden et al. (2010) presented a QSPR method to describe the temperature-dependent viscosities of a diverse set of ILs without needing input of experimental data. The model is based on their correlation with the molecular volume and additional physical observables that remove the anion dependence of the original model (Krossing et al., 2006) and include temperature dependence. They

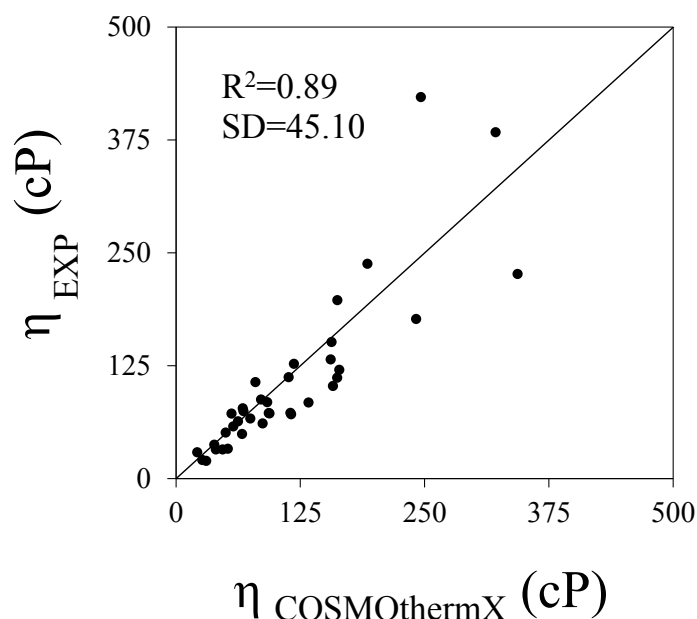


Figure 2.8: Comparison between experiment and the predictions for the viscosity of ionic liquids using COSMOthermX at 298K. Solid line represents perfect agreement. ([C+A] model)

report a R^2 of 0.91 and RMSD of 0.17 for their considered set of ILs (Eiden et al., 2010). This QSPR method is implemented in COSMOthermX. In this work, the viscosities of 37 ILs are calculated at 298 K. The obtained AAD is 28.6 cP, RAAD is 27.0% and RMSD 44.8 cP. As depicted in Figure 2.8, the calculated viscosity values follow the trend of the experimental data for the considered set of ILs, however these results are less accurate than those reported by the authors of the method (Eiden et al., 2010). The best estimates are obtained for those ILs showing the lower viscosity values. We performed an additional validation of the QSPR model by calculating the viscosity temperature-dependent of 3 ILs. These ILs show remarkable different behaviors: (i) [1-ethyl-nicotinic acid ethyl ester][C₂H₅SO₄] shows a large viscosity at 293K but strongly decreases along with increasing temperature, leading

2.4. Evaluation of the transferability of COSMO-RS results to process simulation

to a reasonable viscosity value at a.c. 373 K; (ii) [emim][DCN] is a low viscous IL at low temperatures having a slight decrease of the viscosity with the temperature; (iii) [omim][BF₄] presents an intermediate behavior between two preceding ILs. As can be seen on Figure 2.9, and as expected from previous results, the QSPR model is not accurate for large viscosity values. The QSPR model is suitable to predict viscosities of ILs showing an intermediate temperature-dependent viscosity behavior (such as [omim][BF₄]). The uncertainty of the viscosity predictions obtained by COSMOthermX led us to use viscosity experimental data whenever possible. If they are available, the Andrade's regression parameters from experimental data are specified in Aspen Plus (see Eq. 2.11).

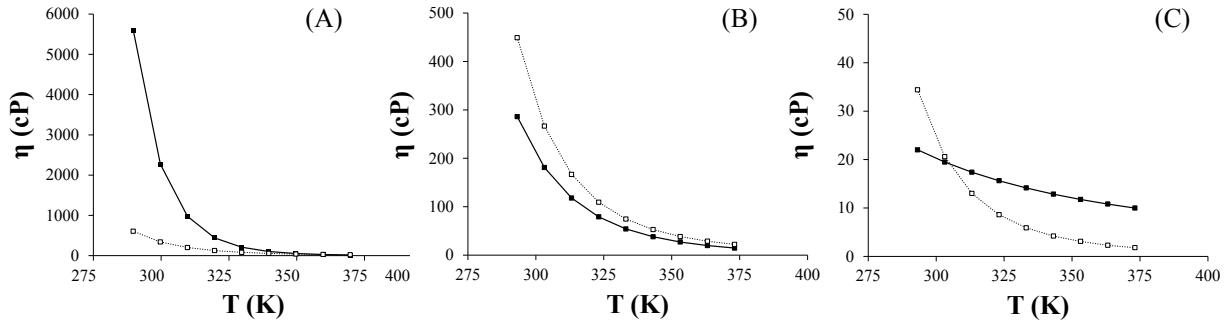


Figure 2.9: Temperature-dependent viscosity behavior of (A) [1-ethyl-nicotinic acid ethyl ester][C₂H₅SO₄], (B) [omim][BF₄], (C) [emim][DCN]. The symbols represent: (black) experimental data, and (white) the obtained calculations using COSMOthermX (QSPR model).

2.5 Concluding remarks

The multiscale approach presented for the conceptual development of a process involving ionic liquids (ILs) implies three stages: molecular simulation, experimental work and process simulation. In this chapter, molecular and process simulation were explained in detail.

The COSMOthermX program based on COSMO-RS calculations is used in the molecular simulation stage to predict thermodynamic properties of pure components (including ILs) and IL-based systems. According to the requirement of the intended application, COSMO-RS allows for multiple options to improve its predictive capacity. The method can be reparameterized, different molecular structures ([CA] and [C+A] models in case of ILs) and optimizations of the geometry (ideal gas phase or condensed phase considering solvent effects) are possible for the COSMO calculations, and some experimental data can be added as inputs.

The COSMO-RS calculations can be transferred to Aspen Tech’s process simulators for both creating non-databank components and specifying the COSMOSAC property model. The non-databank ionic liquids are implemented in the Aspen Plus process simulator. The transferability of the COSMO-RS calculations of ILs properties into Aspen Plus/Aspen HYSYS process simulators was achieved. We are able to operate with COSMO-supported process simulation to design and develop new applications involving ionic liquids (Process Simulation Stage).

Part I

MOLECULAR SIMULATION

Chapter 3

Interactions of ionic liquids and acetone: thermodynamic properties, quantum-chemical calculations, and NMR analysis

THE interactions between ionic liquids (ILs) and acetone have been studied to obtain a further understanding of the behavior of their mixtures, which generally give place to an exothermic process, mutual miscibility, and negative deviation of Raoult's law. COSMO-RS was used to systematically analyze the excess enthalpy of IL-acetone systems, in terms of the intermolecular interactions contributing to the mixture behavior. COSMO-RS results indicated that acetone, as a polar compound with strong hydrogen bond acceptor character, generally establishes favorable hydrogen bonding with ILs. This interaction is strengthened by the presence of an acidic cation and an anion with non-HB acceptor character in the IL. COSMO-RS predictions indicated that gas-liquid and vapor-liquid equilibrium data for IL-acetone systems can be finely tuned by the IL selection. NMR measurements and quantum-chemical calculations by using molecular clusters provided additional evidence of the main role played by hydrogen bonding in the IL-acetone systems.

3.1 Introduction

The efficiency of several potential industrial applications (such as absorption, distillation, liquid-liquid extraction, etc.) depends on the intermolecular interactions between compounds in the liquid mixture (Anthony et al., 2005; Zhao et al., 2005; Seiler et al., 2004). An outstanding variety of organic compounds (aliphatic, aromatic, alkanolic, ketonic, etc.) has been studied in separation process involving ionic liquids (Han and Row, 2010). The *a priori* knowledge of the organic-ILs interactions may help to design more efficient processes.

Depending on the chemical nature of both the ionic liquid and the organic solvent, specific intermolecular interactions such as hydrogen bonding (HB) are established in the mixture fluid with more or less intensity. Other intermolecular interactions such as Van der Waals (vdW) or electrostatic (*Misfit*) interactions are also presented in the mixture. All these interactions affect to the thermodynamic behavior of the system, however HB interactions are more determinants of certain properties. As explained in Chapter II, HB interactions are presented in systems where two sufficiently polar pieces of different polarity interact. ILs have acidic and basic sites on the cation and anion structures. Because of this, HB interactions play an important role in pure ionic liquids and in their mixtures with polar solvents presenting hydrogen bond donor (HBD) or acceptor (HBA) character (Dong et al., 2006; Wang et al., 2010; Maugeri and de María, 2012; Crosthwaite et al., 2005b; Zhang et al., 2010; Gao et al., 2010b; Palomar et al., 2007a; Gao et al., 2010a; Mellein et al., 2007).

The cation-anion interaction can modulate the interaction with another compound (the polar solvent). It has been observed that relevant properties of mixtures including HBD or HBA compounds and ionic liquids, such as phase equilibrium gas-liquid (GLE), vapor-liquid (VLE) or liquid-liquid (LLE), can be drastically affected by the cation-anion selection (Domańska and Marciniak, 2007; Bara et al., 2009b; Anthony et al., 2001; Nebig et al., 2007). In order to study the IL-organic compound interactions (at molecular scale) it is interesting to select an organic with remarkable defined polarity. This means to study the IL contribution in a mixture with an organic with extremely basic, acidic or amphoteric character. In this work we decided to study the IL interactions with an organic compound with distinctly basic character.

Among the growing variety of mixtures studied in the last years formed by ionic liquids and polar organic compounds with outstanding HBA character, those including acetone present attractive applications in new processes. Thus, ionic liquids are being

3. Interactions of ionic liquids and acetone: thermodynamic properties, quantum-chemical calculations, and NMR analysis

investigated for removing acetone from water (Izák et al., 2008), for improving the kinetic and selectivity effects in heterogeneous hydrogenation of acetone (Khodadadi-Moghaddam et al., 2009), for analyzing the presence of acetone by microextraction-gas chromatography (Carda-Broch et al., 2010), and for acting as an entrainer in ternary systems with acetone (Orchillés et al., 2012, 2011; Döker and Gmehling, 2005; Orchillés et al., 2007). Acetone can be used to reduce the viscosity of an ionic liquid, to reduce the ionic liquid consumption in the solvent extraction (Li et al., 2011) or to enhance the kinetic and solvation effects in the synthesis of imidazolium-based ionic liquids (Schleicher and Scurto, 2009). Moreover, acetone has been successfully used as regenerating agent of exhausted adsorbents saturated by ionic liquids (Palomar et al., 2009a; Lemus et al., 2012). As consequence, several properties for the ionic liquid-acetone mixture have been measured, including volumetric and excess properties, LLE and VLE data, etc. (Izák et al., 2008; Pereiro et al., 2006, 2007; González et al., 2012). As remarkably property, acetone behaves as an almost universal solvent for ionic liquids, dissolving as hydrophilic as hydrophobic ionic liquids, only being reported a few cases of immiscibility with acetone (those based on sulfates or phosphate anions) (Kato and Gmehling, 2005a; Iliev et al., 2011).

The excess enthalpy, h^E , is a relevant property in thermodynamic studies of solutions. This is of great utility when analyzing the nature of the molecular interactions in solutions; therefore its knowledge is also interesting for IL-containing systems. The h^E obtained by experimentation is a consequence of the disruption of interactions in the pure compounds and the establishment of new interactions in the mixture. Several research groups have reported experimental excess enthalpies for systems containing ILs and organic solvents, such as water, alcohols, ketones, etc. (Nebig et al., 2007; García-Miaja et al., 2008; He et al., 2010; Ortega et al., 2007, 2008; Navas et al., 2009; Vreekamp et al., 2011; Ren et al., 2011; Ficke and Brennecke, 2010; García-Miaja et al., 2009a; Rai and Kumar, 2011; Porcedda et al., 2011; García-Miaja et al., 2009b).

Ficke and Brennecke (2010) found both exothermic and endothermic behaviors for water-IL systems depending on the IL counterions presented in the aqueous mixture, which were attributed to the capability of the IL to form hydrogen bonds with water. In this sense, Porcedda et al. (2011) found that IL-water interactions became less important as the hydrophobic/hydrophilic ratio increased, along with the length of the alkyl chain in the ILs. Navas et al. (2009) obtained that the hydrophobic [bmim][PF₆] (HBD solvent) mixed endothermically with water and alcohols (polar HBD solvents), whereas a highly exothermicity behavior is observed when ILs are mixed with acetone (HBA solvent), due to favorable hydrogen-bonding interactions. These approaches suggest that h^E is affected

by the nature of both ionic liquid and solvent.

The mixture behavior is determined by the different interactions occurring in solution (Ficke and Brennecke, 2010; García-Miaja et al., 2009a,b). Nevertheless, considering the huge amount of possible organic solvent-IL combinations, the available experimental h^E data are still limited for a systematic analysis. In this context, the COSMO-RS model, capable of predicting thermodynamic data without needing previous experimental data, is very helpful.

COSMO-RS has been shown as a valuable method for predicting a variety of thermodynamic properties of ILs mixtures (Diedenhofen and Klamt, 2010; Manan et al., 2009; Ferreira et al., 2011; Lei et al., 2007; Verma and Banerjee, 2010) providing a useful computational tool for designing ILs with specific properties (Palomar et al., 2008, 2009b). The suitability of COSMO-RS to predict the h^E of binary mixtures formed by the ionic liquids 1-butyl-X-methylpyridinium tetrafluoroborate (X=2, 3 and 4) with alkanols or water has already been reported (Navas et al., 2009; Vreekamp et al., 2011).

An important feature of COSMO-RS is that it provides a description of the different intermolecular interactions (electrostatic forces, hydrogen bonding and van der Waals forces) contributing to the effects on the h^E (Ortega et al., 2007). Furthermore, the gas-liquid (GLE) (Palomar et al., 2011b; González-Miquel et al., 2011; Palomar et al., 2011a; Bedia et al., 2012), liquid-liquid (LLE) (Ortega et al., 2007; Vreekamp et al., 2011), and solid-liquid equilibria (SLE) (Palomar et al., 2009a) have been successfully analyzed using COSMO-RS description of the intermolecular interaction contributions to the excess enthalpies for corresponding IL-based mixtures.

This chapter describes the interactions between ionic liquids and acetone by means of computational and spectroscopic analysis. For this purpose, the COSMO-RS method was applied to screen the h^E predictions of 312 IL-acetone mixtures. The screening includes different IL structures by varying the type of anions (12) and cations (26, including imidazolium, pyridinium, pyrrolidinium, phosphonium, and ammonium). The contributions to h^E from the intermolecular interactions in liquid phase were also estimated. The calculated h^E values were related to other significant thermodynamic properties of mixture, such as GLE and VLE data. Finally, molecular simulations and ^1H -NMR spectroscopic measurements were performed to obtain further insights on the local interactions between IL and acetone in the mixture.

3.2 Computational details

3.2.1 COSMO-RS calculations

The molecular geometry of acetone and IL counterions was optimized at the B3LYP/6-31++G** computational level in the ideal gas phase. The ideal screening charges on the molecular surface for each species was calculated by the COSMO model using BVP86/TZVP/DGA1 level of theory. The molecular model of independent ions is applied in the COSMO-RS calculations ([C+A] model).

3.2.2 Quantum-chemical description of the acetone-IL interactions

The quantum-chemical calculations with molecular models including clusters of acetone with the IL ions allow compute the interaction energies and bond distances between mixed species. These data allow determinate the presence and strength of the hydrogen bonding interactions between species in mixture. Specifically, this technique allows studying in detail the part of the molecules interacting with each other. Two models of cationic structures were considered in cluster optimizations: the single 1- and the di 1,3-substituted imidazolium cations, [eim]⁺ and [mmim]⁺, respectively, along with the [PF6]⁻ anion. These molecular simulations consist of gas phase geometry optimizations at the DFT computational level of different clusters composed of the IL ions and the acetone molecule. The M05-2X density functional and the 6-31++G(d,p) basis sets have been selected to perform these simulations. M05-2X functional is one of the newest DFT methods reproducing weak interactions (Zhao et al., 2006b). Harmonic vibrational frequency calculations are always carried out on the optimized structures to establish the nature of the stationary points.

3.3 NMR spectroscopic analysis procedure

NMR (nuclear magnetic resonance) spectroscopy is an analytical tool that exploits the magnetic properties of certain atomic nuclei. This technique provides detailed information about the structure, dynamics, reaction state, and chemical environment of molecules in a liquid or a solid. Proton NMR (¹H NMR) is the application of NMR spectroscopy respecting to the hydrogen-1 nuclei within the molecules of a substance. NMR spectra are

recorded in solution, and solvent protons must not interfere. For this purpose, deuterated solvents are preferred. ^1H -NMR is one of the most used spectroscopic techniques to investigate 1-alkyl-3-methylimidazolium ionic liquids (Palomar et al., 2007a; Avent et al., 1992; Giernoth et al., 2005). It allows obtaining a better understanding about the nature of cation-anion or solvent-IL interactions appearing in solution. A previous ^1H -NMR study by Zhai et al. (2006) provided experimental evidence of the weakness of the cation-anion interaction as a result of the acetone addition in some 1-alkyl-3-methylimidazolium $[\text{PF}_6]^-$ and $[\text{BF}_4]^-$ ILs. In this work, the ^1H -NMR spectroscopic measurements were performed for selected IL-acetone mixtures at different concentrations. The acetone concentration in the mixture was varied from 0 (neat IL) to 0.95 % mole. These analysis allow experimentally demonstrate the role of hydrogen bonding on the properties of IL-acetone systems. The ^1H -NMR spectra were obtained at room temperature with a Bruker DRX-500 spectrometer (500 MHz), using TMS as calibration standard. Acetone- d_6 , $(\text{CD}_3)_2\text{CO}$, was used as a deuterated solvent for all the measurements. The selected ionic liquids for these analysis were $[\text{eim}][\text{NTf}_2]$ and $[\text{bmim}][\text{NTf}_2]$. They are ionic liquid commercially distributed by Iolitec.

3.4 Results

3.4.1 h^E calculation in (organic + IL) mixtures

The COSMO-RS methodology was applied to predict the h^E of the IL-organic compound mixtures with experimental data reported in the literature. A sample of systems chosen contains 49 mixtures and includes 7 different polar solvents (water, methanol, ethanol, 1-propanol, 1-butanol, acetone and 3-pentanone) and 20 different ILs with a variety of cations and anions. Experimental and COSMO-RS values for the maximum (or minimum) of h^E curves are compared in Figure 3.1. As can be seen on the graph, an appropriate goodness-of-fit is achieved for the wide range of h^E values for IL-organic solvent mixture at different temperatures. The linear fit between experimental and calculated data presents the square correlation coefficient $R^2=0.97$ and standard deviation of 2 kJ/mol. It should be remarked that the reported IL-molecular solvent mixtures present as endothermic and as exothermic behaviors depending on the nature of the solvent and the IL forming the mixture, which would determine the change of intermolecular interactions of the mixture components with respect to the pure compounds. Some authors have explained the significance of the h^E in IL-organic systems in terms of preferential solvation effects between

3. Interactions of ionic liquids and acetone: thermodynamic properties, quantum-chemical calculations, and NMR analysis

the molecules of the mixtures, for the case of polar compounds, such as water, alcohols, or ketones (Mellein et al., 2007).

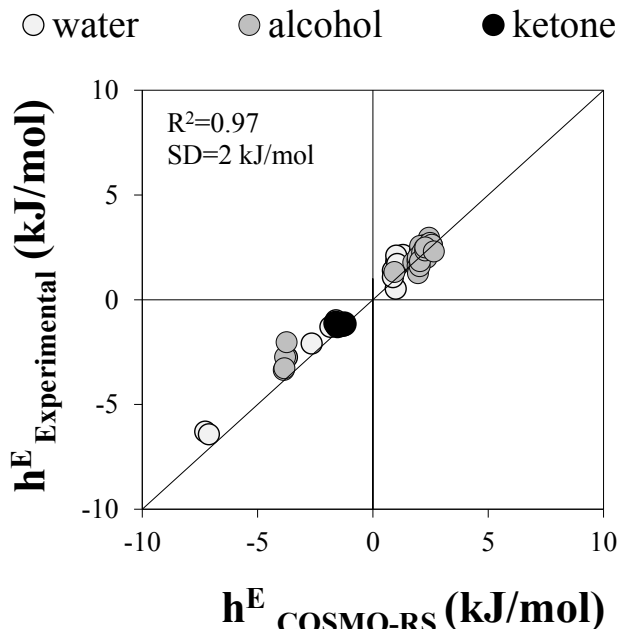


Figure 3.1: Comparison of experimental and COSMO-RS calculated values for the maximum (or minimum) of h^E curves of IL-organic compound mixtures at different temperatures (ranging between 298.15 and 353.15 K). Water (white), alcohols (grey), and ketones (black).

To anticipate the different solvation effects in the mixtures collected in Figure 3.1, we can consider the empirical solvent scales of dipolarity (SdP), polarizability (SP), basicity (SB) and acidity (SA) developed by Catalán (2009) whose normalized values for water, acetone and alcohols are collected in Table 3.1.

Analyzing the water-IL mixtures in Figure 3.1, it was clear that the h^E of the mixture strongly depends on both the cation and the anion selected for the IL. This is the strength of the interactions between water and IL species and the rupture of like forces in pure compounds.

Water is an amphoteric compound, which presents high polarity (SdP=0.681 and SP=0.997), high acidity/HBD character (SA=1.062) and weak basicity/HBA character (SB=0.025) as solvent. As a result, the h^E for the binaries containing water and ILs with common cation (1-ethyl-3-methylimidazolium, [emim]⁺) goes from endothermic for slightly hydrophobic anion, such as [BF₄]⁻ (Rai and Kumar, 2011), to strongly exothermic

3.4. Results

Table 3.1: Empirical Scales of Dipolarity (SdP), Polarizability (SP), Basicity (SB) and Acidity (SA) for Organic Solvents, Developed by [Catalán \(2009\)](#).

Solvent	SdP	SP	SB	SA
water	0.681	0.997	0.025	1.062
methanol	0.608	0.904	0.545	0.605
ethanol	0.633	0.783	0.658	0.4
1-propanol	0.658	0.748	0.782	0.367
1-butanol	0.674	0.655	0.809	0.341
acetone	0.651	0.907	0.475	0

for hydrophilic anion, such as $[\text{CF}_3\text{CO}_2]^-$ or $[\text{CH}_3\text{SO}_3]^-$ ([Ficke and Brennecke, 2010](#)).

Similar endothermic/exothermic behaviors are observed for mixtures of fixed alcohol (also amphoteric polar compounds; see Table 3.1) with different ILs. On the other hand, when the analysis is focused on one IL mixed with alcohols of increasing alkyl chain, it is observed that the decrease of solvent polarizability of the alcohol (see SP values in Table 3.1) implies lower exothermicity (or higher endothermicity) of its mixture with IL, that is, less effective interactions between alcohol and IL species. Therefore, the mixing enthalpies of the IL-organic solvent pairs also depends on the molecular structure of the organic compound.

Remarkably, all the available h^E data for IL-ketone systems evidenced an exothermic mixture behavior, indicating favorable intermolecular interactions between IL and HBA organic compounds, such as acetone. The solvent scale parameter of acetone indicates its high polarity (SdP and SP in Table 3.1) and basicity (SB) associated with the HBA carbonyl group of this compound, but negligible acidic character as solvent (SA in Table 3.1). These results suggest a different behavior of mixtures involving ILs and organic solvents presenting remarkably HBA character, such as acetone.

3. Interactions of ionic liquids and acetone: thermodynamic properties, quantum-chemical calculations, and NMR analysis

The COSMO-RS methodology provides the 3D polarized charge distribution (σ) on the molecular surface, easily visualized on the σ -profile histogram function. This distribution can be used to anticipate the possible interactions of a compound in a fluid. Figure 3.2 shows the σ -profile for the molecular solvents collected in Figure 3.1: alcohol, water and ketones.

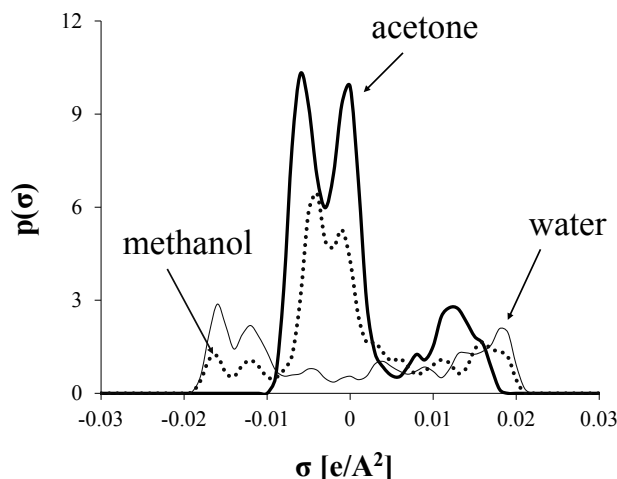


Figure 3.2: The σ -profiles of pure compounds: methanol, acetone and water obtained by COSMO-RS.

The σ -profile of water is dominated by two peaks. One is presented in strongly negative polar regions of the electron lone pairs of the oxygen atom (peak located at $+0.018$ eÅ⁻²). The other peak is located in strongly positive polar region of the hydrogen atoms (peak located at -0.016 eÅ⁻²). The presence of these two peaks agrees with the polar amphoteric character of water (see SdP, SP, SB and SA parameters in Table 3.1).

The σ -profile of methanol also corresponds to an amphoteric compound. However, in this case, a higher amount of electronic density is located in the non-polar regions. It accords with empirical solvent scale parameters where the polarity for methanol -or other alcohol- is lower than water.

A different COSMO-RS description is shown for acetone. Acetone presents an oxygen fragment in the polar positive region (peak at $+0.013$ eÅ⁻²), some charge concentration in the non-polar region, and the absence of atomic fragments with acidic character, anticipating its HBA behavior and relative polarity, in good agreement with the solvent effects measured for this compound (see SdP, SP, SB and SA parameters in Table 3.1). Further analyses in this work were centered on studying the behavior of the IL-acetone solutions, in order to understand the interactions between compounds.

3.4. Results

Figure 3.3 compares experimental h^E points and those estimated by COSMO-RS at 353.15 K for the two cases of IL-acetone mixtures reported by Izák et al. (2008).

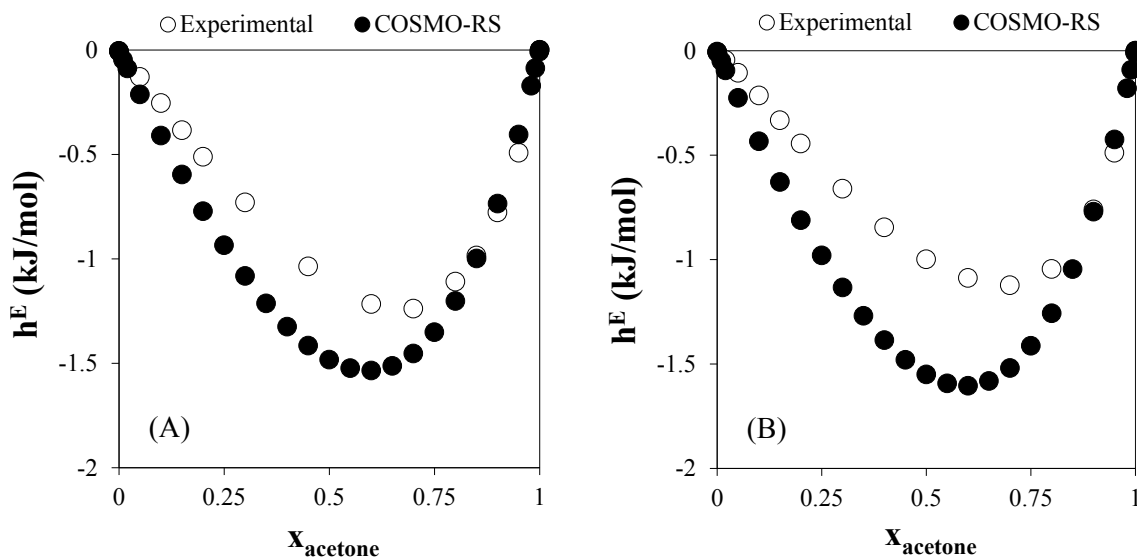


Figure 3.3: Experimental (white) and COSMO-RS (black) curves for excess molar enthalpy of (A) [bmim][NTf₂] + acetone and (B) [hxmim][NTf₂] + acetone mixtures at 353.15 K.

As can be observed, COSMO-RS also provides a reasonable estimation of h^E over the whole range of acetone compositions in the mixture. This is comparable with the predictability observed for other mixtures, such as those of ILs and alcohols (Ortega et al., 2007; García-Miaja et al., 2009a).

Figure 3.4 presents the screening of predicted h^E at 298 K. Qualitatively, the mixing process for the acetone-IL mixtures goes from slightly endothermic to highly exothermic depending on the selection of both cation and anion constituting the IL. The exothermicity of the binaries clearly increases by the presence of HBD groups linked to cation headgroup, such as shown for the imidazolium-based series [eim]⁺ > [e2mim]⁺ > [emim]⁺ > [emmim]⁺. In this sense, for a common anion, it is generally observed more exothermic mixtures in the order [pyrrolidinium]⁺ > [pyridinium]⁺ > [imidazolium]⁺ > [phosphonium]⁺ > [ammonium]⁺, according to the acidic character of the cation family.

In addition, the selection of the anion also determines the excess enthalpy behavior of the IL-acetone mixtures. It is observed that big anions with dispersed charge, lacking the HBA ability, such as [C₆F₁₈P]⁻, [FeCl₄]⁻ or [NTf₂]⁻, are those giving the most negative

3. Interactions of ionic liquids and acetone: thermodynamic properties, quantum-chemical calculations, and NMR analysis

values for excess enthalpies of IL-acetone mixtures; whereas anions with HBA groups, such as $[\text{CH}_3\text{SO}_3]^-$ and $[\text{C}_2\text{H}_5\text{SO}_4]^-$, are the ones providing endothermic systems. These results suggest that the HBA character of these anions favors the anion-cation interaction, restricting the possibility of another interaction (acetone-cation). As a consequence, the most negative h^E values for IL-acetone mixtures (the white and light areas on Figure 3.4), are found for ILs presenting a cation with strong HBD character, which favors cation-acetone interactions, in combination with non-HBA anions, which are not able to promote strong cation-anion hydrogen bonding.

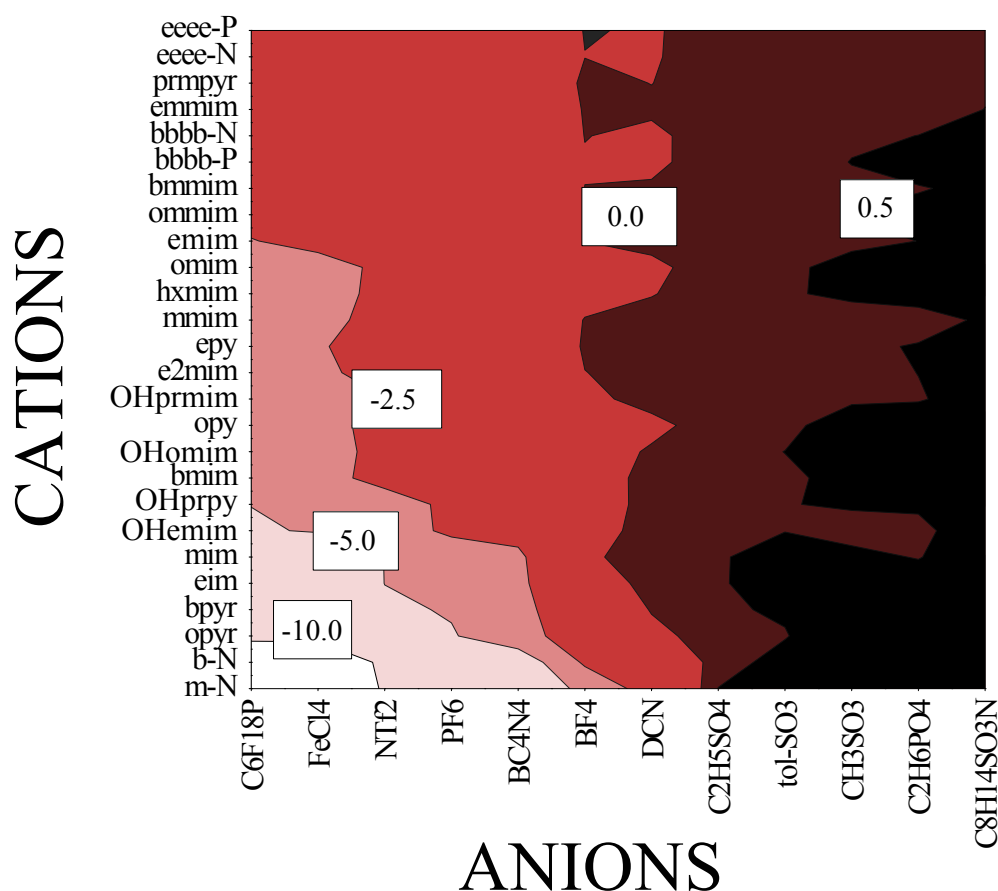


Figure 3.4: Screening of COSMO-RS predicted excess molar enthalpies h^E (kJ/mol) for 312 equimolar acetone-IL mixtures at 298 K.

3.4.1.1 Contributions to h^E

To study in detail the intermolecular interactions established in IL-acetone mixtures, the contributions to the h^E of these systems due to electrostatic (*Misfit*), van der Waals and Hydrogen Bond interactions, were calculated by using COSMO-RS. Figure 3.5 presents the particular energetic contributions (MF), (HB) and (vdW) to the excess enthalpies for equimolar mixtures of acetone with imidazolium-based ILs presenting the common anion $[\text{NTf}_2]^-$, as reference of weakly basic specie. As expected, hydrogen bond interactions dominate the behavior of the mixtures, increasing the exothermicity with the acidity of the cation. Polar misfit contributions are also relevant, nearly following the order of H-bond interactions. The van der Waals interactions are negligible for these mixtures. It should be pointed out that the IL containing an $[\text{eim}]^+$ cation shows the most negative $h^E(\text{HB})$ and $h^E(\text{MF})$ values in its mixture with acetone. These contributions to the h^E are responsible of the extremely exothermic behavior showed in the screening (Figure 3.4).

Figure 3.6 depicts the contributions of the intermolecular interactions to the excess

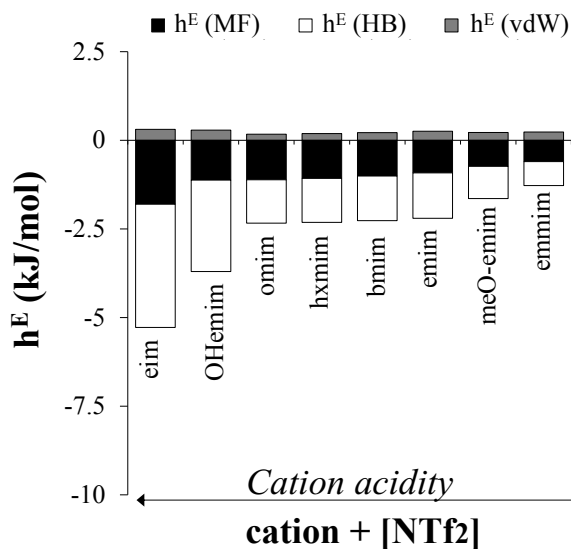


Figure 3.5: Description of the cation effect on the excess molar enthalpy of the acetone-[cation] $[\text{NTf}_2]$ equimolar mixture in terms of the intermolecular interaction contributions h^E (MF), h^E (HB) and h^E (vdW)] computed by COSMO-RS at 298 K.

enthalpy of mixtures with acetone and ILs including a common cation $[\text{eim}]^+$, which presents a strong HBD character as already been discussed. The ILs containing anions without HBA groups, such as $[\text{C}_6\text{F}_{18}\text{P}]^-$, $[\text{FeCl}_4]^-$ or $[\text{NTf}_2]^-$, provide highly exothermic mixtures with acetone (where attractive cation-acetone HB interactions are significant).

3. Interactions of ionic liquids and acetone: thermodynamic properties, quantum-chemical calculations, and NMR analysis

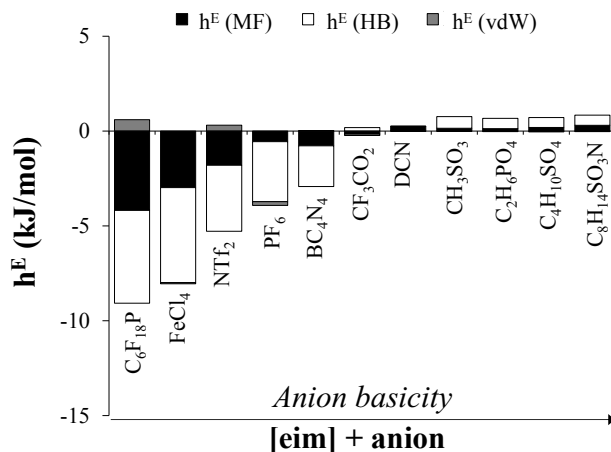


Figure 3.6: Description of the anion effect on the excess molar enthalpy of the acetone-[eim][anion] equimolar mixture in terms of the intermolecular interaction contributions [h^E (MF), h^E (HB) and h^E (vdW)] computed by COSMO-RS at 298 K.

On the contrary, as the anion basicity increases, the h^E (HB) contribution becomes less relevant or even slightly endothermic. This means that cation-anion interactions compete with acetone-cation interactions, decreasing the affinity of the IL for the solvent.

3.4.2 COSMO-RS description of acetone and ILs

The σ -profiles provided by COSMO-RS shown in Figure 3.7 reveal that hydrogen-bond interactions are possible between the acetone and the cations. The interaction is possible through the =O atom of the acetone (red part of its σ -surface) and the acidic hydrogen atoms of the cation (blue part of its σ -surface). The screening results can easily be related to the σ -profiles and σ -surfaces of acetone and selected cations mapped in ascending order of a column and those anions located by shifting to the right in a row of Figure 3.4.

As previously shown in the screening, [eim]⁺ provides high exothermicity in its mixture with acetone. Focusing on the σ -profile of [eim]⁺ (Figure 3.7), the peaks located at lower values than the cutoff $-0.082 \text{ e}\text{\AA}^{-2}$ are those related to the hydrogen atoms of the aromatic ring. These fragments are responsible for HBD capability of cations (the blue part in the σ -surface). There is also a prominent peak with charge distribution in the non-polar region, corresponding to the aliphatic and aromatic groups of the cationic alkyl chain and headgroup. The acidic sites of [eim]⁺ can be observed in Figure 3.8. As can be observed in the figure, the acidity trend of these sites increases as follow $\text{H3} > \text{H2} > \text{H4} \approx \text{H5} >$

3.4. Results

H(CH₃,CH₂) (of the alkyl chain).

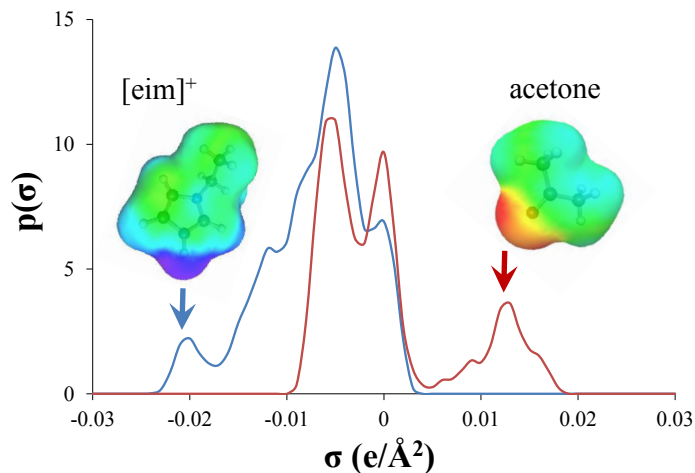


Figure 3.7: σ -profiles and σ -surfaces obtained by COSMO-RS for the [eim]⁺ cation (blue line) and acetone (red line).

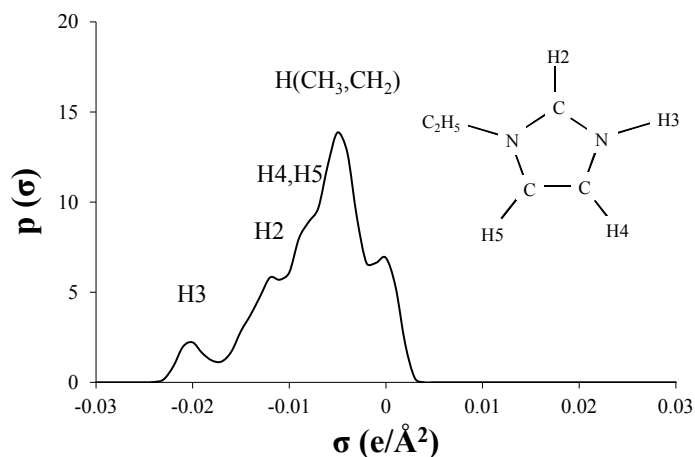


Figure 3.8: σ -profile obtained by COSMO-RS for the [eim]⁺ cation. Labeled peaks correspond to the acid sites of cations.

The σ -profiles of selected cations from the screening are presented in Figure 3.9. The selection was made based on the ascendant acidity trend of these cations ([eim]⁺ > [e2mim]⁺ > [emim]⁺ > [emmim]⁺). There is a particular difference between them in their σ -profile. The peak located at -0.02 eÅ⁻² in the σ -profiles of [eim]⁺ and [e2mim]⁺ (corresponding to the most acidic site of these cations) does not appear in the other two distributions. This is because the replacement of H atoms by the -CH₃ groups eliminates the acid groups in the [emim]⁺ and [emmim]⁺ cations. These two cations show almost no

3. Interactions of ionic liquids and acetone: thermodynamic properties, quantum-chemical calculations, and NMR analysis

deep blue part in their σ -surfaces. The low acidity character of $[\text{emim}]^+$ and $[\text{emmim}]^+$ hinders the interaction with acetone providing less exothermicity in their mixtures (dark color regions in the screening).

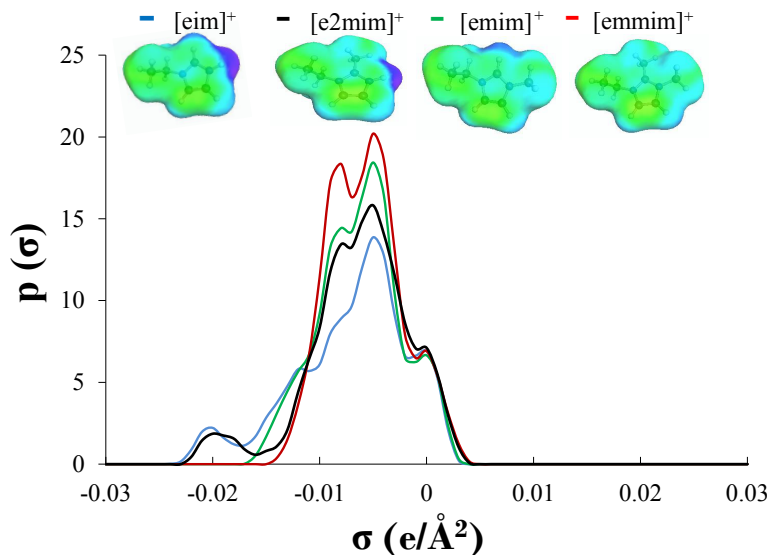


Figure 3.9: σ -profiles and σ -surfaces obtained by COSMO-RS for the $[\text{eim}]^+$ (blue line), $[\text{e2mim}]^+$ (black line), $[\text{emim}]^+$ (green line) and $[\text{emmim}]^+$ (red line) cations.

On the other hand, focusing on the σ -profiles of Figure 3.10, the role of the anion in the IL-acetone interaction can be understood. It can be seen on the distribution, that the $[\text{PF}_6]^-$ and $[\text{BF}_4]^-$ anions show their peaks at lower σ position than acetone. The ILs including these anions provide higher exothermicities in their mixtures with acetone (see Figure 3.4). $[\text{PF}_6]^-$ and $[\text{BF}_4]^-$ have not HBA atomic groups to compete with the basic sites of acetone in the interaction with the cation. The $[\text{PF}_6]^-$ does not contain any HBA group (its σ -surface is totally yellow). The σ -profile of $[\text{BF}_4]^-$ contains a peak located at the negative polar region ($0.011 \text{ e}\text{\AA}^{-2}$), which indicates a weak HBA group character (clear orange appearing in its σ -surface). The $[\text{C}_2\text{H}_5\text{SO}_4]^-$ anion shows a stronger HBA fragment ($-\text{SO}_4$ group, at $0.014 \text{ e}\text{\AA}^{-2}$). A similar description can be done for the $[\text{CH}_3\text{SO}_3]^-$ anion, but in this case, the anion contains a stronger HBA group. These last two anions contain red parts in their σ -surfaces evidencing the presence of strong HBA groups. These groups may interact with the H of the cation, hindering the cation-acetone interaction.

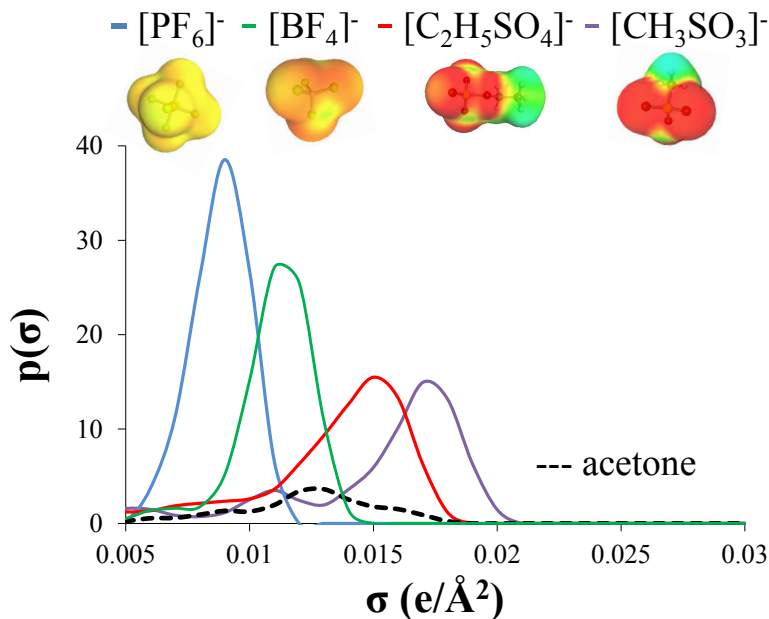


Figure 3.10: σ -profiles and σ -surfaces obtained by COSMO-RS for the $[\text{PF}_6]^-$ (blue solid line), $[\text{BF}_4]^-$ (green solid line), $[\text{C}_2\text{H}_5\text{SO}_4]^-$ (red solid line), $[\text{CH}_3\text{SO}_3]^-$ (purple solid line) anions and acetone (black dashed line)

3.4.3 Thermodynamic analysis of the Gas-Liquid and Vapor-Liquid equilibria in terms of the IL-acetone interactions

Once h^E values for the generally favorable IL-acetone mixtures have been analyzed in terms of intermolecular interactions, the possible relationships to macroscopic properties of interest for these mixtures -such as GLE and VLE data- are evaluated. Previous works showed that h^E analysis by COSMO-RS can be successfully used to design ILs with improved thermodynamic properties, for example, in certain processes, such as absorption (Palomar et al., 2011b; González-Miquel et al., 2011; Palomar et al., 2011a; Bedia et al., 2012), adsorption (Palomar et al., 2009a) and liquid extraction (Ortega et al., 2007; Vreekamp et al., 2011) with the participation of ILs. As can be seen in Figure 3.11A, the more exothermic the mixture is, the higher the solubility of the acetone gas in the liquid.

The VLE data are also relevant information for practical application as distillation involving IL mixtures. Figure 3.11B relates the h^E of mixing to the pressure ratio coefficient ($P_{\text{mixture}}/P_{\text{pure acetone}}$). Considering the negligible partial pressure of the IL at these conditions, $P_{\text{mixture}}/P_{\text{pure acetone}}$ is a parameter of reference for the volatility change of acetone because of IL mixing. The curve shows that, while increasing the exothermicity of the

3. Interactions of ionic liquids and acetone: thermodynamic properties, quantum-chemical calculations, and NMR analysis

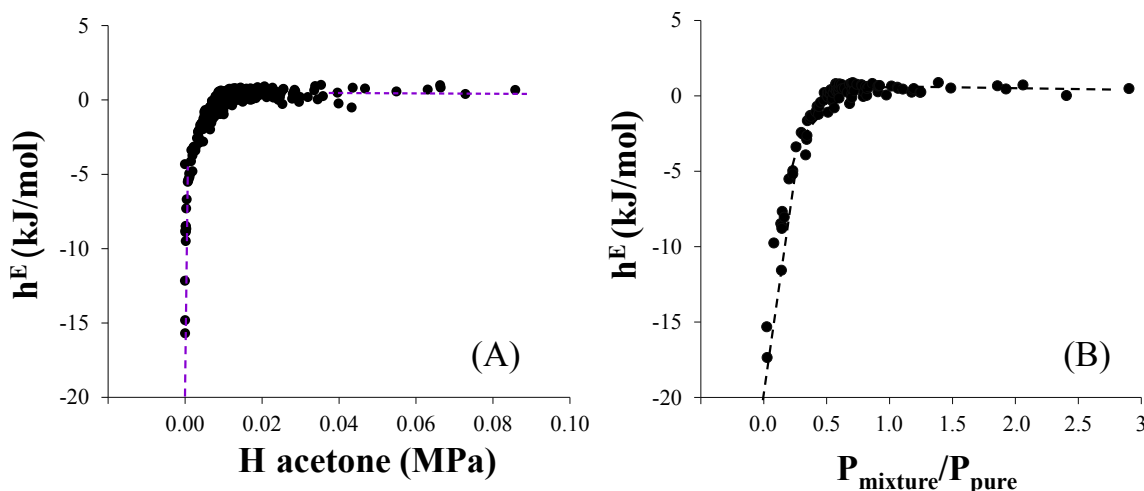


Figure 3.11: Relationship between the h^E of mixing and (A) the acetone Henry's constant in IL and (B) the vapor pressure ratio coefficient for all the studied acetone-IL systems, computed by COSMO-RS at 298 K.

system, the pressure ratio tends to zero. This means that the favorable interactions with ILs significantly decrease the partial pressure of acetone in the mixture. In contrast, when acetone-IL interactions are weaker (h^E values close to zero), the pressure ratio increases toward $P_{\text{mixture}}/P_{\text{pure acetone}}$ values higher than 1. This indicates that IL regeneration by distillation is favorable in these systems.

3.4.4 Molecular overview of the acetone-IL interactions

To obtain further insights on the acetone-IL interactions, quantum chemical molecular simulations including clusters of acetone and IL ionic species as well as spectroscopic analysis based on ^1H -NMR measurements were performed.

As we noted in the above, the σ -profiles provided by COSMO-RS for the cations and acetone reveal that HB donor/acceptor interactions are possible between the acetone and the cations involving the $=\text{O}$ atom of the acetone and the $-\text{H}$ atoms of the cations. This conclusion can also be drawn from their σ -surfaces shown before. The charge distribution in the sigma surfaces suggests that where some potential HBD hydrogen are available, the acidic character decreases in the sequence $\text{H3} > \text{H2} > \text{H4}$. This result is also supported by the atomic Mlliken charges calculated for the gas phase optimized structures of the cations (Figure 3.12). It is interesting to note that atomic charges at the H2 atom is the same for both the $[\text{mmim}]^+$ and the $[\text{eim}]^+$ cations, advising that their HB donating

properties are very similar.

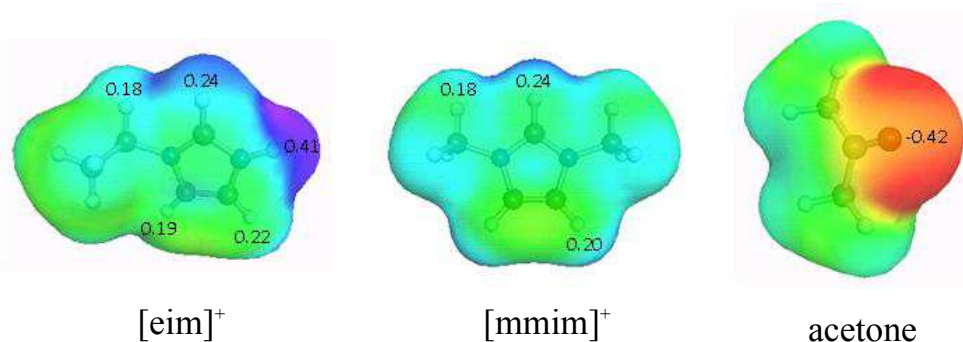


Figure 3.12: Mülliken atomic charges (calculated at M052X/6-311**G(d,p) computational level) at some selected atoms of the $[\text{eim}]^+$, $[\text{mmim}]^+$ and acetone molecules.

The quantum-chemical optimization of clusters including acetone and IL species shows that the total electronic energy of the overall system decreases with respect to that of isolated molecules as a result of the $[\text{cation-acetone}]^+$ complex formation (Figure 3.13). This is coherent with the computed negative excess enthalpies for the mixtures of acetone with ILs. Changes in the total electronic energy, ΔE , for the $[\text{cation-acetone}]^+$ complex formation are very similar, as expected, for $[\text{mmim}]^+$ and $[\text{eim}]^+$ cations when the observed HB interaction takes place with H2 proton involvement. Furthermore, the optimized $\text{H} \cdots \text{O}=\text{C}$ non-bonding distances are close in both cases.

ΔE is less negative for $[\text{eim-acetone}]^+$ complexes in the sequence $\text{H3} > \text{H2} > \text{H4}$, in good agreement with the HBD character of these groups, previously discussed. Moreover, the $\text{H} \cdots \text{O}=\text{C}$ distance is noticeable shorter in H3-complex (1.735 Å) than in H2-complex (2.041 Å). It is important to underline that $[\text{eim-acetone}]^+$ complexes through H4 proton have not been obtained in molecular optimizations. The corresponding final optimized structure in this case is the same to that obtained when acetone directly interacts with H3 proton.

Optimized structures of the $[\text{eim}][\text{PF}_6]$ ion pairs (Figure 3.14) show that the $[\text{PF}_6]^-$ anion is roughly placed at the same cation positions that the acetone molecule in the corresponding complexes (Figure 3.13). This means that the $[\text{PF}_6]^-$ anion and acetone molecule compete for the same proton donor center at the $[\text{eim}]^+$ in a $[\text{eim-PF}_6]$ -acetone mixture. Moreover, optimized structures of the $[\text{eim-acetone}]^+$ complexes and the $[\text{eim-PF}_6]$ ion pair show that cation-acetone interactions have a specific character, as correspond to hydrogen bonding interactions.

3. Interactions of ionic liquids and acetone: thermodynamic properties, quantum-chemical calculations, and NMR analysis

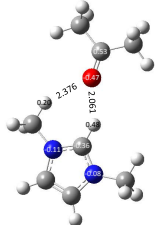
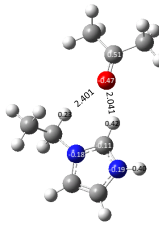
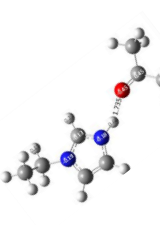
[mmim-acetone]⁺	[eim-acetone]⁺ (-H₂...O=)	[eim-acetone]⁺ (-H₃...O=)
		
$\Delta E = -15.6$ kcal/mol	$\Delta E = -15.9$ kcal/mol	$\Delta E = -19.7$ kcal/mol

Figure 3.13: Optimized structures of the [cation-acetone]⁺ complexes for both [mmim]⁺ and [eim]⁺ cations at the M052X/6-311++G(d,p) computational level. Computed non-bonding interatomic distances (Å) and Mülliken atomic charges for some selected atoms are also included. Energy differences correspond to the total electronic energy (E) being defined as $\Delta E = E_{\text{cation-acetone}} - (E_{\text{cation}} + E_{\text{acetone}})$ for the model process $[\text{cation}]^+ + [\text{acetone}]^0 \longrightarrow [\text{cation-acetone}]^+$.

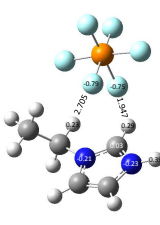
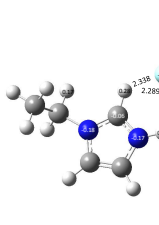
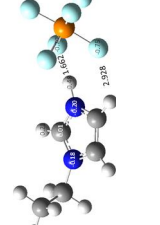
[eimPF₆]		
(-H₂...F- interaction)	(-H₃...F- interaction)	(-H₄...F- interaction)
		
$\Delta E = -80.9$ kcal/mol	$\Delta E = -85.5$ kcal/mol	$\Delta E = -82.4$ kcal/mol

Figure 3.14: Optimized structures of the [eim-PF₆] ion pairs at M052X/6-311++G(d,p) computational level. Computed non-bonding interatomic distances (Å) and Mülliken atomic charges for some selected atoms are also included. Energy differences correspond to the total electronic energy (E) being defined as $\Delta E = E_{[\text{eimPF}_6]} - (E_{[\text{eim}]} + E_{[\text{PF}_6]})$ for the model process $[\text{eim}]^+ + [\text{PF}_6]^- \longrightarrow [\text{eim-PF}_6]$.

3.4. Results

Competence of the acetone molecules and the $[\text{PF}_6]^-$ anion by the acid centers at the $[\text{eim}]^+$ cation is likewise observed in the optimized structures of the $[\text{eim-PF}_6\text{-acetone}]$ clusters. Figure 3.15 shows that acetone is able to displace the anion from its interactions with the most acid H3 center.

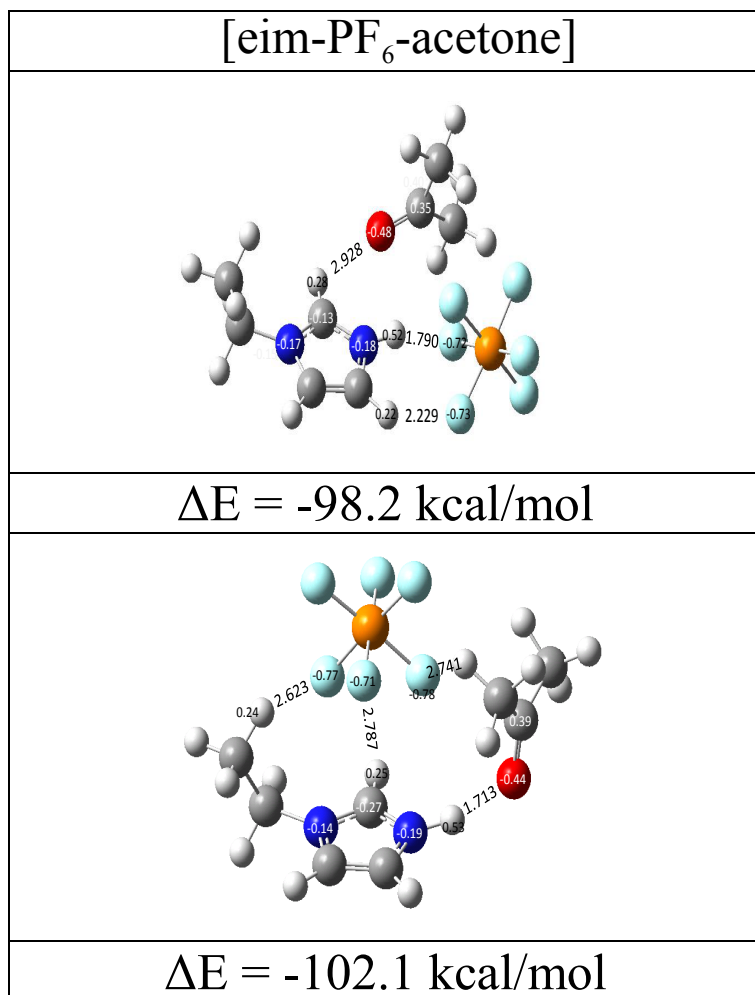


Figure 3.15: Optimized structures of the $[\text{eim-PF}_6\text{-acetone}]$ aggregates at M052X/6-311++G(d,p) computational level. Computed non-bonding interatomic distances (\AA) and Müliken atomic charges for some selected atoms are also included. Energy differences correspond to the total electronic energy (E) being defined as $\Delta E = E_{\text{aggregate}} - (E_{\text{cation}} + E_{\text{anion}} + E_{\text{acetone}})$ for the model process $[\text{cation}]^+ + [\text{anion}]^- + [\text{acetone}]^0 \longrightarrow [\text{cation-anion-acetone}]$.

These theoretical results were finally contrasted with experimental observations made on the IL-acetone systems. $^1\text{H-NMR}$ spectra were obtained at room temperature for

3. Interactions of ionic liquids and acetone: thermodynamic properties, quantum-chemical calculations, and NMR analysis

[bmim][NTf₂]-acetone and [eim][NTf₂]-acetone binary mixtures with different compositions. Figure 3.16A shows ¹H-NMR spectra for [bmim][NTf₂], where most relevant peaks are located between 6 and 10 ppm belonging to aromatic hydrogen atoms (see H2, H4, H5 in Table 3.2). As it can be observed, the value of ¹H chemical shift of the most acidic ring proton (H2) progressively increases with acetone concentration ($\Delta\delta \simeq 1.5$ ppm from neat IL to 5% w/w of IL), assignable to the formation of local interactions (hydrogen bonding) between the acetone's carbonyl group and this cation-acidic hydrogen atom (Bara et al., 2009b).

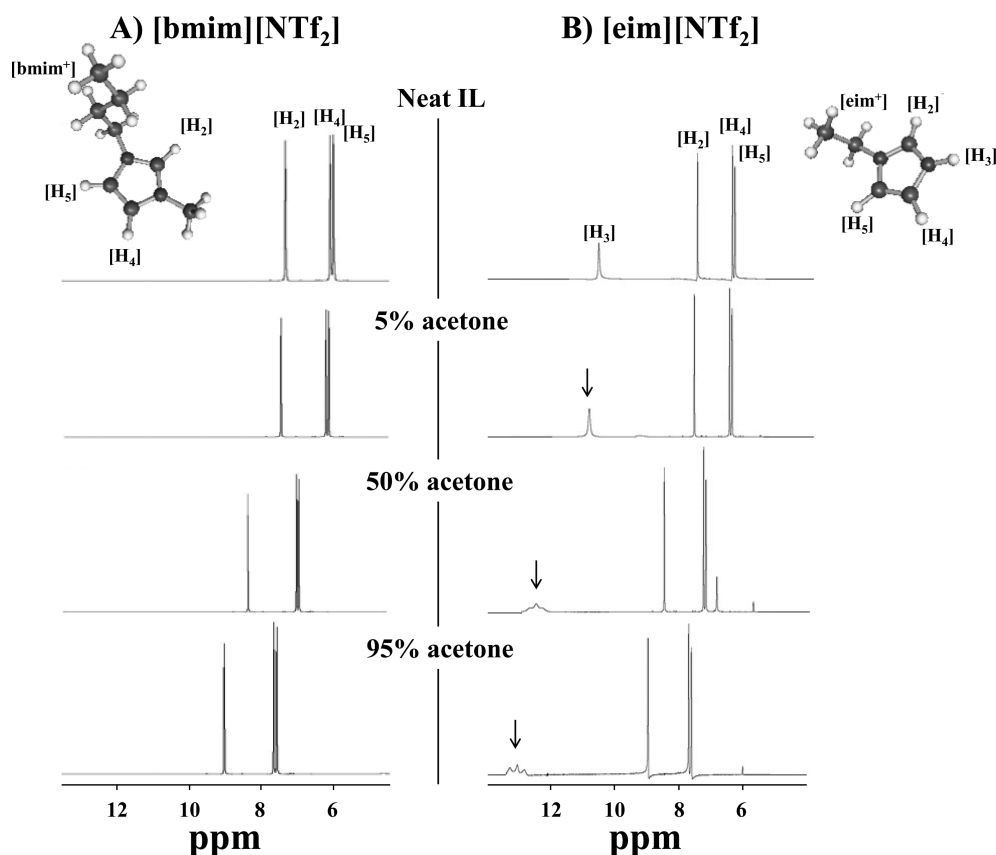


Figure 3.16: ¹H-NMR spectra of (A) [bmim][NTf₂] and (B) [eim][NTf₂]: pure IL and IL-acetone mixtures with increasing mass concentration of acetone.

Figure 3.16B and Table 3.2 show similar displacement of the [H2] signal in [eim][NTf₂] mixtures with acetone. However, a significantly larger displacement is observed for the most acidic proton of the [eim]⁺ cation, [H3]. When acetone concentration increases, this chemical shift ($\Delta\delta \simeq 2.8$ ppm from neat IL to 5% w/w of IL) reveals stronger HB interactions between acetone and the [eim]⁺ cation than that with [bmim]⁺. This agrees

3.4. Results

with the conclusions achieved by COSMO-RS and cluster quantum-chemical simulations.

Table 3.2: Experimental ^1H -NMR chemical shifts (δ , ppm) of neat [bmim][NTf₂] and [eim][NTf₂] and mixtures with acetone at increasing mass concentration of acetone.

	[bmim][NTf ₂]				[eim][NTf ₂]			
H-NMR	H2	H3	H4	H5	H2	H3	H4	H5
neat IL	7.5		6.4	6.2	7.5	10.5	6.4	6.3
5% acetone	7.6		6.5	6.4	7.6	10.9	6.5	6.4
50% acetone	8.4		7.2	7.2	8.5	12.7 / 12.5 / 12.3	7.3	7.2
95% acetone	9		7.7	7.6	9	13.3 / 13.1 / 12.9	7.7	7.7

To complete the analysis, Table 3.3 collects the difference between the computed ^1H and ^{17}O NMR spectra of the complexes [cation-acetone]⁺ and the individual (cations and acetone) species at GIAO/M052X/6-311++G(d,p) quantum-chemical level. The predicted displacements of the chemical shifts (Table 3.3) due to cation-acetone interactions reproduce reasonably well the experimental trends, obtaining additional evidence of the presence of hydrogen bonding between acetone and ILs, which was strengthened by the presence of more acidic centers in the cation.

Table 3.3: Difference between ^1H and ^{17}O NMR chemical shifts ($\Delta\delta$) of [cation-acetone]⁺ complexes and individual species calculated at the GIAO/M052X/6-311++G(d,p) Level^a.

	$\Delta\delta$, ppm			
	H2	H3	H4	O
[mmim-acetone] ⁺	2.8		-0.1	-96.9
[eim-acetone] ⁺ (-H2 ... O=)	2.9	-0.2	-0.1	-98.2
[eim-acetone] ⁺ (-H3 ... O=)	0.3	6	-0.01	-131.1

^aTMS and H₂O are used as reference compound to obtain ^1H and ^{17}O NMR $\Delta\delta$ values, respectively.

3.5 Concluding remarks

COSMO-RS was used as a suitable computational method to systematically analyze the behavior of more than 300 IL-acetone systems in terms of their h^E .

These mixtures generally presented an exothermic behavior where acetone, as polar compound with strong HBA character, establishes favorable HB interactions with ILs.

The HB interaction in IL-acetone mixtures takes place between the cation (HBD character) and acetone. This interaction is strengthened by the presence of an acidic cation and an anion with dispersed charge and non-HBA character.

According to the chemical structure of the IL, the intermolecular interactions in the acetone-IL liquid phase are different, affecting to the gas-liquid and vapor-liquid equilibria. COSMO-RS predictions indicated that gas-liquid and vapor-liquid equilibrium data can be finely tuned by the IL selection.

NMR measurements and quantum-chemical calculations by using molecular clusters evidenced the main role played by the hydrogen-bonding interactions in the IL-acetone mixtures.

The results of this work provide useful insights regarding the selection of ILs to design new technological processes involving acetone-IL systems.

Chapter 4

Separation of small paraffin-olefin mixtures with an ionic liquid. Thermodynamic study using COSMO-RS

Ionic liquids are nonvolatile solvents suitable for separation processes. Because the physicochemical properties of ILs can be tuned by different cation-anion combinations, we use COSMO-RS to select promising ILs for paraffin/olefin separation by absorption or extraction. We estimate Henry's constants for ethane, ethylene, propane, propylene, butane, butene, pentane, pentene, hexane and hexene using the [CA] and [C+A] structural models. Both molecular models appear to be suitable for rough estimates of Henry's constants. We calculate relative volatility and selectivity for some paraffin/olefin systems. We identify some promising ILs for separating ethane, propane, butane, pentane and hexane from their corresponding olefins. This work has been carried out in the Energy Biosciences Institute within the research team led by Prof. Dr. John M. Prausnitz (University of California, Berkeley). This group is working on the separation of paraffins from olefins by selective absorption using phosphonium-based ILs ([Liu et al., 2013b,a](#)).

4.1 Introduction

Light unsaturated hydrocarbons play a significant role in the petrochemical industry. The most widely used process for olefin production is cracking of C4-hydrocarbon fractions, followed by dehydrogenation to produce an equimolar gas mixture of olefins and paraffins. This mixture is difficult to separate because for a fixed carbon number, the properties of paraffin are very similar to those of its corresponding olefin (Eldridge, 1993; Tsou et al., 1994; Safarik and Eldridge, 1998). Absorption/extraction may provide a suitable process for separation. However, traditional solvents often show low selectivity or low capacity for paraffin/olefin separation. Because traditional solvents are volatile, solvent losses may increase process costs. Most ionic liquids (ILs) have favorable properties such as negligible vapor pressure and thermal stability for a broad range of liquid temperature. The physicochemical properties of ILs can be tuned by combining different cations and anions. These desirable properties make ILs potential solvent candidates for extraction and absorption separation processes (Tokuda et al., 2004; Matsumoto et al., 2004; Zhu et al., 2007; Bara et al., 2009c; Yang et al., 2009; Palgunadi et al., 2010).

While many ILs can, in principle, replace conventional solvents for the separation of any low-boiling alkane/alkene mixture (Krummen et al., 2002; Domańska and Laskowska, 2009; Blahut et al., 2010) some are much better than others. The aim of this chapter is to provide a guide for selecting the IL that optimizes a particular paraffin/olefin separation. For this purpose, COSMO-RS calculations were used to obtain Henry's constants (H).

4.2 Thermodynamic analysis

For a binary mixture containing an olefin and a paraffin at a given temperature and composition, the relative volatility is defined as:

$$\alpha = \frac{\left(\frac{y}{x}\right)_p}{\left(\frac{y}{x}\right)_o} \quad (4.1)$$

where subscript p refers to paraffin and subscript o refers to olefin; y is the mole fraction in the vapor and x the mole fraction in the liquid. We now consider a solution of paraffin and olefin in an ionic liquid solvent. When the vapor phase is an ideal gas, the

4. Separation of small paraffin-olefin mixtures with an ionic liquid. Thermodynamic study using COSMO-RS

equations of equilibrium are:

$$y_i \cdot P = \gamma_i \cdot x_i \cdot P_i^o \quad (4.2)$$

where i is paraffin or olefin, P_i^o is vapor pressure of pure liquid i and γ_i is the activity coefficient of i dissolved in the IL solvent. Thus

$$\alpha = \frac{\gamma_p P_p^o}{\gamma_o P_o^o} = s \frac{P_p^o}{P_o^o} \quad (4.3)$$

where s is the selectivity defined as the ratio of activity coefficients of the two hydrocarbons in the IL at a fixed temperature and liquid-phase composition. We consider a very dilute solution of the solute (paraffin or olefin) in the IL; then

$$s = \frac{\gamma_p^\infty}{\gamma_o^\infty} \quad (4.4)$$

where superscript ∞ refers to infinite dilution.

For solute i, Henry's constant is defined by

$$H_i = \lim_{x_i \rightarrow 0} \frac{P_i}{x_i} \quad (4.5)$$

where $P_i = y_i P$ is the partial pressure of i.

Because

$$H_i = \gamma_p^\infty \cdot P_i^o \quad (4.6)$$

it follows that

$$\alpha = \frac{(H_i)_p}{(H_i)_o} \quad (4.7)$$

Considering the large variety of possible cation and anion combinations, computational methods are useful for solvent screening. COSMO-RS provides a convenient method for estimating Henry's constants (Zhang et al., 2008; Manan et al., 2009; Klamt et al., 2010a; Diedenhofen and Klamt, 2010; Sistla and Khanna, 2011; Sumon and Henni, 2011; Palomar

et al., 2011a,b; González-Miquel et al., 2011; Gonzalez-Miquel et al., 2012; Bedia et al., 2012). In this work, we calculate Henry’s constant for some paraffins and olefins in IL solvents using COSMO-RS and the [CA] and [C+A] structural models optimized in solvent phase considering solvent effects. The [C+A] model allows faster and easier calculations as it is the one implemented in the COSMOlogic database. For this reason, the [C+A] model was chosen to calculate Henry’s constant for every solute in 646 ionic liquids at 298 K. Then, we calculate relative volatilities and selectivities using COSMO-RS. We select promising ILs for a given paraffin/olefin separation. We compare our COSMO-RS calculations with experiment whenever possible.

4.3 Computational method

All COSMO-RS calculations were performed using the program package COSMOThermX version C30_1201 (Diedenhofen et al., 2012) developed and distributed by COSMOlogic GmbH & Co. KG. The COSMOThermX calculations use the implicit BP_TZVP_C30_1201 parameterization. Two models were considered to simulate the IL solvents for COSMO-RS calculations:

- **[C+A] solvent effects.** COSMO files for the ions are taken directly from the ILDB-C21-0110 (BP-TZVP-COSMO) database distributed by COSMOlogic. For ions not available in the COSMO database, they are created using TURBOMOLE suit (v 3.1) (Schäfer et al., 2000). Here, the molecular structure of the ions is optimized at BVP-86/TZVP/DGA1 computational level considering solvent effects with a hypothetical solvent having an infinite dielectric constant ($\epsilon \rightarrow \infty$) and Klamt atomic radii. The COSMO file is generated at the same computational level according to the COSMO-RS model developed by Klamt (1995).
- **[CA] solvent effects.** Molecular structures for the [CA] models are optimized at the same computational level as that for individual ions using the TURBOMOLE suit (V 3.1) of programs (Schäfer et al., 2000). Vibrational frequency calculations are performed to obtain an energy minimum. After optimization, the COSMO file containing the ideal screening charges on the molecular surface is computed by the COSMO methodology in a way similar to that for individual ions.

Henry’s constants can be directly calculated using the Henry Constant panel available in COSMOThermX. The temperature is set for each mixture. The activity coefficient at

4. Separation of small paraffin-olefin mixtures with an ionic liquid. Thermodynamic study using COSMO-RS

Table 4.1: Empirical equations used to calculate saturation vapor pressure of solutes at a specific temperature.

Solute	Equation parameters					
	A	B	C	D	E	F
Methane ¹	3.80	403.11	-5.48			
Ethane ¹	3.94	659.74	-16.72			
Ethylene ¹	3.87	584.15	-18.31			
Propane ²	4248	369.83	-6.72	1.33	-2.14	-1.39
Propylene ²	4600	364.9	-6.64	1.22	-1.81	-2.48
Butane ²	3796	425.12	-6.89	1.15	-2.00	-3.13
Butene ²	4020	419.5	-6.88	1.27	-2.26	-2.62
Pentane ²	3370	469.7	-7.29	1.54	-3.08	-1.02
Pentene ²	3560	464.8	-7.05	1.18	-2.45	-2.22
Hexane ²	3025	507.6	-7.47	1.44	-3.28	-2.51
Hexene ²	3210	504.0	-7.76	2.30	-4.44	0.90

¹ Antoine: $\log_{10}(P_i^S) = A - (B/(T+C))$

² Wagner: $\ln(P_i^S) = \ln(A) + 1/(1-\tau)(C\tau + D\tau^{1.5} + E\tau^3 + F\tau^6)$; $\tau = 1 - (T/B)$

infinite dilution is calculated for the output file. Vapor pressures P_i^S were estimated by COSMOthermX, with no additional input, or obtained from experimental data (See Table 4.1). Where experimental Henry's constants are available, errors in Henry's constant calculations using COSMO-RS were determined by the Root Mean Square Deviation (RMSD).

4.4 Results

4.4.1 Henry’s law constants calculation

We consider the separation of an olefin from its corresponding paraffin at 298 K. But firstly, COSMO-RS was evaluated for predicting Henry’s law constants by comparison of calculated and experimental data. The sample included 156 binary mixtures, with Henry’s constants at different temperatures (303-333 K) of 7 solutes (methane, ethane, ethylene, propane, propylene, butane or butene) and a variety of IL solvents (Liu et al., 2013b,a; Lee and Outcalt, 2006).

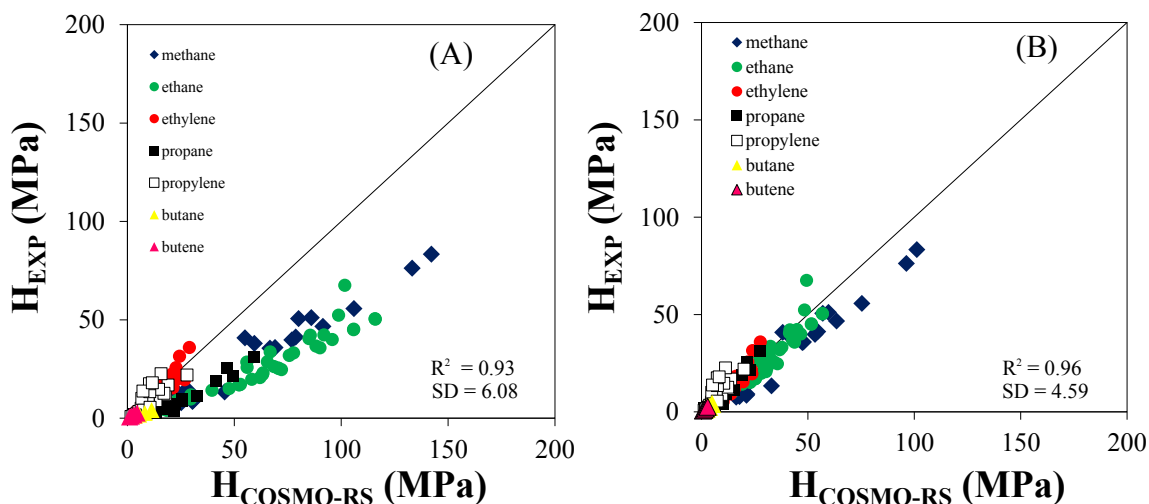


Figure 4.1: COSMO-RS calculated vs. experimental Henry’s constants for solutes in numerous ILs at different temperatures. H are calculated using (A) COSMO-RS or (B) experimental vapor pressures (see Table 4.1). The ILs were simulated by the [C+A] solvent effect model.

Figure 4.1A compares H (experimental) and H (calculated) using vapor pressures predicted by COSMO-RS. In this case, calculated Henry’s constants (using [C+A] solvent effect model) are overestimated ($R^2 = 0.93$, $\text{SD} = 6.08$ MPa and $\text{RMSD} = 1.63$ MPa). In a separate calculation, we calculated activity coefficients at infinite dilution and, to obtain Henry’s constants, we used experimental vapor pressures (Table 4.1). This calculation gave Henry’s constants in better agreement with experiment ($R^2 = 0.96$, $\text{SD} = 4.59$ MPa and $\text{RMSD} = 0.55$ MPa) as shown in Figure 4.1B. The best estimates are obtained for low Henry’s constants, i.e. large solubility.

4. Separation of small paraffin-olefin mixtures with an ionic liquid. Thermodynamic study using COSMO-RS

For ethane, ethylene, hexane and hexene in 646 different ILs at room temperature Henry's constants calculated by COSMO-RS were screened and reflected in maps.

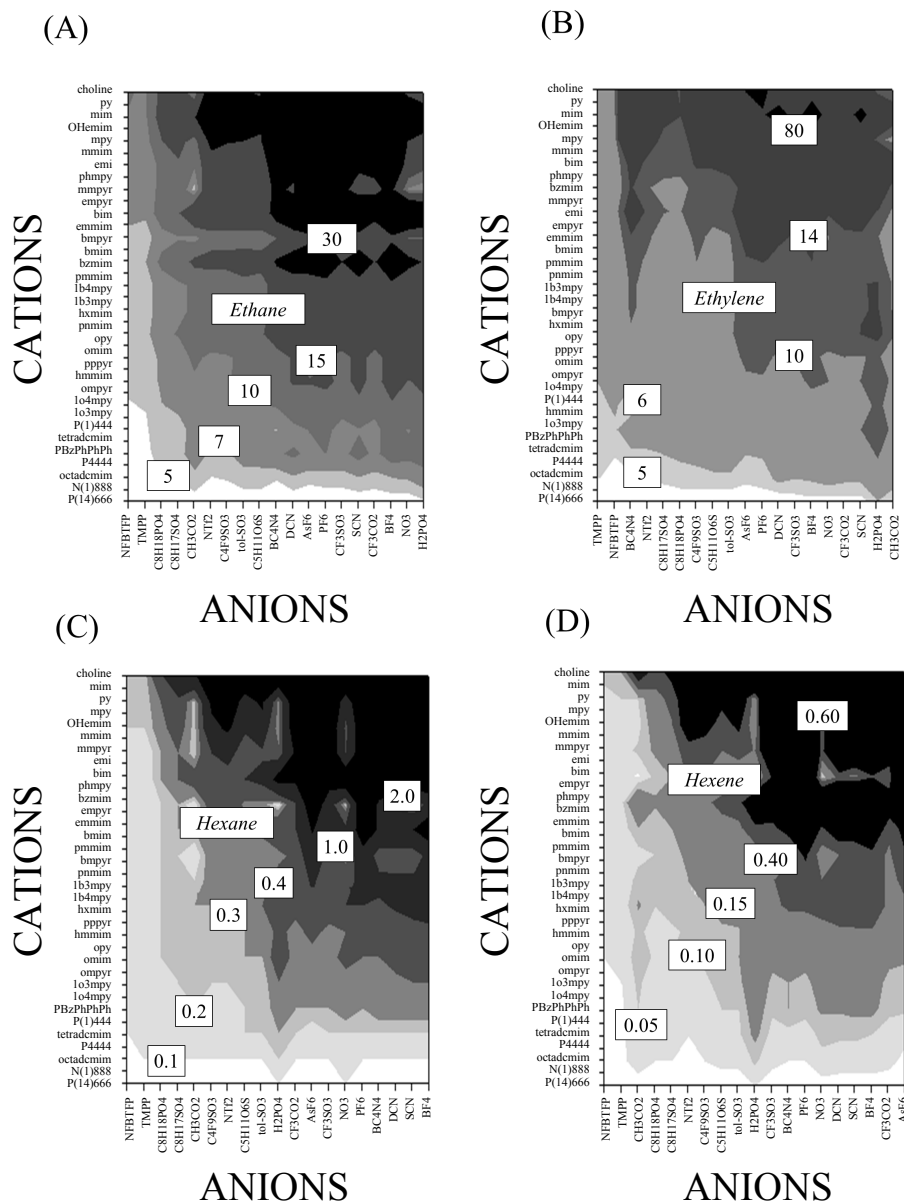


Figure 4.2: Screening of Henry's constants (MPa) of A) ethane, B) ethylene, C) hexane and D) hexene in ILs at 298 K computed by COSMO-RS using the [C+A] solvent effects model.

4.4. Results

Figure 4.2 shows that the lowest Henry’s constants for alkanes in ILs can vary from 5 to 0.1 MPa, and those for alkenes from 5 to 0.05 MPa. Henry’s constants for olefins are lower than those for the corresponding paraffin. Henry’s constants can change by one order of magnitude by tuning the ions chemical structures of the IL. For example, H for ethylene in [P(16)444][TMPP] is 4 MPa while in [choline][DCN] it is 42 MPa. Solubilities of these gases are mainly influenced by the cation. Big cations with strongly aliphatic character, such as [P(14)666]⁺ or [N(1)888]⁺, provide the highest solubilities. However, the anion can play an important role if the IL contains a cation favoring solubility. In this case, big anions with disperse charge, e.g. [TMPP][−] and [NFBTFP][−], enhance solubility.

A good solvent for all hydrocarbons, [P(14)666][TMPP], was given special attention. Figure 4.3 shows that the paraffin or olefin solubility in this IL rises as the hydrocarbon chain of the solute increases. For this solvent, H for paraffins is lower than that for the corresponding olefin. Liu et al. (2013b) experimentally found that [P(16)444][TMPP] IL is the only IL where ethane is more soluble than ethylene.

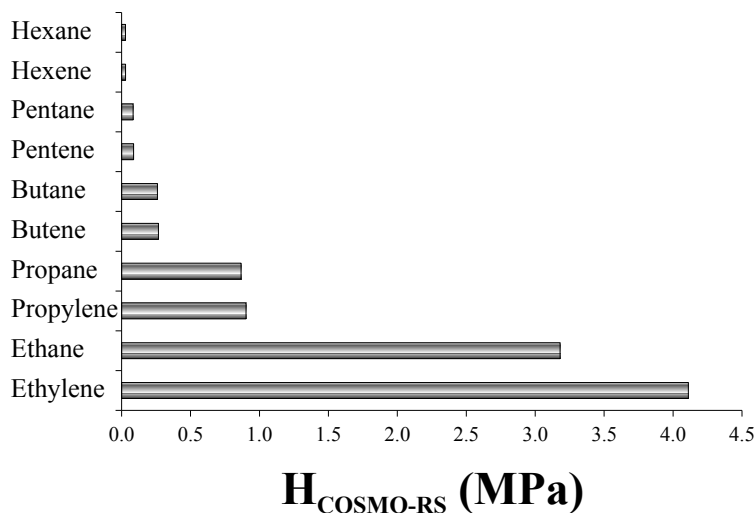


Figure 4.3: Solubility behavior of different hydrocarbons in [P(14)666][TMPP]. The Henry’s constants are calculated from COSMO-RS using vapor pressures from experimental data at 298 K. The IL was simulated by the [C+A] solvent effects model. Line shows perfect agreement between calculated and experiment.

4.4.2 Differences between [CA] and [C+A] models in Henry's constants calculation

Previous results (Fallanza et al., 2013) showed that deviations between calculated and experimental Henry's constants are lower using the ion-pair COSMO-RS model, [CA], instead of the [C+A] model. However, Figure 4.4 shows that the [C+A] model generally provides better results than the [CA] model. For the more favorable solvents (H from 0.6 to 5 MPa), the [CA] model is particularly more accurate. Details can be seen in Table 4.2, where the [CA] model provides better results (AAD=0.48 MPa) than the [C+A] model (AAD=1.43 MPa) for mixtures containing the [P(14)666][TMPP] ionic liquid solvent.

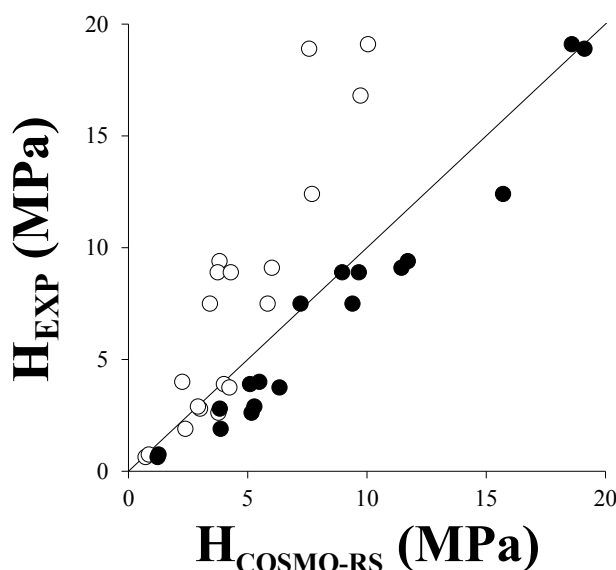


Figure 4.4: Experimental vs. COSMO-RS Henry's constants for paraffins and olefins in ILs at different temperatures. The ILs were simulated by the [C+A] (black) and [CA] (white) solvent effects models. Line shows perfect agreement between calculated and experiment.

As shown in Figure 4.5, activity coefficients using the [CA] model are systematically lower than those using the [C+A] model, but they are similar for low Henry's constants (high solubilities).

4.4.3 Data for the ethane/Ethylene-IL systems

Figure 4.6 shows the experimental and calculated $\alpha_{\text{ethane/ethylene}}$ for several ILs studied at 313.5 K using both [C+A] and [CA] models. Regardless of the model, COSMO-RS

4.4. Results

Table 4.2: COSMO-RS calculations for Henry’s constants of ethane, ethylene, propane and propylene in [P(14)666][TMPP] at 313.15 K.

Solute	H_{EXP} (MPa)	$H_{\text{COSMO-RS}}$ (MPa)	
		[C+A]solvent effects	[CA]solvent effects
Ethane	1.9	3.9	2.4
Ethylene	2.6	5.2	3.8
Propane	0.6	1.2	0.7
Propylene	0.8	1.3	0.9

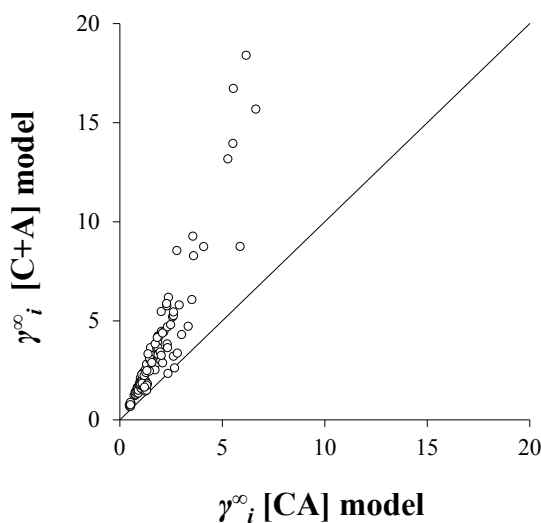


Figure 4.5: Comparison between the [CA] and [C+A] models for estimating activity coefficients at infinite dilution of some paraffins and olefins in ILs. Line shows perfect agreement.

is suitable for predicting $\alpha_{\text{ethane/ethylene}}$, particularly for the case of favorable ILs with low $\alpha_{\text{ethane/ethylene}}$ values. [P4444][TMPP] and [P(14)666][TMPP] are the best solvents for the separation, with $\alpha_{\text{ethane/ethylene}} < 1$, where ethane is more soluble than ethylene. Equation 4.3 shows that the relative volatility depends on both selectivity and on the ratio of vapor pressures in the hydrocarbons. Table 4.3 shows the two terms contributing to $\alpha_{\text{ethane/ethylene}}$ for 4 ILs selected from the COSMO-RS screening (Figure 4.2). The desired IL should provide $\alpha_{\text{ethane/ethylene}}$ much lower than 1.

As shown in Table 4.3, the $P^{\text{s}}_{\text{ethane}}/P^{\text{s}}_{\text{ethylene}}$ ratio contributes favorably to the desired separation because it is lower than 1. Since $\alpha_{\text{ethane/ethylene}}$ decreases with $s_{\text{ethane/ethylene}}$, lower values of $s_{\text{ethane/ethylene}}$ are desired. Table 4.3 shows that the the chemical structure

4. Separation of small paraffin-olefin mixtures with an ionic liquid. Thermodynamic study using COSMO-RS

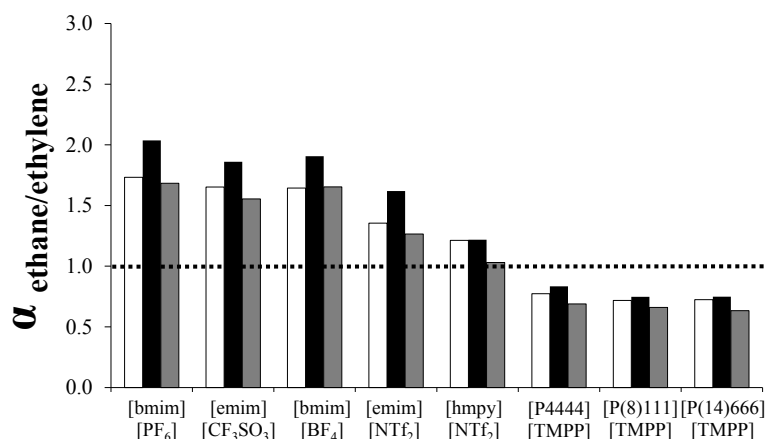


Figure 4.6: Experimental (white bars) and calculated (dark bars) relative volatilities of ethane/ethylene with ILs using vapor pressures from experimental data at 313.15 K. The ILs were simulated by the [C+A] model (black bars) and by the [CA] model (grey bars).

of the IL plays a very important role in selectivity. $S_{\text{ethane/ethylene}}$ falls when increasing the aliphatic character of the cation. Upon increasing the alkyl chain of the phosphonium ion, γ^∞ for ethane and γ^∞ for ethylene decrease, leading to a desired lower values of selectivity, $S_{\text{ethane/ethylene}}$.

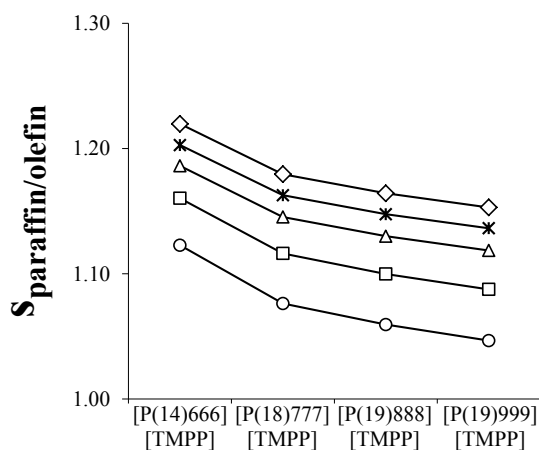


Figure 4.7: Selectivity of the systems: ethane/ethylene (circle), propane/propylene (square), butane/butene (triangle), pentane/pentene (asterisk) and hexane/hexene (diamond), in different ILs simulated by the [C+A] model at 298 K.

Varying the cation structure, new ionic liquids similar to [P(14)666][TMPP] were proposed for ethane/ethylene separation. We created cosmo files for [P(18)777], [P(19)888] and [P(19)999] cations as they are not given in the COSMO-RS database optimizing the

4.4. Results

Table 4.3: Experimental vapor pressure ratio for different solutes. COSMO-RS calculations of selectivity and relative volatility for paraffin/olefin in different ILs at 298 K. The ILs were simulated by the [C+A]solvent effects model.

Ionic Liquid	Paraffin/olefin	P_p^s/P_o^s	s	α
[P(14)666][TMMP]	ethane/ethylene	0.64	1.12	0.72
[P444][TMMP]			1.26	0.81
[P(1)444][TMMP]			1.28	0.82
[hmpy][NTf ₂]			1.91	1.23
[P(14)666][TMMP]	propane/propylene	0.83	1.16	0.96
[P444][TMMP]			1.29	1.07
[P(1)444][TMMP]			1.32	1.09
[hmpy][NTf ₂]			2.02	1.67
[P(14)666][TMMP]	butane/butene	0.82	1.19	0.97
[P444][TMMP]			1.31	1.07
[P(1)444][TMMP]			1.33	1.09
[hmpy][NTf ₂]			1.98	1.62
[P(14)666][TMMP]	pentane/pentene	0.80	1.2	0.96
[P444][TMMP]			1.32	1.05
[P(1)444][TMMP]			1.35	1.08
[hmpy][NTf ₂]			1.99	1.59
[P(14)666][TMMP]	hexane/hexene	0.81	1.22	0.98
[P444][TMMP]			1.34	1.08
[P(1)444][TMMP]			1.37	1.1
[hmpy][NTf ₂]			2.01	1.62

geometry in condensed phase - solvent effects (see Chapter II). Figure 4.7 shows that $s_{\text{ethane/ethylene}}$ decreases as the alkyl chain of the cation rises. [P(19)999][TMPP] may be the most promising IL for ethane/ethylene separation.

4.4.4 Data for the propane/propylene-IL systems

Figure 4.8 shows experimental and calculated $\alpha_{\text{propane/propylene}}$ for 5 ILs at 313.15 K. Regardless of the model, COSMO-RS is again suitable for estimating $\alpha_{\text{propane/propylene}}$, particularly for favorable ILs with low $\alpha_{\text{propane/propylene}}$ values.

Liu et al. (2013b) experimentally found that propane was more soluble in [P(16)444][TMPP] IL than propylene. Both models show higher affinity of [P(14)666][TMPP] for propane than for propylene. Table 4.3 shows the two terms contributing to $\alpha_{\text{propane/propylene}}$ for 4 ILs

4. Separation of small paraffin-olefin mixtures with an ionic liquid. Thermodynamic study using COSMO-RS

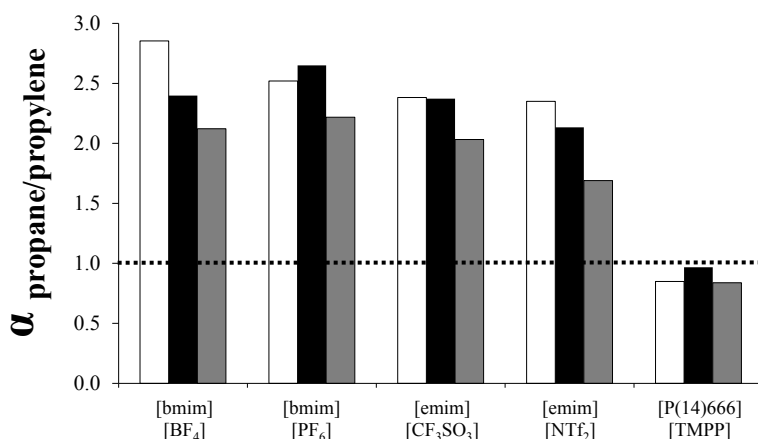


Figure 4.8: Experimental (white bars) and calculated (dark bars) relative volatilities for propane/propylene with ILs using vapor pressures from experimental data at 313.15 K. The ILs were simulated by the [C+A] model (black bars) and by the [CA] model (grey bars).

selected from the screening using the [C+A] model at 298 K. Selection is based on the most promising IL for the separation. The desired IL should provide $\alpha_{\text{propane/propylene}}$ much lower than 1 (see Figure 4.2). As shown in Table 4.3, the $P^s_{\text{propane}}/P^s_{\text{propylene}}$ ratio contributes favorably to the desired separation because α is lower than 1. However, this contribution to relative volatility is less favorable than for ethane/ethylene where $P^s_{\text{ethane}}/P^s_{\text{ethylene}}$ is lower than $P^s_{\text{propane}}/P^s_{\text{propylene}}$. Since $\alpha_{\text{propane/propylene}}$ decreases with selectivity, lower values of $S_{\text{propane/propylene}}$ are preferred. As for ethane/ethylene, studying selectivity can provide a good tool for selecting the most promising IL for the paraffin/olefin separation. Table 4.3 shows that [P(16)444][TMPP] provides the lowest $S_{\text{propane/propylene}}$ at 298 K. This is the only IL where propane is more soluble than propylene. Because $S_{\text{propane/propylene}}$ decreases as the length of the alkyl chain on the cation increases, we evaluate the same ILs that we propose for the ethane/ethylene separation. Figure 4.7 shows that a highly aliphatic IL like [P(19)999][TMPP] is most promising for the propane/propylene separation.

4.4.5 Data for the systems: butane/butene, pentane/pentene or hexane/hexene with an ionic liquid

Figure 4.9 shows $\alpha_{\text{butane/butene}}$ in the [bmim][NTf₂] IL solvent as a function of temperature. The [C+A] COSMO-RS model slightly overestimates the $\alpha_{\text{butane/butene}}$ while the [CA] model underestimates. Nevertheless, both models reproduce the relative volatility decrease with rising temperature.

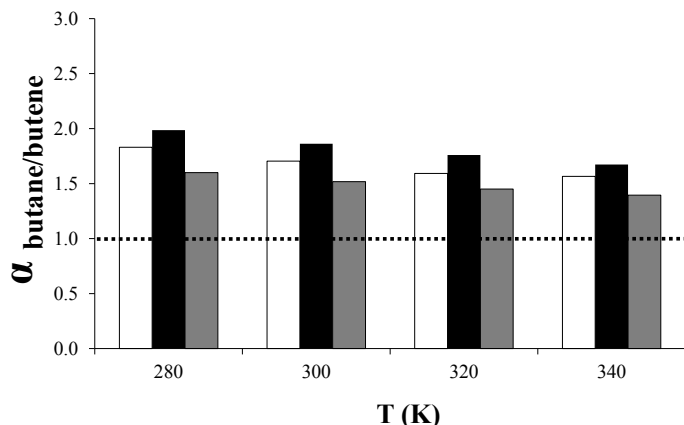


Figure 4.9: Experimental (white bars) and calculated (dark bars) relative volatilities for butane/butene with [bmim][NTf₂] using vapor pressures from experimental data at different temperatures. The ILs were simulated by the [C+A] model (black bars) and by the [CA] model (grey bars).

Once COSMO-RS estimates are validated for several paraffin/olefin systems from 2 to 4 carbon atoms, we calculate α and s using the [C+A] model at room temperature for butane/butene, pentane/pentene and hexane/hexene for 4 ILs (Table 4.3). The desired IL should provide $\alpha_{\text{paraffin/olefin}}$ much lower than 1. Table 4.3 shows that all $P_{\text{paraffin}}^s/P_{\text{olefin}}^s$ ratios contributes favorably to the desired separation because they are different than 1. The vapor pressure ratio is similar to $P_{\text{propane}}^s/P_{\text{propylene}}^s$; it does not change significantly when increasing the alkyl chain of the paraffin and the olefin. $P_{\text{butane}}^s/P_{\text{butene}}^s$, $P_{\text{pentane}}^s/P_{\text{pentene}}^s$ and $P_{\text{hexane}}^s/P_{\text{hexene}}^s$ are similar. At room temperature, [P(16)444][TMPP] provides the lowest $\alpha_{\text{paraffin/olefin}}$, and the only one where paraffin is more soluble than olefin.

As shown for ethane/ethylene and propane/propylene, lower $s_{\text{paraffin/olefin}}$ is favored to obtain $\alpha_{\text{paraffin/olefin}}$ lower than 1. Table 4.3 shows that upon increasing the aliphatic character of the IL, $s_{\text{paraffin/olefin}}$ decreases. As the IL chemical structure plays a very important role in the selectivity for all studied systems, we evaluate the new ILs that we propose for the ethane/ethylene and propane/propylene separation. Figure 4.7 shows

4. Separation of small paraffin-olefin mixtures with an ionic liquid. Thermodynamic study using COSMO-RS

that upon decreasing the alkyl chain of the solute in the IL, the selectivity paraffin/olefin decreases, the affinity of the IL for the paraffin is higher. At the same time, upon increasing the alkyl chain of the cation in the IL, the affinity of the IL for the paraffin also increases. The selection of highly aliphatic ILs can provide better separations where the paraffin is more soluble than the olefin. Hence, [P(19)999][TMPP] can be proposed as a suitable ionic liquid for a paraffin/olefin separation.

4.5 Concluding remarks

We report a comparison of experimental and estimated Henry’s constants for methane, ethane, ethylene, propane, propylene, butane and butene in different ILs using COSMO-RS and the independent-ion model, [C+A]. COSMO-RS overestimates H compared to experiment when COSMO-RS is used to obtain vapor pressures for solutes. However, good agreement with experiment was obtained when experimental vapor pressure for solutes were selected for H calculations. We also consider the molecular ion-pair model, [CA], to simulate the IL in COSMO-RS calculations. The [C+A] model in general provided better estimations for Henry’s constants than the [CA] model. However, the [CA] model provided quantitatively better estimations for low H .

Henry’s constants are screened by COSMO-RS for ethane, ethylene, hexane and hexene in 646 ILs at room temperature using the [C+A] model. Big cation and aliphatic character as in $[P(14)666]^+$ and big anions with disperse charge as $[TMPP]^-$ favor the solubility of the hydrocarbon in the IL. Paraffin or olefin solubility in the IL rises upon increasing the hydrocarbon chain of the solute.

Relative volatilities and selectivities for ethane/ethylene, propane/propylene and butane/butene calculated by COSMO-RS were compared to those obtained from experiment. The better affinity of $[P(14)666][TMPP]$ for paraffins instead of olefins is well reproduced by COSMO-RS.

New phosphonium-based ionic liquids with highly aliphatic character were proposed for the separation of paraffin/olefin systems. The $[P(19)999][TMPP]$ ionic liquid is displayed as a promising option for paraffin/olefin separations from a thermodynamic point of view.

Part II

PROCESS SIMULATION

Chapter 5

Ionic liquids design/selection for separation processes based on operational and economic criteria through the example of their regeneration

THE integration of the COSMO-RS method in the Aspen Tech's process simulators is used in this chapter to elaborate new criteria for designing/selecting ionic liquids for specific applications. The pursued criteria for selecting suitable ionic liquids are related to the operating conditions and energy consumptions. The predictive capacity of the COSMO-RS method for predicting the vapor liquid equilibrium of (organic solvent + IL) binary mixtures is previously assessed. The transfer of the COSMO-RS calculations to Aspen Plus/Aspen HYSYS is tested by comparing calculated heat capacities and VLE with experiment. The capability of this strategy is demonstrated through the example of the IL regeneration from mixtures coming from separation processes.

5.1 Introduction

The optimization criteria used in the design and selection of the IL for taking part in certain separation process are usually related to the equilibrium, i.e. to the thermodynamic properties of the system: relative volatilities, solubilities, partition coefficients, selectivities, etc. However, the development of ILs with real applicability in industrial processes needs a more complete and consistent set of criteria to optimize the ion selection. This set of properties should include parameters related to the operating conditions, energy consumption, operating and capital costs, etc. Thermodynamic and economic criteria for a specific process or system do not often coincide. The information related to the operating conditions and costs can be obtained via process simulation.

ILs have been evaluated in numerous separation processes as, for instance, the separation of aromatic and aliphatic hydrocarbons, purification of gasoline octane boosters and desulphurization processes (Meindersma, 2005; Meindersma et al., 2006; Meindersma and de Haan, 2008; Pereiro and Rodríguez, 2010; Arce et al., 2006b, 2007). Furthermore, ILs have exhibited high capacity as entrainers to separate azeotropic and/or close-boiling mixtures containing alcohols, water, THF, ETBE, ethyl acetate, ketones, aromatic and aliphatic hydrocarbons, hydrofluorocarbons, propene-propane so on (Jork et al., 2004; Seiler et al., 2004; Shiflett and Yokozeki, 2006a; Pereiro and Rodríguez, 2009, 2008a; Pereiro et al., 2010; Pereiro and Rodríguez, 2008b). ILs have also been considered for separating organic acids, phenols and aromatic amines, oil mixtures as well as biomolecules (lipids, proteins, antibodies, etc.) from their growth and/or reacting media (Cascon et al., 2011; Ruivo et al., 2010; Tomé et al., 2010; Domínguez-Pérez et al., 2010; Young et al., 2010; Martínez-Aragón et al., 2009; Egorov et al., 2008; Marták and Schlosser, 2007; Matsumoto et al., 2004).

In any separation process the IL outflow should be regenerated and recycled to the beginning of the process in order to reduce total costs (Fernandez et al., 2011). It is known that the economy of the processes with solvents is determined by the supply of fresh solvent. This is important for ILs, because they are particularly expensive. Their price is estimated in 10-30 €/kg by the BASF, a major producer of imidazole, one of the primary products used in the production of ionic liquids (Meindersma, 2005; Meindersma and de Haan, 2008). Due to the high production costs, any extension of the ILs lifetime by reuse and recycling is interesting (Fernandez et al., 2011).

Some authors have reported either the conceptual design of separation processes using ILs (Meindersma, 2005; Meindersma et al., 2006; Meindersma and de Haan, 2008; Shiflett

5. Ionic liquids design/selection for separation processes based on operational and economic criteria through the example of their regeneration

and Yokozeki, 2006a) and/or simulations of individual separation processes with ionic liquid (Lei et al., 2006; Palomar et al., 2008, 2009b; Meindersma, 2005; Meindersma et al., 2006; Meindersma and de Haan, 2008; Pereiro and Rodríguez, 2010; Arce et al., 2006b, 2007; Seiler et al., 2004; Shiflett and Yokozeki, 2006a; Pereiro and Rodríguez, 2009, 2008a; Pereiro et al., 2010; Pereiro and Rodríguez, 2008b). Some of them present a matter balance specifying the IL recovery. However, they do not solve the phase equilibrium for the corresponding VL operation (Pereiro and Rodríguez, 2010, 2009, 2008a; Pereiro et al., 2010; Pereiro and Rodríguez, 2008b). Then the regeneration is not simulated (Meindersma, 2005; Meindersma and de Haan, 2008; Arce et al., 2006b).

Only a few works simulate the regeneration operation with shortcut distillation models or equilibrium-based VL separators (Arce et al., 2007; Seiler et al., 2004; Shiflett and Yokozeki, 2006a; Pereiro and Rodríguez, 2009). In most cases it has not been possible to develop or optimize the complete process. This happens because of either severe errors occurring in the flowsheet simulation (Meindersma, 2005; Meindersma and de Haan, 2008) or the absence of information on the VL equilibrium, such as the heat capacities of the ILs and their mixtures with conventional organic solvents (Arce et al., 2007).

In these simulations two conflicting issues come into view:

- Since ionic liquids are not available in the simulator (usually Aspen Plus or Aspen HYSYS) databank, the values of parameters for several physical properties of the ionic liquid are estimated, guessed or simply left out (Meindersma, 2005; Meindersma and de Haan, 2008). The simulation crashes if the non-supply or non-consistently estimated information of the pure components is demanded in any critical calculation step.
- The activity coefficients in these simulations are calculated using NRTL or UNIQUAC property models. The binary coefficients are regressed from experimental LL or VLL equilibrium diagrams. Using NRTL and UNIQUAC activity models to correlate experimental SL, LL, VL and VLL data for mixtures of conventional organic solvents and ILs is a common practice (Meindersma, 2005; Meindersma et al., 2006; Meindersma and de Haan, 2008; Pereiro and Rodríguez, 2010; Arce et al., 2006b, 2007; Jork et al., 2004; Kato et al., 2004; Shiflett and Yokozeki, 2006b). However, they are not physically consistent for electrolyte systems as ILs are (Simoni et al., 2008; Chen et al., 2008). The good correlations for LL and VL equilibrium of IL/organic solvent mixtures reached with these activity models have strictly statistic but not predictive character. The inability of these equations to adequately repro-

duce all the features of the physical behavior of this kind of systems along with the strong system-dependent character of these models are, in several cases, the cause of the simulation failures.

In correspondence, both a sufficient specification when creating non-databank IL components and a predictive model for describing the VLE of IL/organic solvent mixtures are needed to simulate the regeneration of ILs with the aim of using it in the theoretical design of new ILs with specific desired properties. The COSMO-RS model ([Diedenhofen and Klamt, 2010](#)) has shown to yield good qualitative and satisfying quantitative predictions for the activity coefficients of neutral compounds in ionic liquids and for mixtures of ionic liquids and neutral solvents. Since this success was achieved without any special parameterization, COSMO-RS has become a widely used and efficient tool for the prediction and screening of ionic liquid properties. COSMO-RS has been successfully applied in the prediction of densities ([Palomar et al., 2007b](#)), vapor pressures and vaporization enthalpies ([Diedenhofen et al., 2007](#)) of ILs, activity coefficients at infinite dilutions ([Diedenhofen et al., 2003](#); [Banerjee and Khanna, 2006](#)) in mixtures of a hydrocarbon, an alcohol or a polar compound in an IL, gas solubilities and Henry’s law constants ([Manan et al., 2009](#); [Palomar et al., 2011a](#)), LLE of binary and ternary mixtures of organic compounds and ILs ([Domańska et al., 2006](#); [Freire et al., 2007](#); [Banerjee et al., 2008](#); [Freire et al., 2008](#)), VLE for binary mixtures including conventional organic solvents and ILs ([Diedenhofen and Klamt, 2010](#); [Freire et al., 2007](#); [Banerjee et al., 2008](#); [Freire et al., 2008](#); [Kato and Gmehling, 2005b](#); [Banerjee et al., 2006](#)).

[Banerjee et al. \(2006\)](#) used a COSMO-RS variant, where the parameters of the model were fitted to the VLE data of neutral systems. They used it for the VLE prediction of 13 IL systems [Cxmim][NTf₂] (x = 1, 2, 4), [mmim][C₂H₆PO₄], [emim][C₂H₅SO₄] with benzene, cyclohexane, acetone, 2-propanol, water and THF. The authors used the ion-pair [CA] model and achieved a good agreement with experiment for vapor pressure, with a root mean square deviation of 6.6%. In a further work ([Banerjee et al., 2008](#)), they reduced the RMSD of these predictions to 3.7% using the [C+A] model.

[Freire et al. \(2008\)](#); [Freire et al. \(2007\)](#) reported COSMO-RS predictions for the VLE of [Cxmim][NTf₂] (x=2, 4, 6), [bmim][C₈H₁₇SO₄] with ethanol, propanol, 2-propanol and methanol, and [Cxmim][NTf₂] (x = 2, 4), [bmim][I], [bmim][BF₄], [Cxmim][PF₆] (x = 4, 8), [mmim][C₂H₆PO₄], [emim][C₂H₅SO₄] with water. They used the general parameterization of COSMO-RS as implemented in the COSMOtherm program package. VLE predictions using the electroneutral ion mixture [C+A] model, are better than that obtained for LLE

5. Ionic liquids design/selection for separation processes based on operational and economic criteria through the example of their regeneration

on similar systems. For the alcohol/IL VLE, the correct temperature dependence of the liquid phase non-ideality, and the positive deviation from Raoult's law with decreasing alkyl chain length, are properly described. An overestimation of the positive deviation of Raoult's law appears for very short chain alcohols, such as methanol. A better accurate in the VLE estimation for the water/IL mixture is obtained when the IL contains a hydrophobic anion, such as $[\text{NTf}_2]$, instead of a more polar anion. The temperature dependence of the pressure is described qualitatively.

Kato and Gmehling (2005b) used the COSMO-RS model modified by Grensemann and Gmehling (2005) (COSMO-RS(O1)) to predict the VLE and other thermodynamical properties of binary mixtures composed by cyclohexane, cyclohexene, methanol and ethanol with $[\text{Cxmim}][\text{NTf}_2]$ ($x = 1, 2, 4, 6$) ILs. The mean relative deviations between experiment and the COSMO-RS(O1) predictions are 79.4%. They used the [C+A] model together with DFT screening charges performed on ion structures optimized at semi-empirical (AM1) gas phase computational level.

Diedenhofen and Klamt (2010) demonstrated that VLE for (fluorinated alkanes + $[\text{bmim}][\text{PF}_6]$) and (ammonia + $[\text{hxmim}][\text{Cl}]$) mixtures can be reasonably well predicted by the COSMO-RS method. This performance has supported the decision adopted in this thesis related to the use of COSMO-RS to generate the information needed both for creating IL non-databank components and for specifying COSMOSAC property model (Lin and Sandler, 2002a) in Aspen Plus (Aspen Technology, 2004a) process simulator.

In this chapter the convenience of introducing operating conditions and economic criteria for designing new ILs is discussed through the example of the IL regeneration in separation processes. Operating conditions and economic evaluation of the IL regeneration are established by process simulations using COSMOSAC property package as implemented in Aspen Plus.

Previously, the capacity of the COSMO-RS method for predicting the VLE of binary mixtures of conventional organic solvents and ILs is discussed. The ILs are created as pseudocomponents making use of the capabilities deployed in the aspenONE software package and the information derived by COSMO-RS method. This work is organized in four parts:

1. Firstly the predictive capacity of the COSMO-RS method with respect to the VLE of binary mixtures composed by ILs and conventional organic solvents is analyzed.
2. Secondly, the transferability of the COSMO-RS results to the Aspen Plus process

simulators is proven.

3. Afterwards, the IL regeneration from their mixtures with organic solvents of different functionalities is simulated. The operating conditions and energetic consumptions of the process are established and systematically studied as a function of the nature of compounds.
4. Finally, the application of new criteria is discussed in the context of an overall process like the separation of aliphatic and aromatic hydrocarbons with ILs.

5.2 Computational details

In this chapter the molecular structures of the considered ILs have been described using the ion-paired [CA] and the ion-separated [C+A] models. The ions and ion-paired structures were optimized at the B3LYP/6-31++G(d,p) computational level in the ideal gas-phase using the quantum chemical Gaussian03 package (Frisch et al., 2003). The version C21_0111 of the COSMOthermX program package (Eckert and Klamt, 2010) and its implicit (BP_TZVP_ C21_0111) parametrization was used to accomplish the calculations of the σ -profiles and the physicochemical data (normal boiling temperatures and densities) of ILs as well as the VLE of (organic solvent + IL) binary mixtures. The organic compounds were selected from the C21-0107-BP-TZVP-COSMO database created by COSMOlogic GmbH & Co. KG.

In process simulations, ILs have been created as pseudocomponents in Aspen Plus specifying their molecular weights, normal boiling temperatures and densities. The organic solvents were selected as conventional components from the Aspen Plus database. The COSMOSAC property model as implemented by default in Aspen Plus was selected to estimate the activity coefficients of the components in the mixtures. The molecular volumes and the σ -profiles of ILs were specified by the user whereas those corresponding to the organic solvents were directly taken from the Aspen Plus database. The information used for both creating IL pseudocomponents and specifying COSMOSAC was obtained from the COSMO-RS calculations. The σ -profile of ILs using the [CA] and [C+A] models were considered in preliminary simulations to evaluate the transferability of the COSMO-RS results to the process simulations. The property packages created in Aspen Plus were imported in Aspen HYSYS. Aspen HYSYS supports the process simulations performed in this chapter including heat capacity and VLE predictions. The version 7.3 of the aspenONE program package (Aspen Technology, 2010) was used.

5.3 Results

5.3.1 Prediction of VLE in the (organic solvent-IL) mixtures using COSMO-RS

The vapor liquid equilibrium diagrams (VLE) of 62 (organic solvent + IL) binary mixtures have been calculated in COSMOtherm using both [CA] and [C+A] COSMO models for the IL structure optimized in gas phase. Some of them are shown in Figure 5.1 and Table 5.1.

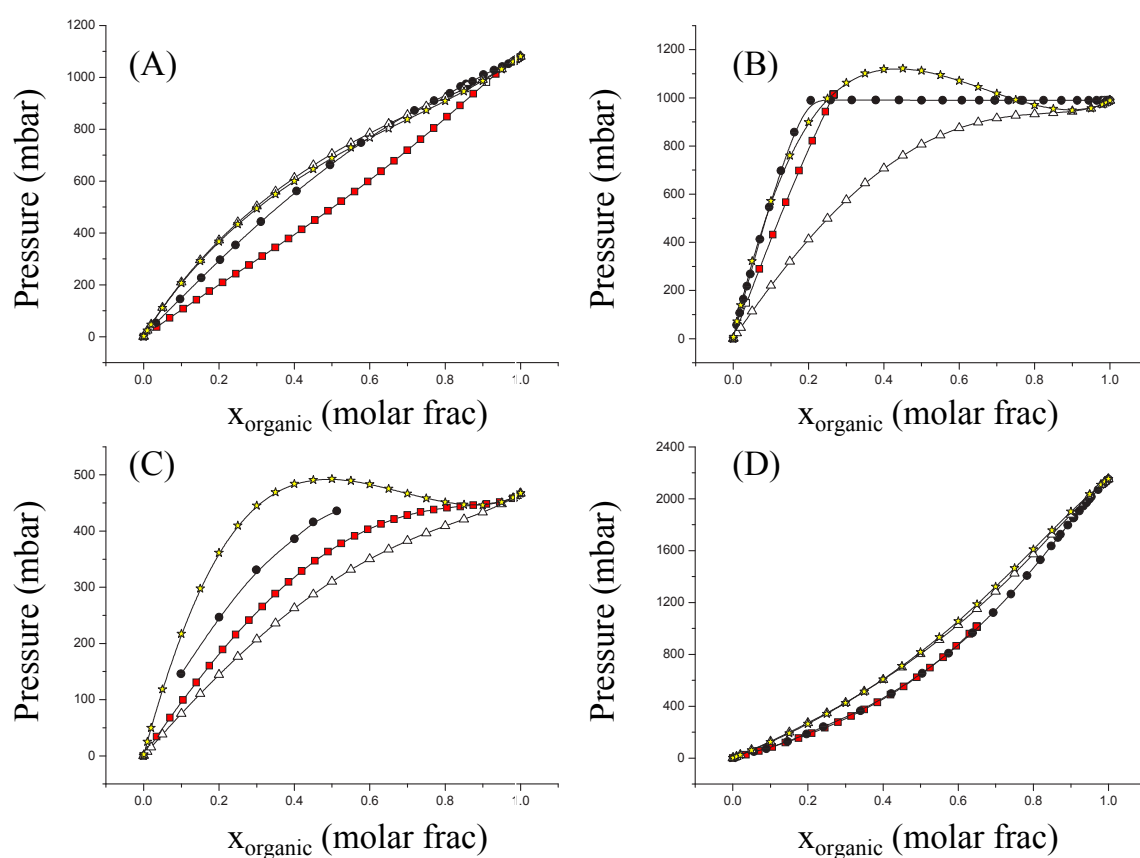


Figure 5.1: VLE diagrams for (A) ethanol/[emim][NTf₂], (B) cyclohexane/[bmim][NTf₂], (C) benzene/[bmim][BF₄] and (D) acetone/[bmim][NTf₂]. Experimental data (black). COSMO-RS calculations using the [CA] (white) and the [C+A] (yellow) models. Aspen HYSYS calculations (red) using the COSMOSAC property model specified with properties of ILs using the [CA] model.

5.3. Results

The binary systems are composed of 1-hexene, 1-octene, 1-propanol, 2-propanol, acetone, benzene, cyclohexane, decane, ethanol, hexane, hexane, methanol, octane, THF, thiophene or water and a very diverse set of ILs (such as imidazoliums or pyridiniums cations and $[\text{NTf}_2]^-$, $[\text{BF}_4]^-$, $[\text{PF}_6]^-$, $[\text{Cl}]^-$, $[\text{C}_2\text{H}_5\text{SO}_4]^-$, $[\text{C}_4\text{H}_{10}\text{PO}_4]^-$, $[\text{C}_2\text{H}_6\text{PO}_4]^-$, $[\text{C}_8\text{H}_{18}\text{PO}_4]^-$, $[\text{C}_8\text{H}_{17}\text{SO}_4]^-$ anions). The COSMO-RS predictions for VLE were validated comparing with experiment (Nebig et al., 2009; Safarov et al., 2006; Verevkin et al., 2005; Döker and Gmehling, 2005; Huo et al., 2009; Kato and Gmehling, 2005a; Calvar et al., 2006; Zhao et al., 2006a; Wang et al., 2007a). The average MRD and RMSD computed between prediction and experiment are, respectively, 32.6% and 56.9 mbar using the [CA] structural model to simulate the ILs. The MRD and RMSD slightly decrease to 30.8% and 44.0 mbar, respectively, using the [C+A] model.

Our results are similar to those obtained by Freire et al. (Freire et al., 2007), (Freire et al., 2008). They are more accurate than those reported by Kato and Gmehling (2005b). The cause of their less accuracy is probably related to the use of an insufficient computational level for the geometry optimization of the ionic liquids. It could also depend on the re-implementation of the COSMO-RS method used by them. On the other hand, our results are worse than those attained by Banerjee et al. (Banerjee et al., 2008, 2006). It suggests that a reparameterization of the COSMO-RS model could be significant to improve the predictive capacity in the VLE calculation.

The average deviations given before correspond to the 62 mixtures studied in this work as a whole. However, the individual values significantly vary depending on the considered system (Figure 5.2). For instance, methanol/[bmim][NTf₂] (MRD 118%), methanol/[omim][BF₄] (MRD 104%) and water/[bmim][BF₄] (MRD 211%) show the highest deviations of the set using the [CA] model. On the other hand, in several cases, the mean relative deviations are appreciably low. For instance, ethanol/[bmim][Cl] (MRD 1.76%), ethanol/[emim][C₂H₅SO₄] (MRD 1.33%) and water/[bmim][Cl] (MRD 1.25%) show the lowest deviations of the set using the [CA] model. Taking into account the diversity of situations, an individual analysis should be recommended in order to study in detail the VLE of IL-based mixtures.

These results should be accurately rationalized and the predictions improved. Nevertheless, they reflect the main tendencies of the VLEs experimentally observed respect to the nature of the IL and the organic solvents (Figure 5.1). In addition, some improvements can be achieved if selecting a suitable molecular structure for the IL ([CA] or [C+A]) as well as a proper optimization for the molecular geometry (gas phase or solvent effects). Basing on the VLE results, the COSMO-RS predictions can be screened for

5. Ionic liquids design/selection for separation processes based on operational and economic criteria through the example of their regeneration

selecting/designing ILs with specific VLE properties.

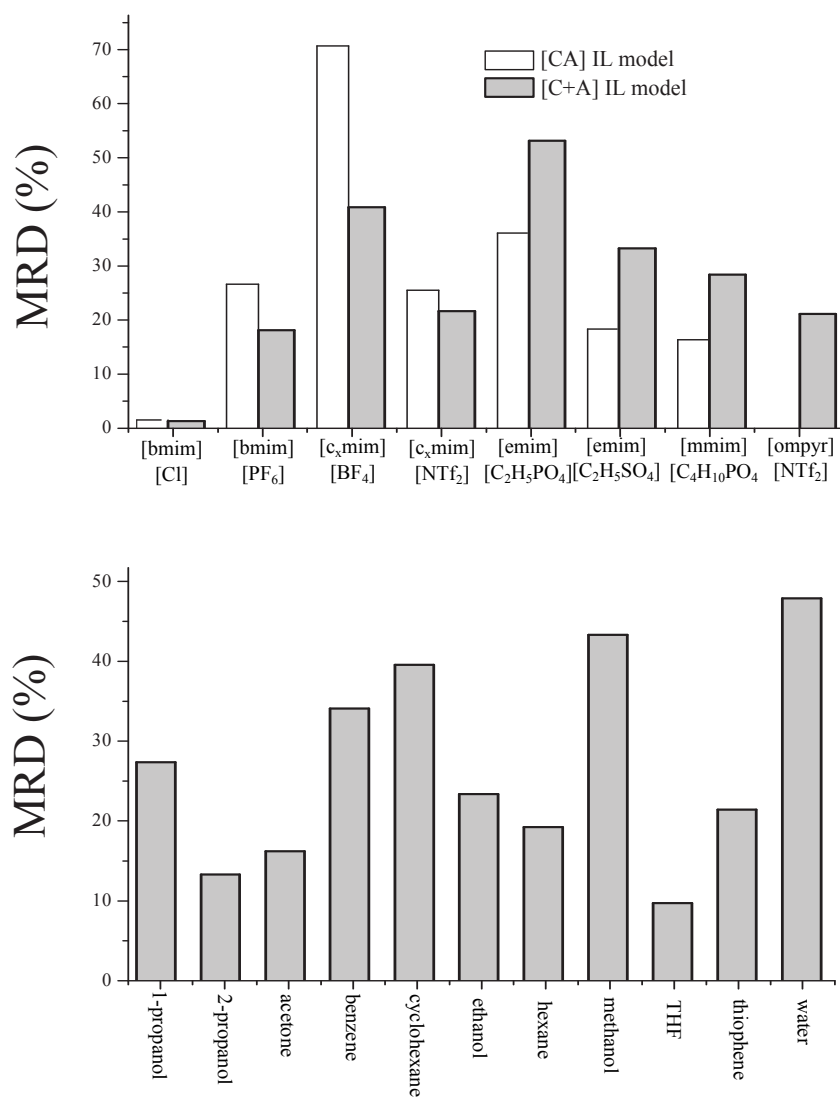


Figure 5.2: Mean relative deviations between COSMO-RS predictions and experimental VLEs of (Organic solvent + IL) binary mixtures depending on the nature of the components.

5.3.2 Prediction of VLE in the (organic solvent-IL) mixtures using Aspen HYSYS

The P-x data of mixtures containing ionic liquids pseudocomponents were calculated using COSMO-supported process simulation to evaluate its predictive capacity.

The MRDs between calculated (with Aspen HYSYS) and experimental VLEs of (organic compound + IL) binary mixtures (Table 5.1) are in the same order of magnitude than those obtained with COSMOthermX. The predictions of Aspen HYSYS are even better in the 50% of the considered systems. The present results validate the computational procedure proposed in this chapter.

The models and computational routes employed by COSMOthermX and Aspen Plus/Aspen HYSYS to compute the studied properties are not only different but also differently implemented in both programs.

The process simulations where the COSMOSAC property model is specified using σ -profiles of the [C+A] IL structures are more deviated with respect to experiment than those achieved with the [CA] model. Thus the following simulations of the IL regeneration process were performed using the σ -profiles of the [CA] IL models to specify COSMOSAC.

5.3.3 Prediction of ILs heat capacities using Aspen HYSYS

In this chapter, we simulate the IL regeneration from its mixture with an organic solvent. The heat capacity of the IL is crucial to evaluate the energy consumption of this process, therefore, to establish selection criteria. The capability for estimating the heat capacities of several ILs in Aspen HYSYS is evaluated.

The heat capacities (Figure 5.3) calculated in Aspen HYSYS for 16 ILs show a mean relative deviations respecting to experiment (ILthermo, 2006) of 12.0% and 18.6%. The COSMOSAC property model was specified by the σ -profiles obtained by the [CA] and the [C+A] models for the ILs, respectively.

5. Ionic liquids design/selection for separation processes based on operational and economic criteria through the example of their regeneration

Table 5.1: Mean relative differences (MRD, %) between the calculations of either COSMO-RS or Aspen HYSYS (using the information obtained in COSMO-RS) and the experimental VLE data for selected (organic solvent + IL) binary mixtures.

Binary mixture	N. points	MRD %			
		COSMO-RS		Aspen HYSYS	
		[CA]	[C+A]	[CA]	[C+A]
1-propanol/[bmim][NTf ₂]	13	10	11.3	–	–
1-propanol/[omim][BF ₄]	6	9.7	8	–	–
2-propanol/[bmim][NTf ₂]	32	10.9	13.1	11.3	24.8
2-propanol/[emim][NTf ₂]	35	9.9	13.4	21	34.7
acetone/[mmim][C ₂ H ₆ PO ₄]	32	19	14.4	36.9	39
acetone/[bmim][NTf ₂]	31	13.8	14.3	2.4	19.7
acetone/[emim][NTf ₂]	29	16.2	19.5	15.9	26.5
benzene/[bmim][BF ₄]	6	16.5	49.3	22.2	74.6
benzene/[bmim][PF ₆]	7	29.2	22.1	6.9	25.8
benzene/[bmim][NTf ₂]	11	6.9	25.9	–	–
benzene/[emim][NTf ₂]	38	7.5	27.5	5.2	18.8
benzene/[mmim][NTf ₂]	35	8.3	35.7	–	–
cyclohexane/[bmim][NTf ₂]	36	24.1	5	19.7	22.7
cyclohexane/[hxmim][NTf ₂]	12	31.9	11.6	25.9	12.9
cyclohexane/[mmim][NTf ₂]	31	27.8	20.6	–	–
cyclohexane/[emim][NTf ₂]	23	28.8	17.8	42.8	28.5
cyclohexane/[hxmim][NTf ₂]	12	23.5	8.6	–	–
ethanol/[bmim][Cl] (Tx) ^a	13	10.4	42.1	–	–
ethanol/[emim][C ₂ H ₅ SO ₄]	4	1.3	3.5	–	–
ethanol/[emim][C ₂ H ₅ SO ₄] (Tx) ^a	15	1.9	2.5	–	–
ethanol/[emim][NTf ₂]	28	7.7	7.4	16	28.9
ethanol/[hxmim][NTf ₂]	28	8.3	5.7	16.4	35.2
hexane/[hxmpyr][NTf ₂]	11	–	16.6	–	–
hexane/[emim][NTf ₂]	40	23.2	13.9	–	–
methanol/[emim][C ₂ H ₅ SO ₄]	14	9	9.7	1.8	6.8
methanol/[hxmim][NTf ₂]	30	23.4	13.8	4.5	19.5
methanol/[mmim][C ₂ H ₆ PO ₄]	28	8.9	7.5	12.4	7.6
THF/[mmim][C ₂ H ₆ PO ₄]	33	–	6.2	45.5	52.4
THF/[emim][NTf ₂]	37	12.9	6.8	34.9	34.9
thiophene/[bmim][BF ₄]	3	40.3	7.2	29.8	29.8
thiophene/[bmim][PF ₆]	4	24	14.2	18.7	19.4
water/[bmim][Cl] (Tx) ^a	25	1.3	0.8	–	–
water/[emim][C ₂ H ₅ SO ₄]	4	10.9	3.6	–	–
water/[emim][NTf ₂]	6	86	37.6	7.5	2.2

^aIsobaric Tx data.

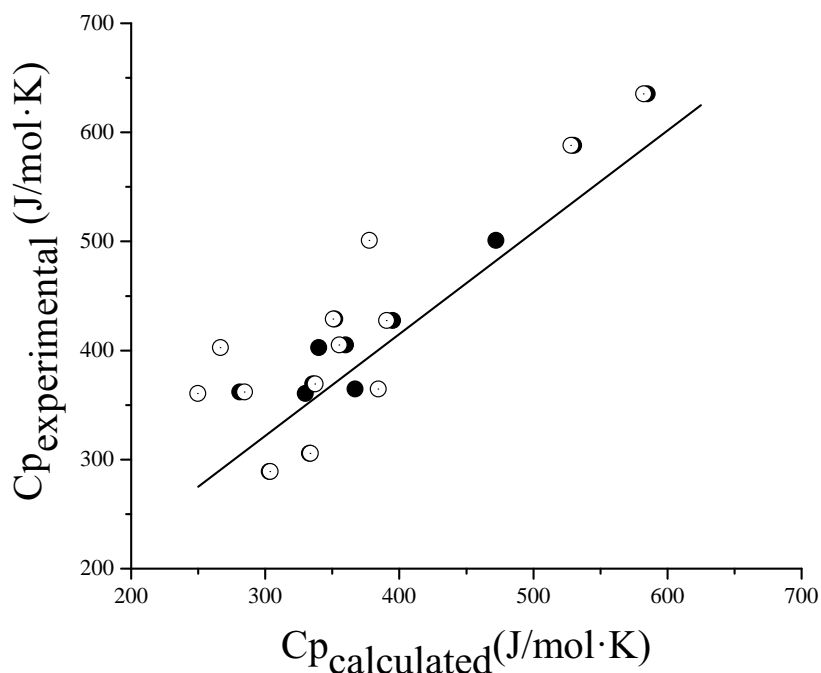


Figure 5.3: Experimental values and Aspen HYSYS calculations for C_p of ILs at 298.15 K (approx.) and atmospheric pressure. The [CA] (black) and [C+A] (white) σ -profiles of the ILs were considered to specify the COSMOSAC model.

5.3.4 Operating conditions and energy consumption of the IL recovery

The conceptual designs developed for separation processes using ILs (Meindersma, 2005; Meindersma et al., 2006; Meindersma and de Haan, 2008; Arce et al., 2007; Shiflett and Yokozeki, 2006a) suggest that ILs could be regenerated from their mixtures with conventional organic solvents by low-pressure evaporation or stripping of the organic solvent.

The viability of the vacuum distillation of ILs has been demonstrated (Taylor et al., 2010) and employed in several applications using ionic liquids:

- The isolation of biaryl products obtained in a Suzuki cross-coupling reaction with [bmim][BF₄] can be carried out at 80°C under vacuum permitting repetitive catalytic runs (Mathews et al., 2000).

5. Ionic liquids design/selection for separation processes based on operational and economic criteria through the example of their regeneration

- Some of the alcohols produced during the reduction of ketones in [bmim][PF₆] could be removed under vacuum. This allowed the reuse of ILs for further reactions (Howarth et al., 2001).
- In the field of enzymatic catalysis. After an application of lipases for an enantioselective reaction in [bmim][NTf₂], the removal of reactants and products was possible at 0.006 kPa and 85°C (Schöfer et al., 2001).
- In an application developed by BASF where ILs modified the equilibrium of several azeotropic systems (Jork et al., 2004). The [emim][MePhSO₃] and [emim][CH₃SO₃] ILs were separated from methanol at 5 kPa and 175°C. High vacuum distillation (ca. $1.33 \cdot 10^{-6}$ kPa) at 120°C was needed to reach a moisture content below 10 ppm in several hydrophobic ILs (Appetecchi et al., 2006).

The VL operation to regenerate the IL is evaluated considering that some ILs (Crosthwaite et al., 2005a; Zaitsau et al., 2006; Heym et al., 2011) with organic solvents undergo significant thermal decomposition at low temperatures. The operative conditions of the IL recovery are limited to determine the pressure of the process for obtaining the IL with a specified purity. Pressure is calculated using the one-stage equilibrium VL operation (flash distillation). Thereby the thermal integrity of compounds is preserved.

We estimate the operating costs related to the energy consumption, but not the capital ones. In the sulfolane process, for example, for separating aromatic from aliphatic hydrocarbons the major costs are related to the heating operations (Meindersma, 2005). The VL separator should not cause an elevated cost. Then it could be neglected in the operating costs. The heat duty to evaporate the organic solvent is required. In these simulations the mechanical work consumed in both fluid transport and vacuum pump is overlooked. The first contribution depends on the process line configuration being out of the scope of this thesis, whereas the second one is relatively small if vacuum is got at low temperatures. Vacuum pumps are expensive affecting the capital cost of the process but they consume low electrical power. Then they provide a low impact on the total operating cost. In this work the energy spending analysis is restricted to that of the fluid heating and vaporization. We consider the major contribution to the total energy balance of the process and the nature of the components to be separated.

Figure 5.4 shows the flowsheet proposed in this work for computing the heat requirement of the organic solvent vaporization and their contributions.

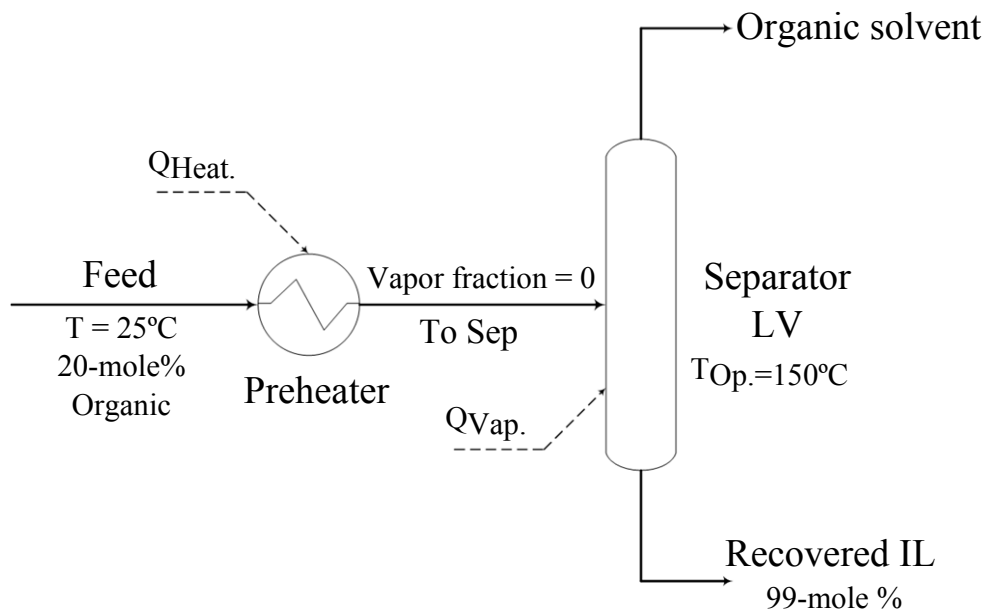


Figure 5.4: Flowsheet and design specifications used in this work for computing the heat duties (and their contributions: $Q_{\text{Vap.}}$ and Q_{Heat}) in the IL regeneration from their mixtures with organic solvents. $\Delta P = 0$ in equipments.

The following design specifications are used in all simulations:

- The (organic solvent + IL) mixture is fed at room temperature. The mixture is preheated to its bubble point. In this form, the total heating load is decomposed in two contributions: Q_{Heat} and $Q_{\text{Vap.}}$.
- The feed to the process has a 20% mole of the organic solvent.
- The recovered IL has a 99% mole of purity.
- The operating temperature of the VL separator is 150°C to avoid the thermal decomposition of compounds. The temperature for the IL decomposition strongly depends on its nature lying in a wide interval. We considered 150°C as limiting situation.
- The pressure drop at the devices is set to 0. This means that the overall flowsheet is at the operating pressure determined by the VLE condition.

5. Ionic liquids design/selection for separation processes based on operational and economic criteria through the example of their regeneration

5.3.4.1 Operating conditions for the VL separator

According to our simulations, the IL regeneration in the considered systems is not achieved at atmospheric pressure and 150°C. In most cases, the calculated operating temperatures for the VL separator are higher than 250 – 300°C. As previously recommended (Meindersma, 2005; Meindersma et al., 2006; Meindersma and de Haan, 2008; Arce et al., 2007; Shiflett and Yokozeki, 2006a), vacuum distillation should be performed to preserve the thermal integrity of the ILs. The pressure has to be reduced up to ca. 5-30 kPa to maintain the operating temperature in the VL separator below 150°C. The calculated pressures are in the same order of magnitude than those obtained in other works (Meindersma, 2005; Meindersma et al., 2006; Meindersma and de Haan, 2008; Arce et al., 2007; Shiflett and Yokozeki, 2006a) where process simulations are supported by NRTL using binary coefficients regressed from experimental VLE data. Pressures also fit well with the experimental results reported by Mathews et al. (2000); Howarth et al. (2001); Schöfer et al. (2001); Appetecchi et al. (2006).

The calculated operating pressure for the studied systems increases 2.5-3.0 times if the temperature rises 1.1-1.3 times (from 150 to 200°C, for instance). This indicates that a dependency between vapor pressure and temperature exists for the considered systems and conditions. The more thermally stable ILs should significantly reduce the vacuum requirements for their regeneration.

The bubble points of the (20% mole organic solvent + IL) mixtures lie in the interval (31.0-76.8)°C at the corresponding operating pressures. These values are 10-65°C higher than the corresponding boiling temperatures of the pure organic solvents at the same pressure. This evidences the strength of the interactions between components in the liquid phase.

The calculated operating pressures depend on the nature of both organic and IL. Due to the difference of volatilities between the components in the mixture, the low-pressure evaporation to regenerate the ILs is a peculiar condition of the VLE. The vapor generated at the VL separator is, for all the studied cases, composed only by the organic solvent. A comparison of the vapor pressure of organic compounds with that of their mixtures with ILs should provide information about the influence of the organic solvent nature on the operating conditions for the IL regeneration.

For the (organic solvent + 99% mole IL) considered mixtures, the vapor pressure of the organic solvents falls approx. two orders of magnitude respect to the pure state as a

5.3. Results

consequence of the interactions in the liquid phase between both components. Moreover, organic solvents undergo similar vapor pressure decreases in their mixtures with the ILs of the same or even relatively different families. Figure 5.5 shows that operating pressure also depends on the length of the alkyl chain in 1-alkyl-3-methyl imidazolium ILs.

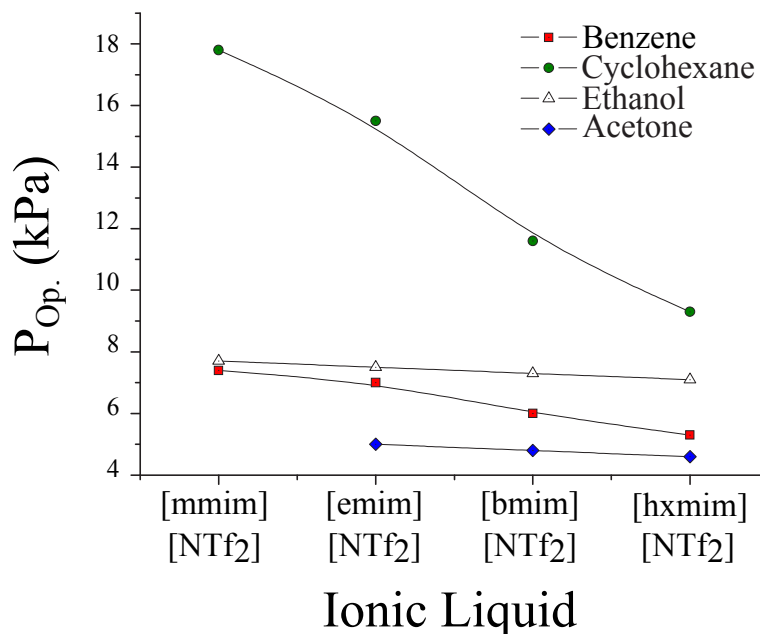


Figure 5.5: Effect of the length of the alkyl chain in 1-alkyl-3-methylimidazolium [NTf₂] on the operating pressure of the IL regeneration from mixtures with organic solvents. Process involves vacuum evaporation of the organic solvent.

The pressure has to be reduced as the length of the alkyl chain increases. This behavior is more acute in nonpolar organic solvents, such as benzene or cyclohexane, than in polar solvents, such as ethanol and acetone.

Figure 5.6 show that operating pressure correlates with the nature of the anion in the IL. This relationship is more general than that observed to the alkyl chain length, i.e. it is significant not only with nonpolar solvents but also with polar ones. The integral evaluation of the results shown in Figure 5.5 and 5.6 allows hypothesizing that shorter chains of the 1-alkyl-3-methyl imidazolium [BF₄] ILs should be regenerated at near-to-atmospheric pressures from mixtures with benzene, for instance.

5. Ionic liquids design/selection for separation processes based on operational and economic criteria through the example of their regeneration

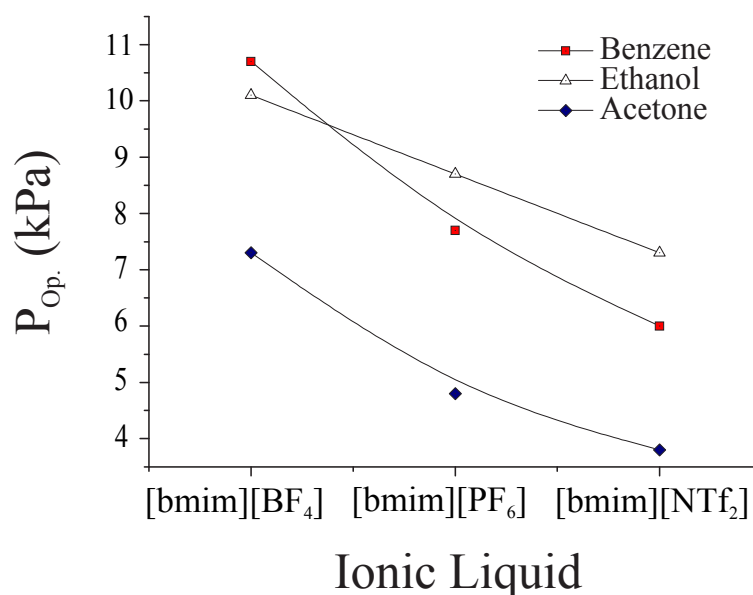


Figure 5.6: Effect of the anion nature on the operating pressure of the IL regeneration from mixtures with organic solvents. Process involves vacuum evaporation of the organic solvent at 150°C.

In fact, our calculations conclude that [bmim][BF₄] could be completely recovered from its mixtures with benzene at atmospheric pressure and temperature over 151.8°C. This result suggests that the computational procedure proposed here is suitable to design ionic liquids using criteria related to process operating conditions.

5.3.4.2 Energy consumptions of the IL recovery process

The energy consumption of the organic solvent vaporization (Q_{vap} in Figure 5.4) from their mixtures with ILs are in the range 120-240 kJ/kg IL regenerated for the considered systems. The duties of the preheating stage (Q_{Heat} in Figure 5.4) fall in the interval (5.0-65.0) kJ/kg (organic solvent + IL) mixture. The heat of vaporization of the organic solvent from their mixtures with ILs (Q_{vap}) is higher than 70% of the total duty ($Q_{\text{vap.}} + Q_{\text{Heat}}$) for the systems studied in this work. It shows an interesting correspondence with the nature of the organic solvent. In fact, $Q_{\text{vap.}}$ is over 75% for polar solvents but rise to approx. 90% when nonpolar solvents are mixed with the same IL. $Q_{\text{vap.}}$ depends on the nature of both IL and organic solvent (Figures 5.7, 5.8 and 5.9).

Figure 5.7 shows that calculated heat of vaporization of the organic solvents from

5.3. Results

their mixtures with ILs are 6.2-14.2 times higher than the heat of vaporization of the pure organic compounds at 150°C.

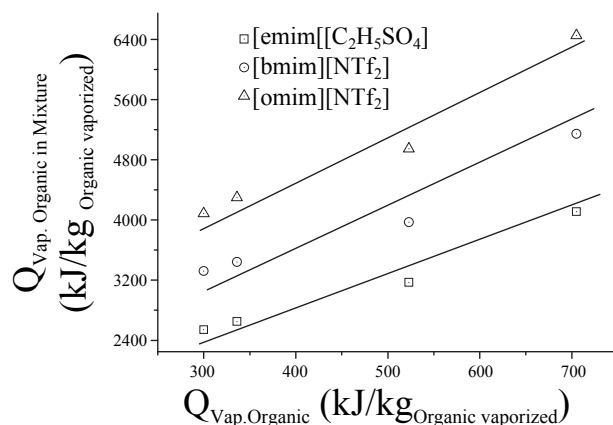


Figure 5.7: The heat of vaporization of an organic solvent in mixture (organic solvent + IL) versus the heat of vaporization of pure organic at 150°C.

This should be taken as a measure of the strength of interactions between ILs and organic solvents in liquid phase. Figure 5.8 shows that $Q_{\text{Vap.}}$ increases with the length of the alkyl chain of cation in mixture. The average ratio is 10.4 kJ per $-\text{CH}_2$ added to the alkyl chain of the cation in the mixtures of [C1,2,4 or 6)mim][NTf₂] and organic solvents of different polarities.

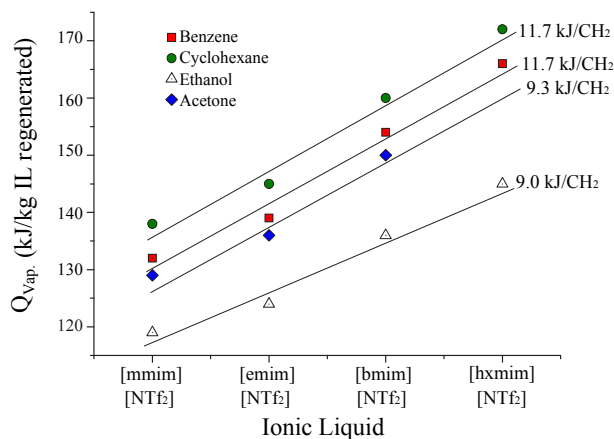


Figure 5.8: Dependence of the heat of vaporization ($Q_{\text{Vap.}}$) of the organic solvent with the alkyl chain length of the cation in the (organic solvent + IL) mixtures.

This means that vaporization heat duty of the same organic solvent from its mixtures

5. Ionic liquids design/selection for separation processes based on operational and economic criteria through the example of their regeneration

with [C1,2,4 or 6)mim][NTf₂] ILs increase approx. 10 times if [hxmim][NTf₂] is used instead of [mmim][NTf₂]. The chain length effect is more acute in nonpolar organic solvents (9.3 to 11.7 times) than that in polar ones (9 times).

Figure 5.9 shows that Q_{vap} depends on the nature of the anion in the IL-organic solvent mixture. The heat spending in evaporating the organic solvent increases approx. 30% when it is mixed with [bmim][BF₄] instead with [bmim][NTf₂] being even higher (approx. 50%) with [1-alkyl-3methyl imidazolium][C₂H₅SO₄] ILs.

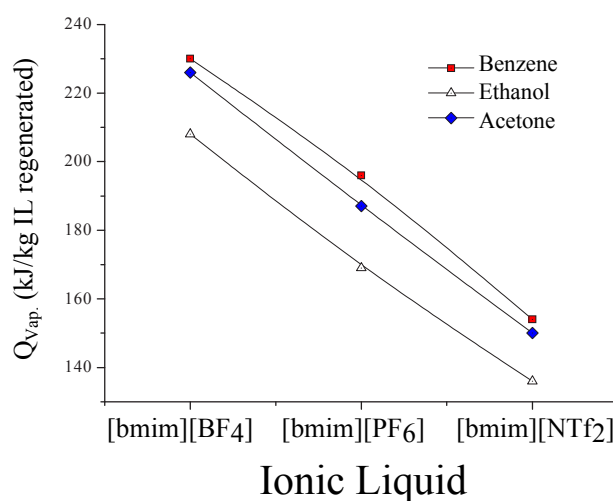


Figure 5.9: Dependence of the heat of vaporization (Q_{vap}) of the organic solvent with the anion nature in the (organic solvent + IL) mixtures.

5.3.5 A case of study: the separation of aromatic/aliphatic hydrocarbons using ILs

The screening performed for selecting/designing suitable ILs for separating aromatic and aliphatic hydrocarbons was based on the separation capacity of the extracting agent (Jork et al., 2005; Palomar et al., 2009b; Meindersma et al., 2006; Meindersma and de Haan, 2008; Arce et al., 2007; González et al., 2010). We reevaluate the IL selection taking also into account the operating conditions and energy consumption needed to regenerate the IL. Figure 5.10 shows the partition coefficients at infinite dilution calculated for the distribution of benzene between cyclohexane and ILs using COSMO-RS. We consider the partition coefficients as a separation capacity criterion.

5.3. Results

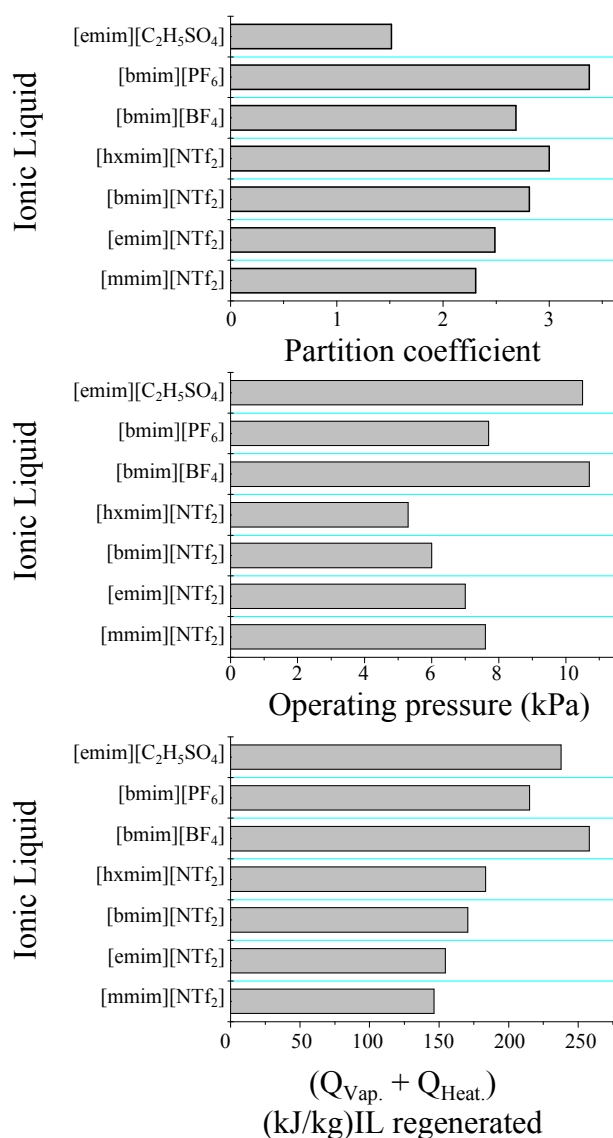


Figure 5.10: Comparison of some ILs as extracting solvents for separating a benzene/cyclohexane mixture. The criteria selected for the comparison are (A) the separation capacity, (B) the operating conditions and (C) the heat duties of the IL regeneration.

The computed solute distribution ratios for different ILs, such as [1-alkyl-3-methyl imidazolium][NTf₂], [bmim][BF₄] or [bmim][PF₆] and [emim][C₂H₅SO₄], agree qualitatively with experiment (González et al., 2010).

As can be seen in Figure 5.10, quantitative patterns for the three criteria considered in this work (partition coefficient in the extraction, operating pressure and the heat duty in the IL regeneration) do not match at all. For the considered systems:

5. Ionic liquids design/selection for separation processes based on operational and economic criteria through the example of their regeneration

1. The [bmim][PF₆] IL ensures the highest aromatic/aliphatic separating capacity in the extraction. (Separation capacity criterion).
2. The mildest operating pressure to achieve the IL regeneration is obtained when [bmim][BF₄] is selected as extractant solvent. (Operating condition criterion).
3. The lowest duty required to regenerate IL (by evaporating benzene from the IL-benzene mixture) is achieved using the [mmim][NTf₂] IL solvent. (Heat duty criterion).

From this, selecting the IL that optimizes the overall (extraction of the solute plus regeneration of the extracting solvent) is not an immediate task. This analysis could turn more complex if other criteria like selectivity of the separation, solvent consumption or capital costs of the process are included.

Finally, we performed a preliminary economical evaluation of the IL regeneration for this process. We considered (average values) $Q_{\text{Vap.}} = 176 \text{ kJ/kg IL regenerated}$ and $Q_{\text{Heat}} = 30.9 \text{ kJ/kg IL regenerated}$. We used the conceptual process developed by [Meindersma \(2005\)](#); [Meindersma and de Haan \(2008\)](#) for the extractive separation of aromatic compounds from an aromatic/aliphatic mixture with an IL. The feed stream flow rate is 300 ton/h with a toluene composition of 10 wt%. The feed stream enters at the bottom of the extraction column. The ionic liquid enters at the top of the extraction column with a flow rate of 1600 ton/hr. The total regeneration of IL by the evaporation of toluene consumes over 1.3 Mton/year of medium vapor pressure. This is approx. 11.4 M€/year (the vapor price is 8.8 €/ton and the capacity factor of the process is assumed to be 90%).

5.4 Concluding remarks

The COSMO-based process simulation is supported by a reasonable predictive capacity of the COSMO-RS method respect to VLE of mixtures (organic solvent + IL). Likewise, the heat capacities of ILs and VLEs for (organic solvent + IL) binary mixtures computed with Aspen HYSYS showed good agreement with experiment. Then a good transferability of the COSMO-RS results into Aspen Plus/Aspen HYSYS process simulators was achieved. This methodology provided results physically coherent and consistent with a molecular interpretation of interactions between both components in liquid phase.

We simulated the IL regeneration from mixtures with conventional organic solvents coming from previous separating processes. Aspen Tech's process simulators allowed for the calculation of operating conditions and heat requirement associated to the IL regeneration. The technical and economic information derived from process simulation could enrich the set of criteria used to select/design the most suitable IL for specific uses.

The regeneration of ILs from mixtures with organic solvents is possible by evaporation of the volatile component under vacuum conditions (approx. 5-30 kPa). The heat requirement for this process was approx. 145-315 kJ/kg IL regenerated. The duty of distillation increases with the alkyl chain length of cation in the 1-alkyl-3-methyl imidazolium ILs. The average heat consume in distillation was 9.7 kJ per $-\text{CH}_2$ added to the cation chain, and it also changes with the nature of the anion.

Chapter 6

Evaluation of ionic liquids as absorbents for ammonia absorption refrigeration cycles using COSMO-based process simulations

THE COSMO-based process simulations using Aspen Plus/Aspen HYSYS are carried out to evaluate the performance of ammonia absorption refrigeration cycles with ionic liquids. The [emim][CH₃CO₂], [emim][C₂H₅SO₄], [emim][SCN], [hxmim][Cl], [choline][NTf₂] and [OHemim][BF₄] ILs are considered as refrigerant absorbents. The [choline][NTf₂] and [OHemim][BF₄] ILs are evaluated by the first time (to our knowledge) in absorption refrigeration after they were recommended as good ammonia absorbents. COSMO-RS method is used for both creating ionic liquid non-databank components and specifying the COSMOSAC property model in Aspen Plus. The COSMOSAC property model gives at once reasonable good property predictions of the vapor (refrigerant) and the condensed (ammonia + ionic liquid) phases. The cycle performances vary in relative wide intervals depending on the ammonia concentration in the (refrigerant + absorbent) solutions. IL mixtures allow not only the tailoring of the working concentration interval of the cycle but also its performance.

6.1 Introduction

The absorption refrigeration cycle (Figure 6.1) is an alternative to the commonly-employed vapor-compression cycle. It uses a source of heat to provide the energy needed to drive the cooling process rather than being dependent on electricity to run a compressor. The system has low-work input requirement, and is fairly simple and economical to operate. It is particularly attractive when an inexpensive source of energy, such as waste heat, is available (Srikhirin et al., 2001; Kim and Infante Ferreira, 2008; Bogart, 1981; Erickson et al., 2004).

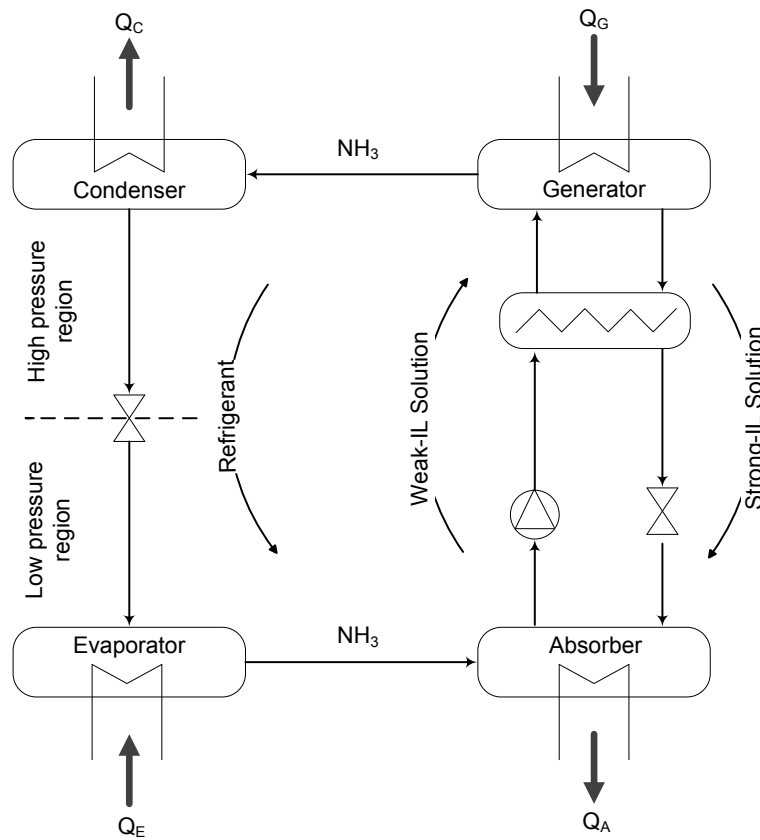


Figure 6.1: Schematic representation of an absorption refrigeration cycle.

In these refrigerators, the gas refrigerant is absorbed in a liquid at relatively low pressure and temperature. Further, a liquid pump drives the refrigerant-absorbent solution to a refrigerant vapor generator. In the generator, a heating source provides the energy required to operate at higher pressure and temperature. The refrigerant is then released in gas phase.

6. Evaluation of ionic liquids as absorbents for ammonia absorption refrigeration cycles using COSMO-based process simulations

Some desirable properties for absorbent/refrigerant pairs include the following (Bogart, 1981):

- The refrigerant should exhibit high solubility in the absorbent.
- The difference in boiling points of refrigerant and absorbent should be large, or else a certain amount of absorbent will contaminate the refrigerant gas produced.
- The heat of mixing of absorbent/refrigerant should be small.
- There should be no crystallization inside the system.
- The solution should not be corrosive.
- Thermal conductivity should be high and viscosity should be small to improve the efficiency of heat transfer and pumping operations.

NH₃/H₂O and H₂O/LiBr are the best known absorption refrigeration systems up to now. Typical commercially-available absorption systems use NH₃/H₂O for moderate-temperature applications such as air conditioning. The H₂O/LiBr systems are usually used for low temperature applications such as refrigeration. In NH₃/H₂O systems some water is evaporated with the ammonia due to their similarities in boiling points. Moreover, NH₃ is toxic and flammable. On the other hand, the H₂O/LiBr systems are limited to up to 0°C to avoid freezing of the refrigerant, and the LiBr aqueous solutions are corrosive. Some studies proposed absorbing fluoroalkane or supercritical CO₂ refrigerants with organic absorbents (Eiseman Jr, 1959; Mastrangelo, 1959; Jones), but problems of fire hazards or gas refrigerant contamination with absorbent persist in using organic absorbents.

A promising option is using ionic liquids (ILs) as refrigerant absorbents (Holbrey and Seddon, 1999b; Shiflett et al., 2006; Yokozeki and Shiflett, 2007a,b; Zhang and Hu, 2011; Kim et al., 2012; Martín and Bermejo, 2010; Chen et al., 2012; Swarnkar et al., 2012). ILs have favorable properties for absorption such as thermal stability and a broad range of liquid temperatures. Their negligible vapor pressure prevents the refrigerant contamination at the generator. Other advantages of ILs are their high heat capacity, high density, non-flammability, low-corrosive character and non-toxicity. They also have a large capacity for dissolving gases such as NH₃ (Yokozeki and Shiflett, 2007a,b; Shiflett and Yokozeki, 2006b; Wang et al., 2007b; Palomar et al., 2011a; Bedia et al., 2012; Yokozeki and Shiflett, 2010; Li et al., 2010; Altamash et al., 2012). Shiflett et al. (2006) patented the application of ILs as absorbents in refrigeration. They studied the NH₃ refrigerant with [emim][BF₄],

[bmim][PF₆], [hxmim][Cl], [emim][NTf₂], [bmim][BF₄], [emim][CH₃CO₂], [emim][SCN], [emim][C₂H₅SO₄] and [DMEA][CH₃CO₂] (Yokozeki and Shiflett, 2007a,b).

Process simulation is a valuable tool for understanding and evaluating absorption refrigeration systems (Shiflett et al., 2006; Yokozeki and Shiflett, 2007a,b; Zhang and Hu, 2011; Kim et al., 2012; Martín and Bermejo, 2010; Chen et al., 2012; Yokozeki and Shiflett, 2010; De Lucas et al., 2007; Imroz Sohel and Dawoud, 2006; Donate et al., 2006; Atmaca et al., 2002; Vargas et al., 1998; Yang and Guo, 1987; Balamuru et al., 2000; Darwish et al., 2008; Steiu et al., 2009; Somers et al., 2011). Furthermore, process simulation can be helpful for selecting and/or designing ILs with optimized properties as refrigerant absorbents.

The thermodynamic description of absorption refrigeration cycles has certain complexity. For instance, the binary (refrigerant+absorbent) vapor liquid equilibrium (VLE) has to be solved in order to establish temperature-pressure-composition and enthalpy-temperature-composition relationships. One way is using equations of states (EOS) for the vapor phase and activity models (NRTL or UNIQUAC) for the liquid phase (Balamuru et al., 2000; Steiu et al., 2009; Van Ness and Abbott, 1982). This way has several limitations:

- EOS's parameters are difficult to set up due to the non-volatile character of the ILs. Hence, information about their critical properties and vapor-pressure data is scarce (Yokozeki, 2005).
- The abundant experimental data on the VLE are also required for correlating the binary parameters of the activity models.
- Activity models are frequently valid for temperatures below the refrigerant critical temperature. Then, modeling (refrigerant + ILs) solutions at generator temperatures would become challenging.
- Activity models are not physically consistent for electrolyte systems (Chen et al., 2008; Simoni et al., 2008) as ILs are.

Yokozeki (2005) developed an EOS-type model (a cubic equation like a generic Redlich-Kwong) for estimating the thermodynamical properties of binary (refrigerant + IL) mixtures. Yokozeki and Shiflett (2007b); Yokozeki (2005) successfully applied this formalism to model NH₃/ILs absorption cycles. However, this procedure demands rigorous and

6. Evaluation of ionic liquids as absorbents for ammonia absorption refrigeration cycles using COSMO-based process simulations

somewhat large experimental data to regress the EOS parameters. It represents a practical limitation when trying to use process simulation for designing/selecting *a priori* new ILs with optimized properties for absorption refrigeration cycles.

We have already successfully integrated COSMO-based methodologies into commercial Aspen Tech process simulators in previous chapters. The COSMOSAC property model as implemented in Aspen Plus is used to estimate the activity coefficients of components in the liquid phase and, simultaneously, the properties of the refrigerant in the vapor phase. COSMOSAC is specified using the results of COSMO-RS calculations. COSMO-RS is used to create/specify the new non-databank IL components. The predicted properties for NH_3 , ILs and their mixtures using COSMO-based Aspen Plus are compared with experimental data reported in literature (Yokozeki and Shiflett, 2007a,b; Bedia et al., 2012). The computed performances for some cycles are compared with those calculated by Yokozeki and Shiflett (2007a); Yokozeki and Shiflett (2007b).

Several ILs are evaluated as absorbents in ammonia absorption refrigerant cycles: some studied by Yokozeki and Shiflett (2007a); Yokozeki and Shiflett (2007b) ([emim][CH_3CO_2], [emim][$\text{C}_2\text{H}_5\text{SO}_4$], [emim][SCN] and [hxmim][Cl]), and some proposed by us ([choline][NTf₂] and [OHemim][BF₄]). We selected the last two ILs after systematic computational and experimental research on the ammonia solubility in ILs (Palomar et al., 2011a; Bedia et al., 2012).

The stepwise strategy developed in this doctoral thesis, in the particular field of ammonia absorption refrigeration cycles, would involve the following phases:

1. A COSMO-RS screening is performed in order to select ILs with potential capability for ammonia absorption (Palomar et al., 2011a; Bedia et al., 2012).
2. The absorption refrigeration cycle performances for the selected ILs are evaluated using process simulations supported by the COSMOSAC property model.
3. The experimental cycle performance with the optimized ILs is carried out.

The scope of this work implies the second stage of the presented approach.

The ILs considered in this work can be classified into two groups according to their capacities for absorbing ammonia:

- The [choline][NTf₂] and [OHemim][BF₄] ionic liquids are considered strong-ammonia absorbents. They are good absorbents of ammonia.

- The [emim][CH₃CO₂], [emim][C₂H₅SO₄], [emim][SCN] and [hxmim][Cl] ionic liquids are considered weak-ammonia absorbents. They absorb the refrigerant lesser than the former.

The mixtures of strong- and week- ammonia absorbent ILs are also evaluated bearing in mind the possible improvement of the cycle’s behavior respect to individual ionic liquids.

6.2 Computational details

6.2.1 Quantum chemical calculations

The molecular structures of the selected ILs have been described by the ion-paired [CA] model. These structures are obtained by geometry optimization at BP-TZVP computational level considering solvent effects through the COSMO-RS continuum solvation model (Klamt, 1995; Andzelm et al., 1995) assuming a hypothetical solvent with $\epsilon \rightarrow \infty$. Vibrational frequency calculations to confirm the presence of an energy minimum are performed. The TURBOMOLE suit (V 3.1) of programs (Schäfer et al., 2000) and the program package COSMOthermX, version C30_1201 (Diedenhofen et al., 2012) are used, respectively, in all the quantum chemical and COSMO-RS calculations. The COSMOthermX calculations use the implicit BP_TZVP_C30_1201 parameterization.

6.2.2 Property package creation

The property packages are generated in Aspen Plus and exported to Aspen HYSYS. ILs are created as pseudo-components specifying their molecular weights, normal boiling temperatures and densities. Additionally, the coefficients of the Andrade’s equation for the viscosity-to-temperature dependency are specified. These coefficients are regressed from experimental data (ILthermo, 2006). Ammonia is selected as conventional component from the Aspen Properties database. The COSMOSAC property model is selected to estimate the activity coefficients of the components in the mixtures, in particular the equation of Lin et al. (2002). Since it modifies the hydrogen bond (HB) term of the original COSMO-SAC equation (Lin and Sandler, 2002a), the description of strongly non-ideal systems is improved. Molecular volumes and σ -profiles of the ILs needed to specify the COSMOSAC model are provided by the user. Those corresponding to ammonia are retrieved from the Aspen Properties database (Aspen Technology, 2011a).

6. Evaluation of ionic liquids as absorbents for ammonia absorption refrigeration cycles using COSMO-based process simulations

For some selected ($\text{NH}_3 + \text{IL}$) binary mixtures (the selection criteria will be explained in the next section), ammonia is specified as Henry component. The coefficients A, B and C in the Equation 2.12 are specified in Aspen Plus. Coefficients are regressed from experimental VLE (or H vs. T) data (Yokozeki and Shiflett, 2007a,b; Bedia et al., 2012; Li et al., 2010). Table 6.1 shows the coefficients used in this work along with the statistical information of the fittings.

Table 6.1: Coefficients used for describing the temperature dependence of the Henry's constant. Number of experimental points (n) considered in the regressions and their R^2 values are also included.

Ionic Liquid	n	R^2	Parameters		
			A	B	C
[emim][$\text{C}_2\text{H}_5\text{SO}_4$]	5	0.9984	-69.3996	1003.3	11.6429
[emim][SCN]	5	0.9999	42.9148	-4214.34	-4.99362

6.2.3 Process simulations

Performance of the absorption refrigeration cycle is based on a simple ideal cycle shown in Figure 6.2. The main specifications used in the simulations are also given. They are similar to those obtained by Yokozeki and Shiflett (2007a); Yokozeki and Shiflett (2007b).

The refrigerant part of the circuit contains a condenser, an expansion valve and an evaporator. The solution section consists of a vapor absorber, a gas generator, a heat exchanger, a pressure control (reducing) valve, and a solution liquid-pump. To simplify, the heat exchanger between the strong- and weak-IL solutions is modeled as two one-side heat exchangers.

The specifications used in this chapter are:

- Temperatures at the generator (T_G), absorber (T_A), condenser (T_C) and evaporator (T_E) are 100, 30, 40 and 10°C, respectively. Selected values of T_G and T_E correspond to a refrigeration cycle which consumes low-quality heat (100°C) to produce (for example) chilled water at 10°C.
- Streams S06 and S08 are ammonia saturated liquid (vapor fraction = 0) and vapor (vapor fraction = 1). From these last two conditions, pressures at the condenser (P_C) and the evaporator (P_E) are the corresponding ammonia VLE pressures: 0.6 and 1.6 MPa.

6.2. Computational details

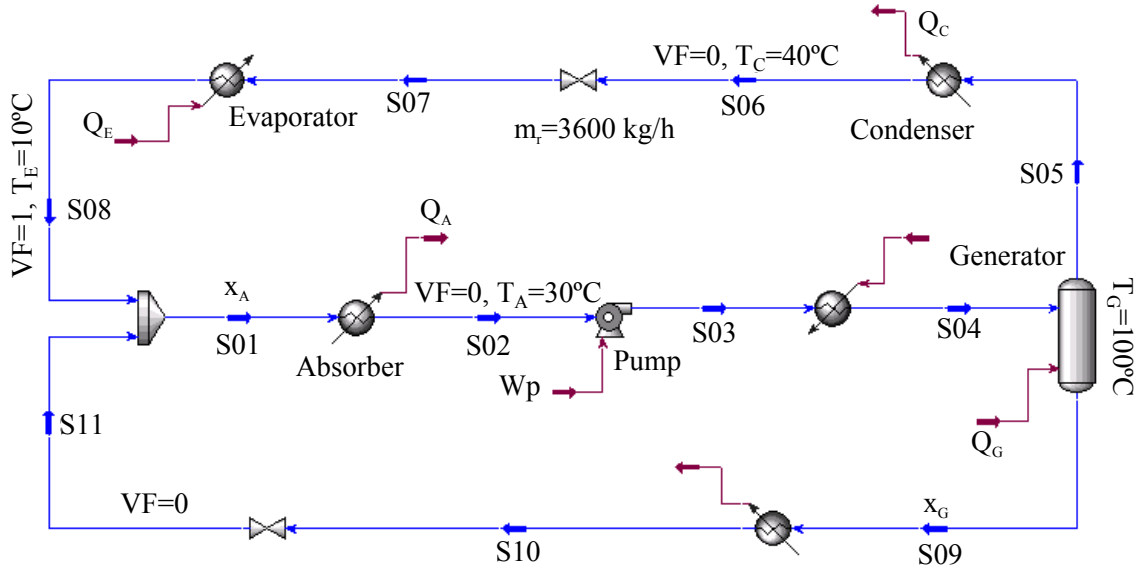


Figure 6.2: Aspen HYSYS process flow diagram used in the current simulations for evaluating the cycle’s performance. The main specifications for the Base Case simulations are also included.

- Composition of the poor- (streams S01 to S04) or rich- (streams S09 to S11) IL solutions (x_A and x_G , respectively) is the degree of freedom of the system directly related to the nature of the ($\text{NH}_3 + \text{IL}$) binary mixtures. x_A is specified taking into account that limiting ammonia concentration in the poor-IL solution is that one corresponding to the saturated ($\text{NH}_3 + \text{IL}$) solution at P_A and T_A . Additionally, x_A and x_G are associated by the VLE condition at the generator:

$$\Theta^{T_G, P_G}(x_A, x_G) = 0 \quad (6.1)$$

As a result, x_A determines the “composition operating window” of the cycle. Its selection should ensure simultaneously the refrigerant vaporization at the generator and the absorption of the refrigerant at the absorber (S02 vapor fraction is set to 0) under their respective operating conditions.

- Refrigerant mass flow at the generator (S05) is 3600 kg/h in all the simulations.
- Pressure drops in the connecting lines are neglected; therefore: $P_C = P_G$ and $P_E = P_A$.
- Stream S11 (strong-IL solution inlet to the absorber) is a solution at the bubble

6. Evaluation of ionic liquids as absorbents for ammonia absorption refrigeration cycles using COSMO-based process simulations

point specified with the absorber pressure (P_A) and the solution concentration of the generator (x_G).

The specification scheme used in this work has two important consequences:

- (i) Stream S05 (condenser inlet) represents a superheated state of pure refrigerant at T_G and P_G .
- (ii) Stream S09 (generator liquid outlet) represents a subcooled quasi-pure ionic liquid under the same conditions (T_G and P_G).

6.2.4 Evaluation of the cycle's performances

The overall energy balance of the cycle is defined as:

$$Q_E + Q_G + W_P = Q_C + Q_A \quad (6.2)$$

where Q_G and Q_E are the heat required in gas generator and evaporator units respectively, W_P the power consumed by the pump and Q_C and Q_A the heat released in condenser and vapor absorber units. Then, the system performance (η) is:

$$\eta = \frac{Q_E}{Q_G + W_P} \quad (6.3)$$

Solution pumping power, W_P , is usually much smaller than Q_G , and it is customary to use a COP (coefficient of performance) defined as just the ratio between Q_E and Q_G . For evaluating absorption chillers it is also used the Solution Circulation Ratio, f , defined as the ratio of the solution flow rate pumped and the refrigerant flow rate:

$$f = \frac{m_s}{m_r} = \frac{x_G}{x_G - x_A} \quad (6.4)$$

where m_r ($m_{S05} = 3600$ kg/h) is the mass flow of refrigerant, and m_s (m_{S09}) is the total mass flow of the reach-IL solution in absorbent. x_G (x_{IL}^{S09}) and x_A (x_{IL}^{S02}) are the mass fractions of the absorbent in the solution leaving the generator and absorber, respectively.

6.3 Results

6.3.1 Prediction of pure component and ($\text{NH}_3 + \text{IL}$) binary mixture properties

6.3.1.1 Prediction of ammonia properties

Calculated equilibrium temperatures at pressures between 5.5 and 20 bar lie in the range of 6.8 to 49.5°C. Moreover calculated mean specific volumes of both saturated liquid and gas at temperatures between 8 and 50°C are 0.0017 and 0.1509 m³/kg. The vaporization of ammonia (between 8 and 50°C) is accomplished with mean enthalpy and entropy changes of 1156 kJ/kg and 3.87 kJ/kg·°C. Table 6.2 shows that predictions match reasonably well with experiment (Haar and Gallagher, 1978). The calculated RAAD for most of the variables lies in the range of 0.08-0.56%, but it is higher for the specific volume of the vapor. The accuracy for predicting superheated ammonia properties is slightly lower than that at equilibrium conditions (RAAD 1.3-5.1%).

6.3.1.2 Prediction of IL properties

Densities, heat capacities and heat of vaporization of the considered ILs at 25°C and 1 atm are in the ranges 1043 - 1444 kg/m³ (mean value 1204 kg/m³), 0.736 - 1.947 kJ/kg·°C (mean value 1.153 kJ/kg·°C) and 170 - 236 kJ/kg (mean value 229 kJ/kg), respectively. The estimated mean viscosity is 277 cP (from 32.4 to 988.1 cP) at same P, T conditions. However, [hxmm][Cl] exhibits a viscosity above 18000 cP. Computed RAAD between predicted IL properties and experiment (Wasserscheid and Welton, 2008; Seddon et al., 2002; Liu et al., 2003; Comminges et al., 2006; Köddermann et al., 2008; Khupse and Kumar, 2009) are lower than approximately 10% (Table 6.2). Current calculations also reproduce the linear decrease of the density and the exponential decay of the viscosity with the temperature observed experimentally for ionic liquids.

6. Evaluation of ionic liquids as absorbents for ammonia absorption refrigeration cycles using COSMO-based process simulations

Table 6.2: RAAD (in %) between calculated (using COSMO-SAC property model in Aspen HYSYS/Aspen Plus process simulations) and experimental values for some thermo-physical and transport properties of pure ammonia and ILs.

Property	Explored range	N. points	RAAD, %
Ammonia saturated liquid and vapor			
T _{Equilibrium}	5 - 20 bar	11	0.56
P _{Equilibrium}	8 - 50°C	12	0.36
V _{Liquid}	8 - 50°C	12	0.21
V _{Vapor}	8 - 50°C	12	14.6
ΔH _{L→V}	8 - 50°C	12	0.08
ΔS _{L→V}	8 - 50°C	12	0.08
Ammonia super-heated vapor			
Molar volume	5 - 20 bar	134	5.1
	8 - 50°C		
ΔH	5 - 20 bar	134	1.3
	8 - 50°C		
ΔS	5 - 20 bar	134	1.4
	8 - 50°C		
Pure ionic liquids ^a			
Density	c.a. 25°C	14	2.50
Viscosity	c.a. 25°C	15	2.34
Heat capacity	c.a. 25°C	14	11.8
Heat of vaporization	c.a. 25°C	16	8.30

^aSome other ILs of the same families are included in the present statistic.

6.3. Results

6.3.1.3 Density and viscosity of the ($\text{NH}_3 + \text{IL}$) binary mixtures

Density and viscosity of the considered mixtures decrease with both the temperature and the ammonia concentration (Figures 6.3 and 6.4). Densities and viscosities of mixtures containing less than 10 wt% of ammonia are lower than those of pure ILs (density and viscosity decrease 50% and 95% in relation to pure ILs).

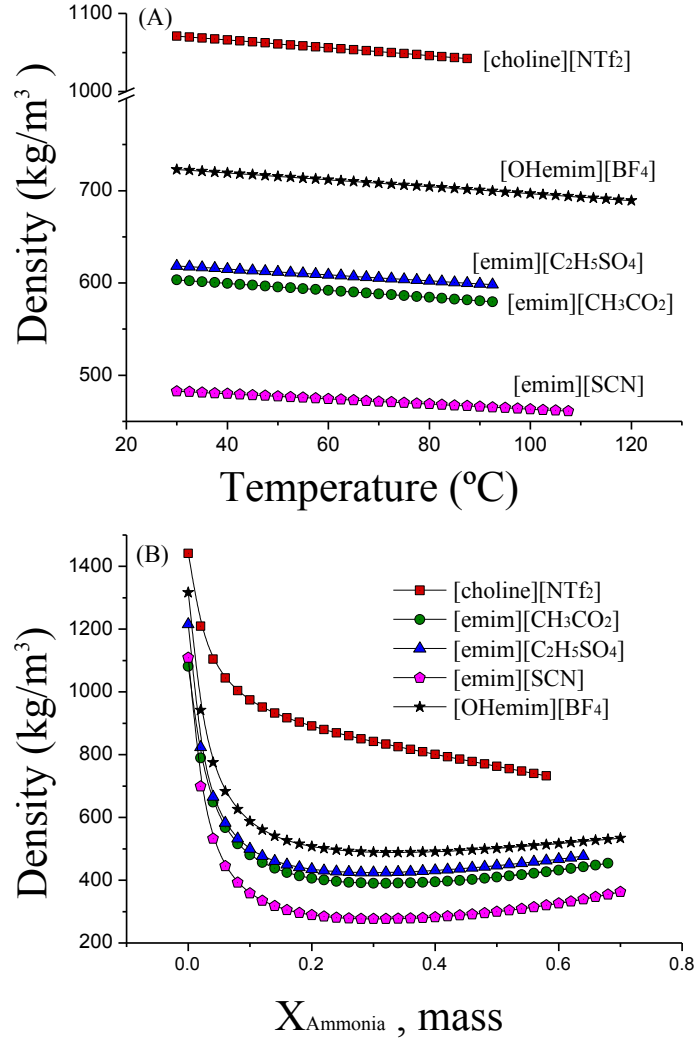


Figure 6.3: Densities of ($\text{NH}_3 + \text{IL}$) binary mixtures calculated in Aspen HYSYS as a function of: (A)- temperature (ammonia mass fraction = 0.05) and (B)- ammonia concentration ($T = 30^{\circ}\text{C}$). $P = 1.1 \text{ MPa}$.

Furthermore, viscosity is similar (between 3 and 9 cP at 30°C) for all the mixtures containing more than c.a. 4 wt% of ammonia. The combined effect of temperature and

6. Evaluation of ionic liquids as absorbents for ammonia absorption refrigeration cycles using COSMO-based process simulations

ammonia concentration on the viscosity of the mixtures is very acute: for temperatures in the interval 60-100°C mixtures containing 2-3 wt% of ammonia have viscosities even lower than 1 cP. These results agree with experiment (Yu et al., 2012; Valderrama and Zarricueta, 2009; Jacquemin et al., 2008; Fredlake et al., 2004; Wasserscheid and Welton, 2008; Seddon et al., 2002; Liu et al., 2003; Comminges et al., 2006; Köddermann et al., 2008; Khupse and Kumar, 2009; Zhu et al., 2009; Rodríguez and Brennecke, 2006; Arce et al., 2006a; González et al., 2007).

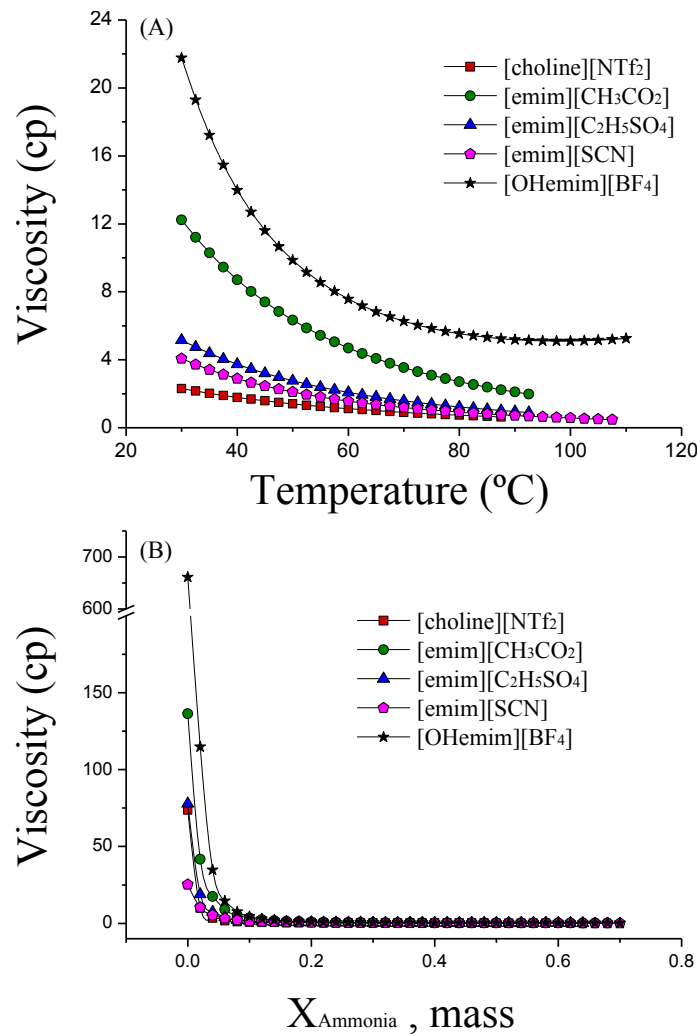


Figure 6.4: Viscosities of (NH₃ + IL) binary mixtures calculated in Aspen HYSYS as a function of: (A)- temperature (ammonia mass fraction = 0.05) and (B)- ammonia concentration (T = 30°C). P = 1.1 MPa.

6.3.1.4 Vapor-liquid behavior of (NH₃ + IL) binary mixtures

Figure 6.5 shows that the COSMO-based property model reproduces the negative deviation respect to the Raoult's law experimentally observed (Yokozeki and Shiflett, 2007a,b; Bedia et al., 2012; Yokozeki and Shiflett, 2010).

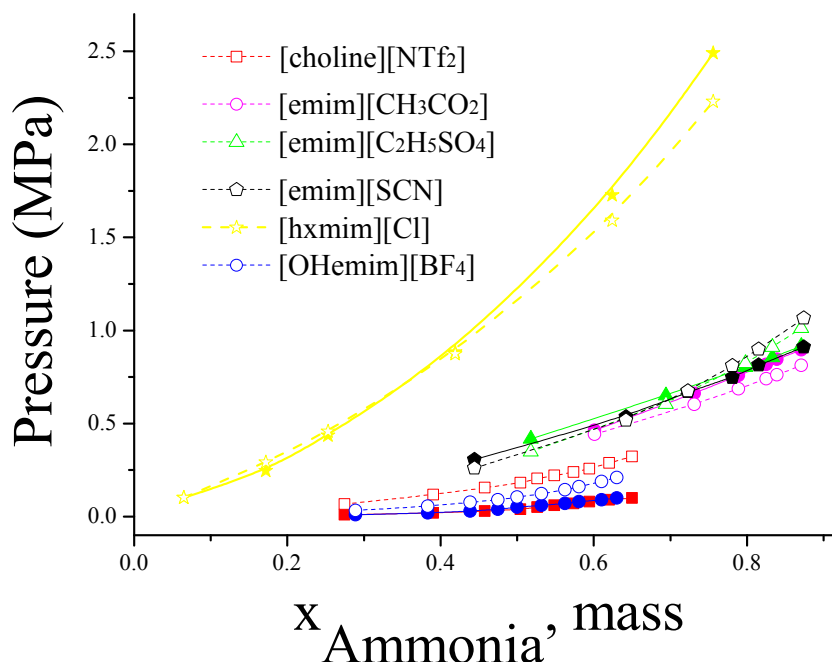


Figure 6.5: Experimental (solid line) and calculated (dashed line) VLE for the (NH₃ + IL) binary mixtures studied in this chapter. Calculations are performed using COSMOSAC property model in Aspen Plus/Aspen HYSYS. In mixtures with [emim][C₂H₅SO₄] and [emim][SCN] Henry components are specified for NH₃. Temperatures are c.a. 300 K.

This model overestimates the vapor pressures of mixtures containing IL good absorbents of ammonia ([choline][NTf₂] and [OHemim][BF₄]) and underestimates the vapor pressures of mixtures with IL poor absorbents of ammonia ([emim][CH₃CO₂], [emim][C₂H₅SO₄], [emim][SCN] and [hxmim][Cl]).

The AADs between calculated and experimental equilibrium vapor pressures of the (NH₃ + IL) mixtures are respectively, 0.101, 0.075, 0.182, 0.157, 0.065 and 0.063 MPa for [choline][NTf₂], [emim][CH₃CO₂], [emim][C₂H₅SO₄], [emim][SCN], [hxmim][Cl] and [OHemim][BF₄] for uncorrected (without Henry component specification) COSMOSAC calculations in Aspen Plus/Aspen HYSYS. AADs is reduced to 0.058 and 0.062 MPa for [emim][C₂H₅SO₄] and [emim][SCN] when ammonia is specified as Henry component in

6. Evaluation of ionic liquids as absorbents for ammonia absorption refrigeration cycles using COSMO-based process simulations

the corresponding mixtures.

As reflected in VLE studies, the vapor pressure of the ($\text{NH}_3 + \text{IL}$) mixtures increases with both the operating temperature of the generator and the ammonia concentration (Figure 6.6). The heat duties of the ammonia vaporization increase abruptly when ammonia mass fraction is lower than 2 wt% (Figure 6.7) and increase with temperature. Thus increasing the generator temperature from 100 to 120°C increases the heat of ammonia vaporization over 7% in ($\text{NH}_3 + [\text{OHemim}][\text{BF}_4]$) mixtures. The low concentrations (c.a. 10 wt%) of ammonia are responsible for both low vapor pressures and high heat vaporization duties. Under low ammonia concentration (less than 10 wt%, for instance) temperature growth has a low influence on the vapor pressure of the mixture (Figure 6.6). On the other hand, the effect of IL nature on the refrigerant generation is less significant for high (more than 50 wt%, for instance) concentrations of ammonia (Figure 6.7).

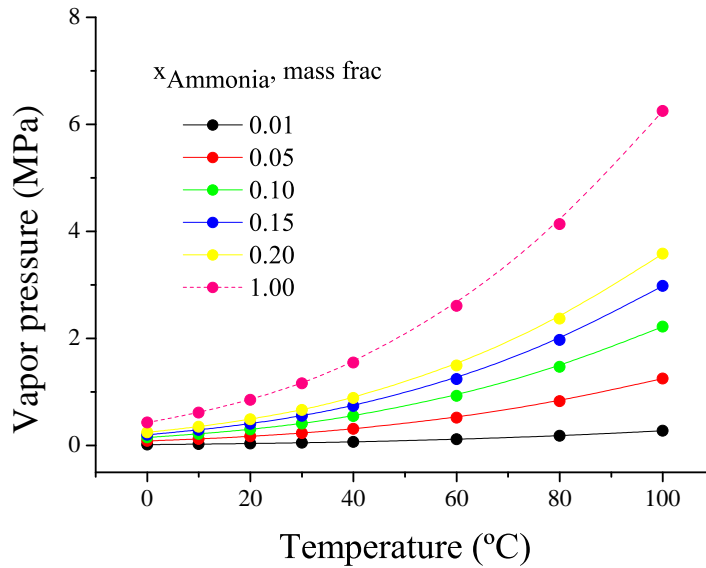


Figure 6.6: Vapor pressure of the ($\text{NH}_3 + [\text{emim}][\text{CH}_3\text{CO}_2]$) binary mixtures as a function of both the temperature and the ammonia concentration. In these calculations vapor fraction of the stream fed to the VL separator is set to 0 and the refrigerant flow rate produced is constant (3600 kg/h).

High vapor pressures in addition to low heat requirements for ammonia vaporization seem to optimize the generator operation but, nonetheless optimization of the generator operation (including the IL selection) is not straightforward.

6.3. Results

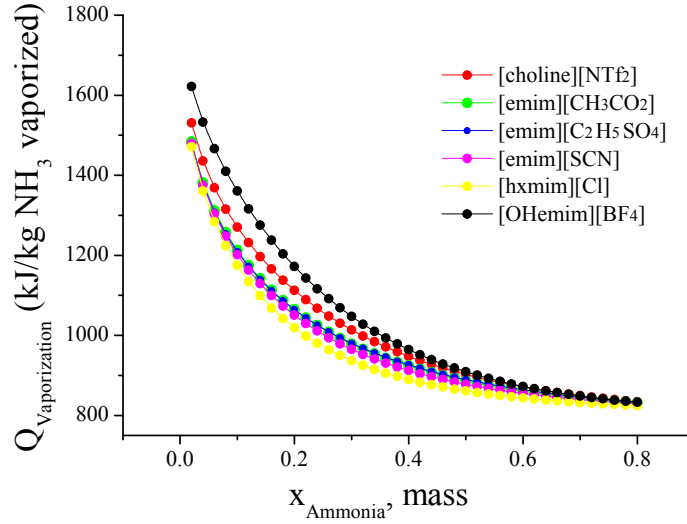


Figure 6.7: Heat duty of ammonia vaporization from its mixtures with ILs as a function of the ammonia concentration at 100°C. In these calculations vapor fraction of the stream fed to the VL separator is set to 0 and the refrigerant flow rate produced is constant (3600 kg/h).

For the Base Case conditions, IL bad absorbents of ammonia yield at once the highest vapor pressures and the lowest heats of vaporization. The picture is the opposite for liquids with high absorption capacity of ammonia ([OHemim][BF₄], for example).

The solubility of ammonia in the ILs under absorber conditions (30°C and 0.6 MPa) ranges approximately from 0.15 to 0.28 (ammonia mass fraction) being [OHemim][BF₄] the best absorbent.

In this work the operating concentration interval (windows) is defined as the ammonia solubility difference under absorber (P_A , T_A) and generator (P_G , T_G) conditions (Figure 6.8).

The good absorbents of ammonia ([OHemim][BF₄]) yield the widest operating concentration intervals for the ammonia absorption refrigeration cycles. However, strong-IL solutions retain relatively elevated refrigerant concentrations.

The high solubility of ammonia in the selected ILs in these mixtures is related with specific solute-solvent interactions in liquid phase like hydrogen bonding. The present calculations find that mixtures of ammonia with [OHemim][BF₄] and [choline][NTf₂] ILs have the most negative calculated excess enthalpies (-1.9 and -0.9 kJ/mol, respectively, in equimolar mixtures). Calculated excess enthalpies are -0.2 and -0.3 kJ/mol in 50 mol%

6. Evaluation of ionic liquids as absorbents for ammonia absorption refrigeration cycles using COSMO-based process simulations

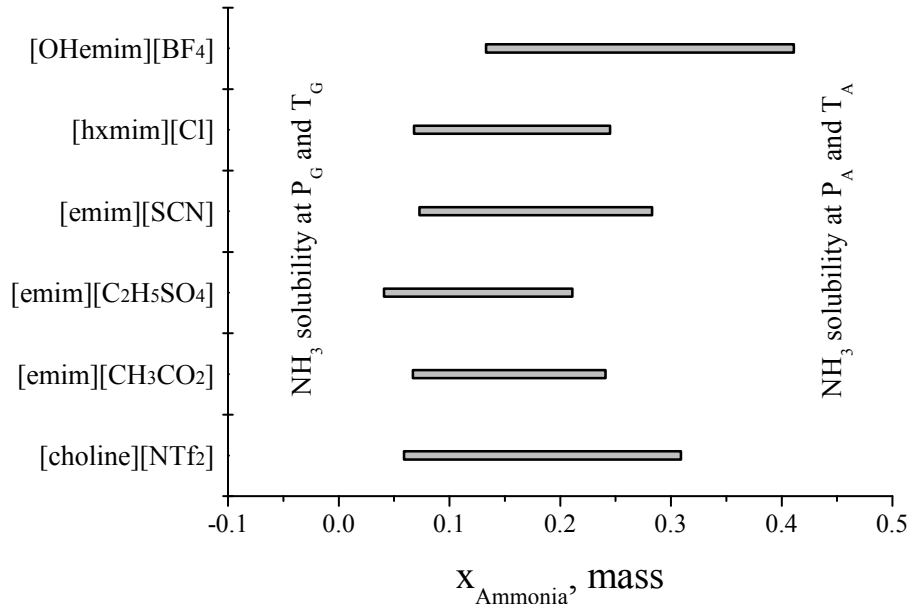


Figure 6.8: Operating concentration intervals in ammonia refrigeration cycles using different ILs as absorbents. Temperatures (T_A and T_G) and pressures (P_A and P_G) correspond to the Base Case considered in this work.

mixtures of ammonia with [emim][C₂H₅SO₄] and [emim][SCN], respectively.

In summary, a reasonably good quantitative prediction is obtained for the properties of the pure (NH₃ and ILs) components and their binary mixtures using the COSMO-based property models in the Aspen Plus/Aspen HYSYS process simulators.

Along with the physical consistency of the obtained results, the integration of the COSMO calculations in the Aspen Tech commercial process simulations is validated for studying the ammonia-IL absorption refrigeration cycles.

6.3.2 Cycle performance

6.3.2.1 Overall cycle's results

Cycle performances obtained in this work (Table 6.3) reasonably agree with those previously obtained by Yokozeki and Shiflett (2007a); Yokozeki and Shiflett (2007b) for the same systems and equivalent conditions.

6.3. Results

Table 6.3: Cycle's performances calculated in this work and reported by [Yokozeki and Shiflett \(2007a\)](#); [Yokozeki and Shiflett \(2007b\)](#) (values in parenthesis). Process specifications: $T_G/T_C/T_A/T_E=100/40/30/10^\circ\text{C}$ are the same to those used in the cited works.

Ionic liquid	f	x_G , IL wt%	$x_A^{(a)}$, IL wt%	COP
[choline][NTf ₂]	9.66	94.3	84.6	0.668
[emim][CH ₃ CO ₂]	11.08(12.55)	93.6(92.3)	85.0(85.0)	0.644(0.573)
[emim][C ₂ H ₅ SO ₄]	21.24(17.55)	93.7(95.2)	89.8(89.8)	0.540(0.485)
[emim][SCN]	12.79(12.42)	92.4(92.7)	85.2(85.2)	0.592(0.557)
[OHemim][BF ₄]	12.34	87.1	80	0.668
[hxmim][Cl]	15.18(14.26)	93.4(93.9)	87.3(87.3)	0.595(0.525)

^(a) x_A values are specified by the user.

For the considered ILs and process specifications, the liquid stream in equilibrium with the vapor refrigerant has x_G (IL wt%) in the interval 87.1 - 93.7 when x_A (ILs wt%) is ranged between 80.0 and 89.8 (IL wt%). f ratio takes values between 9.6 and 21.2. Heat duties in both the generator and the absorber (Q_G and Q_A , respectively) lie in the intervals 1657 - 1879 kW (mean value 1770 kW) and 1579 - 2225 kW (mean value 1881 kW), respectively. Pump powers (W_P) are between 30.4 kW and 61.3 kW (mean value 41.4 kW) approx. 45 times lower than Q_G . This result supports neglecting W_P in the COP definition. Q_E , as expected, is the same for all the binary ($\text{NH}_3 + \text{IL}$) mixtures evaluated here: 1102 kW. This is also the specific cooling capacity (Q_E/m_r) of the cycles. COP takes values in the range between 0.54 and 0.68.

The considered ILs can be roughly divided into two categories according to the cycle performances (Table 6.3):

- ILs providing high COPs and low f ratios (like [choline][NTf₂] and [OHemim][BF₄]) simultaneously exhibit the best ammonia absorption capacities (x_A lies in the interval 15 - 20 wt%). [Liang et al. \(2011\)](#) also suggest that the most favorable (refrigerant + IL) working pairs in absorption heat pumps or chillers are those showing the best refrigerant absorption properties.
- ILs providing low COPs and high f ratios (like [emim][SCN] and [emim][C₂H₅SO₄]). Interactions between these ILs and ammonia are weak in liquid phase.

6. Evaluation of ionic liquids as absorbents for ammonia absorption refrigeration cycles using COSMO-based process simulations

6.3.2.2 Optimizing cycle's behavior

Cycle performances can vary in relatively wide intervals depending on the ammonia concentration in the ($\text{NH}_3 + \text{IL}$) solution (x_A) fed to the generator (Figure 6.9). In fact, the increase of ammonia mass fraction in these solutions provides higher COP values and lower f ratios.

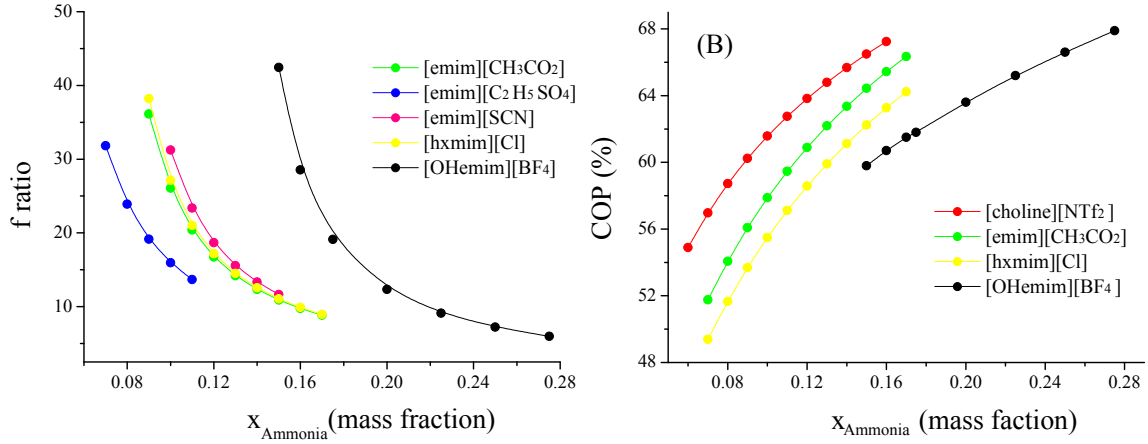


Figure 6.9: (A)- f ratios and (B)- COP for ammonia refrigeration cycles with ILs as absorbents versus ammonia concentration in strong-IL solutions. Remaining specifications correspond to the Base Case of this study.

For instance, ($\text{NH}_3 + [\text{OHemim}][\text{BF}_4]$) mixtures with ammonia mass fractions between 0.150 and 0.275 decreases 36.45 units for f ratio (from 42.4 to 5.98), whereas COP increases 8.1 percent units (from 59.8 to 67.9).

- For low ammonia concentration in the ($\text{NH}_3 + \text{ILs}$) mixtures ($0.10 < x_{\text{Ammonia}} < 0.15$), strong ammonia absorbent ILs provide lower COP and higher f ratio than weak ammonia absorbent ILs. This is because former ILs have lower vapor pressures and require higher duties at refrigerant generator than later ones.
- For high ammonia concentration ($x_{\text{Ammonia}} > 0.20$), ILs having elevated ammonia absorption capacities provide the highest COP values and the lowest f ratios.

The cycle's behavior likewise depends on the heat source temperature (Kim et al., 2012; Yokozeki, 2005; Liang et al., 2011). The temperature of generator represents the quality of the heat source used as driving force in the cycle operation. Figure 6.10 shows

6.3. Results

that both f ratio and COP decrease with the desorber temperature in the range 80 - 120°, at considered conditions. Nevertheless, the shape of dependence is rather different: COP decreases *quasi*-linearly with temperature, while the decrease of f ratio is exponential showing an abrupt decay for relatively low temperatures depending on the nature and/or concentration of the IL.

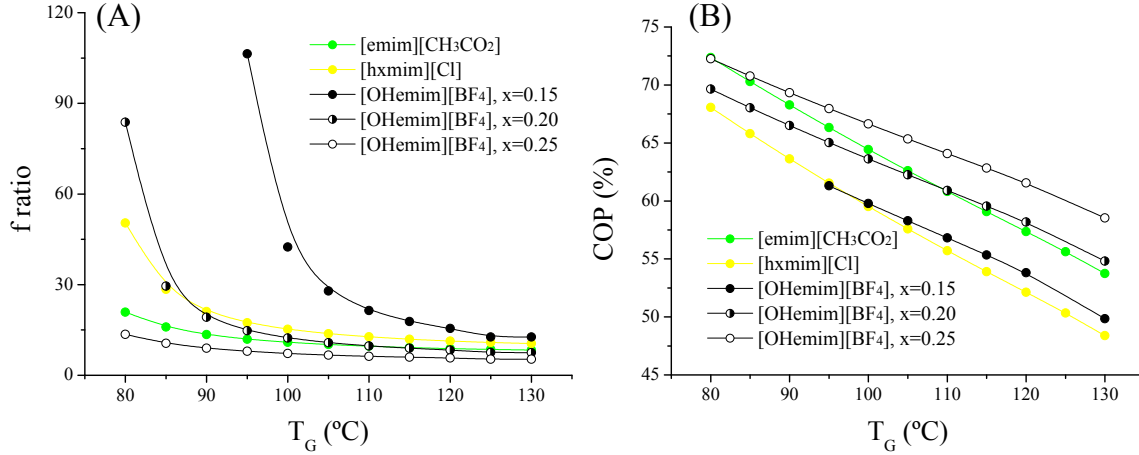


Figure 6.10: Dependence of: (A)- f ratio and, (B)- COP with the cycle heat source (refrigerant generation) temperature for some ILs. Ammonia mass fractions are: 0.150 and 0.127 in mixtures with [emim][CH₃CO₂] and [hxmmim][Cl], respectively. x_{Ammonia} (w/w) takes values 0.15, 0.20 and 0.25 for mixtures with [OHemim][BF₄]. Remaining specifications for the cycle simulations correspond to the Base Case.

When some compositions are possible for the absorption system ([OHemim][BF₄], for instance, in Figure 6.10) the effect of the generation temperature on the cycle performance can show significant differences ongoing from the lower to the higher ammonia concentrations.

The (NH₃ + [OHemim][BF₄]) mixtures having high refrigerant concentrations ($x_{\text{Ammonia}} = 0.20$ in Figure 6.10) behave similarly to the weak ammonia absorbents in spite of the high absorption capacity of [OHemim][BF₄]. High generation temperatures require high ammonia concentrations to ensure refrigerant vapor generation (see data corresponding to mixtures $x_{\text{Ammonia}} = 0.25$ (w/w) with [OHemim][BF₄] in Figure 6.10A). Otherwise, vapor is not produced in the generator.

As shown in Figure 6.11, the COP value slightly and linearly increases as the temperature of the space to be refrigerated (T_E) becomes higher in the interval -5 to 10°C. On the contrary, f ratio does not vary with T_E and depends only on the IL nature and/or

6. Evaluation of ionic liquids as absorbents for ammonia absorption refrigeration cycles using COSMO-based process simulations

concentration in the mixtures (Figure 6.9). Moreover, cycle's performance descriptors (f ratio and COP) are insensitive to changes in the temperature of the absorber (T_A).

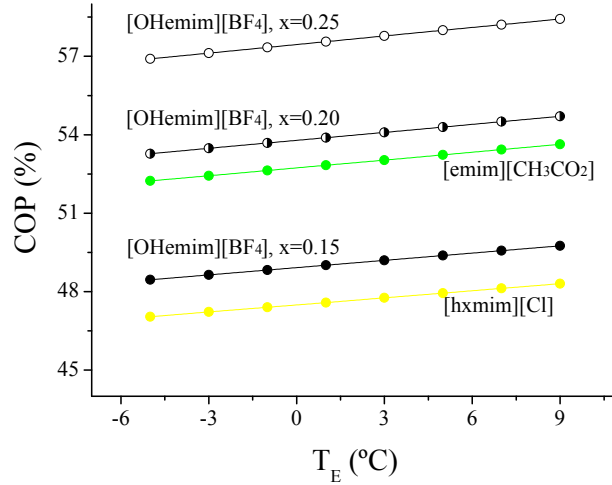


Figure 6.11: Dependence of COP with the temperature of the space to be refrigerated. Ammonia mass fractions are: 0.150 and 0.127 in mixtures with [emim][CH₃CO₂] and [hxvim][Cl], respectively. x_{Ammonia} (wt/wt) takes values 0.15, 0.20 and 0.25 for mixtures with [OHemim][BF₄] IL. Remaining specifications for the cycle simulations correspond to the Base Case.

Figures 6.8 and 6.9 suggest that using IL mixtures instead of pure ILs as refrigerant absorbents could improve the cycle behavior. IL mixtures have already been thoroughly investigated (Taylor et al., 2010; Niedermeyer et al., 2012) and applied to separation processes (García et al., 2012) due to their enhanced properties in respect to individual ionic liquids.

Figure 6.12 demonstrates that the mixtures of ILs having different ammonia absorption capacities ([OHemim][BF₄] and [hxvim][Cl], for example) not only allow the tailoring of the working concentration interval of the cycle (Figure 6.12A) but also its performances (Figure 6.12B). The (NH₃ + [OHemim][BF₄]) mixtures containing 12.5 wt% of ammonia could not be the strong-IL solution of an absorption cycle (Figure 6.8) since vapor generation at 100°C is not possible. However, mixtures with [hxvim][Cl] seem to be suitable as refrigerant absorbents under these conditions. 50-wt% mixture of [OHemim][BF₄] with [hxvim][Cl], for example, gives not only a higher COP but also a lower f ratio (Figure 6.12B) if compared with the systems studied here (Table 6.3).

6.3. Results

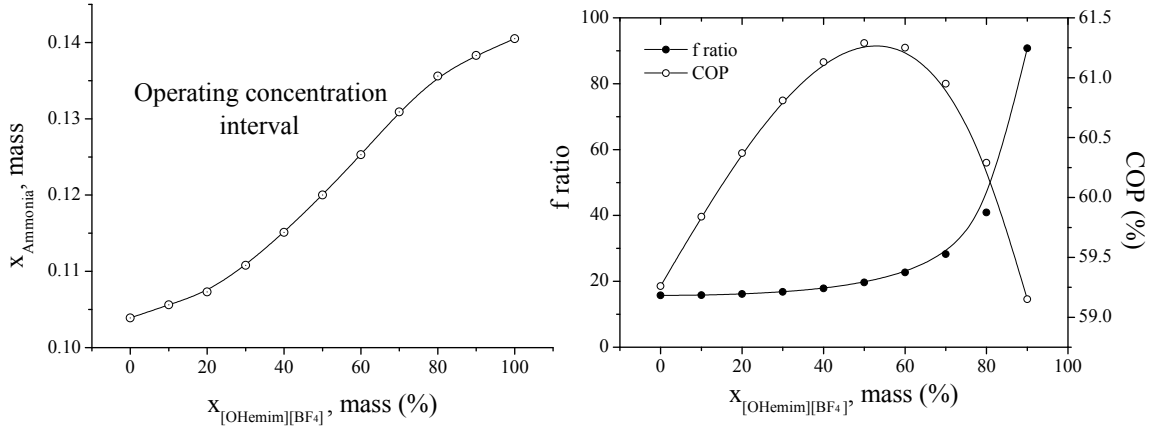


Figure 6.12: (A)- Operating concentration interval of mixtures of [OHemim][BF₄] and [hxmim][Cl] used as absorbent in ammonia absorption cycles. (B)- Performance of ammonia absorption cycles which use [OHemim][BF₄] and [hxmim][Cl] mixtures as absorbents. Operating conditions correspond to the Base Case considered in this work. $x_A = 0.125$.

The presence of a maximum for COP as a function of the [OHemim][BF₄] concentration in the IL-mixture is an outstanding and probably a particular feature of this system. This maximum is related to the exothermic character of the ILs mixing (Niedermeyer et al., 2012) which leads to a lesser external energy consumption (Q_G) to produce the same effect (Q_E). In fact, our calculations show that the ternary ($\text{NH}_3 + ([\text{OHemim}][\text{BF}_4] + [\text{hxmim}][\text{Cl}])$) mixtures have more negative HE than the corresponding ($\text{NH}_3 + \text{ILs}$) binaries due to the negative H^E of the binary (IL + IL) mixture. Negative excess enthalpies for binary mixtures of ILs have been already described in the literature (Niedermeyer et al., 2012). The presence (or not) of a COP maximum, its position and height depend on the nature of the working pair and the operating conditions of the cycle.

It is important to consider that the heat rejected to the ambient at the absorber (Q_A) varies approx. 10% when the [OHemim][BF₄] concentration in its mixtures with [hxmim][Cl] increases up to approx. 0.5 (mass fraction). Further increments of the [OHemim][BF₄] cause an abrupt grow of Q_A . From this, it is evident the need of a more complex thermodynamical second law analysis of the cycle's performances.

6.4 Concluding remarks

COSMO-based process simulations using Aspen Plus/Aspen HYSYS: (i)- adequately predict the properties (density, viscosity, heat capacity, VLE, etc.) of ammonia, ILs and their mixtures and, (ii)- give a reasonably good estimation of the performances in ammonia absorption refrigeration cycles with ILs.

This approach also offers a physical consistent picture about the influence of the operating conditions on the cycle's behavior. Thus, it is a valuable tool in the ILs selection/design with optimized properties to this application.

Cycle's performance depends on both operating conditions of the cycle and ammonia concentration in the strong-IL solutions (x_A). ILs showing low ammonia absorption capacity (as, for example, [hxmim][Cl]) provide low f ratios and high COPs under low ammonia concentrations (x_A) in the strong-IL solution. However, high global ammonia concentrations in the (NH₃ + ILs) binary mixtures are not completely absorbed in the absorber. If considering good ammonia absorbent ILs (like [OHemim][BF₄]): low refrigerant concentrations are not enough to produce refrigerant vapor in the generator but give the best performances and the lowest f ratios among the studied systems when ammonia concentrations are increased.

The ammonia absorption capacity of ILs determines the operating concentration interval of cycles. Using IL mixtures as refrigerant absorbents allow controlling both the working concentration interval of cycle and its performance. These IL mixtures provide new possibilities to optimize the IL selection/design for absorption refrigeration.

Part III

MULTISCALE APPROACH: A case study

Chapter 7

Optimized ionic liquids for toluene absorption

THE three stages of the multiscale approach, molecular simulation-experiment-process simulation, were addressed to select the optimal ionic liquid for toluene absorption. The COSMO-RS method was used to analyze the solute-solvent interactions and to screen Henry's law constant for toluene in 272 ionic liquids (ILs). High-capacity absorbents were selected for experimentation. Thermogravimetric experiments were carried out to evaluate the toluene absorption in selected ILs at different temperatures and atmospheric pressure. The experimental equilibrium data were compared with the COSMO-RS predictions. The separation process rate-based simulation with selected ILs was modeled by the Aspen Plus process simulator. This process was compared with the same one using organic absorbents. Current computational-experimental research allowed selecting a set of suitable ILs for toluene absorption.

7.1 Introduction

Volatile organic compounds (VOCs) are organic substances characterized by their high-vapor pressure at ambient temperature (Hunter and Oyama, 2000). They are involved in atmospheric photochemical reactions and entail one of the most important groups of air pollutants emitted from chemical, petrochemical, and allied industries, leading to serious environmental problems (global warming, acid rain, and health hazard) and economical losses. Due to this, legislations such as Clean Air Act Amendments or European Economic Community (EEC) Directives limit the concentration levels for volatile organic compound emissions into atmosphere. The current methods used in VOC abatement (destructive- and recovery-based) include thermal or catalytic incineration, condensation, absorption, adsorption, membrane separation, and biological treatments, each with particular advantages and limitations (Rafson, 1998).

Selection of an efficient VOC abatement technique depends on the concentration and the nature of the compound, the gas-stream flow rate, and other factors such as safety and economic considerations. Thermal oxidizers, commonly used for the destruction of VOCs, consume large amounts of natural gas to heat air and moisture, generating CO₂ and NO_x emissions, which have negative implications in global warming and air quality (Milota et al., 2007). Catalytic oxidation processes (Bedia et al., 2010; Solsona et al., 2011) reduce the fuel consumption but have the problem of catalyst deactivation. Furthermore, the water vapor presents in most of the gas streams and/or generated from VOCs oxidation frequently deactivates the inorganic catalytic systems. Biological treatments can represent a cost-effective solution for VOC removal, but they are not suitable when the microbial activity is limited by the slow VOC transfer from the gas phase to cell-containing aqueous phase (Arriaga et al., 2006; Quijano et al., 2011). It is also necessary to take into account that any destructive method eliminates the possibility of recovering the VOC. Adsorption of VOCs on different porous materials, such as, activated carbons or zeolites has been extensively studied in the literature (Chiang et al., 2001; Jarraya et al., 2010) but its application may be limited because the moisture in the gas or the deposition of other compounds could block the adsorption sites making difficult the regeneration of the adsorbent. Absorption can provide an effective solution for VOC removal from gas streams with further recovery. The key factor is the selection of an appropriate liquid absorbent (Blach et al., 2008). For hydrophobic components, their low water solubility limits the absorption capacity in aqueous phase (Wang et al., 2001). On the other hand, organic solvents [e.g., hexadecane and di-(2-ethyl) hexyladipate (DEHA) previously stud-

ied for toluene absorption (Quijano et al., 2011)] present the disadvantage of their not negligible volatility. A strategy for improving the solute transfer to the aqueous phase is the addition of a nonaqueous solvent with high affinity for the solute, being silicone oils, n-alkanes, perfluorocarbons, and solid polymers widely used for this purpose (Darracq et al., 2010).

Many of the requirements of VOC removal are fulfilled by an absorption system containing room-temperature ionic liquids (ILs) (Milota et al., 2007; Quijano et al., 2011). Because of their exceptional properties and the possibility of being designed with required properties (Wasserscheid and Welton, 2008; González et al., 1999; Palomar et al., 2010; Giernoth, 2010), ILs have generated significant interest as absorbents in gas separation processes, (Han and Armstrong, 2007; Han and Row, 2010) such as CO₂ capture (Huang and Rüther, 2009; Bara et al., 2009a), absorption of SO₂ (Shiflett and Yokozeki, 2009; Ren et al., 2010), NH₃ (Yokozeki and Shiflett, 2007a; Palomar et al., 2011a; Bedia et al., 2012), hydrofluorocarbons (Shiflett and Yokozeki, 2006c; Shiflett et al., 2011), propylene (Ortiz et al., 2010a,b), or VOCs as dimethylsulfide, dimethyldisulfide, and toluene (Quijano et al., 2011; Ortiz et al., 2010b). In this last reference, the high affinity of conventional imidazolium-based ILs for VOCs compounds was confirmed, being the partition coefficients in [bmim][PF₆] and [bmim][NTf₂] comparable or higher than those of typical organic solvents (Quijano et al., 2011). However, to the best of our knowledge, no systematic investigations on VOCs affinity toward a wide variety of ILs have been reported so far. Computational methods to estimate thermodynamic properties are of great utility for selecting the best cation-anion combinations for absorbing a specific gas (Palomar et al., 2011a). The COSMO-RS method developed by Klamt et al. (2010b) has been demonstrated to be a valuable method for predicting the thermodynamic properties of IL-based mixtures (Diedenhofen and Klamt, 2010), providing an unique *a priori* computational tool for designing ILs with desired properties. In fact, the chapters III and IV, and many publications show the general suitability of COSMO-RS method to reflect the intermolecular interactions in the IL-organic mixtures and to predict the properties of IL systems (Navas et al., 2009; Vreekamp et al., 2011), including solubilities and Henry's law constants of several gases in ILs (Palomar et al., 2011a; Bedia et al., 2012; Palomar et al., 2011b; González-Miquel et al., 2011). Indeed, ILs with optimum characteristics for CO₂ and NH₃ absorption were selected in previous works (Palomar et al., 2011a; Bedia et al., 2012; Palomar et al., 2011b; González-Miquel et al., 2011) on the basis of the excess enthalpy analysis and description of the intermolecular solute-IL interactions using COSMO-RS.

7.1. Introduction

The aim of this work is to propose optimized ILs with high capacities and adequate properties for absorbing toluene. To accomplish that, a research strategy based on a three-step procedure was developed. First, a computational thermodynamic analysis using the COSMO-RS method (molecular simulation) is performed among 272 ILs to select solvents with suitable properties for toluene absorption. Second, experiments are conducted to evaluate the thermodynamics and kinetics of toluene absorption. Thus, absorption-desorption rate curves over selected ILs are obtained by thermogravimetric experiments at different temperatures and atmospheric pressure. As a result, new thermodynamic and kinetic experimental data of interest for toluene absorption by ILs, such as gas-liquid equilibrium data and diffusivities, have been obtained and compared to the available data and calculated values. Third, toluene absorption was modeled in [Aspen Plus \(2010\)](#) v 7.3 at the operating conditions experimentally tested by using equilibrium- and rate-based columns (RADFRAC model). The Aspen Plus simulations of toluene absorption in selected ILs and in other conventional toluene absorbents (such as hexadecane and DEHA) are compared with our own experimental gas-liquid equilibrium and kinetic data. Then, rate-based calculations are performed to estimate the absorption of toluene in tray and packed columns at fixed gas/liquid mass ratio and operating conditions. The recovery of toluene achieved using rate-based approach is compared to the separation obtained using an ideal single equilibrium stage. Thus the importance of kinetics and thermodynamics in the toluene absorption can be analyzed.

Following these steps, a set of optimized ILs are confidently evaluated as potential candidates in the absorption processes for removal toluene from gaseous streams.

7.2 Procedure

7.2.1 Molecular simulation: computational details of COSMO-RS calculations

The molecular geometries of toluene, hexadecane, and ions of ILs were optimized at the B3LYP/6-31++G** computational level in the ideal gas phase using the quantum chemical Gaussian03 package (Frisch et al., 2003). A molecular model of independent counterions was applied in the COSMO-RS calculations, where the IL is treated as an equimolar mixture of a cation and an anion. The version C21_0111 of the COSMOthermX program package (Eckert and Klamt, 2010) and its implicit (BP_TZVP_C21_0111) parameterization were used to accomplish the calculations of the σ -profiles of pure compounds as well as the thermodynamic properties (such as Henry’s law constants for toluene in ILs and detailed contributions to excess enthalpies in equimolar toluene-IL mixtures).

7.2.2 Experimental section

7.2.2.1 Materials

Toluene (purity >99.8%) was purchased from Sigma-Aldrich and used without further purification. The ILs tested as absorbents were: [dcimim][NTf₂], [omim][NTf₂], [hxmim][NTf₂], [bmim][NTf₂], [emim][NTf₂], [dcimim][BF₄], [emim][C₂H₅SO₄], and [bmim][BF₄] supplied by Ionic Liquid Technologies, in the highest purity available (purity >97-98%). All the ILs were also used without further purification. Before each experiment, the ILs were dried under vacuum (10⁻³ Torr) at 298 K over at least 24 h. This procedure ensures working with ILs with very low water content (<250 ppm) (Palomar et al., 2011a; Bedia et al., 2012). Therefore, the water should not significantly affect the absorption capacity, as we have found. Table 7.1 collects the density and viscosity values reported in the literature (Ahosseini and Scurto, 2008; Zhang et al., 2009; Jacquemin et al., 2006) for the different ILs used in this work. As can be seen, the properties measured by us for the IL used as reference [bmim][BF₄] (Palomar et al., 2011a) are fairly close to the reported by other authors (Tokuda et al., 2004).

7.2. Procedure

Table 7.1: Density and viscosity of the ILs reported in literature.

IL	T (K)	ρ (kg/m ³)	μ (mPa·s)	Reference
[dcmim][NTf ₂]	293 ¹	1282	141	Ahosseini and Scurto (2008)
	303	1278	84	
	313	1274	54	
[omim][NTf ₂]	293	1327	115	Zhang et al. (2009)
	303	1320	71	
	313	1358	36	
[hxmim][NTf ₂]	293	1376	91	Ahosseini and Scurto (2008)
	303	1367	56	
	313	1358	36	
[bmim][NTf ₂]	293	1441	63	Jacquemin et al. (2006)
	303	1432	40	
	313	1424	27	
[emim][NTf ₂]	293	1524	41	Ahosseini and Scurto (2008)
	303	1514	28	
	313	1506	20	
[dcmim][BF ₄]	293	1072	928	Ahosseini and Scurto (2008)
	303	1067	456	
	313	1060	248	
[emim][C ₂ H ₅ SO ₄]	293	1241	111	Jacquemin et al. (2006)
	303	1234	75	
	313	122	53	
[bmim][BF ₄]	293	1203 / 1208	123 / 107	Palomar et al. (2011a) Tokuda et al. (2004)
	303	- / 1201	- / 72	
	313	1189 / 1195	48 / 50	

7.2.2.2 Absorption/desorption experiment

Figure 7.1 shows a scheme of the setup used for toluene equilibrium and kinetic absorption experiments. They were carried out in a thermogravimetric analyzer (TGA/SDTA851e Mettler Toledo International Inc.) at atmospheric pressure and temperatures of 293, 303, and 313 K using around 20 mg of IL previously dried as described before. The balance has a weight range of 0-1000 mg with a resolution of 0.1 μ g. The temperature of the sample was maintained constant with an external thermostated bath (Huberminisat 125). Toluene inlet concentration was set by saturation of a nitrogen flow through a saturator at a controlled temperature. Gas-liquid equilibrium data of toluene in ILs were obtained by setting the partial pressure of toluene in the toluene/N₂ gas flow (100 Ncm³/min) and

7. Optimized ionic liquids for toluene absorption

monitoring the increment on weight of the sample. Blank experiments were carried out with neat N_2 gas and no weight increase of the IL samples was detected, consistently with the reported negligible solubility of N_2 in imidazolium-based IL ($<10^{-3}$ molar fraction at 1 atm and 40°C) (Carlisle et al., 2008). It was considered that the IL and the gas have reached equilibrium when at constant pressure no further weight change was observed on time (weight change rate $<0.001\text{ mg h}^{-1}$).

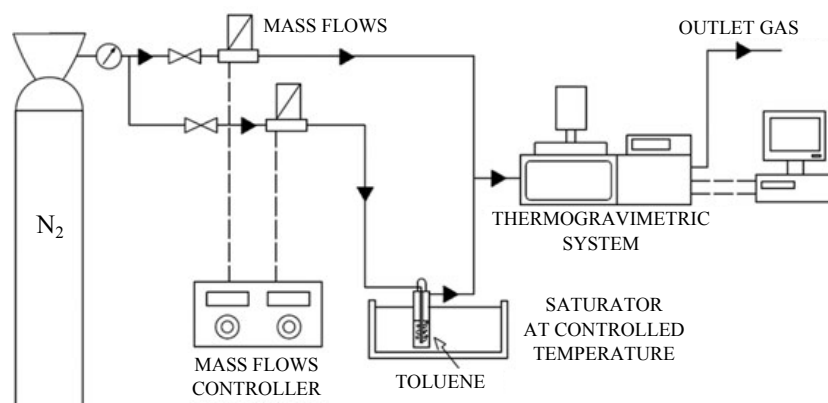


Figure 7.1: Schematic diagram of the atmospheric pressure system for toluene absorption.

The absorption-desorption rate curves were also obtained in the aforementioned thermogravimetric system. Toluene absorption was performed at an inlet toluene partial pressure of 2.0 kPa under continuous gas flow ($100\text{ Ncm}^3/\text{min}$) at 0.1 MPa. The increment of weight was monitored, and once the IL and the gas seem to have reached equilibrium (weight change rate $<0.001\text{ mg h}^{-1}$), desorption was carried out at the absorption temperature with continuous dry nitrogen flow ($100\text{ Ncm}^3/\text{min}$).

7.2.3 Process simulation details

In process simulations, IL new components were created as pseudocomponents in Aspen Plus (v 7.3) specifying their molecular weights, normal boiling temperatures, and densities. Additionally, the coefficients of the Andrade's equation for the viscosity-to-temperature dependency were specified. These coefficients were regressed from experimental data (Palomar et al., 2011a; Ahosseini and Scurto, 2008; Zhang et al., 2009; Tokuda et al., 2004). Toluene and nitrogen were selected as conventional components from the Aspen Plus ASPV73 PURE25 database. The COSMOSAC property model (Aspen Technology, 2004a; Lin and Sandler, 2002a), as implemented by default in Aspen Plus was selected

7.2. Procedure

to estimate the activity coefficients of the components in the mixtures. The molecular volumes and σ -prof-profiles of the ILs, needed for specifying the COSMOSAC model, were set by the user, whereas those corresponding to the organic solvents were directly taken from the Aspen Plus database. The information used for both creating IL pseudo-components (normal boiling temperature and densities) and specifying the corresponding COSMOSAC property models were obtained from the previous COSMO-RS calculations by the COSMOthermX (v C21_0111) program package assuming ion-paired structures (molecular [CA] model) for the ILs. Toluene absorption was simulated with the RADFRAC model of Aspen Plus. In rate-based absorption simulations:

- toluene + IL mixtures were considered as nonreacting systems.
- diffusivities of the toluene in the IL phase were calculated by the Wilke-Chang equation as implemented in Aspen Plus (v 7.3).
- both trayed and packed columns were evaluated.
- dimensions of the tray and pack section were previously estimated by the tray- and pack-sizing utilities available in Aspen Plus.
- correlations used by default in Aspen Plus (v 7.3) to calculate the mass- and heat-transfer coefficients and interfacial areas in rate-based absorption simulations were employed here.

Two rate-based absorption models have been used in this work:

1. **One-Stage Contactor Column.** It was considered for evaluating the absorptive capacity of different ILs using a gas feed with inlet toluene partial pressure of 2.0 kPa. In addition, it allows comparing the separation achieved using rate and equilibrium-based approaches, to evaluate how the kinetics affects in the absorption process. In addition, Murphree tray efficiencies were also evaluated. The feed flows of the IL and gas were fixed at $L=0.01$ and $G = 0.35$ kmol/h, respectively. A G/L of 35 was selected because it allows observing significant deviations of toluene recovery from ideal equilibrium. The inlet streams were fed “on stage” according to the Aspen Plus convention. Sieve tray dimensions were fixed at 0.3 m diameter and 0.15 m height.
2. **Packed Bed Column.** A more realistic absorption model of packed bed column was also considered in this study for the selected IL [dcmmim][NTf₂] and commonly

7. Optimized ionic liquids for toluene absorption

used conventional absorbents (DEHA and n-hexadecane). For the sake, comparison in an industrial-like approach, a column size representative of a pilot plant unit (2 m height, 0.25 m diameter, and 15 mm ceramic Raschig rings) was selected. The G/L molar ratio was chosen taking DEHA as reference solvent for 90% recovery. The obtained G/L molar ratio (17) is in the range of values commonly used in aromatics absorption with conventional organic solvents (Heymes et al., 2006) and was maintained for the other two IL-based systems. The height equivalent to a theoretical plate (HETP) was calculated at those different conditions to characterize the packing efficiency, determined by the rate of the absorption process.

The Height Equivalent per Theoretical Plate (HETP) for packed stages back-calculated by Aspen Rate-Based Distillation from the converged vapor and liquid composition profiles is defined as:

$$HETP = \frac{H}{NT_{av}} \quad (7.1)$$

Where H is the height of packing included in the stage and NT_{av} is the average overall number of transfer units given as $(NT_1 + NT_2 + \dots + NT_n)/n$. These units are calculated by

$$\frac{1}{NT_i} = \frac{1}{NTUV} + K_i \cdot \frac{V}{L} \cdot \frac{1}{NTUL} \quad (7.2)$$

NTUV is the number of transfer units in the vapor phase. This number is calculated by:

$$NTUV = \frac{KV_{av}}{V} \quad (7.3)$$

where V is the superficial vapor phase velocity (kmol/sec) and KV_{av} is the average vapor phase binary mass transfer coefficients (kmol/sec) calculated by

$$KV_{av} = C_v \cdot \frac{1}{\sqrt{\varepsilon - h_t}} \cdot \sqrt{\frac{a_F}{d_K}} \cdot D_{i,K}^V \cdot Re_V^{0.75} \cdot Sc_{V,i,k}^{0.33} \quad (7.4)$$

where C_v is the vapor mass transfer coefficient parameter, characteristic of the shape and structure of the packing, ε is the void fraction of the packing, a_F is the specific area of the packing, h_t is the fractional holdup:

$$h_t = \frac{12 \cdot \mu^L \cdot a_F^2 \cdot u_S^L}{\rho_t^L \cdot g} \quad (7.5)$$

7.2. Procedure

d_K is the hydraulic diameter:

$$d_K = \frac{4 \cdot \varepsilon}{a_F} \quad (7.6)$$

$D_{i,K}^V$ is the diffusivity of the vapor (calculated by the Wilke-Chang equation), Re^V is the Reynolds number for the vapor:

$$Re^V = \frac{\rho_t^V \cdot u_S^V}{\mu^V \cdot a_F} \quad (7.7)$$

u_s^V is the superficial velocity for the vapor:

$$u_s^V = \frac{V}{\bar{\rho}^V} \cdot A_t \quad (7.8)$$

where A_t is the cross-sectional area of the column.

$Sc_{V,i,K}$ is the Schmidt number for the vapor:

$$Sc_{V,i,K} = \frac{\mu^V}{\rho_t^V \cdot D_{i,K}^V} \quad (7.9)$$

NTUL is the number of transfer units in the liquid phase. This number is calculated by:

$$NTUL = \frac{KL_{aV}}{L} \quad (7.10)$$

where L is the superficial liquid phase velocity (kmol/sec, KL_{aV} is the average liquid phase binary mass transfer coefficients (kmol/sec):

$$KL_{aV} = C_L \cdot \left(\frac{g \cdot \rho_t^L}{\mu^L} \right)^{0.167} \cdot \sqrt{\frac{D_{i,K}^L}{d_K}} \cdot \left(\frac{u_S^L}{a_F} \right)^{0.33} \quad (7.11)$$

C_L is the liquid mass transfer coefficient parameter, characteristic of the shape and structure of the packing. $D_{i,K}^L$ is the diffusivity of the liquid phase (calculated by the Wilke-Chang equation), u_s^L is the superficial velocity for the liquid:

$$u_s^L = \frac{L}{\bar{\rho}^L} \cdot A_t \quad (7.12)$$

K_i is the k-value for component i as defined in the Aspen Plus relative volatility calculation methods.

7.3 Results

7.3.1 COSMO-RS screening to select ILs for toluene absorption

It has been explained in Chapter II that the σ -profile of a compound represents its molecular surface polarity distribution obtained from quantum chemical calculations (Klamt et al., 2010b). Figure 7.2 shows the σ -profile of toluene and those belonging to some conventional toluene absorbents. The histogram of toluene is dominated by a series of peaks located at the nonpolar region ($-0.0082 < \sigma < +0.0082$ e/Å²). The neutral character of toluene anticipates predominant misfit (electrostatic) intermolecular interactions. The σ -profile of conventional toluene absorbents, as DEHA or hexadecane (Quijano et al., 2011), is also dominated by peaks located at the nonpolar region (Figure 7.2). This confirms the well-known solute-solvent affinity.

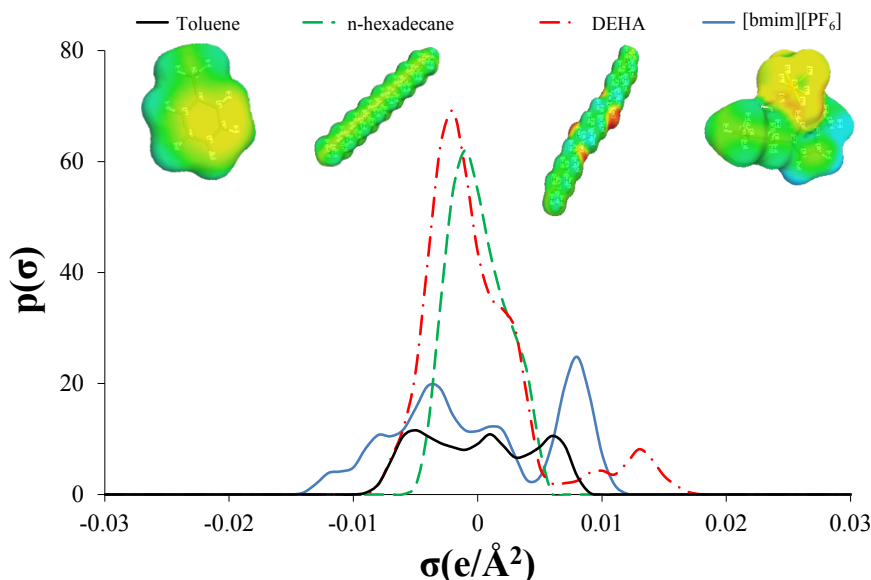


Figure 7.2: The σ -profiles and polarized charge surfaces of toluene and different solvents obtained by COSMO-RS.

Because the [bmim][PF₆] IL solvent was previously used as toluene absorbent (Quijano et al., 2011), its σ -profile was compared with those of the organics. The [bmim][PF₆] IL also shows a significant peak at the nonpolar region. However, it represents polarized charge corresponding to the hydrogen groups of cation located at the hydrogen bond donor region $\sigma < -0.0082$ e/Å², and to the negative charge density of the anion located

7.3. Results

in the hydrogen-bond acceptor region $\sigma > 0.0082 \text{ e}/\text{\AA}^2$. This indicates the higher polar character of IL relative to solvents like DEHA or hexadecane. This is consistent with the experimentally measured higher solubility of toluene in those solvents compared to [bmim][PF₆].

In Chapter III, the COSMO-RS estimates for excess enthalpy, h^E , of acetone-IL mixtures have been studied in terms of the misfit, hydrogen bonding, and van der Waals intermolecular interactions.

$$h^E = h^E(HB) + h^E(Misfit) + h^E(vdW) \quad (7.13)$$

In addition, the excess enthalpy predictions of acetone-IL mixtures were applied to analyze their gas-liquid equilibrium data. In this chapter, the COSMO-RS estimates of Henry's law constants for toluene in DEHA, n-hexadecane, and [bmim][PF₆] at 298 K have been related to the interaction energy contributions to h^E in toluene-solvent systems (Figure 7.3). It is observed that a decrease of repulsive interactions (positive h^E values) accompanies an increasing gas solubility of toluene (decreasing H values).

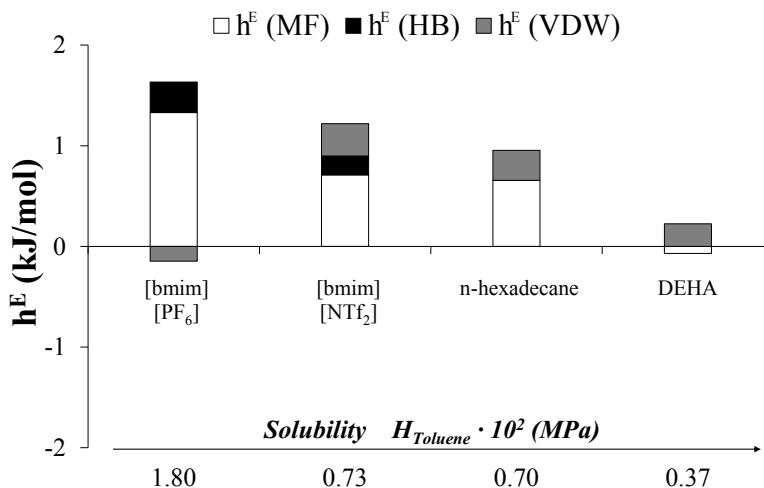


Figure 7.3: Description of the solvent effect on Henry's law constants of toluene at 298 K using the interaction energy contributions [electrostatic, $h^E(\text{MF})$; van der Waals, $h^E(\text{VDW})$, and hydrogen-bonding, $h^E(\text{HB})$] to the excess molar enthalpy of solute-solvent mixtures computed by COSMO-RS.

7. Optimized ionic liquids for toluene absorption

As can be seen, organic solvents present less repulsive interactions than the ionic liquid [bmim][PF₆]. To design optimized ILs for toluene absorption, the COSMO-RS method is applied for predicting Henry's law constants (H) for toluene in 272 ILs at 298 K. Thus, a computational screening was performed over ILs based on different cations and anions being the H values mapped in Figure 7.4.

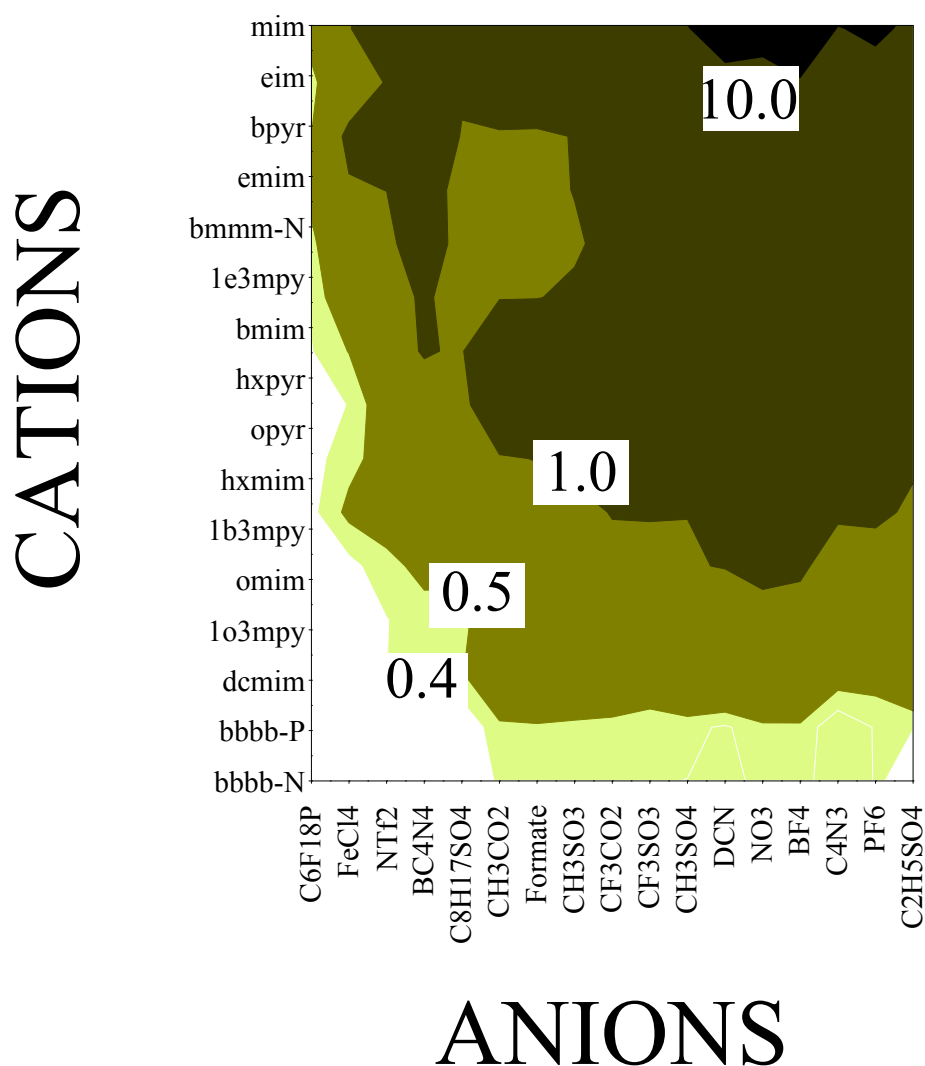


Figure 7.4: Screening of predicted Henry's law constants ($\cdot 10^2$ MPa) for toluene in 272 ILs at 298 K calculated by COSMO-RS.

It is observed that the toluene absorption capacity of ILs is determined by the selection of both cationic and anionic structures. Regarding the cation family effect, and focusing specially on the white region of the map (which corresponds to ILs whose toluene H values

7.3. Results

fall in the order of the benchmark absorbent DEHA), long chain imidazolium cations and tetra-substituted long chain phosphonium or ammonium cations seem to improve the capacity for absorbing toluene. However, taking into account the higher viscosity of ILs based on tetra-substituted long chain ammonium or phosphonium cations (Crosthwaite et al., 2005a; Khupse and Kumar, 2009; Fraser et al., 2007) we decided to select ILs based on imidazolium cations. On the other hand, Figure 7.4 indicates that highly halogenated hydrophobic anions, such as $[C_6F_{18}P]^-$, $[NTf_2]^-$ and $[FeCl_4]^-$, also improve the absorption of toluene.

In the following, the computational analysis is focused on a set of commercially available imidazolium-based ILs with favorable thermodynamics for toluene absorption. Figure 7.5 compares excess enthalpy, h^E , for equimolar toluene-IL mixtures with Henry’s law constants for more than 200 different ILs (those with $H < 5 \cdot 10^{-3}$ MPa), both estimated by COSMO-RS. As a general trend, higher solubilities (decreasing H values) of toluene in ILs are associated to lower endothermicity (decreasing h^E values) of the mixtures.

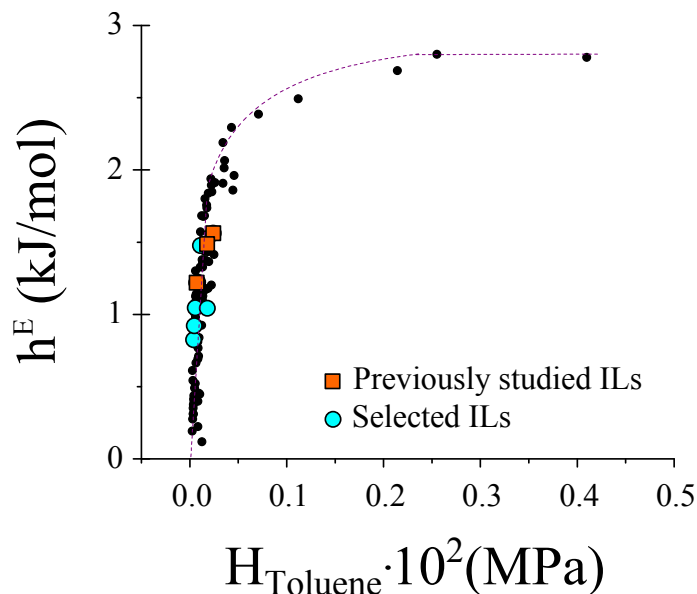


Figure 7.5: Excess molar enthalpies (h^E) of equimolar toluene-IL mixtures versus Henry’s law constants (H) for toluene in >200 ILs, both computed by COSMO-RS at 298K.

Analyzing the computational results of Figures 7.4 and 7.5, it was able to choose five selected ILs where the predicted values of toluene Henry’s constant are lower than those

7. Optimized ionic liquids for toluene absorption

for previously studied ILs in bibliography as toluene absorbents (Quijano et al., 2011). In addition, we decided to evaluate the suitability as toluene absorbent of an IL with relative low cost, based on ethylsulfate anion $[\text{emim}][\text{C}_2\text{H}_5\text{SO}_4]$. Figure 7.6 allows analyzing the absorption of toluene in selected ILs in terms of the contributions of intermolecular interactions to the h^E of toluene-IL mixtures. Electrostatic (Misfit) forces represent in this system the main solute-solvent interactions. They enhance the solubility of toluene in IL when the length of alkyl chain increases, that is, the nonpolar character of the solvent.

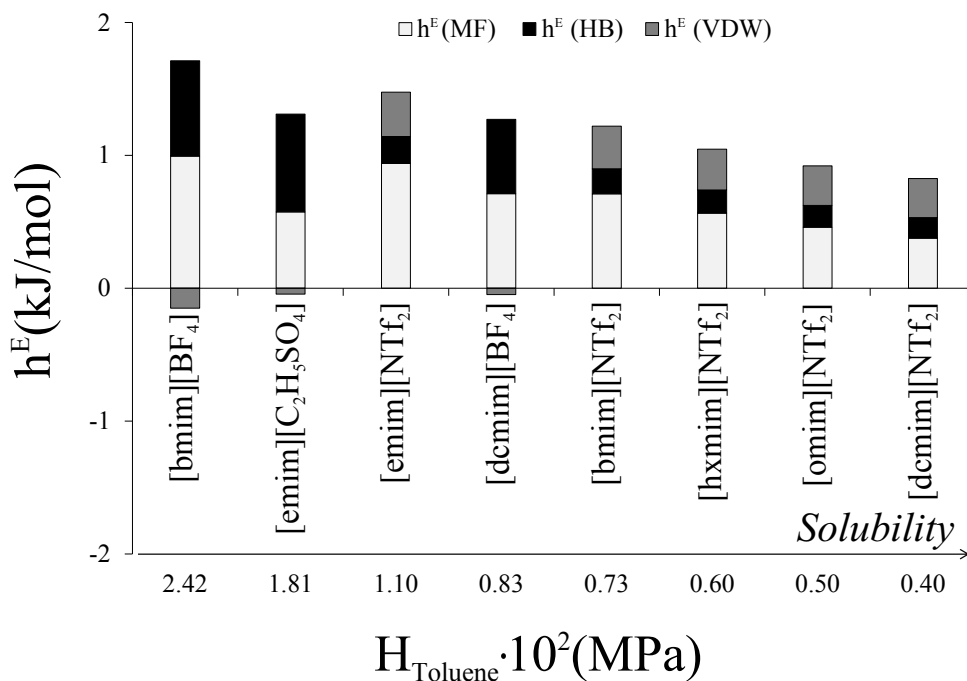


Figure 7.6: Henry's law constants for toluene in ILs vs the excess molar enthalpies of toluene-IL mixtures at 298 K calculated by COSMO-RS.

7.3.2 Toluene absorption experiments

From COSMO-RS computational analysis, we selected the commercially available ILs [dcim][NTf₂], [omim][NTf₂], [hxim][NTf₂], [emim][NTf₂], [dcim][BF₄] and [emim][C₂H₅SO₄] as promising potential solvents to be experimentally tested for toluene absorption. The results will be compared with those reported with [bmim][NTf₂] (Quijano et al., 2011) and the obtained with [bmim][BF₄] as reference conventional IL. Figure 7.7 shows the results of absorption equilibrium experiments performed using toluene/N₂ gas mixtures and [dcim][NTf₂] (the IL with higher toluene solubility predicted by COSMO-RS) at atmospheric pressure and temperatures of 293, 303, and 313 K.

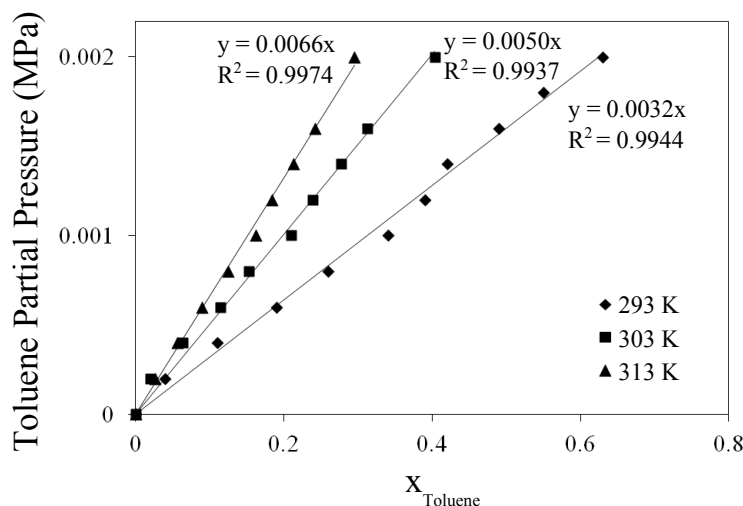


Figure 7.7: Equilibrium curves of toluene absorption on [dcim][NTf₂] ILs measured at 293, 303 and 313 K and total 0.1 MPa.

For an initial toluene concentration of 20000 ppmv, [dcim][NTf₂] absorbs at equilibrium a significant amount of 0.34 g of toluene per gram of IL at 293 K and 1 atm. Figure 7.7 confirms that, as expected, toluene solubilities increase with decreasing temperature and increasing toluene partial pressure. The Henry's law constant could be calculated using the mole fraction of toluene in the IL and the equilibrium pressure, P, by:

$$H_{Tol} = \lim_{x_{Tol} \rightarrow 0} \frac{P}{x_{Tol}} \quad (7.14)$$

This expression is rigorously applied to the toluene gas phase in contact with the IL. In our experimental conditions, we use a binary gas phase mixture of nitrogen and toluene.

7. Optimized ionic liquids for toluene absorption

Table 7.2: Henry’s Law constant (H) for toluene absorption in [dcnim][NTf₂] estimated from equilibrium experiments and predicted by COSMO-RS.

Temperature (K)	Experimental H (MPa)	COSMO-RS H (MPa)
293	0.0032	0.0031
303	0.0050	0.0049
313	0.0066	0.0078

However, taking into account the low solubility of N₂ in imidazolium-based IL ($<10^{-3}$ molar fraction at 1 atm and 313 K) (Carlisle et al., 2008) and assuming a very low interaction between nitrogen and toluene molecules, the effect of nitrogen in the toluene absorption process is neglected. Furthermore, the relation between the equilibrium pressure and the mole fraction of toluene is linear in the entire toluene mole fraction (Figure 7.7) at all the temperatures tested, despite the high values of toluene mole fraction reached in the IL. Considering these assumptions (Vuong et al., 2009; Brodkey and Hershey, 2003), the slopes of linear fits of Figure 7.7 provide representative values of Henry’s Law constant for toluene absorption in the selected IL [dcnim][NTf₂]. The resulting H values from experiment at different temperatures are in very good agreement with COSMO-RS predictions (see Table 7.2).

Figure 7.8 shows the absorption-desorption curves of toluene in (a) ILs with [NTf₂]⁻ anion and (b) other ILs, obtained by thermogravimetric measurements at 293 K and atmospheric pressure and a toluene partial pressure of 2.0 kPa.

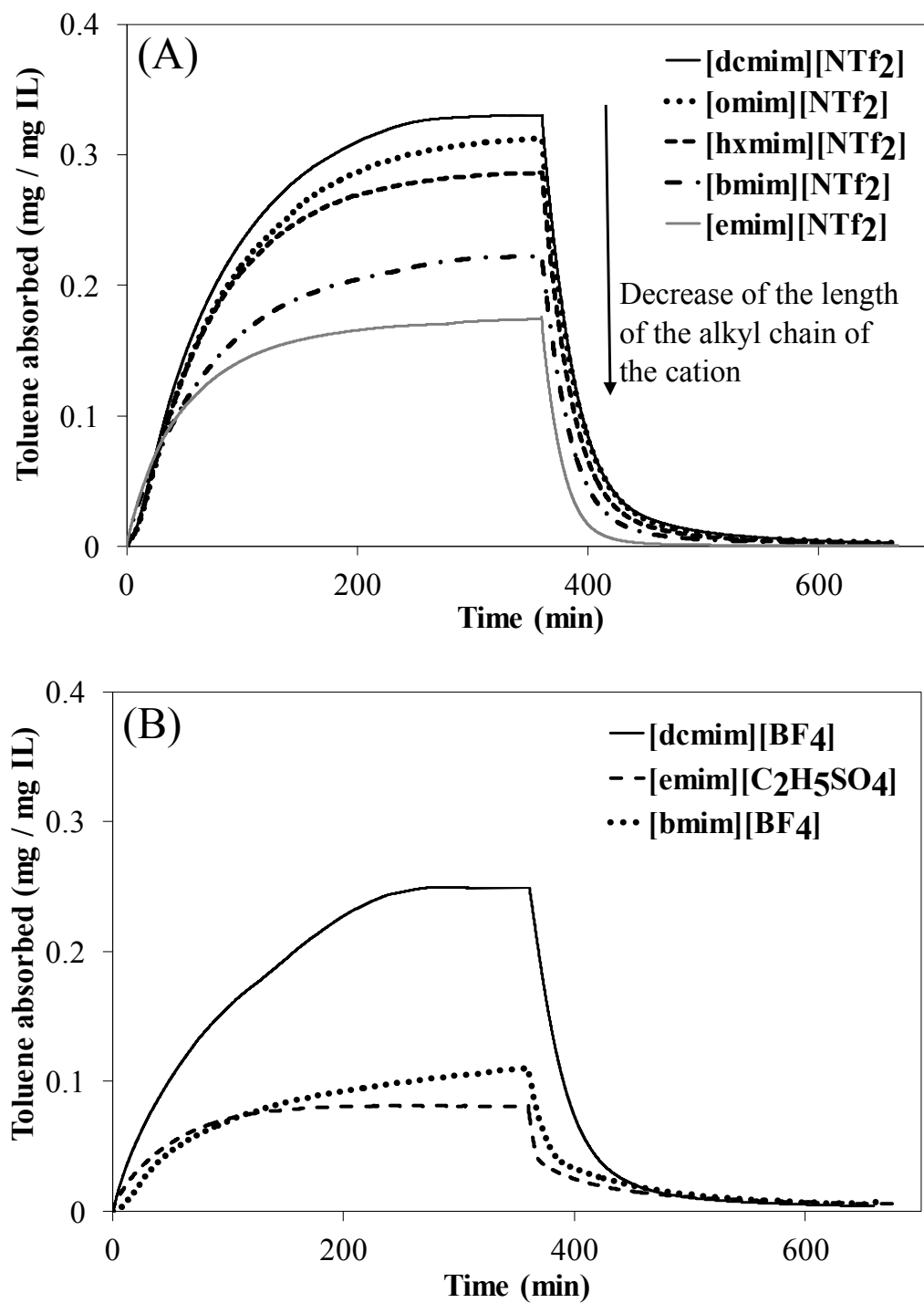


Figure 7.8: Toluene absorption-desorption curves at 293 K and atmospheric pressure in (a) ILs with $[\text{NTf}_2]^-$ anion and (b) other ILs (toluene partial pressure of 2.0 kPa for absorption).

7. Optimized ionic liquids for toluene absorption

Similar curves were obtained at 303 and 313 K (Figures 7.9 and 7.10), decreasing the absorption toluene with increasing temperatures for all the ILs analyzed, as expected.

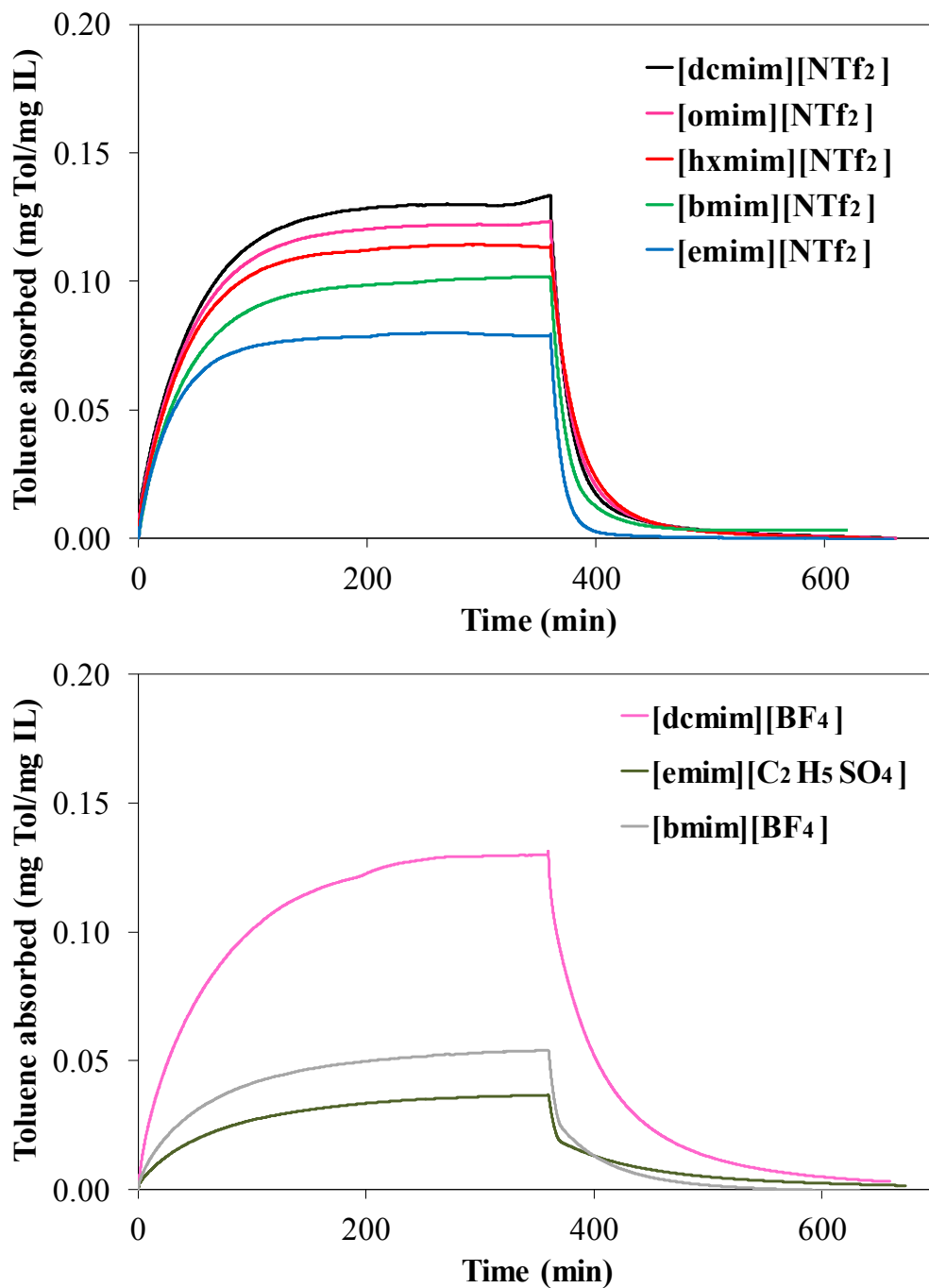


Figure 7.9: Toluene absorption-desorption curves at 303 K in (a) ILs with $[\text{NTf}_2]^-$ anion and (b) other ILs (at a toluene partial pressure of 2.0 kPa for absorption).

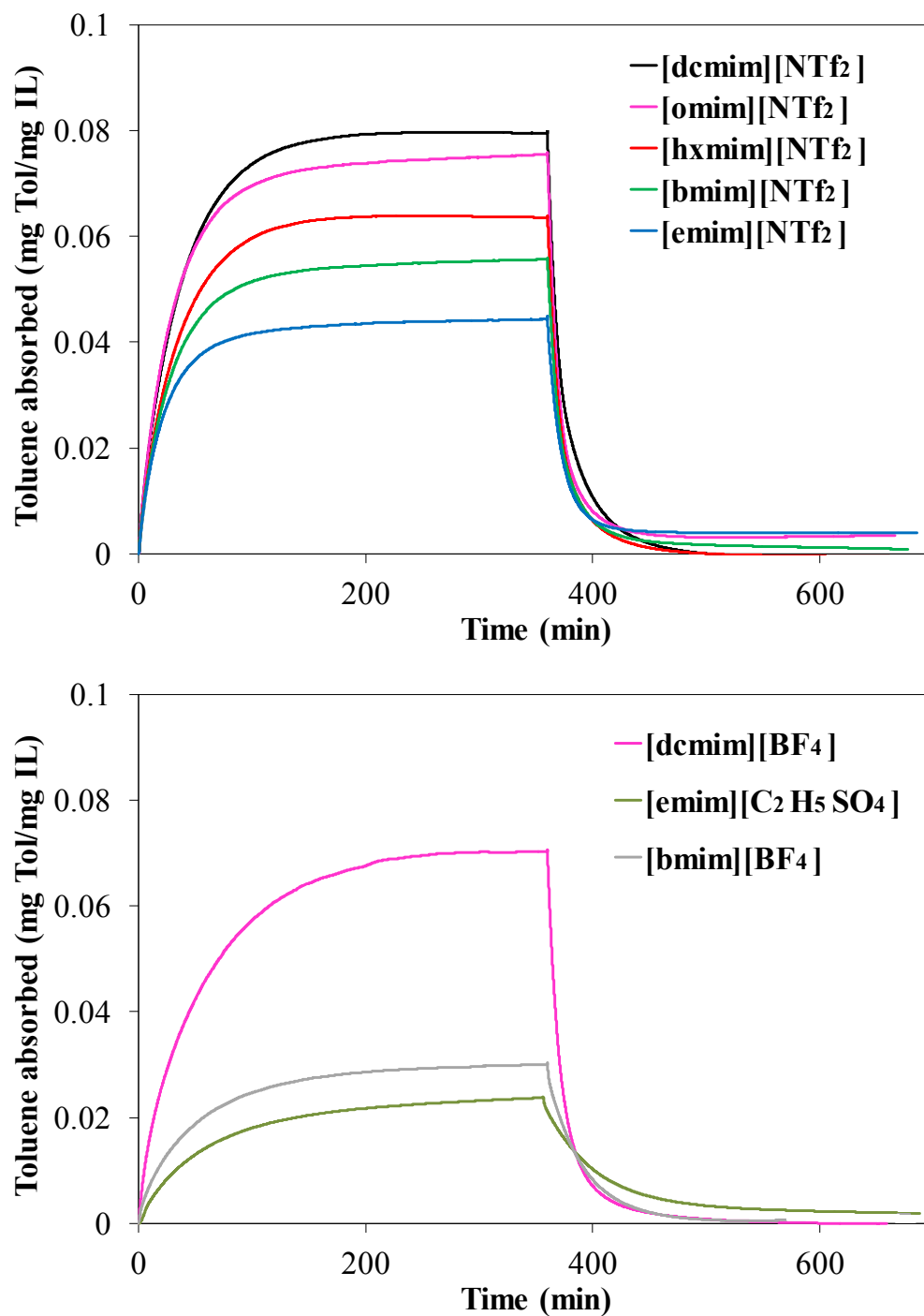


Figure 7.10: Toluene absorption-desorption curves at 313 K in (a) ILs with $[\text{NTf}_2]^-$ anion and (b) other ILs (at a toluene partial pressure of 2.0 kPa for absorption).

Figure 7.8a clearly shows a decrease in the amount of toluene absorbed at saturation

7. Optimized ionic liquids for toluene absorption

as the length of the alkyl chain length of the imidazolium cation decreases. The lowest toluene absorption capacities correspond to ILs with less hydrophobic anions and shorter alkyl chains, [emim][C₂H₅SO₄] and [bmim][BF₄] ILs (Figure 7.8b). These ILs also provided the highest values of the predicted Henry's constants (7.6).

Figure 7.11 shows the good correlation between the COSMO-RS predictions and the experimental toluene absorption capacities. This indicates the validity of H as thermodynamic parameter of reference to select ILs for toluene absorption processes.

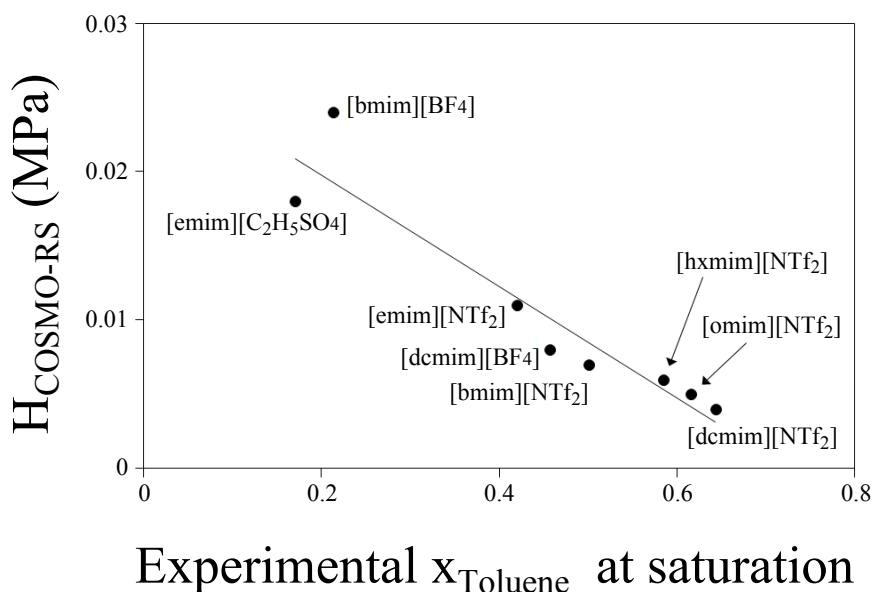


Figure 7.11: COSMO-RS predicted H values at 298 K vs experimental toluene absorption capacities (molar fraction) obtained at 293 K, atmospheric pressure and 2 kPa toluene partial pressure.

Desorption of toluene from the saturated IL is a key issue regarding potential applications. The desorption curves under continuous bare N₂ flow are included in Figure 7.8. Desorption of toluene was complete in all the cases, that is, all the toluene absorbed was desorbed at the absorption temperature, without the need of heating or vacuum which has been reported with other ILs (Huang et al., 2008). Thus, the complete regeneration would be possible by simple stripping at the same ambientlike absorption temperature. To quantify the kinetics of toluene absorption in ILs, diffusion coefficients were estimated by applying a simplified mass diffusion model previously used for CO₂ absorption in ILs (Shiflett and Yokozeki, 2005; Crank, 1979; Hou and Baltus, 2007). The process may be described by one-dimensional mass diffusion due to the local concentration difference. The

7.3. Results

toluene mass balance can be written as

$$\frac{\partial C}{\partial t} = D \cdot \frac{\partial^2 C}{\partial z^2} \quad (7.15)$$

with an initial condition $C=0$ when $t=0$ and $0 < z < L$ and boundary conditions (i) $C=C_s$ when $t > 0$ and $z=0$ and (ii) $\partial C / \partial z = 0$ at $z=L$. C is the concentration of toluene dissolving in the IL as a function of time, t , and vertical location, z . L is the depth of IL in the container (estimated for each case using the weight of IL in the sample pot and the corresponding density reported in Table 7.1). D is the diffusion coefficient that is assumed constant. In this work, D is as an *effective* diffusion coefficient since the toluene-IL mixtures cannot be considered diluted solutions. The simplification of assuming diluted solutions has been previously used by other authors working with CO_2 -ILs systems reaching even higher solute concentration than ours (Shiflett and Yokozeki, 2005). The experimentally measured toluene concentration (mass per unit volume) in IL at a given time corresponds to the space-averaged concentration, \bar{C} , at that time, which can be calculated from the equation:

$$\bar{C} = \frac{1}{L} \int_0^L C dz \quad (7.16)$$

$$\bar{C} = C_s \left[1 - 2 \sum_{n=0}^{\infty} \frac{\exp(-\lambda_n^2 Dt)}{L^2 \lambda_n^2} \right] \quad (7.17)$$

Although this equation contains an infinite summation, only the first four terms are sufficient in practical applications. Fitting the experimental data to this equation, we obtained the saturation concentration (C_s) and the diffusion coefficient (D) at given T and P . The fitting was performed by nonlinear regression. Table 7.3 summarizes the values of the effective diffusion coefficient of toluene in different ILs at the three absorption temperatures tested. The correlation coefficients (R^2) show fairly good values in all the cases ($R^2 > 0.99$). For comparison purposes, the values of D were tentatively estimated by the Wilke-Chang correlation, widely applied in bibliography to predict diffusion coefficients (Wilke and Chang, 1955).

$$D = 7.4 \cdot 10^{-8} \frac{(\phi \cdot M_{IL})^{0.5} T}{\mu_{IL} \cdot V_{Tol}^{0.6}} \quad (7.18)$$

where T is temperature (K), μ_{IL} and V_{Tol} are, respectively, the viscosity of IL (Table 7.1) and the molar volume of toluene at the corresponding temperature, M_{IL} is the molar mass of IL and ϕ is the association parameter (with value of 1, considering in this case IL as unassociated solvent).

7. Optimized ionic liquids for toluene absorption

Table 7.3: Effective diffusion coefficients of toluene in ILs at different temperatures obtained from absorption measurements and estimated by Wilke-Chang correlation.

IL	Temperature (K)	$D \cdot 10^{11}$ (m ² /s)	R^2	$D \cdot 10^{11}$ (m ² /s) (Wilke-Chang)
[dcmim][NTf ₂]	293	3.9	0.994	2.2
	303	7.5	0.996	3.8
	313	8.9	0.998	6.1
[omim][NTf ₂]	293	3.8	0.994	2.6
	303	7.2	0.998	4.3
	313	9.0	0.992	6.8
[hxmim][NTf ₂]	293	3.9	0.992	3.1
	303	7.1	0.995	5.2
	313	10.1	0.998	8.1
[bmim][NTf ₂]	293	4.6	0.998	4.3
	303	7.8	0.995	7.0
	313	10.6	0.993	10.5
[emim][NTf ₂]	293	5.5	0.996	6.3
	303	8.1	0.996	9.5
	313	10.7	0.992	13.6
[dcmim][BF ₄]	293	3.76	0.999	2.5
	303	6.13	0.998	5.3
	313	9.86	0.999	10.0
[emim][C ₂ H ₅ SO ₄]	293	6.5	0.998	1.8
	303	10.2	0.999	2.8
	313	11.0	0.995	4.1
[bmim][BF ₄]	293	7.1	0.992	1.6
	303	8.97	0.998	2.9
	313	10.8	0.998	4.4

Table 7.3 shows a good agreement between D obtained from the absorption experiments and those estimated by Wilke-Chang correlation. The diffusion coefficients increase with the absorption temperature consistently with the decrease of the ILs viscosities (Table 7.1). The effective diffusion coefficients increase when decreasing the length of the imidazolium cation alkyl chain of ILs containing the [NTf₂]⁻ anion. The increase is in agreement with the lower viscosity of the IL with shorter alkyl chain (Table 7.1). It should be indicated that the D values obtained in this work for the absorption of toluene in [bmim][BF₄] are in the order of magnitude of those previously reported for CO₂ with this IL (Shiflett and Yokozeki, 2005).

7.3. Results

7.3.3 Process simulation

In this section, the process simulator Aspen Plus v 7.3 was used for modeling and evaluating the absorption of toluene by ILs (favorable series with the $[\text{NTf}_2]^-$ anion) in separation columns of different types. First, the inclusion of ILs as new components in Aspen Plus was checked by comparing the experimental values of density, viscosity, toluene diffusivity, and toluene absorption equilibrium data for the tested ILs with those predicted by Aspen Plus and using COSMOSAC property model. Table 7.4 shows the good agreement between experimental and simulated property values for the five IL-toluene systems evaluated.

Table 7.4: Experimental and Aspen Plus simulated values for density, viscosity, toluene diffusivity and toluene absorption equilibrium data for the five IL-toluene systems.

IL	T (K)	ρ (kg/m ³)		μ (cP)		D·10 ⁻¹¹ (m ² /s)		H (MPa)	
		Sim.	Exp.	Sim.	Exp.	Sim.	Exp.	Sim.	Exp.
[emim][NTf ₂]	293	1518	1524	40.3	41	6.8	5.5	0.0043	—
	303	1511	1514	27.8	28	9.8	8.1	0.0071	—
	313	1505	1506	19.8	20	13.9	10.7	0.0114	—
[bmim][NTf ₂]	293	1441	1441	65.5	63	4.4	4.6	0.0040	—
	303	1434	1432	41.9	40	6.9	7.8	0.0066	—
	313	1428	1424	27.9	27	10.3	10.6	0.0106	—
[hxmim][NTf ₂]	293	1384	1376	90.6	91	3.4	3.9	0.0036	—
	303	1377	1367	55.8	56	5.4	7.1	0.0060	—
	313	1371	1358	35.8	36	8.4	10.1	0.0096	—
[omim][NTf ₂]	293	1333	1327	123.4	115	2.7	3.8	0.0035	—
	303	1327	1320	73.6	71	4.3	7.2	0.0057	—
	313	1321	1307	45.9	46	6.9	9.0	0.0091	—
[dcmmim][NTf ₂]	293	1288	1282	140.6	141	2.4	3.9	0.0033	0.0032
	303	1282	1278	85.8	84	3.9	7.5	0.0054	0.005
	313	1276	1274	54.6	54	6.2	8.9	0.0086	0.0066
R ²		0.997		0.9961		0.65		0.953	
MRD		0.42%		2.31%		24.14%		11.23%	

It demonstrates both the confidence of ILs implementation as pseudocomponents in Aspen Plus and the capacity of the COSMOSAC property model for estimating thermophysical and equilibrium properties of the (ILs + toluene) mixtures. The recovery of toluene at given operating conditions (C_{Toluene} in gas: 2000 ppmv; G/L=35 in mol, 298 K and 1 atm) was simulated in a single-stage contactor using both equilibrium-and

7. Optimized ionic liquids for toluene absorption

rate-based approaches by RADFRAC in Aspen Plus.

Table 7.5 shows that using rate-based one-stage absorption, the toluene recovery follows the general trend of gas-liquid equilibrium data reported before:

DEHA > [dcimim][NTf₂] > [omim][NTf₂] > n-hexadecane > [hxmim][NTf₂] > [bmim][NTf₂] > [emim][NTf₂]. In addition, toluene separation in rate-based simulation is significantly enhanced at lower-temperatures for all the considered solvents, in spite of the lower diffusion coefficients (Table 7.3). These results suggest that thermodynamics prevails over kinetics, thus being the determining factor in toluene absorption by the ILs tested under experimental conditions of this work.

Table 7.5: Toluene recoveries (%) and Murphree tray efficiencies for the separation of toluene by absorption with ILs and organic solvents in a one-stage contactor, using equilibrium and rate-based models for separation column.

Absorbent	%Toluene recovery						Murphree Tray Efficiency		
	Rate-based model			Equilibrium model					
	293 K	303 K	313 K	293 K	303 K	313 K	293 K	303 K	313 K
[dcimim][NTf ₂]	52.3	40.0	29.6	67.0	50.1	35.4	0.78	0.80	0.84
[omim][NTf ₂]	48.3	36.3	26.5	61.9	45.0	31.2	0.78	0.81	0.85
[hxmim][NTf ₂]	44.7	33.0	23.7	57.0	40.4	27.5	0.78	0.82	0.86
[bmim][NTf ₂]	40.7	29.5	20.9	51.5	35.6	23.8	0.79	0.83	0.87
[emim][NTf ₂]	35.4	25.1	17.5	44.1	29.5	19.5	0.80	0.85	0.90
n-hexadecane	45.8	34.4	25.1	56.8	40.8	28.2	0.80	0.84	0.89
DEHA	64.7	52.6	41.0	81.0	66.3	50.2	0.78	0.80	0.82

Nevertheless, Figure 7.12(A), which compares the percentage of recovered toluene by using rate- and equilibrium-based models for the IL series, suggests that the kinetics also influences toluene absorption by ILs.

Remarkably, the more effective IL absorbents present the less favorable mass transfer properties and, as consequence, lower Murphree tray efficiencies (Figure 7.12(B)). This clearly points to the convenience of taking into account kinetic considerations in the selection of both the IL solvent and the operating conditions. On the other hand, the one-stage absorption results (Table 7.5 and Figure 7.12) indicate that the selected [dcimim][NTf₂] IL solvent could be a promising alternative to conventional organic absorbents, as n-hexadecane or DEHA (Quijano et al., 2011). To evaluate this point, the absorption of toluene gas has been simulated in a packed column using [dcimim][NTf₂], n-hexadecane

7.3. Results

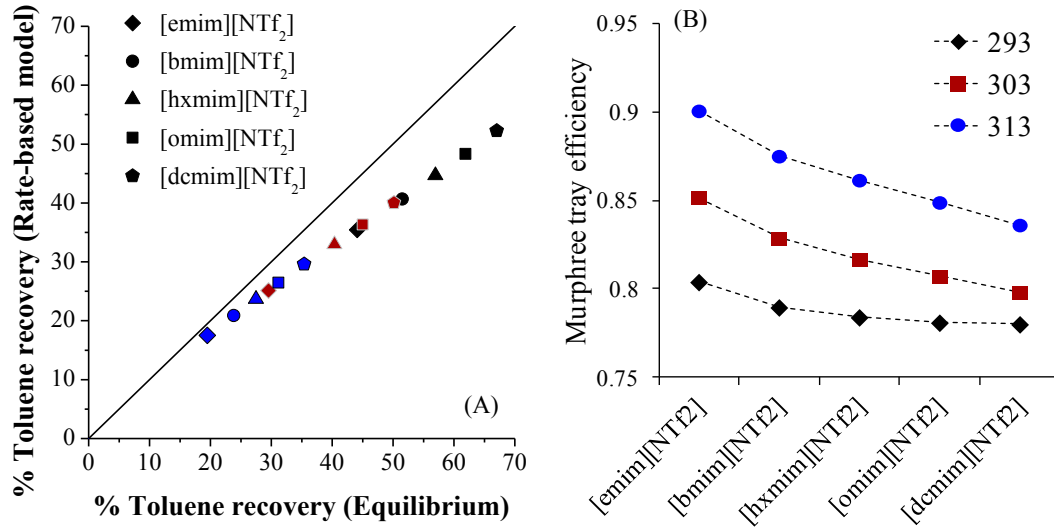


Figure 7.12: (A) Equilibrium- vs. rate-based toluene recovery values at 293 (black), 303 (red) and 313 (blue) K; and (B) Murphree tray efficiencies using different ILs at the considered temperature.

and DEHA as absorbents, operating at 293 K and 1 atm with a molar G/L ratio of 17 and with the column dimensions described in Process simulation details. The main results are summarized in Table 7.6.

Table 7.6: Toluene recovery (%), toluene molar fraction in the exit gas [$y_{\text{Toluene}}(\text{gas out})$] and height equivalent to a theoretical plate (HETP) in a 2 m height absorption packed column at 293 K, 1 atm, G/L= 17 (in mol) and $y_{\text{Toluene}}(\text{gas in})=0.002$, simulated by Aspen Plus.

Absorbent	Toluene Recovery% in mol	y_{Toluene} (Gas out)in mol	HETP (m)
DEHA	90	$1.9 \cdot 10^{-4}$	0.77
[dcimim][NTf ₂]	83	$3.4 \cdot 10^{-4}$	0.57
n-hexadecane	73	$5.2 \cdot 10^{-4}$	1.36

Toluene recovery and concentration in the exit gas stream when using [dcimim][NTf₂] as solvent present intermediate values to the conventional organic solvents, DEHA and n-hexadecane. It should be pointed out that the mass transfer efficiency of the packed column simultaneously depends on gas and liquid flow rate, density, viscosity, and diffusivity (Table 7.7). Aspen Plus simulations show the lowest HETP value when using the IL as absorbent. This implies higher mass transfer efficiency in the packed column, for

7. Optimized ionic liquids for toluene absorption

the selected IL [dcmim][NTf₂] than for the organic solvents DEHA and n-hexadecane.

Table 7.7: Aspen Plus simulated values of gas and liquid flow rate, density, viscosity and toluene diffusivity for DEHA, [dcmim][NTf₂] and n-hexadecane solvents at 293 K and 1 atm.

Absorbent	Gas Flow rate (m ³ /h)	Liquid Flow rate·10 ³ (m ³ /h)	ρ (kg/m ³)	μ (cP)	D·10 ⁻¹¹ (m ² /s)
DEHA	8.54	6.47	915	40.3	6.9
[dcmim][NTf ₂]	8.54	7.89	1288	138	2.42
n-hexadecane	8.54	5.46	772	3.4	57

7.4 Concluding remarks

Basing on the COSMO-RS thermodynamic properties predictions (Henry's constant and excess enthalpy) of more than 200 IL-toluene systems, the [dcmim][NTf₂], [omim][NTf₂], [hxmim][NTf₂], [emim][NTf₂], [dcmim][BF₄] and [emim][C₂H₅SO₄] ILs were selected as promising potential toluene absorbents.

Absorption tests confirmed that selected ILs present high absorption capacities for toluene. Likewise, the experimental results reported a high absorption rate of toluene in these ILs.

Process simulation allowed concluding that thermodynamics considerations prevail in toluene absorption. Nonetheless, Aspen Plus evidenced the need of considering thermodynamic and kinetics aspects in the IL selection and the design of IL-based separation processes.

The results obtained for experimental thermodynamic and kinetic data were in good agreement with theoretical predictions. Then, the computational-experimental strategy research was successfully applied to select ILs with favorable properties for toluene absorption. Imidazolium-based ILs with the [NTf₂]⁻ anion and high length of the cation alkyl chain are found suitable ILs for toluene absorption, considering both kinetic and thermodynamic aspects.

Chapter 8

Conclusions and prospects for the future

The multiscale approach developed in this PhD thesis allows tackling the conceptual development of different processes based on ionic liquids (ILs). The combined use of molecular simulation, experimental work and process simulation is suitable to select/design ILs with optimized properties for a specific task taking into account thermodynamic and kinetic criteria, as well as techno-economic and operating aspects.

It has been demonstrated that COSMO-RS method is valid for predicting thermodynamic properties of pure ILs and their mixtures, such as the acetone-IL binary mixtures and the paraffin/olefin-IL multicomponents mixtures.

Molecular simulation allows for analyzing the intermolecular interactions established in the acetone-IL mixtures. Basing on the molecular simulation results for excess enthalpy of such mixtures, acetone generally forms hydrogen bonding with the most acidic part of the cation. These results have been confirmed by NMR spectroscopy.

The COSMO-RS has been successfully applied for calculating Henry's constants of different paraffin and olefins with ILs. From a thermodynamic point of view, new phosphonium-based ILs with highly aliphatic character have been proposed as promising options for paraffin/olefin separation.

Ionic liquids have been implemented in the commercial process simulator chosen. Property packages have been created in Aspen Plus containing the information required to fully specify the ILs pseudocomponents and the COSMOSAC thermodynamic property method. These specifications have been obtained using COSMOthermX program. The

transferability of the COSMO-RS results to the Aspen Plus process simulator has been demonstrated by comparison with experimental data.

The IL regeneration process from its mixture with an organic component has been simulated in Aspen HYSYS. Based on process simulation results, the IL regeneration is possible by flash distillation at near vacuum conditions. Using Aspen HYSYS, techno-economic criteria have been established in the selection of the optimal IL as solvent to be recovered from a separation process.

Likewise, an absorption refrigeration chiller using ammonia-IL as working pair has been simulated in Aspen HYSYS. The cycle performance has been shown to be increased by those ionic liquids having high absorption capacity of ammonia. This simulation has enabled establishing new criteria for the IL selection based on the efficiency of the process.

The multiscale approach developed here has been successfully applied in the selection of optimized ionic liquids for toluene absorption. Molecular simulation has been used to identify a set of suitable commercial ILs for toluene absorption. The suitability of selected ILs is confirmed with experimental work performed in the laboratories of Universidad Autónoma de Madrid. New thermodynamic and kinetic criteria established in Aspen Plus have allowed identifying the most promising ILs for toluene absorption. According to the multiscale results, those ILs formed by a long chain alkyl imidazolium cation and [NTf₂] anion, such as [dcmim][NTf₂], are optimal for toluene absorption.

This PhD thesis propose a research strategy that allows designing new processes of industrial interest based on ionic liquids. Once the procedure is developed, the implementation options are numerous. The multiscale approach can be applied in other systems, new processes, using other components, other operating conditions, etc. We are able to integrate new components in a commercial process simulator using COSMO-based methodologies. Hereinafter, the estimate of properties required to create pseudocomponents are desired to be improved, an IL database is intended to be developed for its use in Aspen Plus, and other IL-based systems as well as other IL-based processes are being considered to be studied. The aim of this research group is to develop new processes of industrial interest (trying to bet on ionic liquids) taking into account theoretic and experimental results.

Conclusiones globales y perspectivas para el futuro

La estrategia multiescala desarrollada en esta tesis doctoral permite abordar el desarrollo conceptual de diferentes procesos de interés basados en líquidos iónicos (LIs). El uso combinado de las etapas de simulación molecular, experimentación y simulación de procesos resulta adecuado para buscar líquidos iónicos con propiedades optimizadas para su uso potencial en una tarea determinada utilizando criterios tanto termodinámicos como cinéticos, e integrando valoraciones técnico-económicas y operaciones.

Se ha demostrado que el método COSMO-RS es válido para determinar propiedades termodinámicas tanto de los líquidos iónicos puros como de las mezclas binarias LI-acetona o multicomponentes parafina/olefina-LI.

El uso de la herramienta de simulación molecular permite analizar las interacciones intermoleculares establecidas en mezclas acetona-LI. Mediante el cómputo de las entalpías de exceso de dichas mezclas, así como de cálculos químico-cuánticos utilizando agregados moleculares (clusters), se ha determinado que la acetona interacciona con la parte más ácida del catión formando puentes de hidrógeno. Estos resultados han sido confirmados mediante espectroscopía de RMN.

La simulación molecular también se puede aplicar para estimar constantes de Henry de diferentes parafinas y olefinas en sus mezclas con líquidos iónicos. Este estudio ha permitido seleccionar y diseñar LIs con propiedades optimizadas para desempeñar la función de agente separador de estas mezclas. Desde un punto de vista termodinámico, se ha demostrado que los líquidos iónicos basados en fosfonios con alto carácter alifático son adecuados para separar olefinas de parafinas mediante absorción.

Los líquidos iónicos se han integrado en el simulador de procesos comercial elegido. Se han creado paquetes de propiedades en Aspen Plus con las especificaciones necesarias para cada líquido iónico eligiendo como paquete termodinámico el modelo COSMOSAC.

La información requerida para la creación de los líquidos iónicos como pseudocomponentes, así como para especificar COSMOSAC, se ha obtenido mediante el programa COSMOthermX. La transferibilidad de los resultados de COSMO-RS a los simuladores de procesos Aspen Plus y Aspen HYSYS se ha validado mediante comparación con datos experimentales.

Se ha simulado en Aspen HYSYS la regeneración del líquido iónico de mezclas con otros disolventes orgánicos procedentes de un proceso de separación. La regeneración se puede llevar a cabo mediante evaporación del componente orgánico operando en condiciones cercanas al vacío. Además de establecer las condiciones de operación adecuadas en este proceso, la simulación ha permitido considerar aspectos técnico-económicos en la selección del líquido iónico óptimo.

También se ha simulado mediante Aspen HYSYS un ciclo de refrigeración por absorción que opera con amoníaco como agente refrigerante y con un líquido iónico como absorbente del anterior. Se ha demostrado que el tipo de líquido iónico utilizado afecta al rendimiento del ciclo, resultando como absorbente idóneo aquel que presente una mayor capacidad de absorción de amoníaco. Este estudio ha permitido establecer nuevos criterios de selección de líquidos iónicos basados en la eficiencia del proceso.

La metodología multiescala desarrollada se ha aplicado en la selección de líquidos iónicos con propiedades optimizadas para la absorción del tolueno. La simulación molecular ha permitido identificar un set de líquidos iónicos comerciales con una adecuada capacidad de absorción del tolueno en estado gas. En los laboratorios de la Universidad Autónoma de Madrid se han llevado a cabo estudios experimentales que corroboran la idoneidad de los líquidos iónicos previamente propuestos mediante simulación molecular. Aspen Plus ha permitido evaluar criterios termodinámico y cinéticos en el proceso de absorción de tolueno con líquidos iónicos. Teniendo en cuenta las tres etapas, se ha obtenido que los líquidos iónicos basados en cationes de larga cadena alquílica y aniones $[\text{NTf}_2]^-$, como el $[\text{dcim}][\text{NTf}_2]$, son los que resultan óptimos para la captura del gas tolueno.

En definitiva, esta tesis doctoral ofrece una estrategia de investigación que permite diseñar nuevos procesos de interés industrial basados en líquidos iónicos. Una vez desarrollada la técnica, las opciones de aplicación son numerosas, pudiéndose ampliar a otros sistemas de estudio, otros compuestos, otros procesos, otras condiciones de operación, etc. Nos encontramos en capacidad de integrar nuevos componentes en un simulador de procesos comercial aplicando las metodologías COSMO. En lo sucesivo, se desea mejorar la estimación de propiedades necesarias en la creación de pseudocomponentes, se pre-

8. Conclusions and prospects for the future

tende desarrollar una base de datos de líquidos iónicos en Aspen Plus, así como ampliar el número de casos de estudios tanto de simulación como de experimentación (nuevos refrigerantes y/o absorbentes para los ciclos de refrigeración por absorción, otros sistemas para procesos de separación. . .). El objetivo de este grupo de investigación es desarrollar nuevos procesos de interés industrial (intentando apostar por los líquidos iónicos) teniendo en cuenta tanto datos teóricos como experimentales.

finis operis, sed non quaerendum...

(Bernardo de Claraval)

Appendix A

Acronyms for ionic liquids

Table A.1: Anions appearing in this PhD thesis.

Acronym	Anion name
$[\text{AsF}_6]^-$	hexafluoro-arsenate
$[\text{BCl}_4]^-$	tetracyanoborate
$[\text{BF}_4]^-$	tetrafluoroborate
$[\text{Br}]^-$	bromide
$[\text{C}_2\text{H}_5\text{SO}_4]^-$	ethylsulfate
$[\text{C}_2\text{H}_6\text{PO}_4]^-$	dimethylphosphate
$[\text{C}_4\text{F}_9\text{SO}_3]^-$	perfluorobutanesulfonate
$[\text{C}_4\text{H}_{10}\text{SO}_4]^-$	diethyl sulfate
$[\text{C}_4\text{N}_3]^-$	tricyanomethane
$[\text{C}_5\text{H}_{11}\text{O}_6\text{S}]^-$	2-(2-methoxyethoxy)ethylsulfate
$[\text{C}_6\text{F}_{18}\text{P}]^-$	tris(pentafluoroethyl)trifluorophosphate
$[\text{C}_8\text{H}_{14}\text{SO}_3\text{N}]^-$	cyclohexylamine ethylsulfonate
$[\text{C}_8\text{H}_{17}\text{SO}_4]^-$	octylsulfate
$[\text{C}_8\text{H}_{18}\text{PO}_4]^-$	dibutyl phosphate
$[\text{CF}_3\text{CO}_2]^-$	trifluoroacetate
$[\text{CF}_3\text{SO}_3]^-$	trifluoromethanesulfonate
$[\text{CH}_3\text{CO}_2]^-$	acetate
$[\text{CH}_3\text{SO}_3]^-$	methanesulfonate
$[\text{Cl}]^-$	chloride
$[\text{DCN}]^-$	dicyanamide

Continued on next page

Table A.1 – *Continued from previous page*

Acronym	Anion name
[FeCl ₄] ⁻	tetrachloroferrate
[H ₂ PO ₄] ⁻	dihydrogen-phosphate
[MePhSO ₃] ⁻	4-methylbenzenesulfonate
[NFBTFP] ⁻	tris(nonafluorobutyl)trifluorophosphate
[NO ₃] ⁻	nitrate
[NTf ₂] ⁻	bis(trifluoromethanesulfonyl)imide
[PF ₆] ⁻	hexafluorophosphate
[SCN] ⁻	thiocyanate
[TMPP] ⁻	bis(2,4,4-trimethylpentyl)phosphinate
[tol-SO ₃] ⁻	toluene sulfonate

Table A.2: Cations appearing in this PhD thesis.

Acronym	Cation name
[1b3mpy] ⁺	1-butyl-3-methyl-pyridinium
[1b4mpy] ⁺	4-methyl-1-butylpyridinium
[1e3mpy] ⁺	1-ethyl-3-methylpyridinium
[1o3mpy] ⁺	3-methyl-1-octyl-pyridinium
[1o4mpy] ⁺	4-methyl-1-octyl-pyridinium
[bbbb-N] ⁺	tetrabutyl ammonium
[bbbb-P] ⁺	tetrabutyl phosphonium
[bim] ⁺	1-butyl-imidazolium
[bmim] ⁺	1-butyl-3-methylimidazolium
[bmmim] ⁺	1-butyl-2,3-dimethylimidazolium
[bmmm-N] ⁺	trimethylbutan amonium
[bmpyr] ⁺	1-butyl-1-methyl-pyrrolidinium
[b-N] ⁺	butyl ammonium
[bpyr] ⁺	1-butylpyrrolidinium
[bzmim] ⁺	1-benzyl-3-methyl-imidazolium
[c _n mim] ⁺	1-n-alkyl-3-methylimidazolium
[choline] ⁺	(2-hydroxyethyl)-trimethyl ammonium

Continued on next page

A. Acronyms for ionic liquids

Table A.2 – *Continued from previous page*

Acronym	Cation name
[dcmim] ⁺	1-decyl-3-methylimidazolium
[DMEA] ⁺	N,N-dimethylethanolammonium
[e2mim] ⁺	1-ethyl-2-methylimidazolium
[eeee-N] ⁺	tetraethyl ammonium
[eeee-P] ⁺	tetraethyl phosphonium
[eim] ⁺	1-ethylimidazolium
[emim] ⁺	1-ethyl-3-methylimidazolium
[emmim] ⁺	1-ethyl-2,3-dimethylimidazolium
[empyr] ⁺	1-ethyl-1-methyl-pyrrolidinium
[epy] ⁺	1-ethylpyridinium
[hmmim] ⁺	1-hexyl-2-3-methyl-imidazolium
[hmpy] ⁺	1-hexyl-3-methypyridinium
[hxmim] ⁺	1-hexyl-3-methylimidazolium
[hxmpyr] ⁺	1-hexyl-1-methyl-pyrrolidinium
[hxpyr] ⁺	1-hexylpyrrolidinium
[N(1)888] ⁺	methyl-trioctyl-ammonium
[meO-emim] ⁺	1-methoxyethyl-3-methylimidazolium
[mim] ⁺	1-methylimidazolium
[mmim] ⁺	1,3-dimethylimidazolium
[mmpyr] ⁺	1,1-dimethyl-pyrrolidinium
[m-N] ⁺	methyl ammonium
[mpy] ⁺	1-methyl-pyridinium
[OHemim] ⁺	1-(2-hydroxyethyl)-3-methylimidazolium
[OH-omim] ⁺	1-(8-hydroxyoctyl)-3-methylimidazolium
[OH-prmim] ⁺	1-(3-hydroxypropyl)-3-methylimidazolium
[OH-prpy] ⁺	1-(3-hydroxypropyl)-pyridinium
[omim] ⁺	1-octyl-3-methylimidazolium
[ommim] ⁺	1-octyl-2,3-dimethylimidazolium
[ompyr] ⁺	1-octyl-1-methyl-pyrrolidinium
[opy] ⁺	1-octylpyridinium
[opyr] ⁺	1-octylpyrrolidinium
[P(1)444] ⁺	triisobutyl-methyl-phosphonium
[P(8)111] ⁺	trimethyl-octyl-phosphonium

Continued on next page

Table A.2 – *Continued from previous page*

Acronym	Cation name
[P(14)666] ⁺	trihexyl-tetradecyl-phosphonium
[P(18)777] ⁺	triheptyl-octadecyl-phosphonium
[P(19)888] ⁺	trioctyl-nonadecyl-phosphonium
[P(19)999] ⁺	trinonyl-nonadecyl-phosphonium
[P4444] ⁺	tetrabutyl-phosphonium
[phmpy] ⁺	1-(phenylmethyl)pyridinium
[pmmim] ⁺	1-propyl-2-3-methyl-imidazolium
[pppyr] ⁺	1,1-dipropyl-pyrrolidinium
[prmpyr] ⁺	1-propyl-1-methylpyrrolidinium
[py] ⁺	pyridinium
[tetradcmim] ⁺	1-tetradecyl-3-methyl-imidazolium

List of Figures

2.1	The three stages comprising the multiscale approach proposed.	12
2.2	Representation in the COSMO method of the cavity embedding the molecule and the solute-solvent interactions in the COSMO method (Mullins et al., 2006).	14
2.3	Flowchart of a property calculation using COSMO-RS (Eckert and Klamt, 2002).	16
2.4	aspenONE Engineering enables an integrated engineering solution for process design and development (Aspen Technology).	28
2.5	aspenONE Engineering (Aspen Technology).	29
2.6	Normal boiling points calculated by COSMO-RS for different aggregates [C...A] in [emim][C ₂ H ₅ SO ₄].	38
2.7	Comparison between experiment and Aspen HYSYS predictions for the density of ionic liquids at 298K. Solid line represents perfect agreement. The [CA] and [C+A] models are used to simulate the ILs structures.	40
2.8	Comparison between experiment and the predictions for the viscosity of ionic liquids using COSMOthermX at 298K. Solid line represents perfect agreement. ([C+A] model)	41
2.9	Temperature-dependent viscosity behavior of (A) [1-ethyl-nicotinic acid ethyl ester][C ₂ H ₅ SO ₄], (B) [omim][BF ₄], (C) [emim][DCN]. The symbols represent: (black) experimental data, and (white) the obtained calculations using COSMOthermX (QSPR model).	42

LIST OF FIGURES

3.1	Comparison of experimental and COSMO-RS calculated values for the maximum (or minimum) of h^E curves of IL-organic compound mixtures at different temperatures (ranging between 298.15 and 353.15 K). Water (white), alcohols (grey), and ketones (black).	53
3.2	The σ -profiles of pure compounds: methanol, acetone and water obtained by COSMO-RS.	55
3.3	Experimental (white) and COSMO-RS (black) curves for excess molar enthalpy of (A) [bmim][NTf ₂] + acetone and (B) [hxmim][NTf ₂] + acetone mixtures at 353.15 K.	56
3.4	Screening of COSMO-RS predicted excess molar enthalpies h^E (kJ/mol) for 312 equimolar acetone-IL mixtures at 298 K.	57
3.5	Description of the cation effect on the excess molar enthalpy of the acetone-[cation][NTf ₂] equimolar mixture in terms of the intermolecular interaction contributions [h^E (MF), h^E (HB) and h^E (vdW)] computed by COSMO-RS at 298 K.	58
3.6	Description of the anion effect on the excess molar enthalpy of the acetone-[eim][anion] equimolar mixture in terms of the intermolecular interaction contributions [h^E (MF), h^E (HB) and h^E (vdW)] computed by COSMO-RS at 298 K.	59
3.7	σ -profiles and σ -surfaces obtained by COSMO-RS for the [eim] ⁺ cation (blue line) and acetone (red line).	60
3.8	σ -profile obtained by COSMO-RS for the [eim] ⁺ cation. Labeled peaks correspond to the acid sites of cations.	60
3.9	σ -profiles and σ -surfaces obtained by COSMO-RS for the [eim] ⁺ (blue line), [e2mim] ⁺ (black line), [emim] ⁺ (green line) and [emmim] ⁺ (red line) cations.	61
3.10	σ -profiles and σ -surfaces obtained by COSMO-RS for the [PF ₆] ⁻ (blue solid line), [BF ₄] ⁻ (green solid line), [C ₂ H ₅ SO ₄] ⁻ (red solid line), [CH ₃ SO ₃] ⁻ (purple solid line) anions and acetone (black dashed line)	62
3.11	Relationship between the h^E of mixing and (A) the acetone Henry's constant in IL and (B) the vapor pressure ratio coefficient for all the studied acetone-IL systems, computed by COSMO-RS at 298 K.	63

3.12	Mülliken atomic charges (calculated at M052X/6-311**G(d,p) computational level) at some selected atoms of the [eim] ⁺ , [mmim] ⁺ and acetone molecules.	64
3.13	Optimized structures of the [cation-acetone] ⁺ complexes for both [mmim] ⁺ and [eim] ⁺ cations at the M052X/6-311++G(d,p) computational level. Computed non-bonding interatomic distances (Å) and Mülliken atomic charges for some selected atoms are also included. Energy differences correspond to the total electronic energy (E) being defined as $\Delta E = E_{\text{cation-acetone}} - (E_{\text{cation}} + E_{\text{acetone}})$ for the model process $[\text{cation}]^+ + [\text{acetone}]^0 \longrightarrow [\text{cation-acetone}]^+$	65
3.14	Optimized structures of the [eim-PF ₆] ion pairs at M052X/6-311++G(d,p) computational level. Computed non-bonding interatomic distances (Å) and Mülliken atomic charges for some selected atoms are also included. Energy differences correspond to the total electronic energy (E) being defined as $\Delta E = E_{[\text{eimPF}_6]} - (E_{[\text{eim}]} + E_{[\text{PF}_6]})$ for the model process $[\text{eim}]^+ + [\text{PF}_6]^- \longrightarrow [\text{eim-PF}_6]$	65
3.15	Optimized structures of the [eim-PF ₆ -acetone] aggregates at M052X/6-311++G(d,p) computational level. Computed non-bonding interatomic distances (Å) and Mülliken atomic charges for some selected atoms are also included. Energy differences correspond to the total electronic energy (E) being defined as $\Delta E = E_{\text{aggregate}} - (E_{\text{cation}} + E_{\text{anion}} + E_{\text{acetone}})$ for the model process $[\text{cation}]^+ + [\text{anion}]^- + [\text{acetone}]^0 \longrightarrow [\text{cation-anion-acetone}]$	66
3.16	¹ H-NMR spectra of (A) [bmim][NTf ₂] and (B) [eim][NTf ₂]: pure IL and IL-acetone mixtures with increasing mass concentration of acetone.	67
4.1	COSMO-RS calculated vs. experimental Henry's constants for solutes in numerous ILs at different temperatures. H are calculated using (A) COSMO-RS or (B) experimental vapor pressures (see Table 4.1). The ILs were simulated by the [C+A] solvent effect model.	76
4.2	Screening of Henry's constants (MPa) of A) ethane, B) ethylene, C) hexane and D) hexene in ILs at 298 K computed by COSMO-RS using the [C+A] solvent effects model.	77

4.3	Solubility behavior of different hydrocarbons in [P(14)666][TMPP]. The Henry's constants are calculated from COSMO-RS using vapor pressures from experimental data at 298 K. The IL was simulated by the [C+A] solvent effects model. Line shows perfect agreement between calculated and experiment.	78
4.4	Experimental vs. COSMO-RS Henry's constants for paraffins and olefins in ILs at different temperatures. The ILs were simulated by the [C+A] (black) and [CA] (white) solvent effects models. Line shows perfect agreement between calculated and experiment.	79
4.5	Comparison between the [CA] and [C+A] models for estimating activity coefficients at infinite dilution of some paraffins and olefins in ILs. Line shows perfect agreement.	80
4.6	Experimental (white bars) and calculated (dark bars) relative volatilities of ethane/ethylene with ILs using vapor pressures from experimental data at 313.15 K. The ILs were simulated by the [C+A] model (black bars) and by the [CA] model (grey bars).	81
4.7	Selectivity of the systems: ethane/ethylene (circle), propane/propylene (square), butane/butene (triangle), pentane/pentene (asterisk) and hexane/hexene (diamond), in different ILs simulated by the [C+A] model at 298 K.	81
4.8	Experimental (white bars) and calculated (dark bars) relative volatilities for propane/propylene with ILs using vapor pressures from experimental data at 313.15 K. The ILs were simulated by the [C+A] model (black bars) and by the [CA] model (grey bars).	83
4.9	Experimental (white bars) and calculated (dark bars) relative volatilities for butane/butene with [bmim][NTf ₂] using vapor pressures from experimental data at different temperatures. The ILs were simulated by the [C+A] model (black bars) and by the [CA] model (grey bars).	84

5.1	VLE diagrams for (A) ethanol/[emim][NTf ₂], (B) cyclohexane/[bmim][NTf ₂], (C) benzene/[bmim][BF ₄] and (D) acetone/[bmim][NTf ₂]. Experimental data (black). COSMO-RS calculations using the [CA] (white) and the [C+A] (yellow) models. Aspen HYSYS calculations (red) using the COSMOSAC property model specified with properties of ILs using the [CA] model.	95
5.2	Mean relative deviations between COSMO-RS predictions and experimental VLEs of (Organic solvent + IL) binary mixtures depending on the nature of the components.	97
5.3	Experimental values and Aspen HYSYS calculations for Cp of ILs at 298.15 K (approx.) and atmospheric pressure. The [CA] (black) and [C+A] (white) σ -profiles of the ILs were considered to specify the COSMOSAC model.	100
5.4	Flowsheet and design specifications used in this work for computing the heat duties (and their contributions: $Q_{\text{Vap.}}$ and Q_{Heat}) in the IL regeneration from their mixtures with organic solvents. $\Delta P = 0$ in equipments.	102
5.5	Effect of the length of the alkyl chain in 1-alkyl-3-methylimidazolium [NTf ₂] on the operating pressure of the IL regeneration from mixtures with organic solvents. Process involves vacuum evaporation of the organic solvent. . . .	104
5.6	Effect of the anion nature on the operating pressure of the IL regeneration from mixtures with organic solvents. Process involves vacuum evaporation of the organic solvent at 150°C.	105
5.7	The heat of vaporization of an organic solvent in mixture (organic solvent + IL) versus the heat of vaporization of pure organic at 150°C.	106
5.8	Dependence of the heat of vaporization ($Q_{\text{Vap.}}$) of the organic solvent with the alkyl chain length of the cation in the (organic solvent + IL) mixtures.	106
5.9	Dependence of the heat of vaporization ($Q_{\text{Vap.}}$) of the organic solvent with the anion nature in the (organic solvent + IL) mixtures.	107
5.10	Comparison of some ILs as extracting solvents for separating a benzene/cyclohexane mixture. The criteria selected for the comparison are (A) the separation capacity, (B) the operating conditions and (C) the heat duties of the IL regeneration.	108

LIST OF FIGURES

6.1	Schematic representation of an absorption refrigeration cycle.	112
6.2	Aspen HYSYS process flow diagram used in the current simulations for evaluating the cycle's performance. The main specifications for the Base Case simulations are also included.	118
6.3	Densities of ($\text{NH}_3 + \text{IL}$) binary mixtures calculated in Aspen HYSYS as a function of: (A)- temperature (ammonia mass fraction = 0.05) and (B)- ammonia concentration ($T = 30^\circ\text{C}$). $P = 1.1 \text{ MPa}$	122
6.4	Viscosities of ($\text{NH}_3 + \text{IL}$) binary mixtures calculated in Aspen HYSYS as a function of: (A)- temperature (ammonia mass fraction = 0.05) and (B)- ammonia concentration ($T = 30^\circ\text{C}$). $P = 1.1 \text{ MPa}$	123
6.5	Experimental (solid line) and calculated (dashed line) VLE for the ($\text{NH}_3 + \text{IL}$) binary mixtures studied in this chapter. Calculations are performed using COSMOSAC property model in Aspen Plus/Aspen HYSYS. In mixtures with $[\text{emim}][\text{C}_2\text{H}_5\text{SO}_4]$ and $[\text{emim}][\text{SCN}]$ Henry components are specified for NH_3 . Temperatures are c.a. 300 K.	124
6.6	Vapor pressure of the ($\text{NH}_3 + [\text{emim}][\text{CH}_3\text{CO}_2]$) binary mixtures as a function of both the temperature and the ammonia concentration. In these calculations vapor fraction of the stream fed to the VL separator is set to 0 and the refrigerant flow rate produced is constant (3600 kg/h).	125
6.7	Heat duty of ammonia vaporization from its mixtures with ILs as a function of the ammonia concentration at 100°C . In these calculations vapor fraction of the stream fed to the VL separator is set to 0 and the refrigerant flow rate produced is constant (3600 kg/h).	126
6.8	Operating concentration intervals in ammonia refrigeration cycles using different ILs as absorbents. Temperatures (T_A and T_G) and pressures (P_A and P_G) correspond to the Base Case considered in this work.	127
6.9	(A)- f ratios and (B)- COP for ammonia refrigeration cycles with ILs as absorbents versus ammonia concentration in strong-IL solutions. Remaining specifications correspond to the Base Case of this study.	129

6.10	Dependence of: (A)- f ratio and, (B)- COP with the cycle heat source (refrigerant generation) temperature for some ILs. Ammonia mass fractions are: 0.150 and 0.127 in mixtures with [emim][CH ₃ CO ₂] and [hxmim][Cl], respectively. x_{Ammonia} (w/w) takes values 0.15, 0.20 and 0.25 for mixtures with [OHemim][BF ₄]. Remaining specifications for the cycle simulations correspond to the Base Case.	130
6.11	Dependence of COP with the temperature of the space to be refrigerated. Ammonia mass fractions are: 0.150 and 0.127 in mixtures with [emim][CH ₃ CO ₂] and [hxmim][Cl], respectively. x_{Ammonia} (wt/wt) takes values 0.15, 0.20 and 0.25 for mixtures with [OHemim][BF ₄] IL. Remaining specifications for the cycle simulations correspond to the Base Case. . . .	131
6.12	(A)- Operating concentration interval of mixtures of [OHemim][BF ₄] and [hxmim][Cl] used as absorbent in ammonia absorption cycles. (B)- Performance of ammonia absorption cycles which use [OHemim][BF ₄] and [hxmim][Cl] mixtures as absorbents. Operating conditions correspond to the Base Case considered in this work. $x_A = 0.125$	132
7.1	Schematic diagram of the atmospheric pressure system for toluene absorption.	143
7.2	The σ -profiles and polarized charge surfaces of toluene and different solvents obtained by COSMO-RS.	147
7.3	Description of the solvent effect on Henry's law constants of toluene at 298 K using the interaction energy contributions [electrostatic, $h^E(\text{MF})$; van der Waals, $h^E(\text{VDW})$, and hydrogen-bonding, $h^E(\text{HB})$] to the excess molar enthalpy of solute-solvent mixtures computed by COSMO-RS. . . .	148
7.4	Screening of predicted Henry's law constants ($\cdot 10^2$ MPa) for toluene in 272 ILs at 298 K calculated by COSMO-RS.	149
7.5	Excess molar enthalpies (h^E) of equimolar toluene-IL mixtures versus Henry's law constants (H) for toluene in >200 ILs, both computed by COSMO-RS at 298K.	150
7.6	Henry's law constants for toluene in ILs vs the excess molar enthalpies of toluene-IL mixtures at 298 K calculated by COSMO-RS.	151
7.7	Equilibrium curves of toluene absorption on [dcnim][NTf ₂] ILs measured at 293, 303 and 313 K and total 0.1 MPa.	152

LIST OF FIGURES

7.8	Toluene absorption-desorption curves at 293 K and atmospheric pressure in (a) ILs with $[\text{NTf}_2]^-$ anion and (b) other ILs (toluene partial pressure of 2.0 kPa for absorption).	154
7.9	Toluene absorption-desorption curves at 303 K in (a) ILs with $[\text{NTf}_2]^-$ anion and (b) other ILs (at a toluene partial pressure of 2.0 kPa for absorption).	155
7.10	Toluene absorption-desorption curves at 313 K in (a) ILs with $[\text{NTf}_2]^-$ anion and (b) other ILs (at a toluene partial pressure of 2.0 kPa for absorption).	156
7.11	COSMO-RS predicted H values at 298 K vs experimental toluene absorption capacities (molar fraction) obtained at 293 K, atmospheric pressure and 2 kPa toluene partial pressure.	157
7.12	(A) Equilibrium- vs. rate-based toluene recovery values at 293 (black), 303 (red) and 313 (blue) K; and (B) Murphree tray efficiencies using different ILs at the considered temperature.	162

List of Tables

2.1	Boiling point estimates of some ILs using the COSMO-RS calculations and those reported by other authors in literature. The optimization and structural models for the ILs COSMO-RS calculations are [CA] gas and solvent phases.	37
3.1	Empirical Scales of Dipolarity (SdP), Polarizability (SP), Basicity (SB) and Acidity (SA) for Organic Solvents, Developed by Catalán (2009).	54
3.2	Experimental ^1H -NMR chemical shifts (δ , ppm) of neat [bmim][NTf ₂] and [eim][NTf ₂] and mixtures with acetone at increasing mass concentration of acetone.	68
3.3	Difference between ^1H and ^{17}O NMR chemical shifts ($\Delta\delta$) of [cation-acetone] ⁺ complexes and individual species calculated at the GIAO/M052X/6-311++G(d,p) Level ^a	68
4.1	Empirical equations used to calculate saturation vapor pressure of solutes at a specific temperature.	75
4.2	COSMO-RS calculations for Henry's constants of ethane, ethylene, propane and propylene in [P(14)666][TMPP] at 313.15 K.	80
4.3	Experimental vapor pressure ratio for different solutes. COSMO-RS calculations of selectivity and relative volatility for paraffin/olefin in different ILs at 298 K. The ILs were simulated by the [C+A]solvent effects model. .	82

LIST OF TABLES

5.1	Mean relative differences (MRD, %) between the calculations of either COSMO-RS or Aspen HYSYS (using the information obtained in COSMO-RS) and the experimental VLE data for selected (organic solvent + IL) binary mixtures.	99
6.1	Coefficients used for describing the temperature dependence of the Henry's constant. Number of experimental points (n) considered in the regressions and their R^2 values are also included.	117
6.2	RAAD (in %) between calculated (using COSMO-SAC property model in Aspen HYSYS/Aspen Plus process simulations) and experimental values for some thermo-physical and transport properties of pure ammonia and ILs.	121
6.3	Cycle's performances calculated in this work and reported by Yokozeki and Shiflett (2007a); Yokozeki and Shiflett (2007b) (values in parenthesis). Process specifications: $T_G/T_C/T_A/T_E=100/40/30/10^\circ\text{C}$ are the same to those used in the cited works.	128
7.1	Density and viscosity of the ILs reported in literature.	142
7.2	Henry's Law constant (H) for toluene absorption in [dcmim][NTf ₂] estimated from equilibrium experiments and predicted by COSMO-RS.	153
7.3	Effective diffusion coefficients of toluene in ILs at different temperatures obtained from absorption measurements and estimated by Wilke-Chang correlation.	159
7.4	Experimental and Aspen Plus simulated values for density, viscosity, toluene diffusivity and toluene absorption equilibrium data for the five IL-toluene systems.	160
7.5	Toluene recoveries (%) and Murphree tray efficiencies for the separation of toluene by absorption with ILs and organic solvents in a one-stage contactor, using equilibrium and rate-based models for separation column.	161
7.6	Toluene recovery (%), toluene molar fraction in the exit gas [$y_{\text{Toluene}}(\text{gas out})$] and height equivalent to a theoretical plate (HETP) in a 2 m height absorption packed column at 293 K, 1 atm, $G/L=17$ (in mol) and $y_{\text{Toluene}}(\text{gas in})=0.002$, simulated by Aspen Plus.	162

LIST OF TABLES

7.7	Aspen Plus simulated values of gas and liquid flow rate, density, viscosity and toluene diffusivity for DEHA, [dcmim][NTf ₂] and n-hexadecane solvents at 293 K and 1 atm.	163
A.1	Anions appearing in this PhD thesis.	171
A.2	Cations appearing in this PhD thesis.	172

LIST OF TABLES

List of References

- Abdul-Sada, A., Ambler, P., Hodgson, P., Seddon, K., and Stewart, N. 1995. World Patent 9521871 (to BP Chemical Ltd.). August 17. p. 4
- Abrams, D. S. and Prausnitz, J. M. 1975. Statistical thermodynamics of liquid mixtures: a new expression for the excess Gibbs energy of partly or completely miscible systems. *AIChE Journal*, 21(1):116–128. p. 21
- Ahosseini, A. and Scurto, A. 2008. Viscosity of imidazolium-based ionic liquids at elevated pressures: Cation and anion effects. *International Journal of Thermophysics*, 29(4):1222–1243. p. 141, 142, 143
- Altamash, T., Salavera, D., Kumar, A., Patil, K., de Castro, C. N., and Coronas, A. 2012. A review: solubility behavior of natural refrigerants with ionic liquids. In *Proceedings International Workshop on Ionic Liquids - Seeds for New Engineering Applications. Lisbon, Portugal*. p. 113
- Amos, R., Bernhardsson, A., Berning, A., Celani, P., Cooper, D., Deegan, M., et al. 2002. MOLPRO, a package of ab initio programs designed by H. J. Werner and P.J. Knowles, version, 2002. p. 19
- Andzelm, J., Kölmel, C., and Klamt, A. 1995. Incorporation of solvent effects into density functional calculations of molecular energies and geometries. *The Journal of chemical physics*, 103:9312–9320. p. 14, 16, 19, 116
- Anthony, J., Maginn, E., and Brennecke, J. 2002. Solubilities and thermodynamic properties of gases in the ionic liquid 1-n-butyl-3-methylimidazolium hexafluorophosphate. *The Journal of Physical Chemistry B*, 106(29):7315–7320. p. 5
- Anthony, J. L., Anderson, J. L., Maginn, E. J., and Brennecke, J. F. 2005. Anion effects on gas solubility in ionic liquids. *The Journal of Physical Chemistry B*, 109(13):6366–

LIST OF REFERENCES

6374. p. 5, 7, 48
- Anthony, J. L., Maginn, E. J., and Brennecke, J. F. 2001. Solution thermodynamics of imidazolium-based ionic liquids and water. *The Journal of Physical Chemistry B*, 105(44):10942–10949. p. 48
- Appetecchi, G. B., Scaccia, S., Tizzani, C., Alessandrini, F., and Passerini, S. 2006. Synthesis of hydrophobic ionic liquids for electrochemical applications. *Journal of The Electrochemical Society*, 153(9):A1685–A1691. p. 101, 103
- Arce, A., Rodil, E., and Soto, A. 2006a. Volumetric and viscosity study for the mixtures of 2-ethoxy-2-methylpropane, ethanol, and 1-ethyl-3-methylimidazolium ethyl sulfate ionic liquid. *Journal of Chemical & Engineering Data*, 51(4):1453–1457. p. 123
- Arce, A., Rodríguez, H., and Soto, A. 2007. Use of a green and cheap ionic liquid to purify gasoline octane boosters. *Green Chemistry*, 9(3):247–253. p. 90, 91, 100, 103, 107
- Arce, A., Rodríguez, O., and Soto, A. 2006b. A comparative study on solvents for separation of tert-amyl ethyl ether and ethanol mixtures. New experimental data for 1-ethyl-3-methyl imidazolium ethyl sulfate ionic liquid. *Chemical engineering science*, 61(21):6929–6935. p. 90, 91
- Arlt, W., Spuhl, O., and Klamt, A. 2004. Challenges in thermodynamics. *Chemical Engineering and Processing: Process Intensification*, 43(3):221–238. p. 8
- Armstrong, J. P., Hurst, C., Jones, R. G., Licence, P., Lovelock, K. R., Satterley, C. J., and Villar-Garcia, I. J. 2007. Vapourisation of ionic liquids. *Physical chemistry chemical physics*, 9(8):982–990. p. 36
- Arriaga, S., Muñoz, R., Hernández, S., Guieysse, B., and Revah, S. 2006. Gaseous hexane biodegradation by *Fusarium solani* in two liquid phase packed-bed and stirred-tank bioreactors. *Environmental Science & Technology*, 40(7):2390–2395. p. 138
- Aspen Plus, . 2010. Aspen Technology. *Inc., version*, 7.3. p. 9, 140
- Aspen Technology, . <http://www.aspentech.com/products/aspenone-engineering/>. p. 28, 29, 175
- Aspen Technology, . 2004a. How to use COSMO-SAC. Technical Tip ID: 113674. Available at: <http://support.aspentech.com>. . p. 9, 21, 93, 143

LIST OF REFERENCES

- Aspen Technology, . 2004b. What's New in Aspen Plus 12.0? Aspen Plus Documentation. Burlington, MA: Aspen Technology. p. 9, 31
- Aspen Technology, . 2010. Aspen Technology, Inc. Aspen Plus v7.3. Burlington, MA, USA. p. 31, 94
- Aspen Technology, . 2011a. Physical Property Models. AspenONE 7.3 Documentation, Inc. Aspen Physical Property System. Burlington, MA, USA. p. 116
- Aspen Technology, . 2011b. What's New in Aspen ONE V7.3? Aspen ONE Documentation. Burlington, MA: Aspen Technology. p. 9, 31
- Atkins, M., Davey, P., Fitzwater, G., Rouher, O., Seddon, K., and Swindall, J. 2002. Ionic liquids: A map for industrial innovation. In *Report Q001, QUILL. Belfast, UK.* p. 5
- Atmaca, I., Yigit, A., and Kilic, M. 2002. The effect of input temperatures on the absorber parameters. *International communications in heat and mass transfer*, 29(8):1177–1186. p. 114
- Avent, A., Chalones, P., Day, M., Seddon, K., and Welton, T. 1992. Evidence for hydrogen-bonding in solutions of 1-methyl-3-ethyl-imidazolium halides, as determined by ^1H , ^{35}Cl and ^{127}I N.M.R. Spectroscopy, and its implications for room-temperature halogenoaluminate(III) ionic liquids. In *Proceedings of the 8th International Symposium on Molten Salts; The Electrochemical Society. Pennington, USA.* p. 52
- Balamuru, V. G., Ibrahim, O. M., and Barnett, S. M. 2000. Simulation of ternary ammonia-water-salt absorption refrigeration cycles. *International journal of refrigeration*, 23(1):31–42. p. 114
- Baldridge, K. and Klamt, A. 1997. First principles implementation of solvent effects without outlying charge error. *The Journal of chemical physics*, 106:6622–6634. p. 19
- Banerjee, T. and Khanna, A. 2006. Infinite dilution activity coefficients for trihexyltetradecyl phosphonium ionic liquids: measurements and COSMO-RS prediction. *Journal of Chemical & Engineering Data*, 51(6):2170–2177. p. 92
- Banerjee, T., Sahoo, R., Rath, S., Kumar, R., and Khanna, A. 2007. Multicomponent liquid-liquid equilibria prediction for aromatic extraction systems using COSMO-RS. *Industrial & engineering chemistry research*, 46(4):1292–1304. p. 13

- Banerjee, T., Singh, M., and Khanna, A. 2006. Prediction of binary VLE for imidazolium based ionic liquid systems using COSMO-RS. *Industrial & engineering chemistry research*, 45(9):3207–3219. p. [20](#), [92](#), [96](#)
- Banerjee, T., Verma, K. K., and Khanna, A. 2008. Liquid-liquid equilibrium for ionic liquid systems using COSMO-RS: Effect of cation and anion dissociation. *AIChE Journal*, 54(7):1874–1885. p. [92](#), [96](#)
- Bara, J., Carlisle, T., Gabriel, C., Camper, D., Finotello, A., Gin, D., and Noble, R. 2009a. Guide to CO₂ separations in imidazolium-based room-temperature ionic liquids. *Industrial & Engineering Chemistry Research*, 48(6):2739–2751. p. [5](#), [139](#)
- Bara, J. E., Camper, D. E., Gin, D. L., and Noble, R. D. 2009b. Room-temperature ionic liquids and composite materials: platform technologies for CO₂ capture. *Accounts of chemical research*, 43(1):152–159. p. [48](#), [67](#)
- Bara, J. E., Gabriel, C. J., Carlisle, T. K., Camper, D. E., Finotello, A., Gin, D. L., and Noble, R. D. 2009c. Gas separations in fluoroalkyl-functionalized room-temperature ionic liquids using supported liquid membranes. *Chemical Engineering Journal*, 147(1):43–50. p. [72](#)
- Barrett, W. M. and Yang, J. 2005. Development of a chemical process modeling environment based on CAPE-OPEN interface standards and the Microsoft. NET framework. *Computers & chemical engineering*, 30(2):191–201. p. [31](#)
- Bates, E., Mayton, R., Ntai, I., and Davis, J. 2002. CO₂ capture by a task-specific ionic liquid. *Journal of the American Chemical Society*, 124(6):926–927. p. [5](#)
- Bedia, J., Palomar, J., González-Miquel, M., Rodríguez, F., and Rodríguez, J. J. 2012. Screening ionic liquids as suitable ammonia absorbents on the basis of thermodynamic and kinetic analysis. *Separation and Purification Technology*, 95:188–195. p. [50](#), [62](#), [74](#), [113](#), [115](#), [117](#), [124](#), [139](#), [141](#)
- Bedia, J., Rosas, J., Rodríguez-Mirasol, J., and Cordero, T. 2010. Pd supported on mesoporous activated carbons with high oxidation resistance as catalysts for toluene oxidation. *Applied Catalysis B: Environmental*, 94(1-2):8–18. p. [138](#)
-

LIST OF REFERENCES

- Blach, P., Fourmentin, S., Landy, D., Cazier, F., and Surpateanu, G. 2008. Cyclodextrins: a new efficient absorbent to treat waste gas streams. *Chemosphere*, 70(3):374–380. p. 138
- Black, C. 1986. Importance of thermophysical data in process simulation. *International Journal of Thermophysics*, 7(4):987–1002. p. 8
- Blahut, A., Sobota, M., Dohnal, V., and Vrbka, P. 2010. Activity coefficients at infinite dilution of organic solutes in the ionic liquid 1-ethyl-3-methylimidazolium methanesulfonate. *Fluid Phase Equilibria*, 299(2):198–206. p. 72
- Blake, C., Moens, L., Hale, M., Price, H., Kearney, D., and Herrmann, U. 2002. Ionic liquids: designer solvents? In *Proceedings of the 11th Solar PACES International Symposium on Concentrating Solar Power Chemical Energy Technologies*. Zürich, Switzerland. p. 5
- Bogart, M. 1981. *Ammonia absorption refrigeration in industrial processes*. Gulf Pub. Co., Book Division. p. 112, 113
- Bonhote, P., Dias, A., Papageorgiou, N., Kalyanasundaram, K., and Grätzel, M. 1996. Hydrophobic, highly conductive ambient-temperature molten salts. *Inorganic Chemistry*, 35(5):1168–1178. p. 4
- Bösmann, A., Datsevich, L., Jess, A., Lauter, A., Schmitz, C., and Wasserscheid, P. 2001. Deep desulfurization of diesel fuel by extraction with ionic liquids. *Chemical Communications*, (23):2494–2495. p. 5
- Bradley, A., Hatter, J., Nieuwenhuyzen, M., Pitner, W., Seddon, K., and Thied, R. 2002. Precipitation of a dioxouranium (VI) species from a room temperature ionic liquid medium. *Inorganic chemistry*, 41(7):1692–1694. p. 5
- Brodkey, R. and Hershey, H. 2003. *Transport phenomena: a unified approach*, volume 2. Brodkey publishing. p. 153
- Cadoret, L., Yu, C. C., Huang, H. P., and Lee, M. J. 2009. Effects of physical properties estimation on process design: a case study using Aspen Plus. *Asia-Pacific Journal of Chemical Engineering*, 4(5):729–734. p. 9
- Calvar, N., González, B., Gómez, E., and Domínguez, A. 2006. Vapor-liquid equilibria for the ternary system ethanol + water + 1-butyl-3-methylimidazolium chloride and the

LIST OF REFERENCES

- corresponding binary systems at 101.3 kPa. *Journal of Chemical & Engineering Data*, 51(6):2178–2181. p. 96
- Carda-Broch, S., Ruiz-Angel, M. J., Armstrong, D. W., and Berthod, A. 2010. Ionic liquid based headspace solid-phase microextraction-gas chromatography for the determination of volatile polar organic compounds. *Separation Science and Technology*, 45(16):2322–2328. p. 49
- Carlisle, T., Bara, J., Gabriel, C., Noble, R., and Gin, D. 2008. Interpretation of CO₂ solubility and selectivity in nitrile-functionalized room-temperature ionic liquids using a group contribution approach. *Industrial & Engineering Chemistry Research*, 47(18):7005–7012. p. 143, 153
- Cascon, H. R., Choudhari, S. K., Nisola, G. M., Vivas, E. L., Lee, D., and Chung, W. 2011. Partitioning of butanol and other fermentation broth components in phosphonium and ammonium-based ionic liquids and their toxicity to solventogenic clostridia. *Separation and Purification Technology*, 78(2):164–174. p. 90
- Catalán, J. 2009. Toward a generalized treatment of the solvent effect based on four empirical scales: dipolarity (SdP, a new scale), polarizability (SP), acidity (SA), and basicity (SB) of the medium. *The Journal of Physical Chemistry B*, 113(17):5951–5960. p. 53, 54, 183
- Cave, G., Raston, C., , and Scott, J. 2001. Recent advances in solventless organic reactions: towards benign synthesis with remarkable versatility. *Chemical Communications*, (21):2159–2169. p. 1
- Chen, C. C., Simoni, L. D., Brennecke, J. F., and Stadtherr, M. A. 2008. Correlation and prediction of phase behavior of organic compounds in ionic liquids using the nonrandom two-liquid segment activity coefficient model. *Industrial & Engineering Chemistry Research*, 47(18):7081–7093. p. 91, 114
- Chen, W., Liang, S., Guo, Y., Cheng, K., Gui, X., and Tang, D. 2012. Thermodynamic performances of [mmim] DMP/Methanol absorption refrigeration. *Journal of Thermal Science*, 21(6):557–563. p. 113, 114
- Chiang, Y., Chiang, P., and Huang, C. 2001. Effects of pore structure and temperature on VOC adsorption on activated carbon. *Carbon*, 39(4):523–534. p. 138

LIST OF REFERENCES

- CO-LaN, . The CAPE-OPEN Laboratories Network. Available at: <http://www.colan.org/>. p. 31
- Commings, C., Barhdadi, R., Laurent, M., and Troupel, M. 2006. Determination of viscosity, ionic conductivity, and diffusion coefficients in some binary systems: ionic liquids + molecular solvents. *Journal of Chemical & Engineering Data*, 51(2):680–685. p. 120, 123
- COSMOlogic GmbH & Co. KG, . Excess properties. <http://www.cosmologic.de/index.php?cosId=4302&crId=4>. p. 13
- COSMOthermX, . 2011. A Graphical User Interface to the COSMOtherm Program . *Version C30_1201; COSMOlogic GmbH & Co. KG., Leverkusen, Germany*. p. 20
- Crank, J. 1979. *The mathematics of diffusion*. Oxford university press. p. 157
- Crosthwaite, J., Muldoon, M., Dixon, J., Anderson, J., and Brennecke, J. 2005a. Phase transition and decomposition temperatures, heat capacities and viscosities of pyridinium ionic liquids. *The Journal of Chemical Thermodynamics*, 37(6):559–568. p. 3, 101, 150
- Crosthwaite, J. M., Aki, S. N., Maginn, E. J., and Brennecke, J. F. 2005b. Liquid phase behavior of imidazolium-based ionic liquids with alcohols: effect of hydrogen bonding and non-polar interactions. *Fluid phase equilibria*, 228:303–309. p. 48
- Darracq, G., Couvert, A., Couriol, C., Amrane, A., Thomas, D., Dumont, E., Andres, Y., and Le Cloirec, P. 2010. Silicone oil: an effective absorbent for the removal of hydrophobic volatile organic compounds. *Journal of Chemical Technology and Biotechnology*, 85(3):309–313. p. 139
- Darwish, N., Al-Hashimi, S., and Al-Mansoori, A. 2008. Performance analysis and evaluation of a commercial absorption-refrigeration water-ammonia (ARWA) system. *International Journal of Refrigeration*, 31(7):1214–1223. p. 114
- (DDBSP GmbH, . 1989. Dortmund Data Bank Software Package. <http://www.ddbst.com>. p. 5
- De Lucas, A., Donate, M., and Rodríguez, J. F. 2007. Absorption of water vapor into new working fluids for absorption refrigeration systems. *Industrial & engineering chemistry research*, 46(1):345–350. p. 114

- Delley, B. 2006. Ground-state enthalpies: Evaluation of electronic structure approaches with emphasis on the density functional method. *The Journal of Physical Chemistry A*, 110(50):13632–13639. p. 19
- DeSimone, J. 2002. Practical approaches to green solvents. *Science*, 297(5582):799–803. p. 1
- Deyko, A., Lovelock, K. R., Corfield, J., Taylor, A. W., Gooden, P. N., Villar-Garcia, I. J., Licence, P., Jones, R. G., Krasovskiy, V. G., Chernikova, E. A., et al. 2009. Measuring and predicting $\Delta_{\text{vap}}H_{298}$ values of ionic liquids. *Physical Chemistry Chemical Physics*, 11(38):8544–8555. p. 36
- Diedenhofen, M., Eckert, F., Hellweg, A., Huniar, U., Klamt, A., Loschen, C., Reinisch, J., Schroer, A., Steffen, C., Thomas, C., Wichmann, K., and Ikeda, H. 2012. COSMOthermX, Version C30_1201, Release 01.11; COSMOlogic GmbH & Co. KG., Leverkusen, Germany. p. 19, 74, 116
- Diedenhofen, M., Eckert, F., and Klamt, A. 2003. Prediction of infinite dilution activity coefficients of organic compounds in ionic liquids using COSMO-RS. *Journal of Chemical & Engineering Data*, 48(3):475–479. p. 92
- Diedenhofen, M. and Klamt, A. 2010. COSMO-RS as a tool for property prediction of IL mixtures - A review. *Fluid Phase Equilibria*, 294(1):31–38. p. 6, 7, 50, 73, 92, 93, 139
- Diedenhofen, M., Klamt, A., Marsh, K., and Schäfer, A. 2007. Prediction of the vapor pressure and vaporization enthalpy of 1-n-alkyl-3-methylimidazolium-bis-(trifluoromethanesulfonyl) amide ionic liquids. *Physical Chemistry Chemical Physics*, 9(33):4653–4656. p. 24, 37, 92
- Döker, M. and Gmehling, J. 2005. Measurement and prediction of vapor-liquid equilibria of ternary systems containing ionic liquids. *Fluid phase equilibria*, 227(2):255–266. p. 49, 96
- Domańska, U. and Laskowska, M. 2009. Measurements of activity coefficients at infinite dilution of aliphatic and aromatic hydrocarbons, alcohols, thiophene, tetrahydrofuran, MTBE, and water in ionic liquid [BMIM][SCN] using GLC. *The Journal of Chemical Thermodynamics*, 41(5):645–650. p. 72
- Domańska, U. and Marciniak, A. 2007. Phase behaviour of 1-hexyloxymethyl-3-methylimidazolium and 1, 3-dihexyloxymethyl-imidazolium based ionic liquids with alcohols,

- water, ketones and hydrocarbons: The effect of cation and anion on solubility. *Fluid Phase Equilibria*, 260(1):9–18. p. 48
- Domańska, U., Pobudkowska, A., and Eckert, F. 2006. Liquid-liquid equilibria in the binary systems (1, 3-dimethylimidazolium, or 1-butyl-3-methylimidazolium methylsulfate + hydrocarbons). *Green Chemistry*, 8(3):268–276. p. 92
- Domínguez-Pérez, M., Tomé, L. I., Freire, M. G., Marrucho, I. M., Cabeza, O., and Coutinho, J. A. P. 2010. (Extraction of biomolecules using) aqueous biphasic systems formed by ionic liquids and aminoacids. *Separation and Purification Technology*, 72(1):85–91. p. 90
- Donate, M., Rodriguez, L., Lucas, A. D., and Rodríguez, J. F. 2006. Thermodynamic evaluation of new absorbent mixtures of lithium bromide and organic salts for absorption refrigeration machines. *International journal of refrigeration*, 29(1):30–35. p. 114
- Dong, K., Zhang, S., Wang, D., and Yao, X. 2006. Hydrogen bonds in imidazolium ionic liquids. *The Journal of Physical Chemistry A*, 110(31):9775–9782. p. 48
- Dong, Q., Muzny, C., Kazakov, A., Diky, V., Magee, J., Widegren, J., Chirico, R., Marsh, K., and Frenkel, M. 2007. ILThermo: A free-access web database for thermodynamic properties of ionic liquids. *Journal of Chemical & Engineering Data*, 52(4):1151–1159. p. 5
- Doyle, M., Choi, S., and Proulx, G. 2000. High-Temperature Proton Conducting Membranes Based on Perfluorinated Ionomer Membrane-Ionic Liquid Composites. *Journal of the Electrochemical Society*, 147(1):34–37. p. 5
- Earle, M., Esperança, J., Gilea, M., Canongia Lopes, J., Rebelo, L., Magee, J., Seddon, K., and Widegren, J. 2006. The distillation and volatility of ionic liquids. *Nature*, 439(7078):831–834. p. 3
- Eckert, F. 2007. COSMOthermCO: Using COSMOtherm in Process Modelling Environments. White Paper. COSMOlogic GmbH & Co. KG., Leverkusen, Germany. p. 9, 31
- Eckert, F. and A., K. COSMOlogic GmbH & Co. KG. COSMOthermCO-C21-0111. Leverkusen, Germany. p. 31
- Eckert, F. and Klamt, A. 2001. Validation of the COSMO-RS method: Six binary systems. *Industrial & engineering chemistry research*, 40(10):2371–2378. p. 13
-

LIST OF REFERENCES

- Eckert, F. and Klamt, A. 2002. Fast solvent screening via quantum chemistry: COSMO-RS approach. *AIChE Journal*, 48(2):369–385. p. 16, 175
- Eckert, F. and Klamt, A. 2008. COSMOtherm Version C21 Revision 0108; COSMOlogic GmbH & Co. KG., Leverkusen, Germany. p. 19, 20
- Eckert, F. and Klamt, A. 2010. COSMOthermX, Version C2.1, Release 01.11; COSMOlogic GmbH & Co. KG., Leverkusen, Germany. p. 19, 94, 141
- Eckert, F., van Baten, J., and Baur, R. 2006. The CAPE-OPEN Interface to COSMO-RS. White Paper. COSMOlogic GmbH & Co. KG., Leverkusen, Germany. p. 9, 31
- Egorov, V. M., Smirnova, S. V., and Pletnev, I. V. 2008. Highly efficient extraction of phenols and aromatic amines into novel ionic liquids incorporating quaternary ammonium cation. *Separation and Purification Technology*, 63(3):710–715. p. 90
- Eiden, P., Bulut, S., Köchner, T., Friedrich, C., Schubert, T., and Krossing, I. 2010. In silico predictions of the temperature-dependent viscosities and electrical conductivities of functionalized and nonfunctionalized ionic liquids. *The Journal of Physical Chemistry B*, 115(2):300–309. p. 25, 41
- Eiseman Jr, B. 1959. Comparison of fluoroalkane absorption refrigerants. *ASHRAE Transactions*, 15:635–50. p. 113
- Eldridge, R. B. 1993. Olefin/paraffin separation technology: a review. *Industrial & engineering chemistry research*, 32(10):2208–2212. p. 72
- Erickson, D. C., Anand, G., and Kyung, I. 2004. SYMPOSIUM PAPERS-AN-04-07 Absorption/Sorption Heat Pumps and Refrigeration Systems-Heat-Activated Dual-Function Absorption Cycle. *ASHRAE Transactions-American Society of Heating Refrigerating Airconditioning Engin*, 110(1):515–524. p. 112
- Fadeev, A. and Meagher, M. 2001. Opportunities for ionic liquids in recovery of biofuels. *Chemical Communications*, (3):295–296. p. 5
- Fallanza, M., González-Miquel, M., Ruiz, E., Ortiz, A., Gorri, D., Palomar, J., and Ortiz, I. 2013. Screening of RTILs for propane/propylene separation using COSMO-RS methodology. *Chemical Engineering Journal*. p. 22, 79

LIST OF REFERENCES

- Falling, S., Monnier, J., Phillips, G., Kanel, J., and Godleski, S. 2005. First International Congress on Ionic Liquids (COIL-1), Salzburg, Austria. p. [2](#)
- Fernandez, J. F., Neumann, J., and Thoming, J. 2011. Regeneration, recovery and removal of ionic liquids. *Current Organic Chemistry*, 15(12):1992–2014. p. [90](#)
- Ferreira, A. R., Freire, M. G., Ribeiro, J. C., Lopes, F. M., Crespo, J. G., and Coutinho, J. A. P. 2011. An overview of the liquid- liquid equilibria of (ionic liquid + hydrocarbon) binary systems and their modeling by the Conductor-like Screening Model for Real Solvents. *Industrial & Engineering Chemistry Research*, 50(9):5279–5294. p. [7](#), [50](#)
- Ferro, V., Ruiz, E., Tobajas, M., and Palomar, J. 2012. Integration of COSMO-based methodologies into commercial process simulators: Separation and purification of reuterin. *AIChE Journal*, 58(11):3404–3415. p. [33](#)
- Ficke, L. E. and Brennecke, J. F. 2010. Interactions of ionic liquids and water. *The Journal of Physical Chemistry B*, 114(32):10496–10501. p. [49](#), [50](#), [54](#)
- Franke, R. 2007. Process intensification - an industrial point of view. *Modeling of Process Intensification*, pages 9–23. p. [8](#)
- Fraser, K., Izgorodina, E., Forsyth, M.S., J. L., and MacFarlane, D. 2007. Liquids intermediate between molecular and ionic liquids: Liquid Ion Pairs? *Chemical communications*, (37):3817–3819. p. [150](#)
- Fredenslund, A., Jones, R. L., and Prausnitz, J. M. 1975. Group-contribution estimation of activity coefficients in nonideal liquid mixtures. *AIChE Journal*, 21(6):1086–1099. p. [18](#), [21](#)
- Fredlake, C., Crosthwaite, J., Hert, D., Aki, S., and Brennecke, J. 2004. Thermophysical properties of imidazolium-based ionic liquids. *Journal of Chemical & Engineering Data*, 49(4):954–964. p. [3](#), [123](#)
- Freemantle, M. 1998. Designer solvents-ionic liquids may boost clean technology development. *Chemical & engineering news*, 76(13):32–37. p. [3](#), [4](#)
- Freemantle, M. 2003. BASF’s smart ionic liquid. *Chemical & Engineering News*, 81(13):9. p. [2](#)

- Freire, M. G., Santos, L. M. N. B. F., Marrucho, I. M., and Coutinho, J. A. P. 2007. Evaluation of COSMO-RS for the prediction of lle and vle of alcohols + ionic liquids. *Fluid phase equilibria*, 255(2):167–178. p. [92](#), [96](#)
- Freire, M. G., Ventura, S. P. M., Santos, L. M. N. B. F., Marrucho, I. M., and Coutinho, J. A. P. 2008. Evaluation of cosmo-rs for the prediction of lle and vle of water and ionic liquids binary systems. *Fluid Phase Equilibria*, 268(1):74–84. p. [92](#), [96](#)
- Frisch, M., Trucks, G., Schlegel, H., Scuseria, G., Robb, M., Cheeseman, J., and others. 2003. Gaussian03, revision B. 05; Gaussian: Pittsburgh, PA. p. [18](#), [19](#), [94](#), [141](#)
- Fuller, J., Breda, A., and Carlin, R. 1997. Ionic Liquid-Polymer Gel Electrolytes. *Journal of the Electrochemical Society*, 144(4):L67–L70. p. [5](#)
- Gamero-Castaño, M. and Hruby, V. 2001. Electrospray as a source of nanoparticles for efficient colloid thrusters. *Journal of Propulsion and Power*, 17(5):977–987. p. [5](#)
- Gao, T., Andino, J. M., and Alvarez-Idaboy, J. R. 2010a. Computational and experimental study of the interactions between ionic liquids and volatile organic compounds. *Physical Chemistry Chemical Physics*, 12(33):9830–9838. p. [48](#)
- Gao, Y., Zhang, L., Wang, Y., and Li, H. 2010b. Probing electron density of H-Bonding between cation-anion of imidazolium-based ionic liquids with different anions by vibrational spectroscopy. *The Journal of Physical Chemistry B*, 114(8):2828–2833. p. [48](#)
- García, S., Larriba, M., García, J., Torrecilla, J. S., and Rodríguez, F. 2012. Separation of toluene from n-heptane by liquid-liquid extraction using binary mixtures of [bpy][BF₄] and [4bmpy][Tf₂N] ionic liquids as solvent. *The Journal of Chemical Thermodynamics*, 53:119–124. p. [131](#)
- García-Miaja, G., Troncoso, J., and Romaní, L. 2008. Excess properties for binary systems ionic liquid + ethanol: Experimental results and theoretical description using the ERAS model. *Fluid Phase Equilibria*, 274(1):59–67. p. [49](#)
- García-Miaja, G., Troncoso, J., and Romaní, L. 2009a. Excess enthalpy, density, and heat capacity for binary systems of alkyimidazolium-based ionic liquids + water. *The Journal of Chemical Thermodynamics*, 41(2):161–166. p. [49](#), [50](#), [56](#)
- García-Miaja, G., Troncoso, J., and Romaní, L. 2009b. Excess molar properties for binary systems of alkyimidazolium - based ionic liquids + nitromethane. experimental results

LIST OF REFERENCES

- and eras - model calculations. *The Journal of Chemical Thermodynamics*, 41(3):334–341. p. 49, 50
- Gardas, R. L. and Coutinho, J. A. P. 2008. Extension of the Ye and Shreeve group contribution method for density estimation of ionic liquids in a wide range of temperatures and pressures. *Fluid Phase Equilibria*, 263(1):26–32. p. 39
- Giernoth, R. 2010. Task-specific ionic liquids. *Angewandte Chemie International Edition*, 49(16):2834–2839. p. 139
- Giernoth, R., Bankmann, D., and Schlörer, N. 2005. High performance NMR in ionic liquids. *Green Chemistry*, 7(5):279–282. p. 52
- Gislason, J., Conoco, P., and Livia, W. 2008. Using Aspen Simulation Workbook to make confident feedstock selections. AspenTech. in *AspenTech User Conference*, Houston, April. p. 30
- Gmehling, J. 1985. Dortmund Data Bank-Basis for the development of prediction methods. *CODATA Bulletin*, (58):56–64. p. 5
- González, E. J., Calvar, N., González, B., and Domínguez, A. 2010. Liquid extraction of benzene from its mixtures using 1-ethyl-3-methylimidazolium ethylsulfate as a solvent. *Journal of Chemical & Engineering Data*, 55(11):4931–4936. p. 107, 108
- González, E. J., Domínguez, Á., and Macedo, E. A. 2012. Excess properties of binary mixtures containing 1-hexyl-3-methylimidazolium bis (trifluoromethylsulfonyl) imide ionic liquid and polar organic compounds. *The Journal of Chemical Thermodynamics*, 47:300–311. p. 49
- González, E. J., González, B., Calvar, N., and Domínguez, A. 2007. Physical properties of binary mixtures of the ionic liquid 1-ethyl-3-methylimidazolium ethyl sulfate with several alcohols at $t=(298.15, 313.15, \text{ and } 328.15)$ K and atmospheric pressure. *Journal of Chemical & Engineering Data*, 52(5):1641–1648. p. 123
- González, J., Carmona, J., Garcia De La Fuente, I., and Cobos, J. 1999. DISQUAC predictions on thermodynamic properties of ternary and higher multicomponent mixtures: I. results for total pressure measurements at isothermal conditions of ternary systems. *Thermochimica acta*, 326(1):53–67. p. 139

- González-Miquel, M., Palomar, J., Omar, S., and Rodríguez, F. 2011. CO₂/N₂ selectivity prediction in supported ionic liquid membranes (SILMs) by COSMO-RS. *Industrial & Engineering Chemistry Research*, 50(9):5739–5748. p. 50, 62, 74, 139
- Gonzalez-Miquel, M., Palomar, J., and Rodriguez, F. 2012. Selection of ionic liquids for enhancing the gas solubility of Volatile Organic Compounds. *The Journal of Physical Chemistry B*, 117(1):296–306. p. 74
- Gordon, C. 2001. New developments in catalysis using ionic liquids. *Applied Catalysis A: General*, 222(1):101–117. p. 3
- Grätzel, M. 1995. Low cost and efficient photovoltaic conversion by nanocrystalline solar cells. *Chemie Ingenieur Technik*, 67(10):1300–1305. p. 5
- Grensemann, H. and Gmehling, J. 2005. Performance of a conductor-like screening model for real solvents model in comparison to classical group contribution methods. *Industrial & engineering chemistry research*, 44(5):1610–1624. p. 20, 93
- Gutowski, K., Broker, G., Willauer, H., Huddleston, J., Swatloski, R., Holbrey, J., and Rogers, R. 2003. Controlling the aqueous miscibility of ionic liquids: aqueous biphasic systems of water-miscible ionic liquids and water-structuring salts for recycle, metathesis, and separations. *Journal of the American Chemical Society*, 125(22):6632–6633. p. 5
- Haar, L. and Gallagher, J. S. 1978. *Thermodynamic properties of ammonia*. American Chemical Society and the American Institute of Physics for the National Bureau of Standards. p. 120
- Han, D. and Row, K. 2010. Recent applications of ionic liquids in separation technology. *Molecules*, 15(4):2405–2426. p. 48, 139
- Han, X. and Armstrong, D. 2007. Ionic liquids in separations. *Accounts of chemical research*, 40(11):1079–1086. p. 139
- He, Z., Zhao, Z., Zhang, X., and Feng, H. 2010. Thermodynamic properties of new heat pump working pairs: 1,3-dimethylimidazolium dimethylphosphate and water, ethanol and methanol. *Fluid Phase Equilibria*, 298(1):83–91. p. 49
- Heintz, A. 2005. Recent developments in thermodynamics and thermophysics of non-aqueous mixtures containing ionic liquids. A review. *The Journal of Chemical Thermodynamics*, 37(6):525–535. p. 3
-

LIST OF REFERENCES

- Hendriks, E., Kontogeorgis, G. M., Dohrn, R., de Hemptinne, J. C., Economou, I. G., Zilnik, L. F., and Vesovic, V. 2010. Industrial requirements for thermodynamics and transport properties. *Industrial & Engineering Chemistry Research*, 49(22):11131–11141. p. 8
- Hervier, A. and Klamt, A. 2006. Boiling Points. http://www.cosmologic.de/application_examples. p. 13
- Heym, F., Etzold, B. J., Kern, C., and Jess, A. 2011. Analysis of evaporation and thermal decomposition of ionic liquids by thermogravimetric analysis at ambient pressure and high vacuum. *Green Chemistry*, 13(6):1453–1466. p. 101
- Heymes, F., Manno, D., Charbit, F., Fanlo, J., and Moulin, P. 2006. Hydrodynamics and mass transfer in a packed column: case of toluene absorption with a viscous absorbent. *Chemical engineering science*, 61(15):5094–5106. p. 145
- Holbrey, J., Plechkova, N., and K.R., S. 2006. Recalling coil. *Green chemistry*, 8(5):411–414. p. 2
- Holbrey, J. and Seddon, K. 1999a. The phase behaviour of 1-alkyl-3-methylimidazolium tetrafluoroborates; ionic liquids and ionic liquid crystals. *Journal of the Chemical Society, Dalton Transactions*, (13):2133–2140. p. 4
- Holbrey, J. D. and Seddon, K. R. 1999b. Ionic liquids. *Clean Products and Processes*, 1(4):223–236. p. 113
- Hou, Y. and Baltus, R. 2007. Experimental measurement of the solubility and diffusivity of CO₂ in room-temperature ionic liquids using a transient thin-liquid-film method. *Industrial & Engineering Chemistry Research*, 46(24):8166–8175. p. 157
- Howarth, J., James, P., and Dai, J. 2001. Immobilized baker’s yeast reduction of ketones in an ionic liquid,[bmim] [PF₆] and water mix. *Tetrahedron Letters*, 42(42):7517–7519. p. 101, 103
- Huang, J., Riisager, A., Berg, R., and Fehrmann, R. 2008. Tuning ionic liquids for high gas solubility and reversible gas sorption. *Journal of Molecular Catalysis A: Chemical*, 279(2):170–176. p. 157
- Huang, J. and Rüther, T. 2009. Why are ionic liquids attractive for CO₂ absorption? an overview. *Australian Journal of Chemistry*, 62(4):298–308. p. 139

LIST OF REFERENCES

- Hunter, P. and Oyama, S. 2000. *Control of volatile organic compound emissions: conventional and emerging technologies*. John Wiley. p. 138
- Huo, Y., Xia, S., Yi, S., and Ma, P. 2009. Measurement and correlation of vapor pressure of benzene and thiophene with [BMIM][PF₆] and [BMIM][BF₄] ionic liquids. *Fluid Phase Equilibria*, 276(1):46–52. p. 96
- IFP, . 2004. Annual report. p. 2
- Iliev, B., Smiglak, M., Swierczynska, A., and Schubert, T. 2011. Iolitec, Ionic Liquids Technologies GmbH. . in *1st International conference on ionic liquids separation and purification technology (ILSEPT) Conference*, Sitges, Spain, Sept. p. 49
- ILthermo, . 2006. ILthermo, 2006. <http://ilthermo.boulder.nist.gov>. p. 5, 98, 116
- Imroz Sohel, M. and Dawoud, B. 2006. Dynamic modelling and simulation of a gravity-assisted solution pump of a novel ammonia-water absorption refrigeration unit. *Applied thermal engineering*, 26(7):688–699. p. 114
- Izák, P., Ruth, W., Fei, Z., Dyson, P. J., and Kragl, U. 2008. Selective removal of acetone and butan-1-ol from water with supported ionic liquid-polydimethylsiloxane membrane by pervaporation. *Chemical Engineering Journal*, 139(2):318–321. p. 49, 56
- Jacquemin, J., Ge, R., Nancarrow, P., Rooney, D. W., Costa Gomes, M. F., Pádua, A. A., and Hardacre, C. 2008. Prediction of ionic liquid properties. I. Volumetric properties as a function of temperature at 0.1 MPa. *Journal of Chemical & Engineering Data*, 53(3):716–726. p. 123
- Jacquemin, J., Husson, P., Padua, A., and Majer, V. 2006. Density and viscosity of several pure and water-saturated ionic liquids. *Green Chemistry*, 8(2):172–180. p. 141, 142
- Jarraya, I., Fourmentin, S., Benzina, M., and Bouaziz, S. 2010. VOC adsorption on raw and modified clay materials. *Chemical Geology*, 275(1):1–8. p. 138
- Jeapes, A., Rooney, G., Hatter, J., and Welton, T. 2000. World Patent 0115175 (to British Nuclear Fuels PLC). August 21. p. 5
- Jessop, P. and Leitner, W. 2008. *Chemical synthesis using supercritical fluids*. Wiley. com. p. 2
- Jones, J. Champagne Heat Pump, NASA Technical Support Package, www.techbriefs.com/tsp. p. 113

- Jones, R. G., Licence, P., Lovelock, K. R., and Villar-Garcia, I. J. 2007. Comment on “critical properties, normal boiling temperatures, and acentric factors of fifty ionic liquids”. *Industrial & Engineering Chemistry Research*, 46(18):6061–6062. p. 36, 37
- Jork, C., Kristen, C., Pieraccini, D., Stark, A., Chiappe, C., Beste, Y., and Arlt, W. 2005. Tailor-made ionic liquids. *The Journal of Chemical Thermodynamics*, 37(6):537–558. p. 6, 7, 107
- Jork, C., Seiler, M., Beste, Y. A., and Arlt, W. 2004. Influence of ionic liquids on the phase behavior of aqueous azeotropic systems. *Journal of Chemical & Engineering Data*, 49(4):852–857. p. 90, 91, 101
- Kapavarapu, V. M. R. and Kuwait Oil Company, . 2011. Process optimization using simulation and integrated economics. in *1st MEPEC Conference*, Manama, Bahrain, October. p. 29
- Kato, R. and Gmehling, J. 2005a. Measurement and correlation of vapor-liquid equilibria of binary systems containing the ionic liquids [EMIM][(CF₃SO₂)₂N],[BMIM][(CF₃SO₂)₂N],[MMIM][(CH₃)₂PO₄] and oxygenated organic compounds respectively water. *Fluid phase equilibria*, 231(1):38–43. p. 49, 96
- Kato, R. and Gmehling, J. 2005b. Systems with ionic liquids: Measurement of VLE and γ data and prediction of their thermodynamic behavior using original UNIFAC, mod. UNIFAC (Do) and COSMO-RS (Ol). *The Journal of Chemical Thermodynamics*, 37(6):603–619. p. 6, 92, 93, 96
- Kato, R., Krummen, M., and Gmehling, J. 2004. Measurement and correlation of vapor-liquid equilibria and excess enthalpies of binary systems containing ionic liquids and hydrocarbons. *Fluid Phase Equilibria*, 224(1):47–54. p. 91
- Kelkar, M. S. and Maginn, E. J. 2007. Calculating the enthalpy of vaporization for ionic liquid clusters. *The Journal of Physical Chemistry B*, 111(32):9424–9427. p. 36
- Khodadadi-Moghaddam, M., Habibi-Yangjeh, A., and Gholami, M. R. 2009. Solvent effects on the reaction rate and selectivity of synchronous heterogeneous hydrogenation of cyclohexene and acetone in ionic liquid/alcohols mixtures. *Journal of Molecular Catalysis A: Chemical*, 306(1):11–16. p. 49
- Khupse, N. and Kumar, A. 2009. Dramatic change in viscosities of pure ionic liquids upon addition of molecular solvents. *Journal of solution chemistry*, 38(5):589–600. p. 120, 123, 150

- Kim, D. and Infante Ferreira, C. 2008. Solar refrigeration options - a state - of - the - art review. *International journal of refrigeration*, 31(1):3–15. p. 112
- Kim, Y. J., Kim, S., Joshi, Y. K., Fedorov, A. G., and Kohl, P. A. 2012. Thermodynamic analysis of an absorption refrigeration system with ionic-liquid/refrigerant mixture as a working fluid. *Energy*, 44(1):1005–1016. p. 113, 114, 129
- Klamt, A. 1995. Conductor-like screening model for real solvents: a new approach to the quantitative calculation of solvation phenomena. *The Journal of Physical Chemistry*, 99(7):2224–2235. p. 7, 8, 13, 16, 18, 21, 31, 74, 116
- Klamt, A. 2002. Comments on “A Priori Phase Equilibrium Prediction from a Segment Contribution Solvation Model” . *Industrial & Engineering Chemistry Research*, 41(9):2330–2331. p. 20, 21, 30
- Klamt, A. 2005. *COSMO-RS: from quantum chemistry to fluid phase thermodynamics and drug design*. Elsevier Science Ltd. p. 26
- Klamt, A. and Eckert, F. 2000. COSMO-RS: a novel and efficient method for the a priori prediction of thermophysical data of liquids. *Fluid Phase Equilibria*, 172(1):43–72. p. 13, 14, 16, 19, 21
- Klamt, A. and Eckert, F. 2008. Comment on “Refinement of COSMO-SAC and the Applications” . *Industrial & Engineering Chemistry Research*, 47(4):1351–1352. p. 20, 21
- Klamt, A., Eckert, F., and Arlt, W. 2010a. COSMO-RS: an alternative to simulation for calculating thermodynamic properties of liquid mixtures. *Annual review of chemical and biomolecular engineering*, 1:101–122. p. 13, 73
- Klamt, A., Eckert, F., and Arlt, W. 2010b. COSMO-RS: an alternative to simulation for calculating thermodynamic properties of liquid mixtures. *Annual review of chemical and biomolecular engineering*, 1:101–122. p. 139, 147
- Klamt, A., Eckert, F., and Diedenhofen, M. 2009. Prediction of the Free Energy of Hydration of a Challenging Set of Pesticide-Like Compounds. *The Journal of Physical Chemistry B*, 113(14):4508–4510. p. 13
- Klamt, A., Eckert, F., Diedenhofen, M., and Beck, M. 2003. First principles calculations of aqueous p K a values for organic and inorganic acids using COSMO-RS reveal an

- inconsistency in the slope of the p K a scale. *The Journal of Physical Chemistry A*, 107(44):9380–9386. p. 13
- Klamt, A., Eckert, F., Hornig, M., Beck, M., and Bürger, T. 2002. Prediction of aqueous solubility of drugs and pesticides with COSMO-RS. *Journal of computational chemistry*, 23(2):275–281. p. 13
- Klamt, A., Jonas, V., Bürger, T., and Lohrenz, J. 1998. Refinement and parametrization of COSMO-RS. *The Journal of Physical Chemistry A*, 102(26):5074–5085. p. 13, 16, 18, 20
- Klamt, A. and Schüürmann, G. 1993. COSMO: a new approach to dielectric screening in solvents with explicit expressions for the screening energy and its gradient. *J. Chem. Soc., Perkin Trans. 2*, (5):799–805. p. 7, 13, 14, 16
- Koch, V., Nanjundiah, C., , and Carlin, R. 1996. World Patent 9702252 (to Covalent Associates, Inc., USA). June 28. p. 5
- Köddermann, T., Ludwig, R., and Paschek, D. 2008. On the validity of Stokes-Einstein and Stokes-Einstein-Debye relations in ionic liquids and ionic-liquid mixtures. *ChemPhysChem*, 9(13):1851–1858. p. 120, 123
- Kreher, U., Rosamilia, A., Raston, C., Scott, J., and Strauss, C. 2004. Self-associated, “distillable” ionic media. *Molecules*, 9(6):387–393. p. 3
- Krossing, I., Slattey, J., Daguenet, C., Dyson, P., Oleinikova, A., and Weingärtner, H. 2006. Why are ionic liquids liquid? A simple explanation based on lattice and solvation energies. *Journal of the American Chemical Society*, 128(41):13427–13434. p. 2, 41
- Krummen, M., Wasserscheid, P., and Gmehling, J. 2002. Measurement of activity coefficients at infinite dilution in ionic liquids using the dilutor technique. *Journal of Chemical & Engineering Data*, 47(6):1411–1417. p. 72
- Kubo, W., Kitamura, T., Hanabusa, K., Wada, Y., and Yanagida, S. 2002. Quasi-solid-state dye-sensitized solar cells using room temperature molten salts and a low molecular weight gelator. *Chemical Communications*, (4):374–375. p. 5
- Lazzús, J. A. 2009. ρ (T, p) model for ionic liquids based on quantitative structure–property relationship calculations. *Journal of Physical Organic Chemistry*, 22(12):1193–1197. p. 39
-

LIST OF REFERENCES

- Lazzús, J. A. 2010. Prediction of flash point temperature of organic compounds using a hybrid method of group contribution + neural network + particle swarm optimization. *Chinese Journal of Chemical Engineering*, 18(5):817–823. p. 39
- Lee, B.-C. and Outcalt, S. L. 2006. Solubilities of gases in the ionic liquid 1-n-butyl-3-methylimidazolium bis (trifluoromethylsulfonyl) imide. *Journal of Chemical & Engineering Data*, 51(3):892–897. p. 76
- Lei, Z., Arlt, W., and Wasserscheid, P. 2006. Separation of 1-hexene and n-hexane with ionic liquids. *Fluid Phase Equilibria*, 241(1):290–299. p. 6, 7, 91
- Lei, Z., Arlt, W., and Wasserscheid, P. 2007. Selection of entrainers in the 1-hexene/n-hexane system with a limited solubility. *Fluid Phase Equilibria*, 260(1):29–35. p. 7, 50
- Lemus, J., Palomar, J., Heras, F., Gilarranz, M. A., and Rodríguez, J. J. 2012. Developing criteria for the recovery of ionic liquids from aqueous phase by adsorption with activated carbon. *Separation and Purification Technology*, 97:11–19. p. 49
- Li, G., Zhou, Q., Zhang, X., Zhang, S., Li, J., et al. 2010. Solubilities of ammonia in basic imidazolium ionic liquids. *Fluid Phase Equilibria*, 297(1):34–39. p. 113, 117
- Li, X., Sun, W., Wu, G., He, L., Li, H., and Sui, H. 2011. Ionic liquid enhanced solvent extraction for bitumen recovery from oil sands. *Energy & Fuels*, 25(11):5224–5231. p. 49
- Liang, S., Chen, W., Cheng, K., Guo, Y., and Gui, X. 2011. The latent application of ionic liquids in absorption refrigeration. *Application of ionic liquids in science and technology, InTechOpen, Croatia*, pages 467–494. p. 128, 129
- Lin, S., Mathias, P., Song, Y., Chen, C., and Sandler, S. 2002. Improvements of phase-equilibrium predictions for hydrogen-bonding systems from a new expression for COSMO solvation models. *Presented at the AIChE Annual Meeting*, Indianapolis, IN, November. p. 21, 31, 116
- Lin, S. and Sandler, S. 1999. Infinite dilution activity coefficients from ab initio solvation calculations. *AIChE journal*, 45(12):2606–2618. p. 20
- Lin, S. and Sandler, S. 2002a. A priori phase equilibrium prediction from a segment contribution solvation model. *Industrial & engineering chemistry research*, 41(5):899–

913. p. [8](#), [20](#), [21](#), [30](#), [31](#), [93](#), [116](#),
[143](#)
 - Lin, S. and Sandler, S. 2002b. Reply to comments on “a priori phase equilibrium prediction from a segment contribution solvation model” . *Industrial & Engineering Chemistry Research*, 41:2332–2334. p. [30](#)
 - Lischka, H., Shepard, R., Shavitt, I., Pitzer, R., Dallos, M., Müller, T., et al. 2003. COLUMBUS, an ab initio electronic structure program. p. [19](#)
 - Liu, X., Afzal, W., and Prausnitz, J. M. 2013a. Solubilities of small hydrocarbons in tetrabutylphosphonium bis (2, 4, 4-trimethylpentyl) phosphinate and in 1-ethyl-3-methylimidazolium bis (trifluoromethylsulfonyl) imide. *Industrial & Engineering Chemistry Research*. p. [71](#),
[76](#)
 - Liu, X., Afzal, W., Yu, G., He, M., and Prausnitz, J. M. 2013b. High solubilities of small hydrocarbons in trihexyl tetradecylphosphonium bis (2, 4, 4-trimethylpentyl) phosphinate. *The Journal of Physical Chemistry B*. p. [71](#), [76](#), [78](#), [82](#)
 - Liu, Z., Wu, W., Han, B., Dong, Z., Zhao, G., Wang, J., Jiang, T., and Yang, G. 2003. Study on the phase behaviors, viscosities, and thermodynamic properties of CO₂/[C4mim][PF₆]/methanol system at elevated pressures. *Chemistry-a European Journal*, 9(16):3897–3903. p. [120](#), [123](#)
 - Ludwig, R. 2008. Thermodynamic properties of ionic liquids-a cluster approach. *Physical Chemistry Chemical Physics*, 10(29):4333–4339. p. [36](#), [37](#), [39](#)
 - Maase, M. 2005. *Multiphase Homogeneous Catalysis*, volume 2. ed. Cornils, B. and Herrmann, W.A. and Horvath, I.T. and Leitner, W. and Mecking, S. and Olivier-Bourbigou, H. and Vogt, D. John Wiley & Sons. p. [2](#)
 - Maase, M. and Massonne, K. 2005. *Biphasic acid scavenging utilizing ionic liquids: The first commercial process with ionic liquids*, volume 902 of *Ionic Liquids IIIb: Fundamentals, Progress, Challenges and Opportunities: Transformations and Processes*. ed. Robin D. R., Kenneth R. S. ACS Symposium Series. American Chemical Society, Washington, USA. p. [2](#)
 - MacFarlane, D., Forsyth, S., Golding, J., and Deacon, G. 2002. Ionic liquids based on imidazolium, ammonium and pyrrolidinium salts of the dicyanamide anion. *Green Chemistry*, 4(5):444–448. p. [3](#)
-

- Majewski, P., Pernak, A., Grzymisławski, M., Iwanik, K., and Pernak, J. 2003. Ionic liquids in embalming and tissue preservation.: Can traditional formalin-fixation be replaced safely? *Acta histochemica*, 105(2):135–142. p. 5
- Manan, N., Hardacre, C., Jacquemin, J., Rooney, D. W., and Youngs, T. 2009. Evaluation of gas solubility prediction in ionic liquids using COSMOthermX. *Journal of Chemical & Engineering Data*, 54(7):2005–2022. p. 7, 50, 73, 92
- Marták, J. and Schlosser, Š. 2007. Extraction of lactic acid by phosphonium ionic liquids. *Separation and Purification Technology*, 57(3):483–494. p. 90
- Martín, A. and Bermejo, M. D. 2010. Thermodynamic analysis of absorption refrigeration cycles using ionic liquid+ supercritical CO₂ pairs. *The Journal of Supercritical Fluids*, 55(2):852–859. p. 113, 114
- Martínez-Aragón, M., Burghoff, S., Goetheer, E., and de Haan, A. 2009. Guidelines for solvent selection for carrier mediated extraction of proteins. *Separation and Purification Technology*, 65(1):65–72. p. 90
- Mastrangelo, S. 1959. Solubility of some chlorofluorohydrocarbons in tetraethylene glycol dimethyl ether. *ASHRAE Journal*, 1(10):64–68. p. 113
- Mathews, C. J., Smith, P. J., and Welton, T. 2000. Palladium catalysed suzuki cross-coupling reactions in ambient temperature ionic liquids. *Chemical Communications*, (14):1249–1250. p. 100, 103
- Matsumoto, M., Mochiduki, K., Fukunishi, K., and Kondo, K. 2004. Extraction of organic acids using imidazolium-based ionic liquids and their toxicity to *Lactobacillus rhamnosus*. *Separation and Purification Technology*, 40(1):97–101. p. 72, 90
- Maugeri, Z. and de María, P. D. 2012. Novel choline-chloride-based deep-eutectic-solvents with renewable hydrogen bond donors: levulinic acid and sugar-based polyols. *RSC Advances*, 2(2):421–425. p. 48
- Meindersma, G. and De Haan, A. 2012. Cyano-containing ionic liquids for the extraction of aromatic hydrocarbons from an aromatic/aliphatic mixture. *Science China Chemistry*, 55(8):1488–1499. p. 3
- Meindersma, G. W. 2005. *Conceptual process design for the extraction of aromatic compounds with ionic liquids*. In “Extraction of aromatics from naphtha with ionic liquids:

LIST OF REFERENCES

- from solvent development to pilot RDC evaluation.*”. Thesis, University of Twente.
p. [90](#), [91](#), [100](#), [101](#), [103](#), [109](#)
- Meindersma, G. W. and de Haan, A. 2008. Conceptual process design for aromatic/aliphatic separation with ionic liquids. *Chemical Engineering Research and Design*, 86(7):745–752. p. [90](#), [91](#), [100](#), [103](#), [107](#), [109](#)
- Meindersma, G. W., Podt, A., Klaren, M. B., and De Haan, A. B. 2006. Separation of aromatic and aliphatic hydrocarbons with ionic liquids. *Chemical Engineering Communications*, 193(11):1384–1396. p. [90](#), [91](#), [100](#), [103](#), [107](#)
- Mellein, B. R., Aki, S. N., Ladewski, R. L., and Brennecke, J. F. 2007. Solvatochromic studies of ionic liquid/organic mixtures. *The Journal of Physical Chemistry B*, 111(1):131–138. p. [48](#), [53](#)
- Milota, M., Mosher, P., and Li, L. 2007. VOC and HAP removal from dryer exhaust gas by adsorption into ionic liquids. *Forest Products Journal*, 57:73 – 77. p. [138](#), [139](#)
- Mokrushina, L., Buggert, M., Smirnova, I., Arlt, W., and Schomäcker, R. 2007. COSMO-RS and UNIFAC in prediction of micelle/water partition coefficients. *Industrial & Engineering Chemistry Research*, 46(20):6501–6509. p. [13](#)
- Mu, T., Rarey, J., and Gmehling, J. 2007a. Group contribution prediction of surface charge density profiles for COSMO-RS (Ol). *AIChE Journal*, 53(12):3231–3240. p. [20](#)
- Mu, T., Rarey, J., and Gmehling, J. 2007b. Performance of COSMO-RS with sigma profiles from different model chemistries. *Industrial & Engineering Chemistry Research*, 46(20):6612–6629. p. [20](#)
- Mullins, E., Liu, Y., Ghaderi, A., and Fast, S. D. 2008. Sigma profile database for predicting solid solubility in pure and mixed solvent mixtures for organic pharmacological compounds with COSMO-based thermodynamic methods. *Industrial & Engineering Chemistry Research*, 47(5):1707–1725. p. [31](#)
- Mullins, E., Oldland, R., Liu, Y., Wang, S., Sandler, S., Chen, C., Zwolak, M., and Seavey, K. 2006. Sigma-profile database for using COSMO-based thermodynamic methods. *Industrial & engineering chemistry research*, 45(12):4389–4415. p. [14](#), [20](#), [31](#), [175](#)

- Navas, A., Ortega, J., Vreekamp, R., Marrero, E., and Palomar, J. 2009. Experimental Thermodynamic Properties of 1-Butyl-2-methylpyridinium Tetrafluoroborate [b2mpy][BF₄] with Water and with Alkan-1-ol and Their Interpretation with the COSMO-RS Methodology. *Industrial & Engineering Chemistry Research*, 48(5):2678–2690. p. 7, 49, 50, 139
- Nebig, S., Bölts, R., and Gmehling, J. 2007. Measurement of vapor-liquid equilibria (VLE) and excess enthalpies (HE) of binary systems with 1-alkyl-3-methylimidazolium bis (trifluoromethylsulfonyl) imide and prediction of these properties and γ^∞ using modified UNIFAC (Dortmund). *Fluid phase equilibria*, 258(2):168–178. p. 48, 49
- Nebig, S., Liebert, V., and Gmehling, J. 2009. Measurement and prediction of activity coefficients at infinite dilution (γ^∞), vapor-liquid equilibria (VLE) and excess enthalpies (HE) of binary systems with 1, 1-dialkyl-pyrrolidinium bis (trifluoromethylsulfonyl) imide using mod. UNIFAC (Dortmund). *Fluid Phase Equilibria*, 277(1):61–67. p. 96
- Neese, F. 2009. Orca. *An ab Initio, Density Functional and Semiempirical Program Package version, 2*. p. 19
- Niedermeyer, H., Hallett, J. P., Villar-Garcia, I. J., Hunt, P. A., and Welton, T. 2012. Mixtures of ionic liquids. *Chemical Society Reviews*, 41(23):7780–7802. p. 131, 132
- O’Connell, J. P., Gani, R., Mathias, P. M., Maurer, G., Olson, J. D., and Crafts, P. A. 2009. Thermodynamic property modeling for chemical process and product engineering: some perspectives. *Industrial & Engineering Chemistry Research*, 48(10):4619–4637. p. 8
- Orchillés, A. V., Miguel, P. J., González-Alfaro, V., Vercher, E., and Martínez-Andreu, A. 2012. 1-ethyl-3-methylimidazolium dicyanamide as a very efficient entrainer for the extractive distillation of the acetone + methanol system. *Journal of Chemical & Engineering Data*, 57(2):394–399. p. 49
- Orchillés, A. V., Miguel, P. J., Llopis, F. J., Vercher, E., and Martínez-Andreu, A. 2011. Influence of some ionic liquids containing the trifluoromethanesulfonate anion on the vapor-liquid equilibria of the acetone + methanol system. *Journal of Chemical & Engineering Data*, 56(12):4430–4435. p. 49
- Orchillés, A. V., Miguel, P. J., Vercher, E., and Martínez-Andreu, A. 2007. Ionic liquids as entrainers in extractive distillation: isobaric vapor-liquid equilibria for acetone +

- methanol + 1-ethyl-3-methylimidazolium trifluoromethanesulfonate. *Journal of Chemical & Engineering Data*, 52(1):141–147. p. 49
- Ortega, J., Vreekamp, R., Marrero, E., and Penco, E. 2007. Thermodynamic properties of 1-butyl-3-methylpyridinium tetrafluoroborate and its mixtures with water and alkanols. *Journal of Chemical & Engineering Data*, 52(6):2269–2276. p. 49, 50, 56, 62
- Ortega, J., Vreekamp, R., Penco, E., and Marrero, E. 2008. Mixing thermodynamic properties of 1-butyl-4-methylpyridinium tetrafluoroborate [b4mpy][BF₄] with water and with an alkan-1-ol (methanol to pentanol). *The Journal of Chemical Thermodynamics*, 40(7):1087–1094. p. 49
- Ortiz, A., Galán, L., Gorri, D., de Haan, A., and Ortiz, I. 2010a. Kinetics of reactive absorption of propylene in RTIL-Ag⁺ media. *Separation and Purification Technology*, 73(2):106–113. p. 139
- Ortiz, A., Galán, L., Gorri, D., de Haan, A., and Ortiz, I. 2010b. Reactive ionic liquid media for the separation of propylene/propane gaseous mixtures. *Industrial & Engineering Chemistry Research*, 49(16):7227–7233. p. 139
- Palgunadi, J., Kim, H. S., Lee, J. M., and Jung, S. 2010. Ionic liquids for acetylene and ethylene separation: Material selection and solubility investigation. *Chemical Engineering and Processing: Process Intensification*, 49(2):192–198. p. 72
- Palomar, J., Ferro, V. R., Gilarranz, M. A., and Rodríguez, J. J. 2007a. Computational approach to nuclear magnetic resonance in 1-alkyl-3-methylimidazolium ionic liquids. *The Journal of Physical Chemistry B*, 111(1):168–180. p. 48, 52
- Palomar, J., González-Miquel, M., Bedia, J., Rodríguez, F., and Rodríguez, J. J. 2011a. Task-specific ionic liquids for efficient ammonia absorption. *Separation and Purification Technology*, 82:43–52. p. 50, 62, 73, 92, 113, 115, 139, 141, 142, 143
- Palomar, J., González-Miquel, M., Polo, A., and Rodríguez, F. 2011b. Understanding the physical absorption of CO₂ in ionic liquids using the COSMO-RS method. *Industrial & Engineering Chemistry Research*, 50(6):3452–3463. p. 7, 22, 50, 62, 74, 139
- Palomar, J., Lemus, J., Gilarranz, M., and Rodríguez, J. 2009a. Adsorption of ionic liquids from aqueous effluents by activated carbon. *Carbon*, 47(7):1846–1856. p. 49, 50, 62

LIST OF REFERENCES

- Palomar, J., Torrecilla, J., Ferro, V., and Rodríguez, F. 2007b. Density and molar volume predictions using COSMO-RS for ionic liquids. An approach to solvent design. *Industrial & Engineering Chemistry Research*, 46(18):6041–6048. p. 7, 25, 40, 92
- Palomar, J., Torrecilla, J., Ferro, V., and Rodríguez, F. 2008. Development of an a priori ionic liquid design tool. 1. Integration of a novel COSMO-RS molecular descriptor on neural networks. *Industrial & Engineering Chemistry Research*, 47(13):4523–4532. p. 6, 7, 8, 50, 91
- Palomar, J., Torrecilla, J., Ferro, V., and Rodríguez, F. 2009b. Development of an a priori ionic liquid design tool. 2. ionic liquid selection through the prediction of COSMO-RS molecular descriptor by inverse neural network. *Industrial & Engineering Chemistry Research*, 48(4):2257–2265. p. 6, 7, 8, 50, 91, 107
- Palomar, J., Torrecilla, J., Lemus, J., Ferro, V., and Rodríguez, F. 2010. A COSMO-RS based guide to analyze/quantify the polarity of ionic liquids and their mixtures with organic cosolvents. *Physical Chemistry Chemical Physics*, 12(8):1991–2000. p. 7, 139
- Papageorgiou, N., Athanassov, Y., Armand, M., Bonho, P., Pettersson, H., Azam, A., Grätzel, M., et al. 1996. The performance and stability of ambient temperature molten salts for solar cell applications. *Journal of the Electrochemical Society*, 143(10):3099–3108. p. 5
- Parshall, G. 1972a. Catalysis in molten salt media. *Journal of the American Chemical Society*, 94(25):8716–8719. p. 4
- Parshall, G. 1972b. U.S. Patent 3657368 (to E.I. du Pont de Nemours and Company). April 18. p. 4
- Pereiro, A., Canosa, J., and Rodríguez, A. 2007. Liquid-liquid equilibria of 1, 3-dimethylimidazolium methyl sulfate with ketones, dialkyl carbonates and acetates. *Fluid phase equilibria*, 254(1):150–157. p. 49
- Pereiro, A., Deive, F., Esperança, J., and Rodríguez, A. 2010. Alkylsulfate-based ionic liquids to separate azeotropic mixtures. *Fluid phase equilibria*, 294(1):49–53. p. 90, 91
- Pereiro, A., Tojo, E., Rodríguez, A., Canosa, J., and Tojo, J. 2006. Properties of ionic liquid hmimpf6 with carbonates, ketones and alkyl acetates. *The Journal of Chemical Thermodynamics*, 38(6):651–661. p. 49

- Pereiro, A. B. and Rodríguez, A. 2008a. Azeotrope-breaking using [BMIM][MeSO₄] ionic liquid in an extraction column. *Separation and Purification Technology*, 62(3):733–738. p. [90](#), [91](#)
- Pereiro, A. B. and Rodríguez, A. 2008b. Separation of ethanol - heptane azeotropic mixtures by solvent extraction with an ionic liquid. *Industrial & Engineering Chemistry Research*, 48(3):1579–1585. p. [90](#), [91](#)
- Pereiro, A. B. and Rodríguez, A. 2009. Purification of hexane with effective extraction using ionic liquid as solvent. *Green Chemistry*, 11(3):346–350. p. [90](#), [91](#)
- Pereiro, A. B. and Rodríguez, A. 2010. An ionic liquid proposed as solvent in aromatic hydrocarbon separation by liquid extraction. *AIChE Journal*, 56(2):381–386. p. [90](#), [91](#)
- Poliakoff, M., Fitzpatrick, J., Farren, T., , and Anastas, P. 2002. Green chemistry: science and politics of change. *Science*, 297(5582):807–810. p. [2](#)
- Porcedda, S., Marongiu, B., Schirru, M., Falconieri, D., and Piras, A. 2011. Excess enthalpy and excess volume for binary systems of two ionic liquids + water. *Journal of Thermal Analysis and Calorimetry*, 103:29–33. p. [49](#)
- Preiss, U. P., Slattey, J. M., and Krossing, I. 2009. In silico prediction of molecular volumes, heat capacities, and temperature-dependent densities of ionic liquids. *Industrial & Engineering Chemistry Research*, 48(4):2290–2296. p. [25](#)
- Pulay, P., Baker, J., and Wolinski, K. 2003. Paralell Quantum Solutions (PQS). Fayetteville, AR. p. [19](#)
- Putnam, R., Taylor, R., Klamt, A., Eckert, F., and Schiller, M. 2003. Prediction of infinite dilution activity coefficients using COSMO-RS. *Industrial & engineering chemistry research*, 42(15):3635–3641. p. [13](#)
- Quijano, G., Couvert, A., Amrane, A., Darracq, G., Couriol, C., Le Cloirec, P., Paquin, L., and Carrié, D. 2011. Potential of ionic liquids for VOC absorption and biodegradation in multiphase systems. *Chemical Engineering Science*, 66(12):2707–2712. p. [138](#), [139](#), [147](#), [151](#), [152](#), [161](#)
- Raabe, G. and Köhler, J. 2008. Thermodynamical and structural properties of imidazolium based ionic liquids from molecular simulation. *The Journal of chemical physics*, 128:154509. p. [36](#), [40](#)
-

- Rafson, H. 1998. *Odor and VOC control handbook*. McGraw-Hill handbooks. McGraw-Hill. p. 138
- Rai, G. and Kumar, A. 2011. An enthalpic approach to delineate the interactions of cations of imidazolium-based ionic liquids with molecular solvents. *Physical Chemistry Chemical Physics*, 13(32):14716–14723. p. 49, 53
- Rebelo, L., Canongia Lopes, J., Esperança, J., and Filipe, E. 2005. On the critical temperature, normal boiling point, and vapor pressure of ionic liquids. *The Journal of Physical Chemistry B*, 109(13):6040–6043. p. 3, 36, 37, 39
- Ren, J., Zhao, Z., and Zhang, X. 2011. Vapor pressures, excess enthalpies, and specific heat capacities of the binary working pairs containing the ionic liquid 1-ethyl-3-methylimidazolium dimethylphosphate. *The Journal of Chemical Thermodynamics*, 43(4):576–583. p. 49
- Ren, S., Hou, Y., Wu, W., Liu, Q., Xiao, Y., and Chen, X. 2010. Properties of ionic liquids absorbing SO₂ and the mechanism of the absorption. *The Journal of Physical Chemistry B*, 114(6):2175–2179. p. 139
- Rhodes, C. 1996. The process simulation revolution: Thermophysical property needs and concerns. *Journal of Chemical & Engineering Data*, 41(5):947–950. p. 8
- Rodríguez, H. and Brennecke, J. F. 2006. Temperature and composition dependence of the density and viscosity of binary mixtures of water + ionic liquid. *Journal of Chemical & Engineering Data*, 51(6):2145–2155. p. 123
- Rogers, R. and Seddon, K. 2003. Ionic liquids—solvents of the future? *Science*, 302(5646):792–793. p. 2
- Rogers, R., Seddon, K., of Industrial, A. C. S. D., Chemistry, E., and Meeting, A. C. S. 2002. *Ionic liquids: industrial applications for green chemistry*. ACS symposium series. American Chemical Society. p. 4, 5
- Rogers, R. and Voth, G. 2007. Guest editorial-Ionic liquids. p. 5
- Ruivo, R., Couto, R., and Simões, P. C. 2010. Screening of ionic liquids as promising separation agents of oil mixtures for application in membranes. *Separation and Purification Technology*, 76(1):84–88. p. 90
-

- Safarik, D. J. and Eldridge, R. B. 1998. Olefin/paraffin separations by reactive absorption: a review. *Industrial & engineering chemistry research*, 37(7):2571–2581. p. 72
- Safarov, J., Verevkin, S. P., Bich, E., and Heintz, A. 2006. Vapor pressures and activity coefficients of n-alcohols and benzene in binary mixtures with 1-methyl-3-butylimidazolium octyl sulfate and 1-methyl-3-octylimidazolium tetrafluoroborate. *Journal of Chemical & Engineering Data*, 51(2):518–525. p. 96
- Sandler, S., Wang, S., Lin, S., and Goddard, W. 2008. Reply to “Comments on Refinement of COSMO-SAC and the Applications” . *Industrial & Engineering Chemistry Research*, 47(4):1353–1354. p. 20
- Schäfer, A., Klamt, A., Sattel, D., Lohrenz, J., and Eckert, F. 2000. COSMO Implementation in TURBOMOLE: Extension of an efficient quantum chemical code towards liquid systems. *Physical Chemistry Chemical Physics*, 2(10):2187–2193. p. 13, 19, 74, 116
- Schleicher, J. C. and Scurto, A. M. 2009. Kinetics and solvent effects in the synthesis of ionic liquids: imidazolium. *Green chemistry*, 11(5):694–703. p. 49
- Schöfer, S. H., Kaftzik, N., Wasserscheid, P., and Kragl, U. 2001. Enzyme catalysis in ionic liquids: lipase catalysed kinetic resolution of 1-phenylethanol with improved enantioselectivity. *Chemical Communications*, (5):425–426. p. 101, 103
- Schröder, B., Santos, L., Rocha, M., Oliveira, M., Marrucho, I., and Coutinho, J. 2010. Prediction of environmental parameters of polycyclic aromatic hydrocarbons with COSMO-RS. *Chemosphere*, 79(8):821–829. p. 13
- Schumann, D., Gregory, D. V., and Piyush, S. 2009. Application of simulation models in operations - A success story. AspenTech. in *AspenTech User Conference*, Houston, May. p. 30
- Seddon, K. 1995. Room-temperature ionic liquids: neoteric solvents for clean catalysis. *Kinetics and Catalysis*, 37(5):693–697. p. 2, 4
- Seddon, K. 1997. Ionic liquids for clean technology. *Journal of Chemical Technology and Biotechnology*, 68(4):351–356. p. 4
- Seddon, K. 1999. Ionic liquids: designer solvents? in *The International George Papatheodorou Symposium*, Eds. S. Boghosian, V. Dracopoulos, C.G. Kontoyannis and

- G.A. Voyiatzis (Institute of Chemical Engineering and High Temperature Processes), Patras. p. 4
- Seddon, K. 2003. Ionic liquids: a taste of the future. *Nature materials*, 2(6):363–365. p. 2
- Seddon, K. R., Stark, A., and Torres, M. J. 2002. *Viscosity and density of 1-alkyl-3-methylimidazolium ionic liquids*. In *Clean Solvents. Alternative media for chemical reactions and processing*. Eds. Abraham, M.A. and Moens, L. American Chemical Society. p. 120, 123
- Seiler, M., Jork, C., Kavarnou, A., Arlt, W., and Hirsch, R. 2004. Separation of azeotropic mixtures using hyperbranched polymers or ionic liquids. *AIChE Journal*, 50(10):2439–2454. p. 7, 48, 90, 91
- Sheldon, R. 2001. Catalytic reactions in ionic liquids. *Chemical Communications*, (23):2399–2407. p. 3
- Shiflett, M. B., Shiflett, A., and Yokozeki, A. 2011. Separation of tetrafluoroethylene and carbon dioxide using ionic liquids. *Separation and Purification Technology*, 79(3):357–364. p. 139
- Shiflett, M. B. and Yokozeki, A. 2005. Solubilities and diffusivities of carbon dioxide in ionic liquids:[bmim][PF₆] and [bmim][BF₄]. *Industrial & engineering chemistry research*, 44(12):4453–4464. p. 157, 158, 159
- Shiflett, M. B. and Yokozeki, A. 2006a. Separation of difluoromethane and pentafluoroethane by extractive distillation using ionic liquid. *Chimica Oggi-Chemistry Today*, 24(2):28–30. p. 90, 91, 100, 103
- Shiflett, M. B. and Yokozeki, A. 2006b. Solubility and diffusivity of hydrofluorocarbons in room-temperature ionic liquids. *AIChE journal*, 52(3):1205–1219. p. 91, 113
- Shiflett, M. B. and Yokozeki, A. 2006c. Solubility and diffusivity of hydrofluorocarbons in room-temperature ionic liquids. *AIChE journal*, 52(3):1205–1219. p. 139
- Shiflett, M. B. and Yokozeki, A. 2009. Chemical absorption of sulfur dioxide in room-temperature ionic liquids. *Industrial & Engineering Chemistry Research*, 49(3):1370–1377. p. 139

- Shiflett, M. B., Yokozeki, A., et al. 2006. World Patent 2006084262 (to Covalent Associates, Inc., USA). August 11. p. [113](#), [114](#)
- Simoni, L. D., Lin, Y., Brennecke, J. F., and Stadtherr, M. A. 2008. Modeling liquid-liquid equilibrium of ionic liquid systems with nrtl, electrolyte-nrtl, and uniquac. *Industrial & Engineering Chemistry Research*, 47(1):256–272. p. [91](#), [114](#)
- Sistla, Y. S. and Khanna, A. 2011. Validation and Prediction of the Temperature-Dependent Henry’s Constant for CO₂-Ionic Liquid Systems Using the Conductor-like Screening Model for Realistic Solvation (COSMO-RS). *Journal of Chemical & Engineering Data*, 56(11):4045–4060. p. [73](#)
- Solsona, B., García, T., Aylón, E., Dejoz, A., Vázquez, I., Agouram, S., Davies, T., and Taylor, S. 2011. Promoting the activity and selectivity of high surface area Ni-C-O mixed oxides by gold deposition for VOC catalytic combustion. *Chemical Engineering Journal*, 175(0):271 – 278. p. [138](#)
- Somers, C., Mortazavi, A., Hwang, Y., Radermacher, R., Rodgers, P., and Al-Hashimi, S. 2011. Modeling water/lithium bromide absorption chillers in ASPEN Plus. *Applied Energy*, 88(11):4197–4205. p. [114](#)
- Srikhirin, P., Aphornratana, S., and Chungpaibulpatana, S. 2001. A review of absorption refrigeration technologies. *Renewable and sustainable energy reviews*, 5(4):343–372. p. [112](#)
- Steiú, S., Salavera, D., Bruno, J. C., and Coronas, A. 2009. A basis for the development of new ammonia-water-sodium hydroxide absorption chillers. *International Journal of Refrigeration*, 32(4):577–587. p. [114](#)
- Sumon, K. Z. and Henni, A. 2011. Ionic liquids for CO₂ capture using COSMO-RS: Effect of structure, properties and molecular interactions on solubility and selectivity. *Fluid Phase Equilibria*, 310(1):39–55. p. [73](#)
- Swarnkar, S. K., Venkatarathnam, G., Ayoub, D. S., Bruno, J. C., and Coronas, A. 2012. A review on absorption heat pumps and chillers using ionic liquids as absorbents. In *Proceedings International Workshop on Ionic Liquids - Seeds for New Engineering Applications. Lisbon, Portugal*. p. [113](#)

LIST OF REFERENCES

- Swatloski, R., Spear, S., Holbrey, J., and Rogers, R. 2002. Dissolution of cellulose with ionic liquids. *Journal of the American Chemical Society*, 124(18):4974–4975. p. 5
- Taylor, A. W., Lovelock, K. R., Deyko, A., Licence, P., and Jones, R. G. 2010. High vacuum distillation of ionic liquids and separation of ionic liquid mixtures. *Physical Chemistry Chemical Physics*, 12(8):1772–1783. p. 100, 131
- Thied, R., Seddon, K., Pitner, W., and Rooney, D. 1999. World Patent 9941752 (to British Fuels PLC). August 19. p. 5
- Tian, X., Zhang, X., Wei, L., Zeng, S., Huang, L., and Zhang, S. 2010. Multi-scale simulation of the 1, 3-butadiene extraction separation process with an ionic liquid additive. *Green Chemistry*, 12(7):1263–1273. p. 9
- Tokuda, H., Hayamizu, K., Ishii, K., Susan, M., and Watanabe, M. 2004. Physicochemical properties and structures of room temperature ionic liquids. 1. Variation of anionic species. *The Journal of Physical Chemistry B*, 108(42):16593–16600. p. 72, 141, 142, 143
- Tomasi, J., Mennucci, B., and Cammi, R. 2005. Quantum mechanical continuum solvation models. *Chemical Reviews*, 105(8):2999–3094. p. 18
- Tomé, L. I., Catambas, V. R., Teles, A. R., Freire, M. G., Marrucho, I. M., and Coutinho, J. A. P. 2010. Tryptophan extraction using hydrophobic ionic liquids. *Separation and Purification Technology*, 72(2):167–173. p. 90
- Tripp, J. T. 1987. UNEP Montreal Protocol: Industrialized and Developing Countries Sharing the Responsibility for Protecting the Stratospheric Ozone Layer. *The New York University Journal of International Law and Politics*, 20:733–752. p. 1
- Trouton, F. 1883. On a relation existing between the latent heats, specific heats, and relative volumes of volatile bodies. *Nature*, 27:292. p. 36
- Trouton, F. 1884. On molecular latent heat. *The London, Edinburgh, and Dublin Philosophical Magazine and Journal of Science*, 18(110):54–57. p. 36
- Tsou, D. T., Blachman, M. W., and Davis, J. C. 1994. Silver-facilitated olefin/paraffin separation in a liquid membrane contactor system. *Industrial & engineering chemistry research*, 33(12):3209–3216. p. 72

LIST OF REFERENCES

- Valderrama, J. and Robles, P. 2007a. Critical properties, normal boiling temperatures, and acentric factors of fifty ionic liquids. *Industrial & engineering chemistry research*, 46(4):1338–1344. p. 37
- Valderrama, J. and Robles, P. 2007b. Reply to “Comment on Critical Properties, Normal Boiling Temperature, and Acentric Factor of Fifty Ionic Liquids”. *Industrial & Engineering Chemistry Research*, 46(18):6063–6064. p. 37
- Valderrama, J. O., Reategui, A., and Rojas, R. E. 2009. Density of ionic liquids using group contribution and artificial neural networks. *Industrial & Engineering Chemistry Research*, 48(6):3254–3259. p. 39
- Valderrama, J. O. and Zarricueta, K. 2009. A simple and generalized model for predicting the density of ionic liquids. *Fluid Phase Equilibria*, 275(2):145–151. p. 39, 123
- Van Ness, H. C. and Abbott, M. M. 1982. *Classical thermodynamics of nonelectrolyte solutions: with applications to phase equilibria*. McGraw-Hill Companies. p. 114
- Vargas, J., Horuz, I., Callander, T., Fleming, J., and Parise, J. 1998. Simulation of the transient response of heat driven refrigerators with continuous temperature control: Simulation de la réponse transitoire des réfrigérateurs utilisant une source de chaleur avec maîtrise de la température en continu. *International journal of refrigeration*, 21(8):648–660. p. 114
- Verevkin, S. P., Safarov, J., Bich, E., Hassel, E., and Heintz, A. 2005. Thermodynamic properties of mixtures containing ionic liquids: Vapor pressures and activity coefficients of n-alcohols and benzene in binary mixtures with 1-methyl-3-butyl-imidazolium bis(trifluoromethyl-sulfonyl) imide. *Fluid phase equilibria*, 236(1):222–228. p. 96
- Verma, V. K. and Banerjee, T. 2010. Ionic liquids as entrainers for water + ethanol, water + 2-propanol, and water + THF systems: A quantum chemical approach. *The Journal of Chemical Thermodynamics*, 42(7):909–919. p. 7, 50
- Virginia Tech, . 2006. VT Sigma Profile Database. Virginia Polytechnic Institute and State University. Available at: <http://www.design.che.vt.edu/>. Blacksburg, VA:. p. 31, 32
- Vreekamp, R., Castellano, D., Palomar, J., Ortega, J., Espiau, F., Fernández, L., and Penco, E. 2011. Thermodynamic behavior of the binaries 1-butylpyridinium tetrafluoroborate with water and alkanols: their interpretation using ¹H NMR spectroscopy and

- quantum-chemistry calculations. *The Journal of Physical Chemistry B*, 115(27):8763–8774. p. [49](#), [50](#), [62](#), [139](#)
- Vuong, M., Couvert, A., Couriol, C., Amrane, A., Le Cloirec, P., and Renner, C. 2009. Determination of the Henry’s constant and the mass transfer rate of VOCs in solvents. *Chemical Engineering Journal*, 150(2):426–430. p. [153](#)
- Walden, P. 1914. Molecular weights and electrical conductivity of several fused salts. *Bull. Acad. Sci. St. Petersburg*, 405:22. p. [2](#)
- Wang, J. F., Li, C. X., and Wang, Z. H. 2007a. Measurement and prediction of vapor pressure of binary and ternary systems containing 1-ethyl-3-methylimidazolium ethyl sulfate. *Journal of Chemical & Engineering Data*, 52(4):1307–1312. p. [96](#)
- Wang, J.-F., Li, C.-X., Wang, Z.-H., Li, Z.-J., and Jiang, Y.-B. 2007b. Vapor pressure measurement for water, methanol, ethanol, and their binary mixtures in the presence of an ionic liquid 1-ethyl-3-methylimidazolium dimethylphosphate. *Fluid phase equilibria*, 255(2):186–192. p. [113](#)
- Wang, N.-N., Zhang, Q.-G., Wu, F.-G., Li, Q.-Z., and Yu, Z.-W. 2010. Hydrogen Bonding Interactions between a Representative Pyridinium-Based Ionic Liquid [BuPy][BF₄] and Water/Dimethyl Sulfoxide. *The Journal of Physical Chemistry B*, 114(26):8689–8700. p. [48](#)
- Wang, S., Sandler, S., and Chen, C. 2007c. Refinement of COSMO-SAC and the applications. *Industrial & Engineering Chemistry Research*, 46(22):7275–7288. p. [20](#)
- Wang, X., Daniels, R., and Baker, R. 2001. Recovery of VOCs from high-volume, low-VOC-concentration air streams. *AIChE journal*, 47(5):1094–1100. p. [138](#)
- Wasserscheid, P. and Welton, T. 2008. *Ionic liquids in synthesis*, volume 1. Wiley Online Library. p. [39](#), [120](#), [123](#), [139](#)
- Welton, T. 1999. Room-temperature ionic liquids. Solvents for synthesis and catalysis. *Chemical reviews*, 99(8):2071–2084. p. [3](#)
- Wilke, C. and Chang, P. 1955. Correlation of diffusion coefficients in dilute solutions. *AIChE Journal*, 1(2):264–270. p. [158](#)
-

LIST OF REFERENCES

- Wilkes, J. 2002. A short history of ionic liquids - from molten salts to neoteric solvents. *Green Chemistry*, 4(2):73–80. p. 4
- Wilkes, J. and Zaworotko, M. 1992. Air and water stable 1-ethyl-3-methylimidazolium based ionic liquids. *Journal of the Chemical Society, Chemical Communications*, (13):965–967. p. 4
- Yang, Q., Xing, H., Cao, Y., Su, B., Yang, Y., and Ren, Q. 2009. Selective separation of tocopherol homologues by liquid - liquid extraction using ionic liquids. *Industrial & Engineering Chemistry Research*, 48(13):6417–6422. p. 72
- Yang, W. J. and Guo, K. H. 1987. Solar-assisted lithium-bromide absorption cooling systems. In *Solar Energy Utilization*, pages 409–423. Springer. p. 114
- Ye, C., Liu, W., Chen, Y., and Yu, L. 2001. Room-temperature ionic liquids: a novel versatile lubricant. *Chemical Communications*, (21):2244–2245. p. 5
- Ye, C. and Shreeve, J. M. 2007. Rapid and accurate estimation of densities of room-temperature ionic liquids and salts. *The Journal of Physical Chemistry A*, 111(8):1456–1461. p. 39
- Yokozei, A. 2005. Theoretical performances of various refrigerant-absorbent pairs in a vapor-absorption refrigeration cycle by the use of equations of state. *Applied Energy*, 80(4):383–399. p. 114, 129
- Yokozei, A. and Shiflett, M. 2010. Water solubility in ionic liquids and application to absorption cycles. *Industrial & Engineering Chemistry Research*, 49(19):9496–9503. p. 5, 113, 114, 124
- Yokozei, A. and Shiflett, M. B. 2007a. Ammonia solubilities in room-temperature ionic liquids. *Industrial & engineering chemistry research*, 46(5):1605–1610. p. 113, 114, 115, 117, 124, 127, 128, 139, 184
- Yokozei, A. and Shiflett, M. B. 2007b. Vapor-liquid equilibria of ammonia + ionic liquid mixtures. *Applied Energy*, 84(12):1258–1273. p. 113, 114, 115, 117, 124, 127, 128, 184
- Yoshizawa, M., Xu, W., and Angell, C. 2003. Ionic liquids by proton transfer: vapor pressure, conductivity, and the relevance of $\Delta p K_a$ from aqueous solutions. *Journal of the American Chemical Society*, 125(50):15411–15419. p. 3

LIST OF REFERENCES

- Young, G., Nippgen, F., Titterbrandt, S., and Cooney, M. J. 2010. Lipid extraction from biomass using co-solvent mixtures of ionic liquids and polar covalent molecules. *Separation and Purification Technology*, 72(1):118–121. p. 90
- Yu, G., Zhao, D., Wen, L., Yang, S., and Chen, X. 2012. Viscosity of ionic liquids: Database, observation, and quantitative structure-property relationship analysis. *AIChE Journal*, 58(9):2885–2899. p. 123
- Zaitsau, D. H., Kabo, G. J., Strechan, A. A., Paulechka, Y. U., Tschersich, A., Verevkin, S. P., and Heintz, A. 2006. Experimental vapor pressures of 1-alkyl-3-methylimidazolium bis (trifluoromethylsulfonyl) imides and a correlation scheme for estimation of vaporization enthalpies of ionic liquids. *The Journal of Physical Chemistry A*, 110(22):7303–7306. p. 36, 37, 39, 101
- Zhai, C., Wang, J., Zhao, Y., Tang, J., and Wang, H. 2006. A NMR study on the interactions of 1-alkyl-3-methylimidazolium ionic liquids with acetone. *Zeitschrift für Physikalische Chemie*, 220(6/2006):775–785. p. 52
- Zhang, Q.-G., Wang, N.-N., and Yu, Z.-W. 2010. The hydrogen bonding interactions between the ionic liquid 1-ethyl-3-methylimidazolium ethyl sulfate and water. *The Journal of Physical Chemistry B*, 114(14):4747–4754. p. 48
- Zhang, S., Lu, X., Zhou, Q., Li, X., Zhang, X., and Li, S. 2009. *Ionic Liquids:: Physicochemical Properties*. Access Online via Elsevier. p. 141, 142, 143
- Zhang, X. and Hu, D. 2011. Performance simulation of the absorption chiller using water and ionic liquid 1-ethyl-3-methylimidazolium dimethylphosphate as the working pair. *Applied Thermal Engineering*, 31(16):3316–3321. p. 113, 114
- Zhang, X., Liu, Z., and Wang, W. 2008. Screening of ionic liquids to capture CO₂ by COSMO-RS and experiments. *AIChE Journal*, 54(10):2717–2728. p. 73
- Zhang, Z. 2006. *Catalysis in ionic liquids*. Eds. Gates, B.C. and Knozinger, H. Advances in Catalysis. Advances in Catalysis Series. Elsevier Science & Technology Books. p. 5
- Zhao, H., Xia, S., and Ma, P. 2005. Use of ionic liquids as “green” solvents for extractions. *Journal of chemical technology and biotechnology*, 80(10):1089–1096. p. 7, 48

- Zhao, J., Li, C.-X., and Wang, Z.-H. 2006a. Vapor pressure measurement and prediction for ethanol + methanol and ethanol + water systems containing ionic liquids. *Journal of Chemical & Engineering Data*, 51(5):1755–1760. p. 96
- Zhao, Y., Schultz, N. E., and Truhlar, D. G. 2006b. Design of density functionals by combining the method of constraint satisfaction with parametrization for thermochemistry, thermochemical kinetics, and noncovalent interactions. *Journal of Chemical Theory and Computation*, 2(2):364–382. p. 51
- Zhu, A., Wang, J., Han, L., and Fan, M. 2009. Measurements and correlation of viscosities and conductivities for the mixtures of imidazolium ionic liquids with molecular solutes. *Chemical Engineering Journal*, 147(1):27–35. p. 123
- Zhu, J.-Q., Chen, J., Li, C.-Y., and Fei, W.-Y. 2007. Centrifugal extraction for separation of ethylbenzene and octane using 1-butyl-3-methylimidazolium hexafluorophosphate ionic liquid as extractant. *Separation and purification technology*, 56(2):237–240. p. 72

LIST OF REFERENCES

Publications related to this PhD Thesis

This dissertation is the result of the following papers recently published by the author:

- Interactions of Ionic Liquids and Acetone: Thermodynamic Properties, Quantum Chemical Calculations and NMR Analysis.
- High Solubilities of Methane, Ethane, Ethylene and Propane in [P8111][TMPP].
- Introducing process simulation in ionic liquids design/selection for separation processes based on operational and economic criteria through the example of their regeneration.
- Evaluation of ionic liquids as absorbents for ammonia absorption refrigeration cycles using COSMO-based process simulations.
- Optimized ionic liquids for toluene absorption.

Besides the digital version of this PhD thesis (PDF file), the publications mentioned above are available in the CD-ROM included in this book. The thesis in PDF format contains hyperlinks that contribute to a greater reading agility.